NASA CR-121127

INVESTIGATION OF NOISE SUPPRESSION BY SONIC INLETS FOR TURBOFAN ENGINES

Volume II: Appendixes

D6-40855-1

July 1973

by F. Klujber, J. C. Bosch,
R. W. Demetrick, and W. L. Robb

BOEING COMMERCIAL AIRPLANE COMPANY

prepared for

NATIONAL AERONAUTICS AND SPACE ADMINISTRATION

NASA Lewis Research Center
Contract NAS3-15574

(NASA-CR-121127) INVESTIGATION OF NOISE SUPPRESSION BY SONIC INLETS FOR TURBOFAN ENGINES. VOLUME 2: APPENDIXES (Boeing Commercial Airplane Co., Seattle) 219 p CSCL 2_A G3/28

N73-28732
Unclas
_9955

222

PRECEDING PAGE BLANK NOT FILMED

INVESTIGATION OF NOISE SUPPRESSION BY SONIC INLETS FOR TURBOFAN ENGINES

BY: F. KLUJBER,
J. C. BOSCH, R. W. DEMETRICK, AND W. L. ROBB

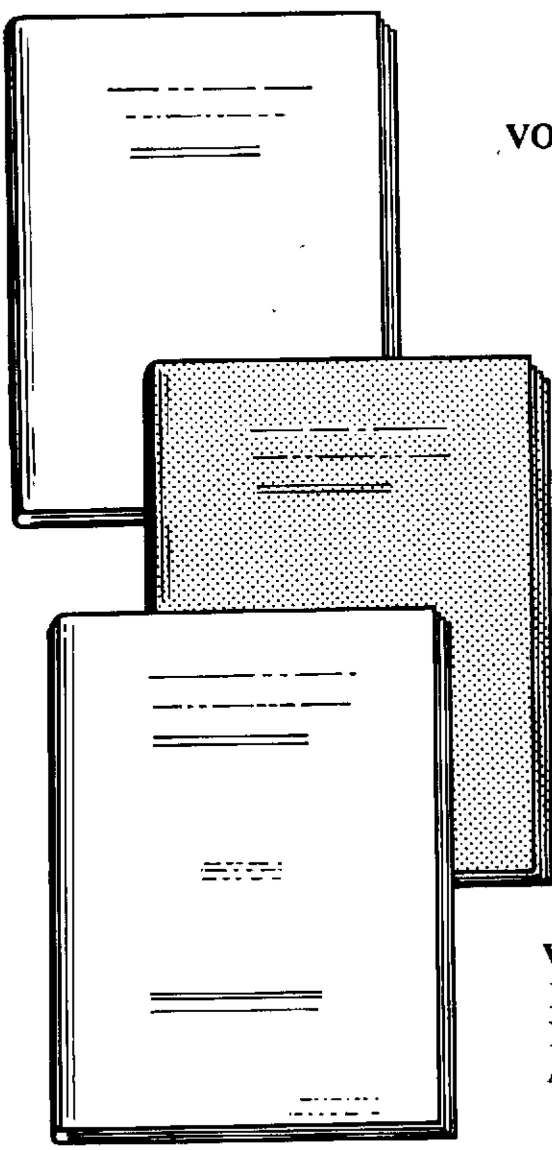

VOLUME I: PROGRAM SUMMARY

CR-121126 D6-40855

VOLUME II: APPENDIXES

CR-121127 D6-40855-1

A. MECHANICAL DESIGN STUDY AND TEST CONFIGURATION SELECTION

B. DETAIL DESIGN OF MODELS

C. INSTRUMENTATION DETAILS

D. DATA ANALYSIS PROCEDURE

E. CONCEPT SCREENING.

VOLUME III: AN EXPERIMENTAL INVESTIGATION OF THE INTERNAL NOISE FIELD OF TWO MODEL AXISYMMETRIC SONIC INLETS

CR-121128 D6-40818

CONTENTS

APPENDIX A

MECHANICAL DESIGN STUDY
AND TEST CONFIGURATION SELECTION

SUMMARY

This appendix contains the results of design studies to establish the best mechanical design that meets the criteria for a single- or multipassage sonic inlet on a STOL airplane propulsion system. Conclusions from the study had a major influence on selection of sonic inlet models for testing.

The desired throat area reduction of 27% from cruise to approach was best achieved in the multipassage group with a translating radial vane and centerbody configuration, for a vane-type sonic inlet, and a translating ring and centerbody configuration, for a ring-type sonic inlet. An articulated radial vane configuration is discussed and was chosen to be tested for performance evaluation.

In the single-passage group, the translating centerbody was considered to be the most suitable.

A.1 INTRODUCTION

The total program for investigation of noise suppression by sonic inlets for turbofan engines is outlined in technical proposal document D6-40195-1, dated September 24, 1971. Mechanical design configuration studies were proposed under task III of the program. Studies conducted to determine mechanical design influence on selection of candidate configurations for model screening tests of single-passage and multipassage sonic inlets are outlined in this document. Preliminary design layouts, design criteria, evaluation charts, and conclusions and comments are included.

A.2 DESIGN CRITERIA

The following criteria were followed in all design studies to ensure comparison of configurations within the same parameters.

1) The designs were tailored to the engine requirements for a STOL airplane. However, design flexibility, for application to engines having greater area change requirements, was also considered in design selection.

2) The inlets were evaluated as both two-position devices and multiposition devices until test results and/or analysis defined noise and performance payoffs for trade against system complexity.

3) Actuation time from approach to takeoff was considered compatible with engine acceleration capabilities and tolerance to transient flow variations.

A.3 CONFIGURATIONS

A.3.1 Vane-Type Sonic Inlets

A.3.1.1 Rotating Radial Vane Sonic Inlet

Figure A-1, LO-INSP-003, depicts a rotating radial vane sonic inlet configured to the criteria outlined in section A-2.

Throat area reduction to increase the throat Mach number for noise reduction at takeoff and approach is achieved by rotating the vanes from their partially stowed horizontal cruise position in the outer cowl to a vertical position in the inlet throat area. The maximum thickness line for the vane airfoil was chosen to coincide with the internal inlet surface to minimize seal problems when the vanes are stowed in cruise position. This leaves a portion of the vane in the inlet flow stream during cruise. If further analysis and test show that vane protrusion at cruise is a greater problem than leakage, alternate versions of the basic concept are possible. Twenty vanes having a t/c of 0.24 and a taper ratio of 6/1 are shown. The t/c and taper ratio can be reduced by increasing the number of vanes or increasing vane chord length, or both, and accepting the penalties associated with greater cowl penetration and vane protrusion in the diffuser during cruise. As configured, the desired area reduction of 27% for approach is achieved with 8.9 in. of actuation travel.

The outer cowl is of conventional skin and frame construction, with longitudinal stiffening and supports in the area of rotating vane penetration. The vanes are pivoted from cowl structure and driven by links from an actuator-driven unison ring. The actuation system shown consists of four engine-bleed-air-driven piston actuators that are also connected to racks that drive gear boxes interconnected by flex shafting for synchronization. An alternate, and perhaps preferable system, would be hydraulic actuators with transducer position feedback to transfer valves for uniform actuator position control.

Section A.4 outlines additional characteristics and provides a comparison to other concepts.

A.3.1.2 Translating Parallel Vane Sonic Inlet

Figure A-2, LO-INSP-004, shows a single-grid translating parallel vane inlet configured to the criteria outlined in section A.2. The desired throat area reduction of 27% for approach is achieved by translating the vanes 22.4 in. from their stowed cruise position in the diffuser section to the throat area of the inlet.

The outer cowl is of conventional skin and frame construction, with longitudinal stiffening and supports in the area of vane translation. The vane ends extend through slots in the cowl wall and attach rigidly to an actuator-driven unison ring that rides on slide blocks and tracks. Slot closure doors are shown as a schematic means for sealing at cruise. Smoothness and leakage elimination at cruise will be a function of how well the complex detail seal design problems are resolved. Slots are left open during approach. As in the rotating radial vane configuration, the actuation system shown consists of four pneumatic actuators with gear boxes and flexible shafting for synchronization. Here also, a preferable system could be hydraulic actuators with transducer feedback to transfer values for uniform actuator position control.

Section A.4 outlines additional characteristics and provides a comparison to other concepts.

A.3.1.3 Translating Radial Vane Sonic Inlet

Figure A-3, LO-INSP-005, shows a translating radial vane sonic inlet configured to the criteria outlined in section A.2.

The desired throat area reduction of 27% for approach is achieved when a set of radial vanes, that are positioned in the diffuser during cruise, are translated 10 in. forward to alternating positions between radial vanes that are fixed to the cowl.

The outer cowl is of conventional skin and frame construction with longitudinal stiffening and supports in the area of vane translation. The vane ends extend through slots in the cowl wall and attach to an actuator-driven unison ring that moves on slide blocks and guide rails. Sliding filler strips are shown as slot seals. As in the rotating radial and parallel vane configurations, hydrualic actuators with transducer feedback to transfer valves, for control of relative position, may be preferable to the pneumatic actuation with mechanical interconnect that is shown.

Additional characteristics are outlined in section A.4, together with a comparison to other concepts.

A.3.1.4 Expanding Radial Vane Sonic Inlet

Figure A-4, LO-INSP-007, shows an expanding radial vane sonic inlet configured to the criteria outlined in section A.2.

The desired throat area reduction of 27% is achieved when engine bleed air valving is opened to allow flow to air bags that expand inside radial vanes. Air bag pressure overcomes spring load of hinged panels that form the vanes, forcing them outward to increase the vane thickness and reduce throat area.

The outer cowl is of conventional skin and frame construction. Vane venting is required to bring spring forces to a reasonable level. As configured, the concept may have potential as a two-position device with spring forces working against stops in one position and air bag pressure against stops in the other position. Selection of midpoints using air pressure control is not feasible.

Section A.4 outlines additional characteristics and provides a comparison to other concepts.

A.3.1.5 Translating Radial Vane and Centerbody Sonic Inlet

Figure A-5, LO-INSP-008, depicts a translating radial vane and centerbody sonic inlet configured to the criteria outlined in section A.2.

The desired throat area reduction of 27% is obtained when radial vanes fixed to a centerbody are translated, with the centerbody, 20.0 in. from their cruise position in the diffuser section, to the throat area of the inlet. Part of the area change results from centerbody vane blockage of area between fixed vanes on the cowl and centerbody blockage of area in the center of the inlet at the tips of the cowl vanes.

The outer cowl is of conventional skin and frame construction, with longitudinal bridging between frames for attachment of radial vanes. Fixed fins are attached to the diffuser wall to control flow Mach number at cruise. The centerbody with its radial vanes translates on slide blocks and tracks supported by structure attached to an engine case extension with struts or IGVs. No sealing of moving parts is required except in the anti-ice system. Translation is accomplished with a single actuator using pneumatics if a two-position system is found adequate and hydraulics with transducer position feedback to a transfer valve if multiple position is necessary.

Figure A-6, LO-INSP-016, presents a possible variation of the translating radial vane and centerbody sonic inlet concept, in which the radial vanes rotate and are partially stowed in the cowl during cruise. This is similar to the rotating vane concept shown in figure A-1. It was configured as part of the overall study because of the possibility of better cruise inlet performanance with the vanes rotated out of the inlet flow. However, the study indicates that increased weight will negate inlet performance gains on a short-range STOL airplane. Therefore, there is very little, if any, benefit from the added complexity.

Section A.4 outlines additional characteristics and provides a comparison to other concepts.

A.3.2 Ring-Type Inlets

A.3.2.1 Translating Ring Sonic Inlet

Figure A-7, LO-INSP-006, shows a translating ring sonic inlet configured to the criteria outlined in section A.2.

The desired 27% area reduction is achieved by translation of a ring that is positioned outside the basic inlet, in what is normally free stream, during cruise and translated 21.3 in. aft into the throat area of the inlet for approach.

The outer cowl is of conventional skin and frame construction. The centerbody is supported by struts or IGVs from an engine case extension. The translating ring is supported by struts from a center housing that forms trackage for translation on slide blocks attached to the fixed centerbody. No sealing of moving parts is required except in the ring anti-ice system. A single pneumatic actuator will accomplish translation for a two-position system. A hydraulic actuator with transducer position feedback to a transfer valve will provide multiposition capability.

Section A.4 outlines additional characteristics and provides a comparison to other concepts.

A.3.2.2 Translating Ring and Centerbody Sonic Inlet

Figure A-8, LO-INSP-013, shows a translating ring and centerbody sonic inlet configured to the criteria outlined in section A.2.

The desired 27% area reduction is achieved by translating a ring and centerbody 21.8 in. from a cruise position in the diffuser section to a position in the inlet throat for approach.

The outer cowl is of conventional skin and frame construction. The centerbody with its strut-supported ring translates on slide blocks and tracks supported by structure attached to an engine case extension by struts. Sliding seals will be required for the centerbody and ring anti-ice system. A single pneumatic actuator will provide translation for a two-position system. A hydraulic actuator with transducer position feedback to a transfer valve will provide multiposition capability.

Figure A-9, LO-INSP-015, shows a variation of figure A-8 that utilizes a translating ring and centerbody in conjunction with a fixed ring supported from the cowl. All the comments made regarding figure A-8 apply except that translation has been reduced from 21.8 to 18.5 in.

The double ring arrangement of figure A-9 provides a method of achieving a better Mach number match of exit airflow from the separated flow paths.

Section A.4 outlines additional characteristics and provides a comparison to other concepts.

A.3.3 Articulated Radial Vane Sonic Inlet

Figure A-10, LO-INSP-014, shows an articulated radial vane sonic inlet configured to the criteria outlined in section A.2.

Area reduction is achieved by rotating two sets of radial vanes. The first set has a variable trailing edge and, when rotated, establishes a high throat Mach number for suppression. The second set has a variable leading edge and acts as a straightening vane for flow to the fan. Approximately 40° vane rotation is required to achieve the desired 27% area reduction.

The outer cowl is of conventional skin and frame construction. The radial vanes are supported by an extension of the engine case and nose dome. The vanes are rotated by cranks that are link driven from a unison ring that rotates around the engine case when actuated. A single actuator is shown that could be pneumatic for a two-position system or hydraulic with transducer position feedback to a transfer valve for multiple position.

Section A.4 outlines additional characteristics and provides a comparison to other concepts.

A.3.4 Translating Centerbody Sonic Inlet

Figure A-11, LO-INSP-001, depicts a translating centerbody sonic inlet configured to the criteria outlined in section A.2.

Throat area reduction to increase the throat Mach number for noise reduction at takeoff and approach is achieved by translating the centerbody forward from its stowed cruise position in the inlet diffuser section. The desired area reduction of 27% for approach is achieved with 27 in. of centerbody translation. It appears that further study and test could reduce this stroke.

The outer cowl is conventional skin and frame construction. The centerbody support structure is attached to an extended section of the engine case by struts or structural inlet guide vanes. The centerbody is supported vertically and horizontally by tracks that ride on structure-mounted slide blocks. The fore and aft positions of the centerbody are variable and are maintained in the position desired by a single actuator. A two-position pneumatic piston actuator is shown. However, in the final analysis, a hydraulic actuator with transfer valve and position feedback for infinite position control will more than likely be used.

Area change capability with a single actuator moving one part and minimal seal problems are the major design advantages of the translating centerbody configuration. Section A.4 outlines additional characteristics of this configuration.

A.3.5 Variable Cowl Wall Sonic Inlet

Figure A-12, LO-INSP-002, depicts a variable cowl wall sonic inlet configured to the criteria outlined in section A.2. The configuration is similar to the one tested on NASA contract NAS1-7129 and reported in document D6-60120-5.

Eight sets of two leaves are used to vary throat area. The forward leaves rotate from a fixed pivot on the forward end and are attached to the aft leaves by a moving pivot that is driven by links from an actuated unison ring. The aft ends of the aft leaves are pivoted in tracks mounted to structure. The unison ring is actuated by four ball screws that are gear-box-driven by an air rotor with the gear boxes synchronized by flex shafting. The actuation system could be simplified by using eight hydraulic actuators driving the leaves directly, with transducer feedback to transfer valves for uniform actuator position control. The outer surface of the cowl is conventional skin attached to frames. The inner surface in the area of the leaves is a combination of closure pan and leaf support beams. The support beams also form a side wall for the leaves to seal against.

Figure A-13, LO-INSP-002A, shows a variation with flexing material replacing pivot points at the inlet throat. A variable cowl wall approach to single throat sonic inlets becomes more attractive as the amount of required throat area variation increases. Section A.4 outlines additional characteristics.

A.4 COMPARATIVE EVALUATION

Figure A-14 presents a matrix of design considerations for comparison of the multipassage sonic inlets briefly described in section A.3 and depicted in figures A-1 through A-9. The inlets are categorized for comparative purposes as vane-type and ring-type inlets, with the articulated vane inlet a separate category.

Areas of significant differences for vane-type inlets (figs. A-1 through A-5) are tabulated in table A-1. Table A-2 is a tabulation of areas of significant differences for ring-type inlets, (figs. A-7 and A-8).

Figure A-15 presents a matrix of design considerations for comparison of a translating centerbody sonic inlet (fig. A-11) and a variable cowl wall sonic inlet (fig. A-12). Areas of significant differences are tabulated in table A-3, with preferences indicated.

A.4.1 Vane-Type Sonic Inlets

The translating radial vane and centerbody configuration (fig. A-5) provides the best vane-type sonic inlet with regard to structure, mechanism, seal requirements, actuation, control, smoothness, bird-strike vulnerability, leakage, and cruise flow restrictions. The other vane-type inlets have some advantages; however, their overall complexity in conjunction with minimum benefits make the translating radial vane and centerbody the obvious choice of the vane-type configurations evaluated.

A.4.2 Ring-Type Sonic Inlets

The translating ring and centerbody configuration (fig. A-8 or A-9) is considered the best of the two ring-type sonic inlets due to superior characteristics with regard to lines, range of application, angle-of-attack sensitivity, flow passage Mach number mismatch, and cruise flow restrictions.

A.4.3 Articulated Radial Vane Sonic Inlet

This configuration (fig. A-10) represents a unique type and is thus difficult to compare directly to the vane- and ring-type sonic inlets without additional analysis and test to more clearly define the design requirements. Estimates at this point indicate that there may be some weight penalty. However, this cannot be established without additional analysis and test development work to better define vane shape, size, and number.

Split vanes with rotation of leading and trailing edges, as shown on figure A-10, are a possible solution to the large performance losses expected from a leading edge angle of incidence of 40°. Rotation of a single vane as in the alternate concept shown in detail I on figure A-10 would be preferable from a mechanical design viewpoint but is subject to the noted losses.

The concept has potential from a design standpoint, and model testing to determine noise suppression capability and performance is in order.

A.4.4 Translating Centerbody Sonic Inlet

The translating centerbody configuration will provide a better design with respect to contour lines, smoothness, mechanism, sealing, actuation and control, vulnerability to bird strike, and installation of acoustic material.

A.4.5 Variable Cowl Wall Sonic Inlet

The variable cowl wall appears to have an advantage if larger throat area changes are required, but final determination is subject to review of inlet length, diffusion angles, and possibility of boundary layer control requirements on the particular configuration under consideration.

A.5. CONCLUSIONS AND COMMENTS

On the basis of comparisons presented in section A.4, it is concluded that a radial vane and translating centerbody configuration of the type shown in figure A-5 provides the best mechanical design approach of the vane-type sonic inlets studied. It is further concluded that use of a translating centerbody in conjuntion with rings provides the best mechanical design approach of the ring-type sonic inlets studied.

In addition to the comparative considerations presented in section A.4, there is a basic geometry consideration that favors centerbody-type configurations. This applies to any sonic inlet that requires stowage of blockage material in the diffuser section when high Mach number throat flow for suppression is not desired. A centerbody is a natural extension of the engine hub and must be there in some form to divert the cylindrical inlet flow to annular fan flow This hub area is a natural location for stowage of blockage material, and if it is not utilized the outer diffuser surface must be expanded to provide stowage area elsewhere. Outer surface expansion will require greater inlet length or steeper diffusion angles, or both.

The probability for success in design of a good sonic inlet is also enhanced to some extent when engine fan hub/tip ratio increases because a larger hub provides a larger area for stowage of blockage material.

The articulated radial vane approach to a sonic inlet has been considered and evaluated within the limits of available data. Additional testing and analysis are required to better define design parameters. However, this approach to a sonic inlet appears feasible and does have potential from a mechanical design standpoint.

The conclusions noted are made specifically for inlets configured to the criteria outlined in section A.2. It is important to note, however, that for different design criteria other conclusions could be made. This is particularly true if larger area changes are required. Increased area change requires increased centerbody translation, and at some point the amount of translation will become prohibitive and one would choose the variable cowl wall concept or continue the search for another approach.

Idealized inlet lines have been used in these studies for comparative purposes. Analysis and testing of shorter translating centerbody inlets should be completed to establish the best weight/performance trade prior to finalization of inlet lines. Figure A-16, LO-INSP-010, and figure A-17, LO-INSP-011, showing inlet lines with length/diameter ratios of 1.0 and 1.2, respectively, are included to emphasize the potential benefits of shorter inlets. It is estimated that a weight reduction from 480 to 370 lb is possible if the L/D of 1.4 shown in figure A-11 is reduced to the L/D of 1.0 shown in figure A-16.

TABLE A-1.—SIGNIFICANT DIFFERENCES—VANE-TYPE SONIC INLETS[a]

Area of significant difference	Configuration				
	1 Rotating radial vanes	2 Translating parallel vanes	3 Translating radial vanes	4 Expanding radial vanes	5 Translating radial vane and centerbody
Basic design					
A. Lines				+	
B. Structure					+
C. Mechanism					+
D. Seals					+
Actuation					+
Control					+
Smoothness					+
Bird Strike					+
Anti-ice system				+	
Performance concerns					
A. Leakage					+
B. Angle-of-attack sensitivity	+	+	+	+	
C. Flow passage Mach No. mismatch	+		+	+	
D. Cruise flow restrictions					+

[a]For use with figure A-14

TABLE A-2.–SIGNIFICANT DIFFERENCES–RING-TYPE SONIC INLETS[a]

Area of significant difference	Configuration	
	6 Translating ring	7 Translating ring and centerbody
Basic design		
A. Lines		+
E. Range of application		+
Performance concerns		
B. Angle-of-attack sensitivity		+
E. Diffusion angle	+	
G. Flow passage Mach No. mismatch		+
H. Cruise flow restrictions		+

[a]For use with figure A-14

TABLE A-3.–SIGNIFICANT DIFFERENCES–SINGLE-PASSAGE SONIC INLET

Area of significant difference	Translating centerbody	Variable cowl wall
Basic design:		
A. Lines	+ (Approach)	
C. Mechanism	+	
D. Seals	+	
E. Range of application		+
Actuation	+	
Control	+	
Smoothness	+	
Bird strike	+	
Acoustic treatment	+	

The variable cowl wall appears to have an advantage if larger throat area variations are required, because movement of the larger outer perimeter surface areas will provide the greatest throat area variation with the least motion. However, a longer inlet or steeper diffusion angles with a boundary layer control system might be required, and the impact should be evaluated prior to a configuration selection.

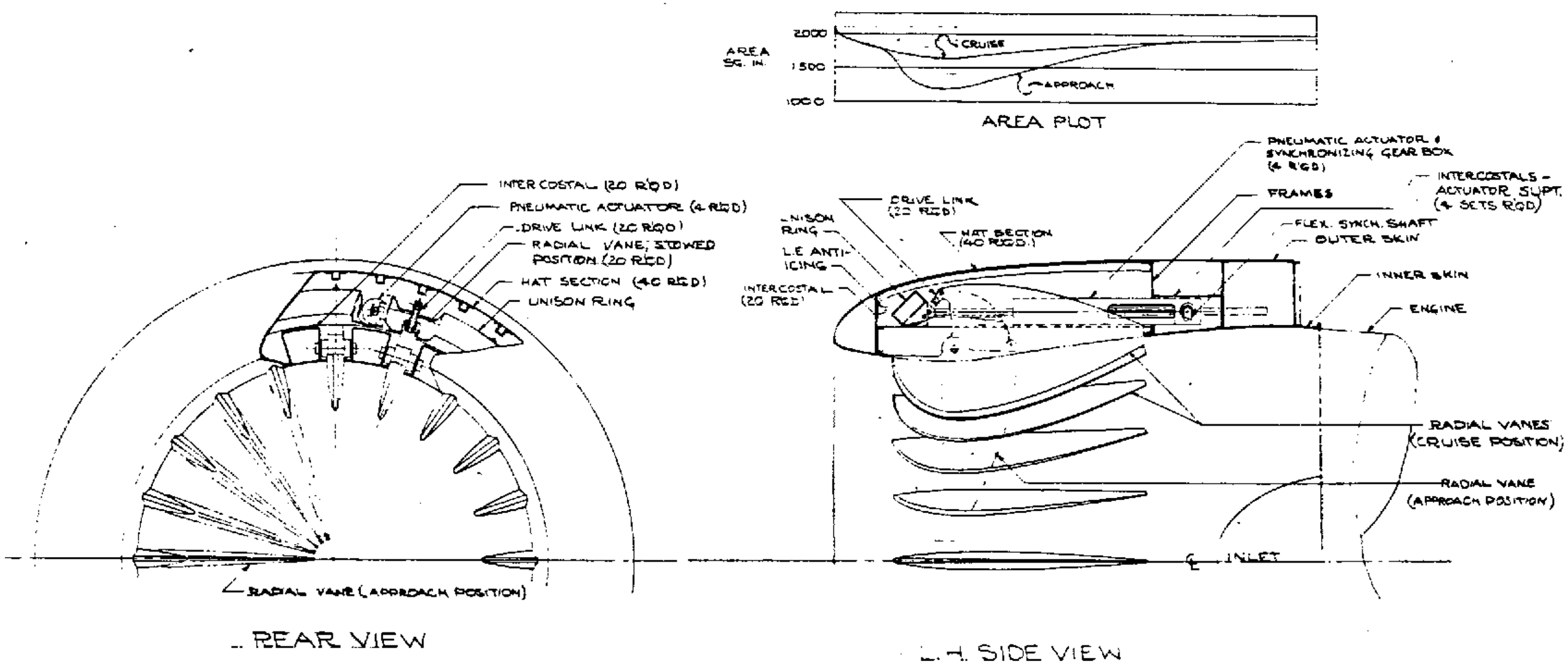

FIGURE A-1.—LO-INSP-003—ROTATING RADIAL VANE SONIC INLET

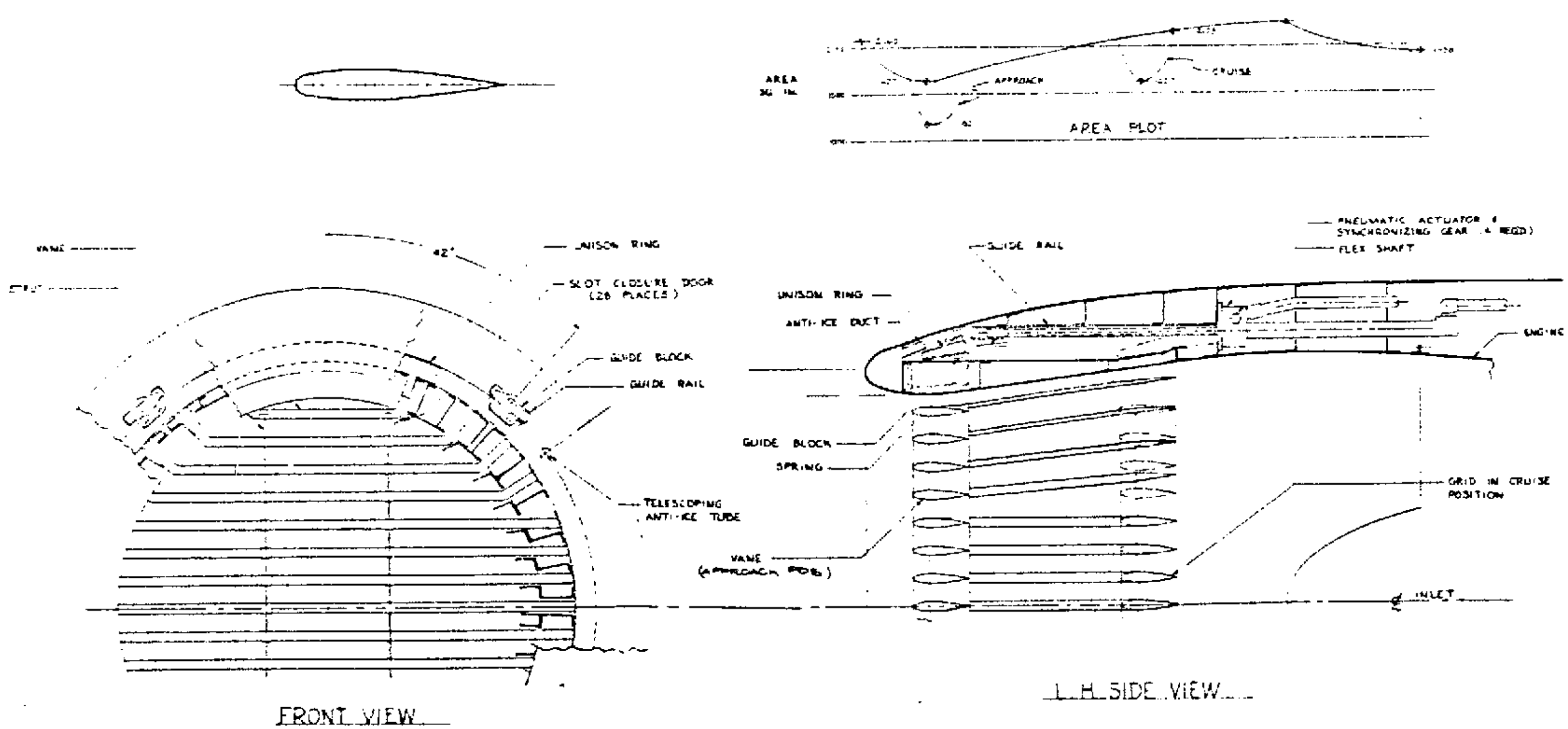

FIGURE A-2.—LO-INSP-004—TRANSLATING PARALLEL VANE SONIC INLET

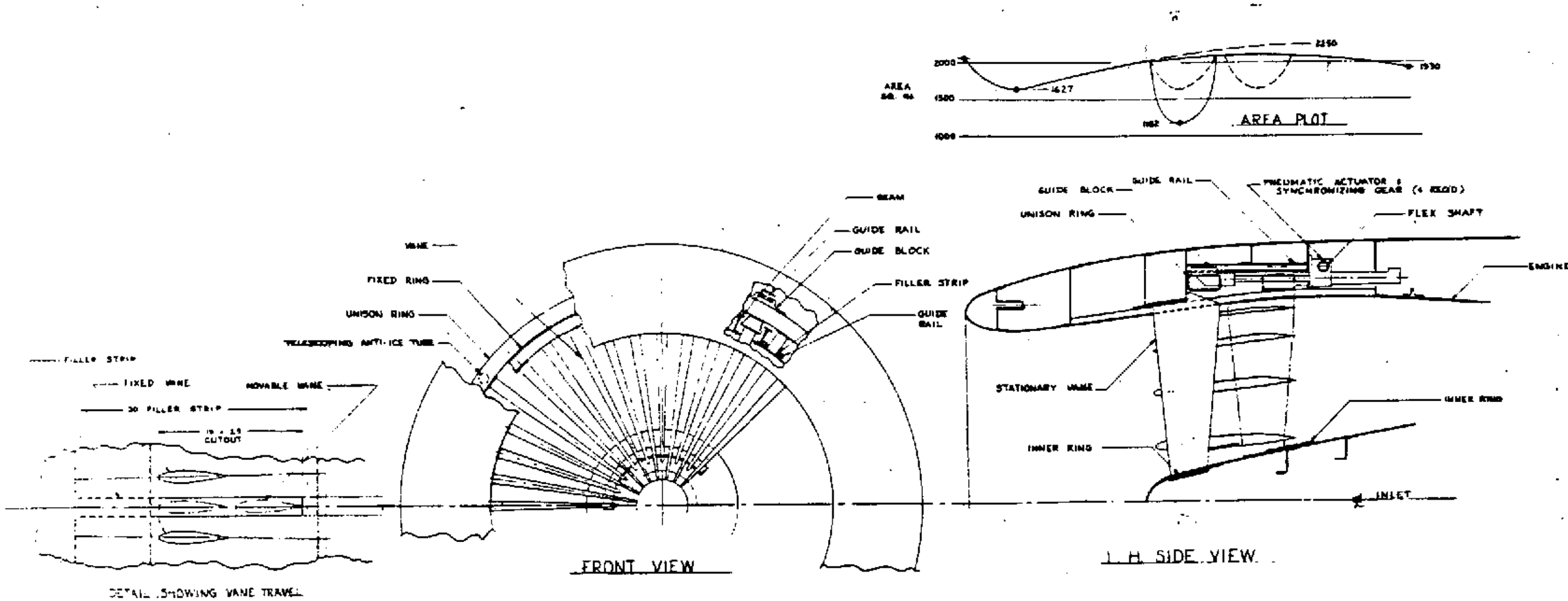

FIGURE A-3.—LO-INSP-005—TRANSLATING RADIAL VANE SONIC INLET

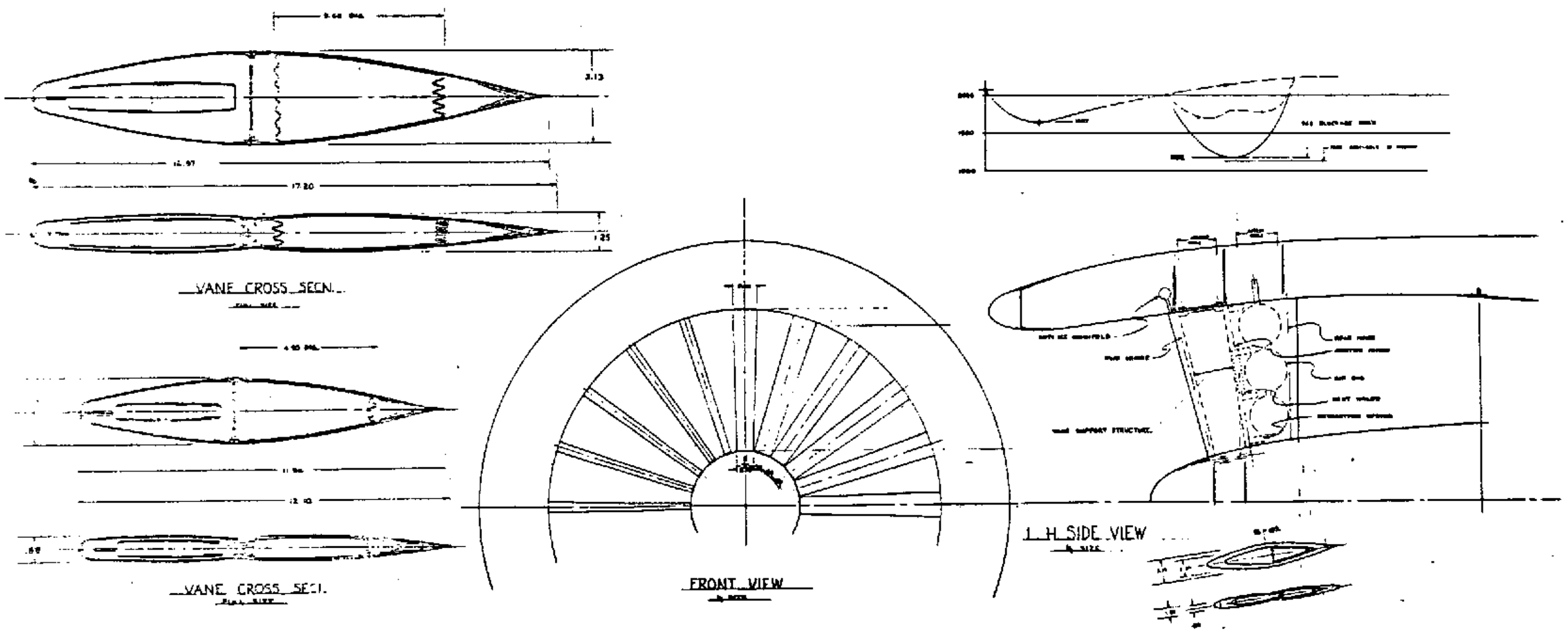

FIGURE A-4.—LO-INSP-007—EXPANDING RADIAL VANE SONIC INLET

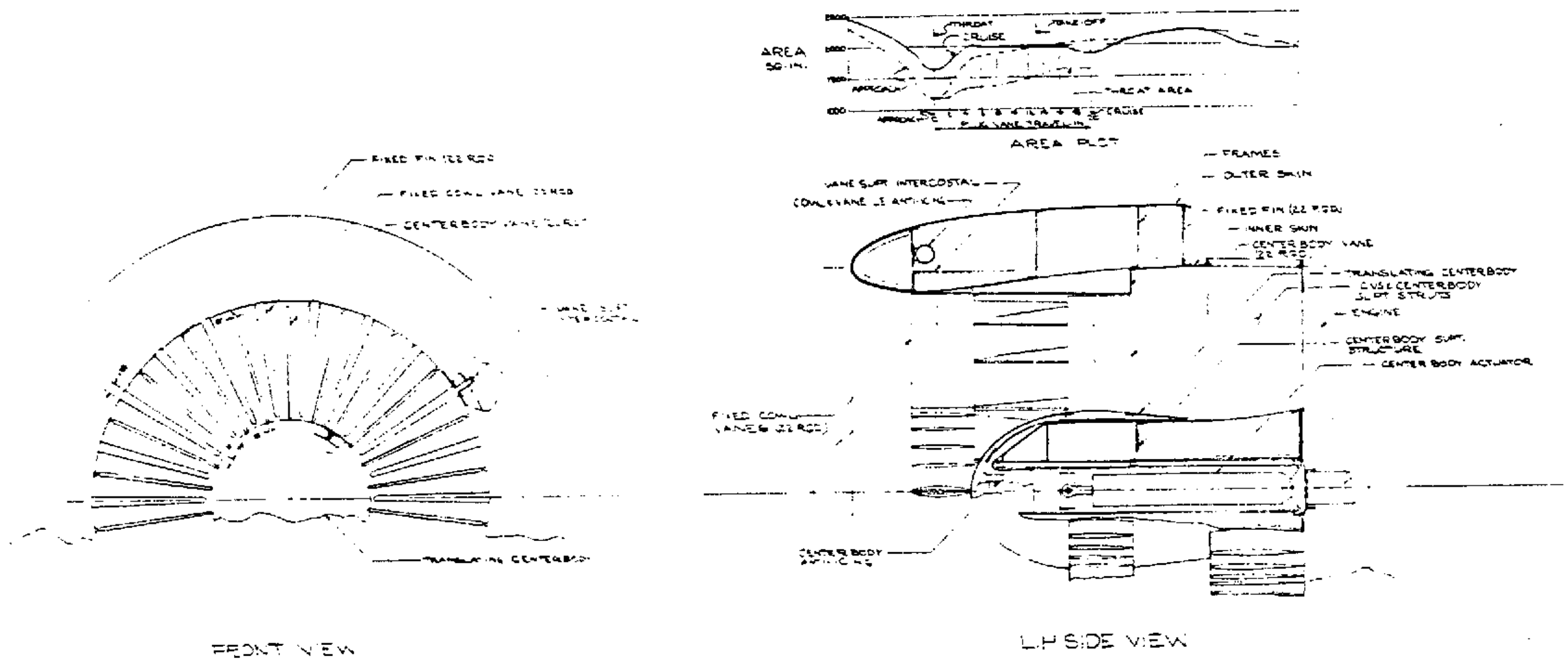

FIGURE A-5.—LO-INSP-008—TRANSLATING RADIAL VANE AND CENTERBODY SONIC INLET

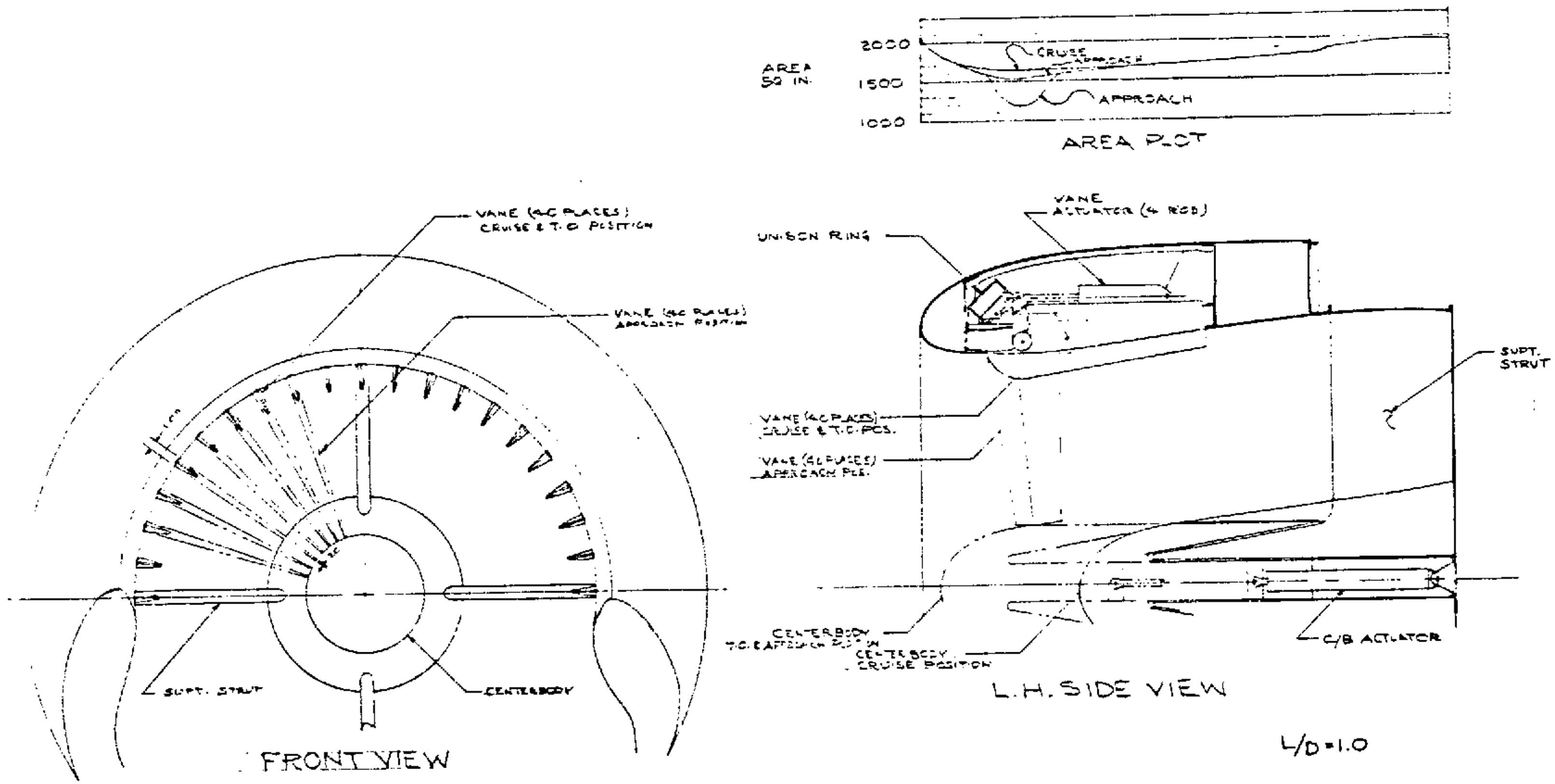

FIGURE A-6.—LO-INSP-016—TRANSLATING CENTERBODY AND ROTATING RADIAL VANE SONIC INLET

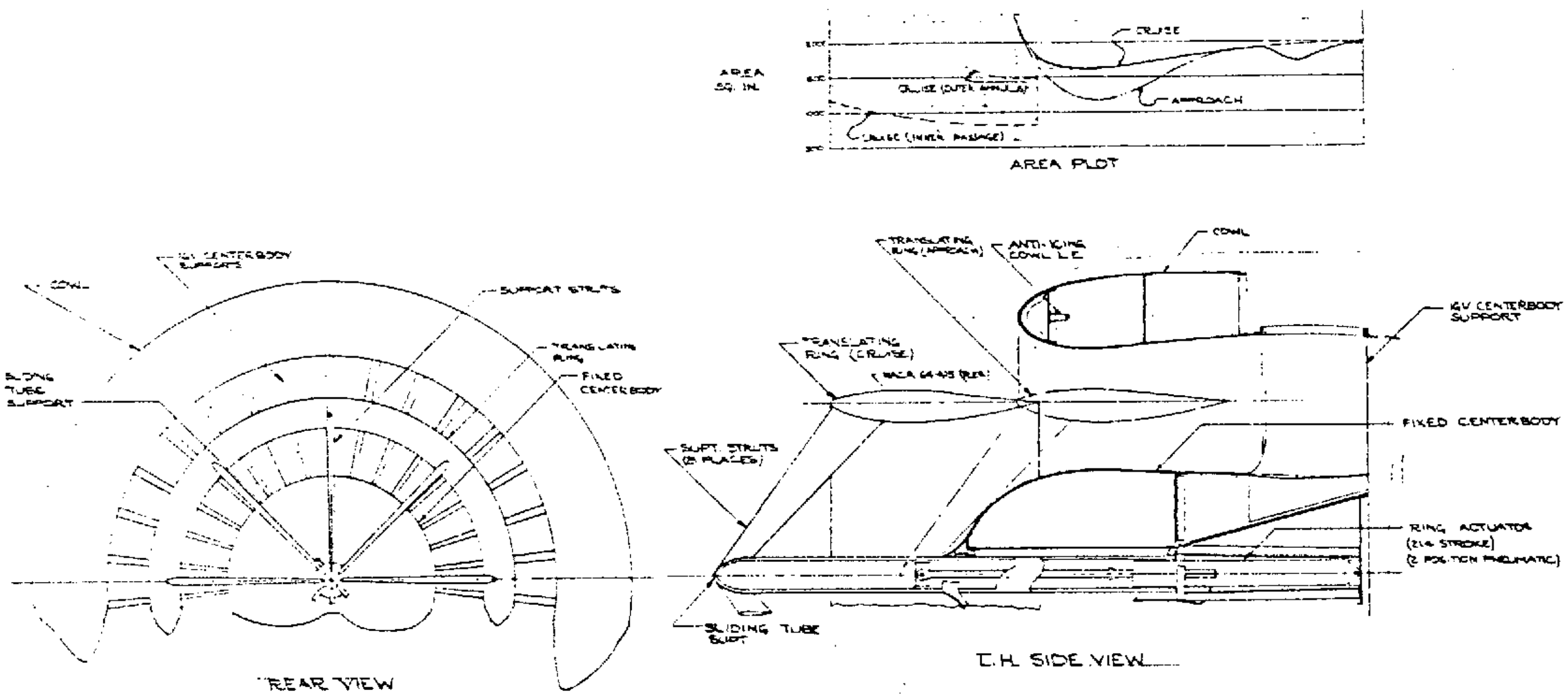

FIGURE A-7.—LO-INSP-006—TRANSLATING RING SONIC INLET

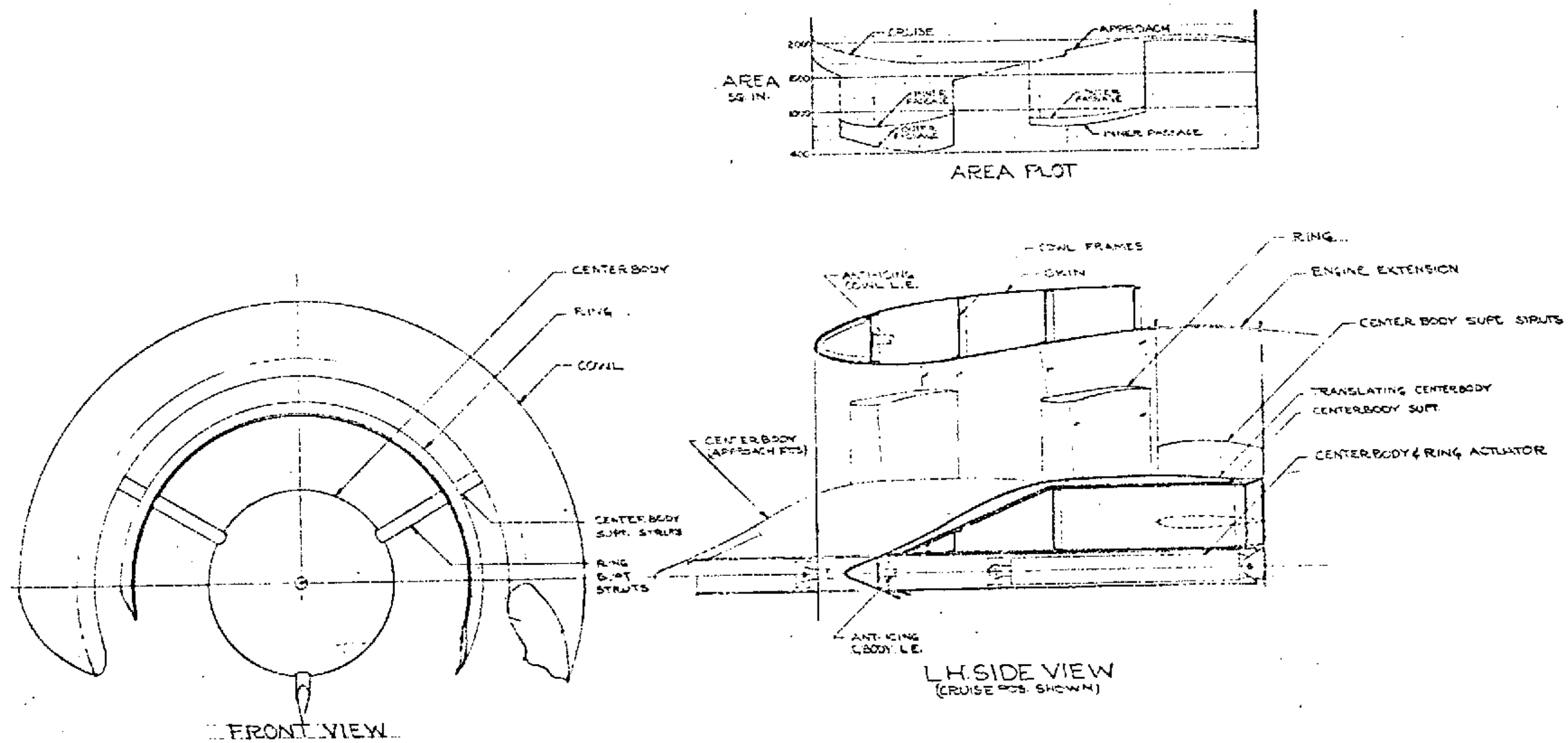

FIGURE A-8.—LO-INSP-013—TRANSLATING RING AND CENTERBODY SONIC INLET

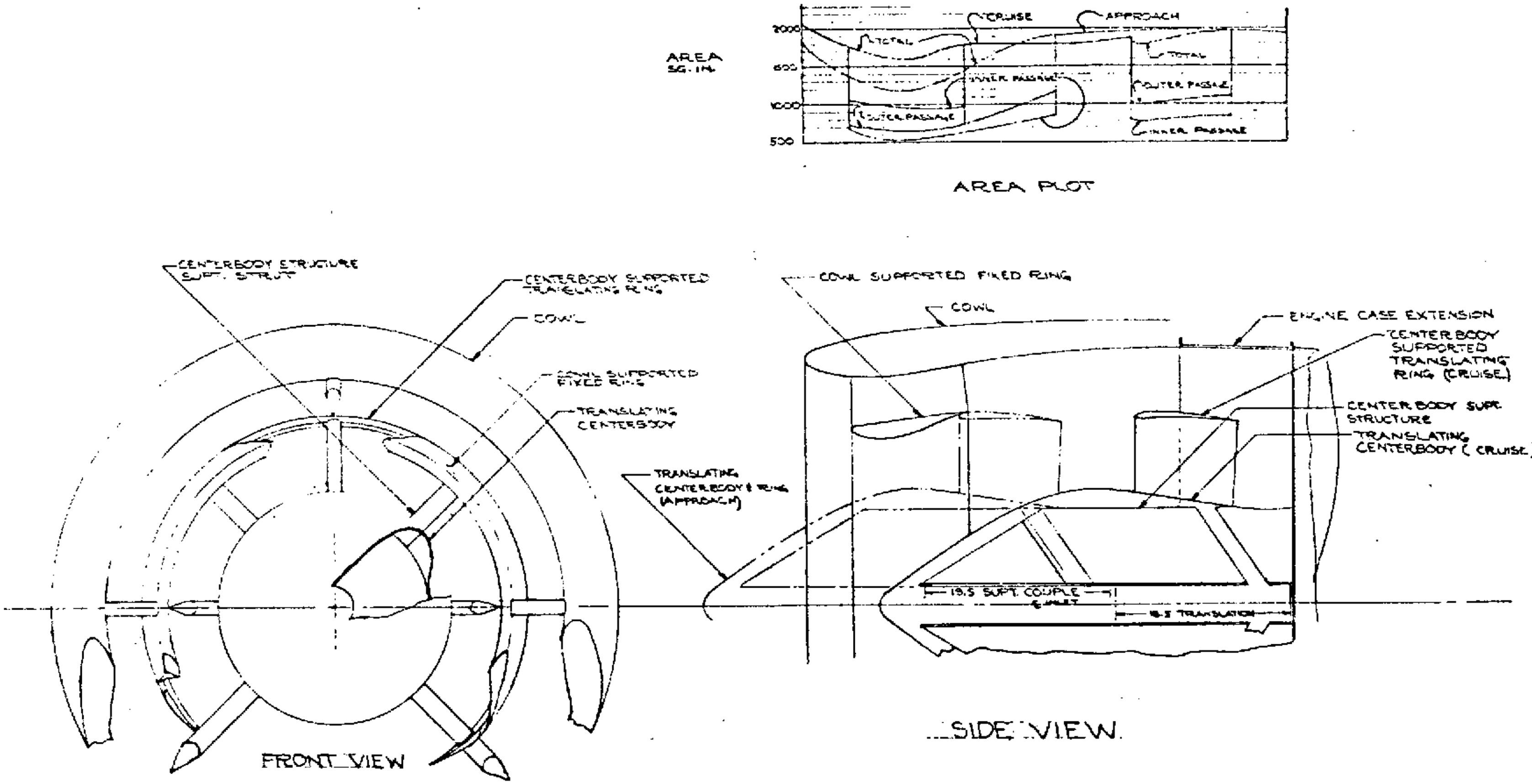

FIGURE A-9.—LO-INSP-015—TRANSLATING RING AND FIXED RING SONIC INLET

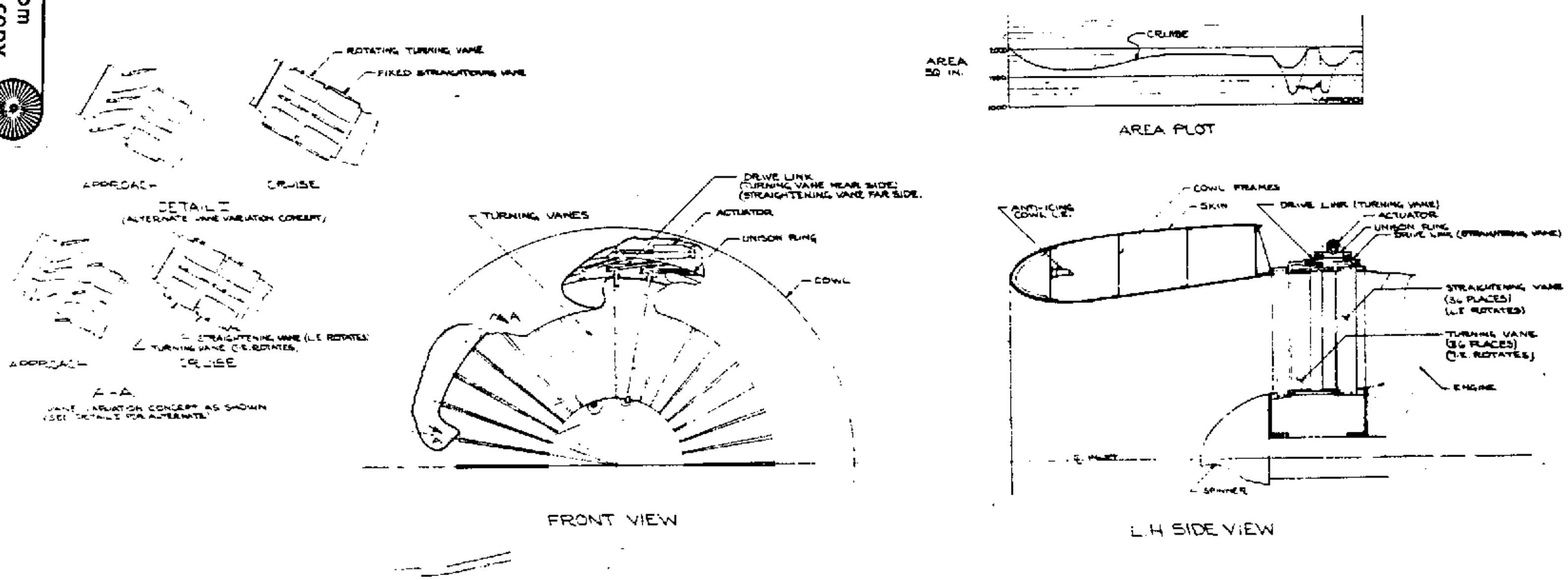

FIGURE A-10.—LO-INSP-014—ARTICULATED RADIAL VANE SONIC INLET

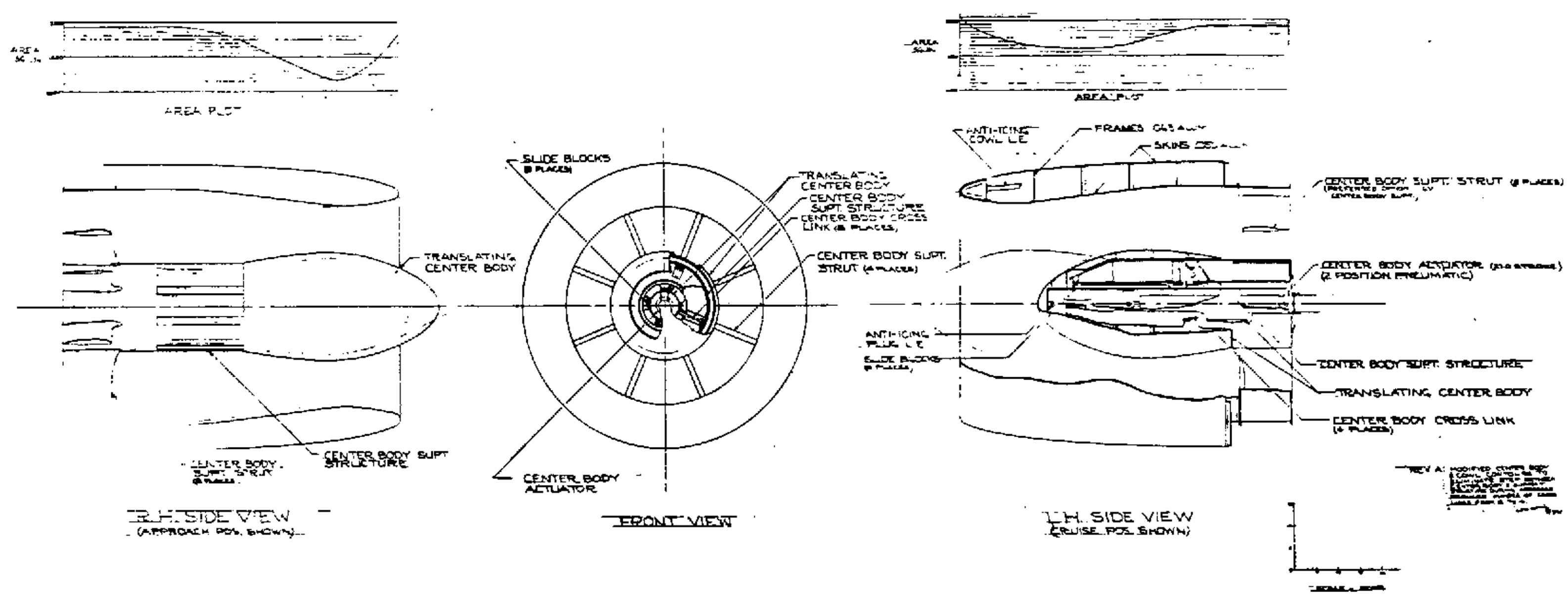

FIGURE A-11.—LO-INSP-001—TRANSLATING CENTERBODY SONIC INLET

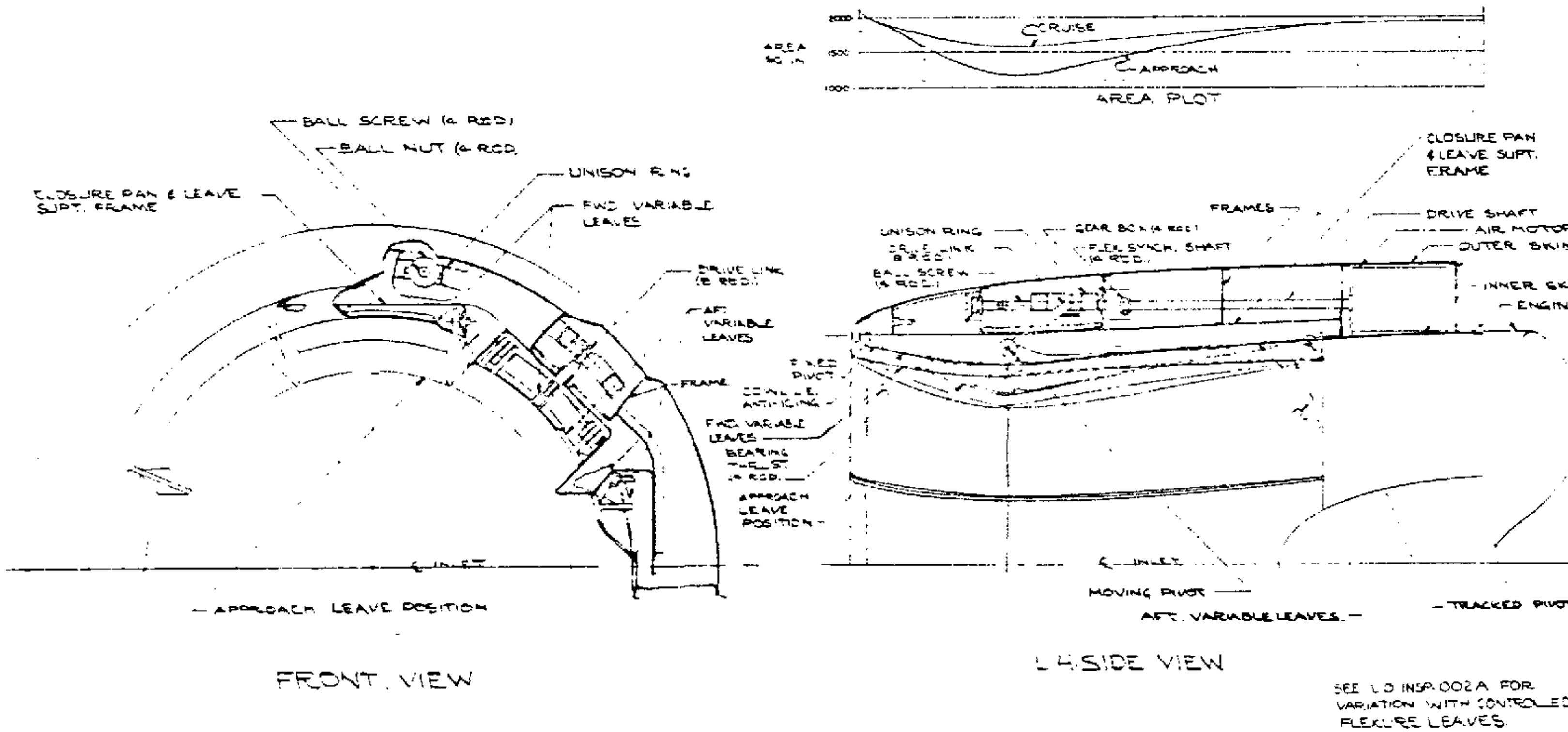

FIGURE A-12.—LO-INSP-002—VARIABLE COWL WALL SONIC INLET

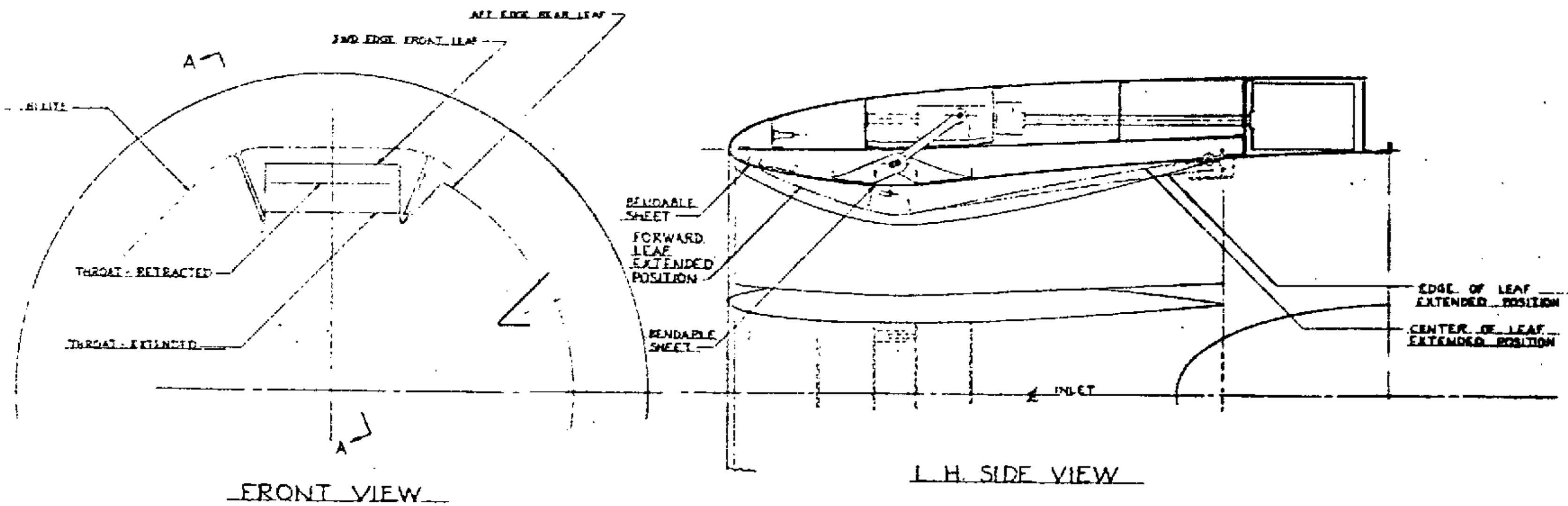

FIGURE A-13.—LO-INSP-002A—VARIABLE COWL WALL SONIC INLET USING FLEXING MATERIAL

Rotating Radial Vanes (1)

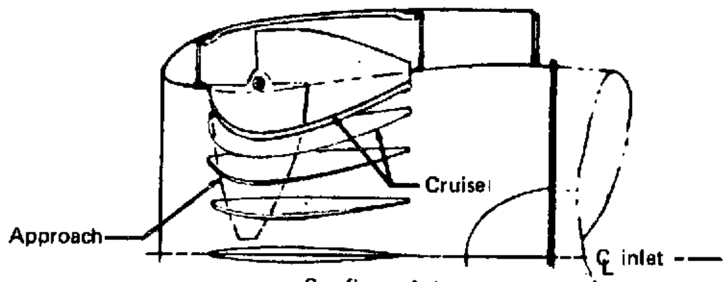

See figure A-1

Design Consideration		Rotating Radial Vanes (1)
Basic design	Lines	Good area progression; vane and actuation stowage influences shape of exterior lines; L/D = 1.05
	Structure	Conventional skin and frame cowl with longitudinal stiffening and support in area of vane penetration
	Mechanism	Actuator-driven unison ring driving links to rotating vanes
	Seals	30.0 in. of seal required around each vane; relatively simple for cruise-only seal, complex otherwise
	Range of application	Larger area changes can be achieved by adding vanes and cowl compromise
Actuation	Power source	Engine bleed air for two-position; pneumatic system hydraulic pump for multiple position
	Type of actuation	Pneumatic or hydraulic piston
	Load and stroke	Load ≈ 2400 lb; stroke = 8.9 in.
	Synchronization	Mechanical load limit or position feedback control
	Failsafe potential	Pressure loads tend to move vanes toward open throat position; balance point not established
Control	Two position	
	Multiple position	Electronic input to electromechanical transfer valve nulled by a linearly variable differential transducer position feedback with position selected as a function of engine rpm and total pressure at the fan face
Weight estimate (lb)		Basic cowl 236.0 Nose dome 10.0 Radial vanes 74.0 Actuation and control 96.0 Anti-icing system 78.0 Total inlet 494.0 Engine penalty 48.0 Total 542.0
Smoothness		Exposed slots in cowl wall during approach (can be minimized or eliminated with added complexity)
Bird strike		Shock-absorbing linkage or beef-up required
Anti-icing system		Complicated multiple routing to vanes
Performance concerns	Leakage	Minimum at cruise: a concern in other positions
	Angle-of-attack sensitivity	Comparable to current inlets
	Distortion	Radial wakes (circumferential distortion)
	Diffusion angle	7.5° (good)
	Vane airfoil	T/C = 0.14; taper ratio = 6/1 (add vanes to decrease) (T/C = thickness/chord)
	Flow passage Mach no. mismatch	Minimal
	Cruise flow restrictions	Vanes protrude in flow path
Acoustic potential		Has potential of flow choking and lining of vanes and cowl wall

FIGURE A-14.—EVALUATION CHART—MULTIPLE THROAT SONIC INLETS

Design Consideration		Translating Parallel Vanes (2)
		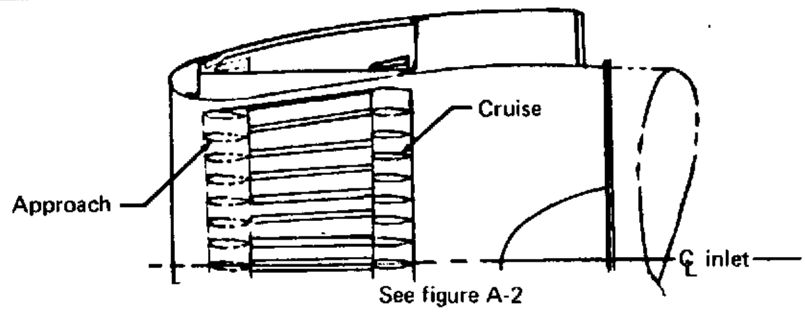
Basic design	Lines	Vane support and actuation could influence shape of external lines; L/D = 1.1
	Structure	Conventional skin and frame cowl with longitudinal bridging in area of vane penetration
	Mechanism	Vanes attached to actuator-driven unison ring
	Seals	Difficult and complex seal design required for vane penetration slot closure
	Range of application	Limited by the amount of diffuser expansion possible for vane stowage; diffusion angle or inlet length and vane translation would increase
Actuation	Power source	Same as (1)
	Type of actuation	Same as (1)
	Load and stroke	Load ≈ 800 lb; stroke = 22.4 in.
	Synchronization	Same as (1)
	Failsafe potential	Friction forces will probably counteract pressure forces, and vanes will remain in position last called for if actuation fails
Control	Two position	
	Multiple position	Same as (1)
Weight estimate (lb)		Basic cowl 184.0 Nose dome 10.0 Vanes 43.0 Actuation and control 58.0 Anti-icing system 59.0 Total inlet 390.0 Engine penalty 37.0 Total 427.0
Smoothness		Open slots in cowl wall during approach; smoothness at cruise will be a function of how well a difficult seal design problem is resolved
Bird strike		Shock-absorbing support plus vane beef-up required
Anti-icing system		Complicated routing to multiple translating vanes
Performance concerns	Leakage	Function of seal design at cruise; concern in other positions
	Angle-of-attack sensitivity	Same as (1)
	Pressure recovery	Same as (1)
	Distortion	Complicated distortion pattern
	Diffusion angle	Same as (1)
	Vane airfoil	T/C = 0.167
	Flow passage Mach no. mismatch	Vanes adjacent to cowl could be a problem
	Cruise flow restrictions	Stowed vanes create a second throat
Acoustic potential		Same as (1)

FIGURE A-14.—Continued

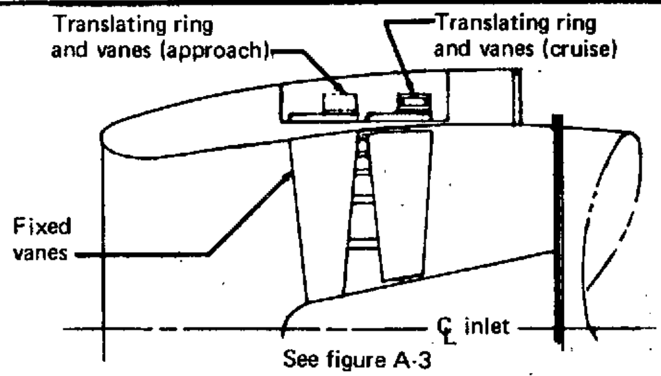

Design Consideration		Translating Radial Vanes (3)
Basic design	Lines	External lines could be affected as in (2); L/D = 1.1
	Structure	Same as (2)
	Mechanism	Same as (2)
	Seals	Vane penetration sealing similar to (2); not quite as difficult
	Range of application	Same limitations as (2)
Actuation	Power source	Same as (1)
	Type of actuation	Same as (1)
	Load and stroke	Load ≈ 600 lb; stroke = 10.0 in.
	Synchronization	Same as (1)
	Failsafe potential	Same as (2)
Control	Two position	
	Multiple position	Same as (1)
Weight estimate (lb)		Basic cowl 248.0 Nose dome 12.0 Radial vanes 67.0 Actuation and control 60.0 Anti-icing system 64.0 Total inlet 451.0 Engine penalty 45.0 Total 496.0
Smoothness		Same as (2)
Bird strike		Same as (2)
Anti-icing system		Same as (2)
Performance concerns	Leakage	Similar to (2)
	Angle-of-attack sensitivity	Same as (1)
	Pressure recovery	Same as (1)
	Distortion	Same as (1)
	Diffusion angle	Same as (1)
	Vane airfoil	T/C = 0.16
	Flow passage Mach no. mismatch	Same as (1)
	Cruise flow restrictions	Same as (2)
Acoustic potential		Same as (1)

FIGURE A-14.—Continued

Design Consideration		Expanding Radial Vanes (4)
		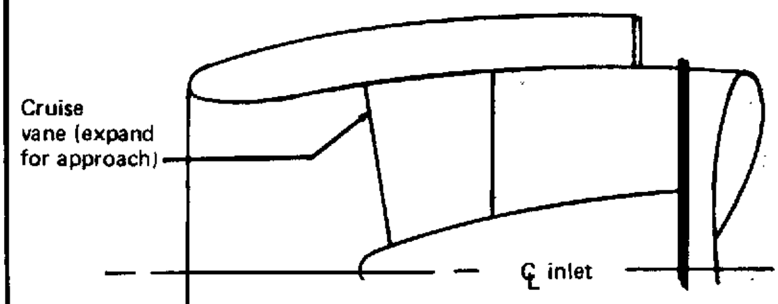 See figure A-4
Basic design	Lines	Good area progression; L/D = 1.2
	Structure	Conventional skin and frame cowl
	Mechanism	Vane panels hinged for expansion and spring loaded to the collapsed cruise position
	Seals	Required at vane ends
	Range of application	Same limitations as (2)
Actuation	Power source	Engine bleed air
	Type of actuation	Pneumatic diaphrams and spring returns
	Load and stroke	Load ≈ 450 lb vane; stroke = 1.6 in.
	Synchronization	None; vane expansion will vary with ability to provide uniform airflow
	Failsafe potential	Vanes go to cruise position with loss of pneumatic power
Control	Two position	Electrical signal to air valve
	Multiple position	No positive way to control
Weight estimate (lb)		Basic cowl 186.0 Nose dome 17.0 Radial vanes and actuation and control 110.0 Anti-icing system 66.0 Total inlet 379.0 Engine penalty 34.0 Total 413.0
Smoothness		Depression in vane cross section at cruise
Bird strike		Can be handled structurally
Anti-icing system		Can be accomplished with fixed plumbing
Performance concerns	Leakage	Not as big a problem as (1), (2), and (3)
	Angle-of-attack sensitivity	Same as (1)
	Pressure recovery	Same as (1)
	Distortion	Same as (1)
	Diffusion angle	Same as (1)
	Vane airfoil	Cruise T/C = 0.073; approach T/C = 0.185
	Flow passage Mach no. mismatch	Same as (1)
	Cruise flow restrictions	Less restriction than (1), (2), and (3)
Acoustic potential		Acoustic material on vanes would have less area and be less effective than (1), (2), and (3)

FIGURE A-14.—Continued

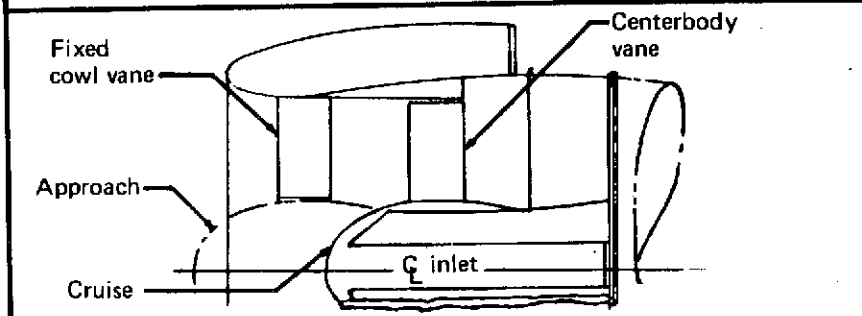

See figure A-5

Design Consideration		Translating Radial Vane and Centerbody (5)
Basic design	Lines	Good area progression; L/D = 1.07
	Structure	Conventional skin and frame outer cowl with centerbody supported by IGVs or struts
	Mechanism	Actuator-driven centerbody translating on slide blocks and tracks
	Seals	None required
	Range of application	Same limitations as (2)
Actuation	Power source	Same as (1)
	Type of actuation	Same as (1)
	Load and stroke	Load ≈ 3500 lb; stroke = 20.0 in.
	Synchronization	None required (single actuator)
	Failsafe potential	Plug venting or locking devices required to counteract adverse pressure loads
Control	Two position	
	Multiple position	Same as (1)
Weight estimate (lb)		Basic cowl 140.0 Translating centerbody 38.0 IGV modification or centerbody 34.0 Support struts centerbody support structure 69.0 Vanes 88.0 Actuation and control 20.0 Anti-icing system 75.0 Total inlet 464.0 Engine penalty 32.0 Total 496.0
Smoothness		No surface roughness anticipated
Bird strike		Can be handled structurally
Anti-icing system		Outer cowl leading edge comparable to existing inlets; telescopic routing to centerbody and vane leading edges required
Performance concerns	Leakage	Not a problem
	Angle-of-attack sensitivity	Centerbody extension at approach could create adverse flow conditions
	Pressure recovery	Same as (1)
	Distortion	Same as (1)
	Diffusion angle	Same as (1)
	Vane airfoil	Maximum T/C = 0.09
	Flow passage Mach no. mismatch	Diffusion angles differ on sides of flow passages at approach
	Cruise flow restrictions	Stowed vanes disrupt diffusion
Acoustic potential		Same as (1) plus centerbody lining is also possible

FIGURE A-14.—Continued

Design Consideration		Translating Ring (6)
		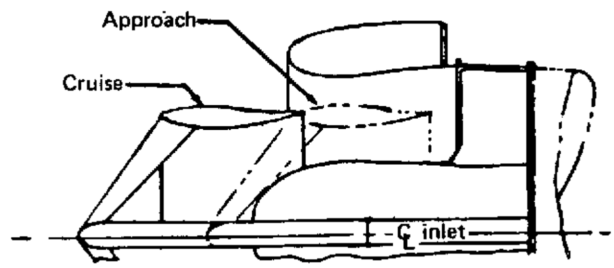 See figure A-7
Basic design	Lines	Achievement of good area progression is complicated by shape and position of ring; $L/D_{cowl} = 0.75$, $L/D_{ring} = 1.14$
	Structure	Conventional skin and frame outer cowl with centerbody and ring supported by IGVs or struts
	Mechanism	Actuator-driven centerbody translating on slide block and tracks
	Seals	None required
	Range of application	Larger area changes can be achieved by increased ring size and cowl length
Actuation	Power source	Same as (1)
	Type of actuation	Same as (1)
	Load and stroke	Load ≈ 2000 lb; stroke = 21.3 in.
	Synchronization	Same as (5)
	Failsafe potential	Will probably stay in last position called for if actuator fails
Control	Two-position	
	Multiple position	Same as (1)
Weight estimate (lb)		Basic cowl 91.0 Translating ring 50.0 Fixed centerbody 66.0 Ring support 33.0 IGV modification or struts 34.0 Actuation and control 20.0 Anti-icing system 75.0 Total inlet 369.0 Engine penalty 30.0 Total 399.0
Smoothness		No major surface roughness anticipated
Bird strike		Can be handled structurally
Anti-icing system		Outer cowl comparable to existing inlets; telescopic routing to translating centerbody and ring required
Performance concerns	Leakage	Not a problem
	Angle-of-attack sensitivity	Could be a major problem
	Pressure recovery	Same as (1)
	Distortion	Circumferential wake (radial distortion)
	Diffusion angle	5.5°
	Vane airfoil	NACA 64-415
	Flow passage Mach no. mismatch	Positioning ring to match exit Mach numbers from flow passages at both cruise and approach will be a problem
	Cruise flow restrictions	Ring and support struts in freestream
Acoustic potential		Has potential for choking plus acoustic material on ring, cowl, and centerbody

FIGURE A-14.—Continued

Design Consideration		Translating Ring and Centerbody (7)
		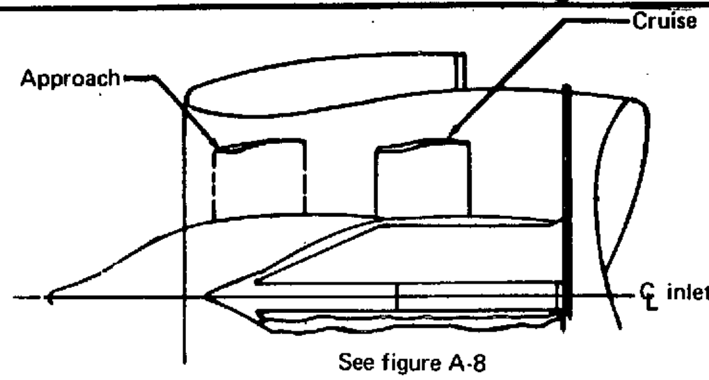 See figure A-8
Basic design	Lines	Same as (6) except L/D = 0.95
	Structure	Conventional skin and frame outer cowl with centerbody supported by IGVs or struts
	Mechanism	Same as (6)
	Seals	None required
	Range of application	Larger area changes possible by increasing cowl length and translation
Actuation	Power source	Same as (1) and (6)
	Type of actuation	Same as (1) and (6)
	Load and stroke	Load ≈ 3500 lb; stroke = 21.8 in.
	Synchronization	Same as (5)
	Failsafe potential	Same as (6)
Control	Two position	
	Multiple position	Same as (1)
Weight estimate (lb)		Basic cowl 126.0 Translating centerbody 55.0 IGV modification or support struts 34.0 Centerbody support structure 70.0 Actuation and control 22.0 Anti-icing system 65.0 Total inlet 387.0 Engine penalty 20.0 Total 407.0
Smoothness		Same as (6)
Bird strike		Same as (6)
Anti-icing system		Same as (6)
Performance concerns	Leakage	Not a problem
	Angle-of-attack sensitivity	Less cause for concern than (6)
	Pressure recovery	Same as (1)
	Distortion	Same as (6)
	Diffusion angle	9.5°
	Vane airfoil	T/C = 0.08
	Flow passage Mach no. mismatch	Similar problem but to a lesser degree than (6)
	Cruise flow restrictions	Ring and support struts in diffuser
Acoustic potential		Same as (6)

FIGURE A-14.—Continued

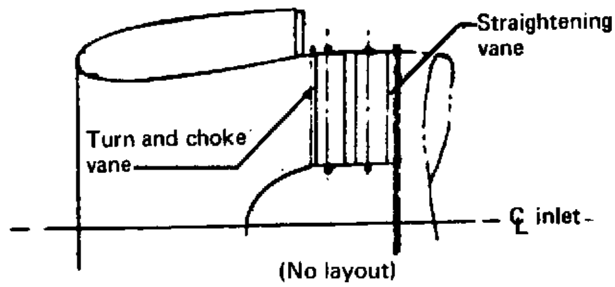

Design Consideration		Variable Inlet Guide Vanes 8
Basic design	Lines	Comparable to current inlets; L/D = 0.94
	Structure	Conventional skin and frame outer cowl with engine case and shaft extended for vane support
	Mechanism	Actuator-driven unison ring that rotates around engine driving links that rotate vanes
	Seals	72 rotary seals required as configured
	Range of application	A Mach 0.80 throat requires close to limit vane turning of 40°
Actuation	Power source	Same as 1
	Type of actuation	Same as 1
	Load and stroke	Load ≈ 1500 lb; stroke = 2.04 in.
	Synchronization	Same as 5
	Failsafe potential	Vane pivot points should be forward of center of pressure for vanes to trail in failsafe position (see detail I on LO-INSP-014)
Control	Two position	
	Multiple position	Same as 1
Weight estimate (lb)		Basic cowl 111.0 Engine case extension 49.0 IGVs 230.0 Vane support hub 19.0 Shaft extension and spinner 15.0 Actuation and control 54.0 Anti-icing system 56.0 Total inlet 535.0 Engine penalty 12.0 Total 547.0
Smoothness		Surface imperfections will occur at vane ends due to rotation within curved surfaces
Bird strike		Bird strike with vanes at 40°rotation could be difficult to handle
Anti-icing system		Outer cowl comparable to existing inlets; vane leading edge requires multiple complex routing
Performance concerns	Leakage	Not a problem
	Angle-of-attack sensitivity	Comparable to current inlets
	Pressure recovery	Unknown
	Distortion	Same as 1
	Diffusion angle	7.7°
	Vane airfoil	T/C = 0.087
	Flow passage Mach no. mismatch	Not a problem from an area standpoint
	Cruise flow restrictions	IGVs in diffuser
Acoustic potential		Same as 1

FIGURE A-14.—Concluded

Design Consideration		Translating Centerbody
		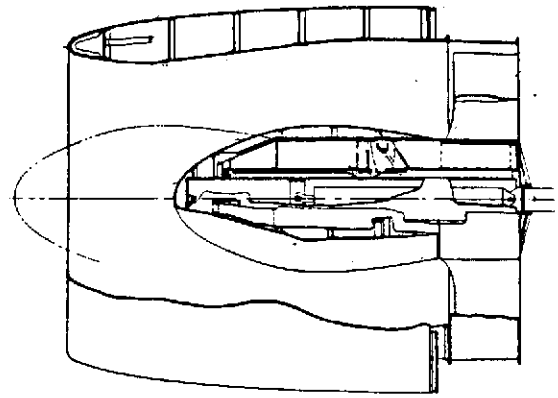 See figure A-11
Basic design	Lines	Good area progression profile with maximum cowl wall diffusion angle of 7.5° and L/D of 1.4; external lines not affected
	Structure	Conventional skin and frame outer cowl with centerbody support integrated with engine inlet guide vane design
	Mechanism	Actuator-driven centerbody translating on slide blocks and tracks
	Seals	Static seals only
	Range of application	Larger area changes can be achieved at the expense of increased inlet length and/or diffusion angle
Actuation	Power source	Engine bleed air for two-position pneumatic system; hydraulic for multiple position
	Type of actuation	Pneumatic piston for two position; hydraulic piston for multiple position
	Load and stroke	Load ≈3500 lb; stroke = 27.0 in.
	Synchronization	None required
	Failsafe potential	Careful venting of plug and/or locking devices required to counteract adverse pressure loads
Control	Two position	Electrical signal to air control valve
	Multiple position	Electronic input to electromechanical transfer valve nulled by linearly variable differential transducer position feedback with position selected as a function of engine rpm and total pressure at the fan face 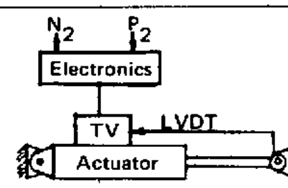
Weight estimate (lb)		Basic cowl 174.0 Translating centerbody 55.0 IGV modification 34.0 Centerbody support structure 89.0 Actuation and control 22.0 Anti-icing system 65.0 Total inlet 439.0 Engine penalty 40.0 Total 479.0 Comparative weight of 707-320B nonsonic inlet = 220 lb (scaled)
Smoothness		Imperfections limited to joint between centerbody and support structure
Bird strike		Hazard no greater than current inlets
Anti-icing system		Outer cowl leading edge comparable to existing inlets; telescopic routing to centerbody leading edge required
Acoustic treatment		Wall treatment more effective

FIGURE A-15.—EVALUATION CHART—SINGLE THROAT SONIC INLETS

Design Consideration		Variable Cowl Wall 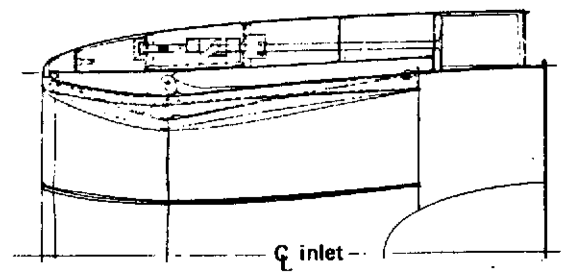 See figure A-12
Basic design	Lines	Good area progression profile at cruise; 11° diffusion angle during approach; $L/D = 1.35$
	Structure	Conventional skin and frame outer surface with combination closure pan and leaf support beams on inner surface
	Mechanism	Eight sets of two leaves with link connected to track-mounted unison ring or driven by individual actuators; option: replace eight sets of two leaves with eight leaves with controlled flexure for throat variation
	Seals	Approximately 700 in. of leaf edge requires variable degree of sealing
	Range of application	Has advantage of maximum area change with minimum diameter change at outer surface
Actuation	Power source	Engine bleed air for two-position pneumatic system; hydraulics for multiple position
	Type of actuation	Four ball screws, gear box driven from air motor, driving unison ring or eight individual actuators
	Load and stroke	Load ≈ 20,000 lb; stroke = 5.4 in.
	Synchronization	Flex shaft between gear boxes for unison ring drive or common input to transfer valves on independent actuators having linearly variable differential transducer position feedback
	Failsafe potential	Pressure loads are adverse
Control	Two position	Electrical signal to air control valve
	Multiple position	Electronic input to electromechanical transfer valves nulled by linearly variable differential transducer position feedback with position selected as a function of engine rpm and total inlet pressure at the fan face 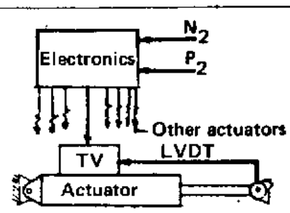
Weight estimate (lb)		Basic cowl 168.0 Nose dome 10.0 Variable leaves 104.0 Actuation and control 105.0 Anti-icing system 56.0 Total inlet 443.0 Engine penalty 41.0 Total 484.0 Comparative weight of 707-320B nonsonic inlet = 220 lb (scaled)
Smoothness		Leaf support beams protrude into airstream during cruise; longitudinal and circumferential joints around leaves; variable gap in surface continuity at aft end of leaves 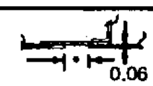 *Approach ≈ 0.80; cruise = 0.02
Bird strike		Leaf damage could cause failures that result in leaf ingestion (throat variation using leaves with controlled flexure would minimize this hazard)
Anti-icing system		Leading edge anti-icing is readily accomplished; leaf jamming is a possibility
Acoustic treatment		Wall treatment less effective

FIGURE A-15.—Concluded

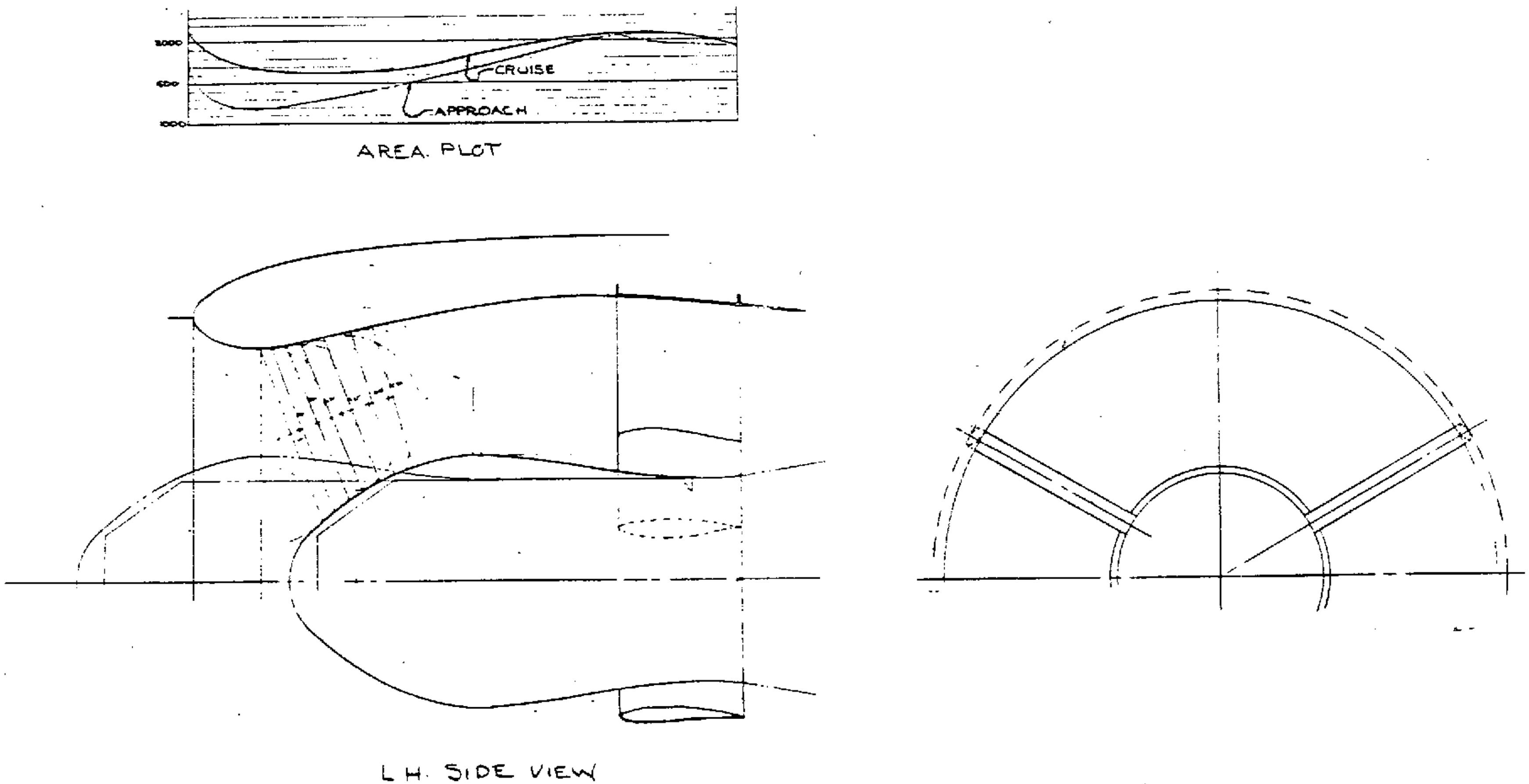

FIGURE A-16.—LO-INSP-010—SONIC INLET LINES, TRANSLATING CENTERBODY, L/D = 1.0

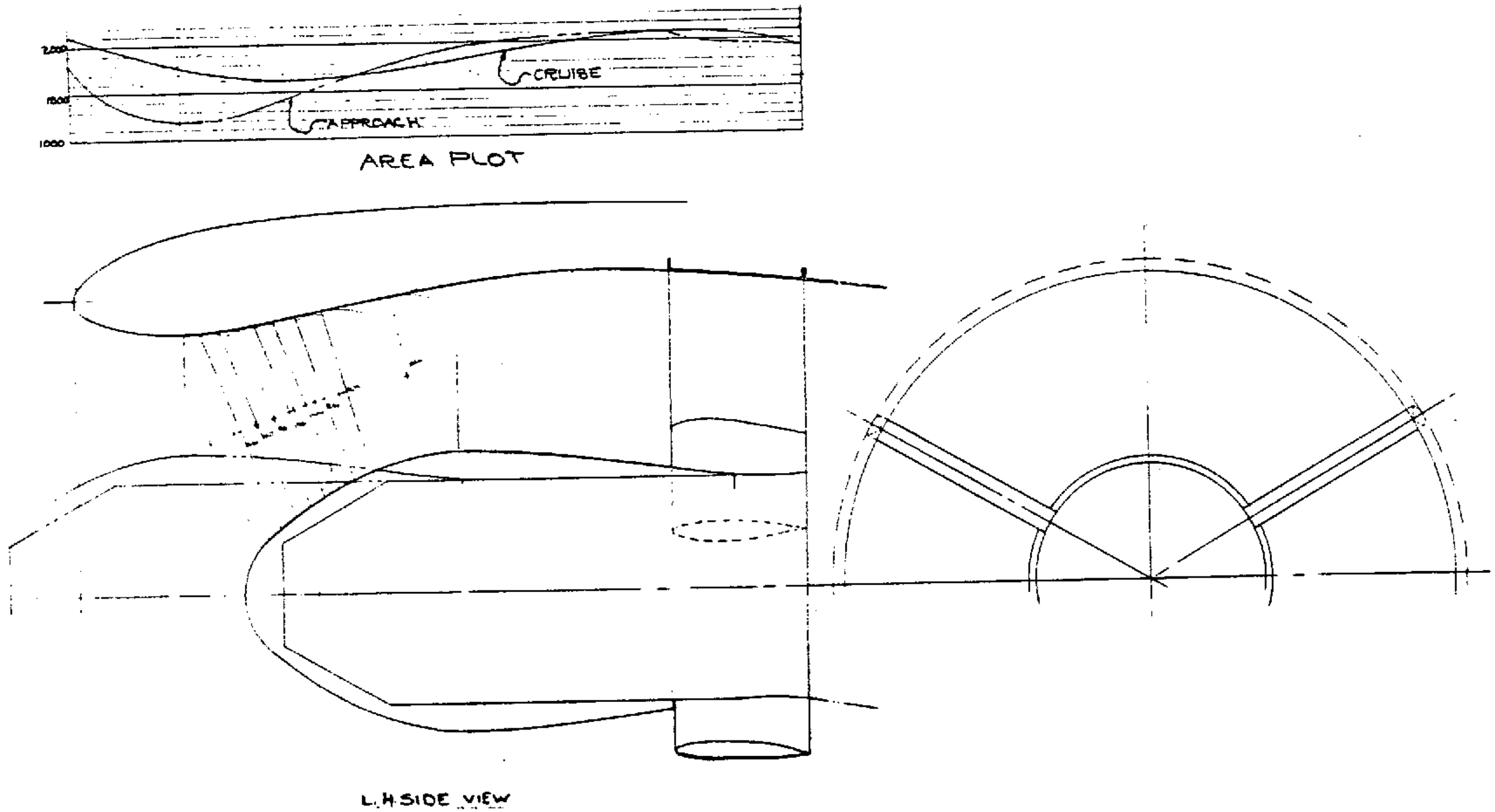

FIGURE A-17.—LO-INSP-011—SONIC INLET LINES, TRANSLATING CENTERBODY, L/D = 1.2

PRECEDING PAGE BLANK NOT FILMED

APPENDIX B

DETAIL DESIGN OF MODELS

B.1 INTRODUCTION

Two inlet concepts were studied, a single-passage and a multipassage type, and each embraced two different configurations: contracting cowl wall or translating centerbody for the single-passage type, and radial vanes or double articulated vanes for the multipassage type.

The basic design parameters for all configurations at full scale were as follows:

Approach = 402 lb/sec
Takeoff = 515 lb/sec
Maximum Cruise = 476 lb/sec

These were based on engine criteria used for system design and evaluation studies of jet STOL aircraft under another NASA contract (ref. 2).

B.2 DETAIL DESIGN OF INLET MODELS

B.2.1 Single-Passage Type

The design procedure for the single-passage inlets was similar for each model. Because the throat and diffuser exit areas were defined by the engine airflow requirements, the prime variables were diffuser length (L/D) and diffuser shape (area distribution). These variables were initially selected on a trial-and-error basis and evaluated with the aid of a computerized potential flow program combined with a boundary layer program. Surface Mach number, boundary layer shape factors, and boundary layer thickness were calculated and plotted as a function of diffuser length. The criterion used for inlet optimization was the attainment of minimum length without boundary layer separation or excessive boundary layer thickness. A shape factor of 2.8 was defined as the limit before separation occurred.

During design of the contracting cowl wall inlets, solutions were obtained for both model- and full-scale inlets. The full-scale inlet was based on the requirements of a typical augmentor wing-type turbofan engine requiring the above-mentioned corrected airflows at critical design conditions. Other variables used in the calculations included average throat Mach number, shape of the fan spinner, and shape of the cowl wall. Since the design computer program would not handle supersonic flow it was necessary to use average throat Mach numbers low enough to ensure that local supersonic velocities on the surface of the cowl were avoided. The principal average throat Mach numbers studied were 0.80, 0.85, and 0.90.

The cowl wall slope had a significant effect on the boundary layer shape factor and was used to good advantage in determining the shortest inlet having good boundary layer characteristics. In general, it was found that a steep slope at the early stages of diffusion with lower slopes near the end resulted in the optimum design. However, danger of separation near the throat existed when using this technique; although the boundary layer was thin, local surface Mach number could be high and Mach number gradient across the channel severe. Examples of shape factor and cowl wall slope given on figure B-1 show that accurate prediction of shape factor was necessary to avoid separation.

Reynolds number exerted a major influence on shape factor and boundary layer thickness, as indicated by the curves comparing model scale and full scale on figure B-2.

B.2.1.1 Contracting Cowl Wall, L/D = 2.0, Model 1

The computerized potential flow program combined with the boundary layer analysis program was used to generate the flow properties of the "fundamental" inlets. Model 1, which was conservatively designed using L/D = 2.0, was the first to be studied. The cowl boundary layer characteristics expected at model scale for an average throat Mach number of 0.8 are shown on figure B-3. The transition from laminar to turbulent flow in the boundary layer occurred slightly downstream of the inlet throat. The analysis indicated that the compressible shape factor for this condition would not exceed 2.0 anywhere in the diffuser and would be close to 1.5 at the diffuser exit. Predicted inlet Mach number distribution is shown on figure B-4. Details of inlet geometry are presented on figure B-5.

B.2.1.2 Contracting Cowl Wall, L/D = 1.0, Model 2

The same design procedure was used for both the approach and takeoff configurations of model 2, but only the takeoff configuration, details of which are presented in figure B-6, was critical. The internal flow characteristics for model scale Reynolds number and an average throat Mach number of 0.80 are presented in figure B-7, which shows the duct Mach number as a function of inlet length. Figure B-8 shows boundary layer thickness, and figure B-9 shows boundary layer shape factor.

B.2.1.3 Translating Centerbody, L/D = 1.3, Model 3 and L/D = 1.0, Model 4

The translating centerbody inlets with L/D = 1.3, and 1.0 (models 3 and 4, respectively), were also designed using similar methods, and the same engine characteristics, as previously described.

The inlet lines for model 3 are shown on figure B-10; this inlet was tested in its basic configuration and with various degrees of acoustic treatment. Model 3A, shown on figure B-11, was lined completely; model 3B, shown on figure B-12, had the lining removed from the forward section of the centerbody; and model 3C, shown on figure B-13, had a lining applied only to the diffuser section of the cowl and centerbody.

To achieve L/D = 1.0 on the centerbody inlet it was necessary to shorten both the diffuser length and the distance from the highlight to the throat; to have used a conventional elliptical lip shape would have resulted in surface overvelocity. To avoid this, the contour between highlight and throat was modified, and the shape used is compared to the elliptical shape in figure B-14. This change reduced the curvature in the throat and hence the surface Mach number, but it also increased the channel Mach number. The increased curvature behind the throat necessary to enable a short translation of the centerbody, by virtue of a "shortened" centerbody coupled with rapid cowl diffusion, had the effect of delaying boundary layer transition to a location downstream of the throat.

Principal dimensions of the full-scale inlet used for the analysis are given in figure B-15. This shows a centerbody translation of 22 in. (full scale) from the approach to takeoff and cruise positions, which was necessary to satisfy the airflow variation between these flight conditions when the throat Mach number at takeoff is limited to 0.8. The coordinates of the test model internal contours are presented in figure B-16. Because of computer progam limitations, it was necessary to limit the average throat Mach number at takeoff to 0.8, based on mass flow and the "rolling ball" minimum area, to avoid supersonic surface velocities on the cowl surface. For test purposes the centerbody translation was determined by recovery and noise performance and was approximately 17 in. full scale.

The results of the computerized analysis are presented below.

Approach: The compressible boundary layer shape factor distributions are shown for both cowl and centerbody on figure B-17. An average throat Mach number of 0.9 was used which represented an engine corrected airflow of 402 lb/sec at an inlet recovery of 0.995. The centerbody was in the extended position. At full-scale Reynolds number, no adverse boundary layer characteristics were observed. The boundary layer thickness is shown on figure B-18 and surface Mach number distribution on figure B-19.

Takeoff: Similar data are presented for the centerbody translated to its takeoff position 22 in. behind the approach position and with a corrected engine airflow of 515 lb/sec. The boundary layer shape factor is shown on figure B-20, boundary layer thickness on figure B-21, and Mach number distribution on figure B-22. The irregular characteristics shown for the cowl were a result of the rapid rate of surface curvature necessary to achieve the short inlet. An average throat Mach number of 0.8 was achieved based on minimum flow area.

Cruise: The average throat Mach number was 0.66 because of the reduced corrected airflow of 476 lb/sec. Boundary layer thickness is plotted on figure B-23, shape factor on figure B-24, and Mach number distribution on figure B-25.

The full-scale cowl surface compressible shape factor was compared to the model-scale shape factor, which indicated a value of 2.32 for the model and 1.82 for the full-scale inlet (fig. B-21). To compensate for this effect of Reynolds number, the rate of diffusion was relieved on the model. The modification reduced the maximum shape factor on the cowl surface from 2.32 to 2.06 (fig B-26).

B.2.2 Multipassage Type

B.2.2.1 Radial Vane, L/D = 1.0, Model 5

The basic design configuration for the radial vane inlet (model 5A) was a length-to-diameter ratio of one and a full-length centerbody. The throat, formed by 36 radial vanes, was sized for approach airflow. The centerbody was constant in diameter, with 2:1 elliptical nose dome. A symmetrical airfoil with 14% thickness-to-chord ratio was used for the vanes, which tapered uniformly toward zero chord and thickness at the inlet centerline. Maximum thickness was at 40% chord. The maximum diffuser angle on the cowl wall downstream of the vanes was 5.5°. The geometry is presented on figure B-27.

The inlet model was modified slightly for the second phase of testing (model 5B). Flow separation in the hub region was evident during the first phase. It was believed to have been caused by the rate of flow diffusion necessary to reduce flow velocities near the vane row entrance. The alteration involved the introduction of a continuously accelerating flow passage ahead of the vane row. A comparison of the two inlets is presented on figure B-28. The geometry is presented in figure B-29.

B.2.2.2 Articulated Vane, L/D = 1.0, Model 6

The double-articulated radial vane inlet (model 6) was also designed to have an inlet-to-fan-diameter ratio of one. Details of the geometry are shown on figures B-30 and B-31. The front vanes were used to turn the flow to provide a sonic throat and the second row of vanes returned the flow to an axial direction.

A computerized compressor design procedure was used to obtain uniform flow at the exit of the front vanes. To achieve this flow condition, it was necessary to contour both the cowl and centerbody and to radially distribute the vane turning angle as shown in figure B-32.

The front vanes were NACA 63 series airfoil basic thickness distribution. The thickness-to-chord ratios were 8% and 4% at nominal tip and hub radii, respectively, and the chord length varied linearly radially to attain uniform blockage (13.3%). The vanes were designed to be hinged (flight inlet) at a point 25% chord length from the leading edge. The rear vanes had NACA 64 series airfoil basic thickness distribution, and the same thickness-to-chord ratios as the front vanes. However, the blockage was 8% and the hinge point at 40% chord length from the leading edge.

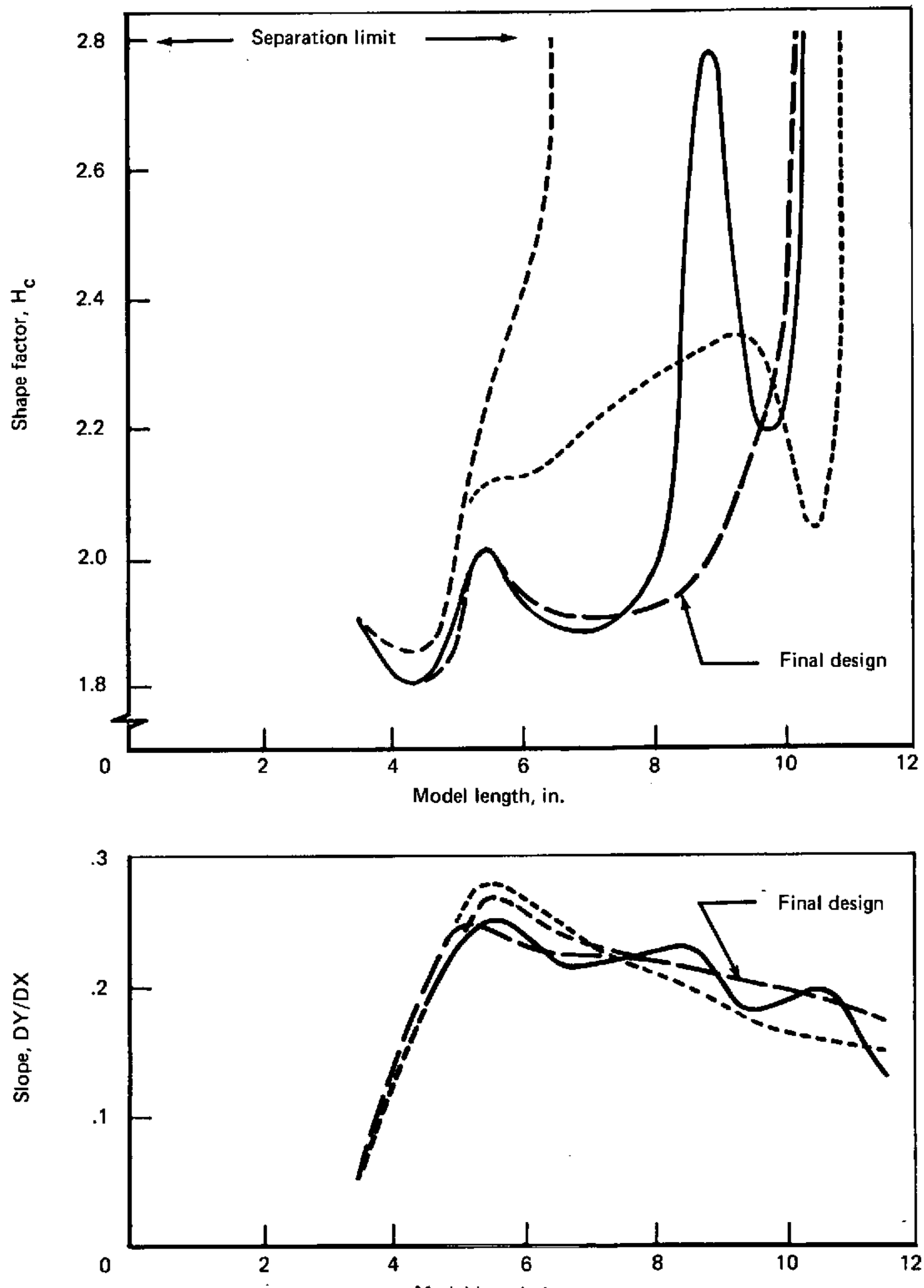

FIGURE B-1.—RELATIONSHIP BETWEEN COWL WALL SLOPE AND BOUNDARY LAYER SHAPE FACTOR—MODEL 2, L/D = 1.0, APPROACH CONFIGURATION

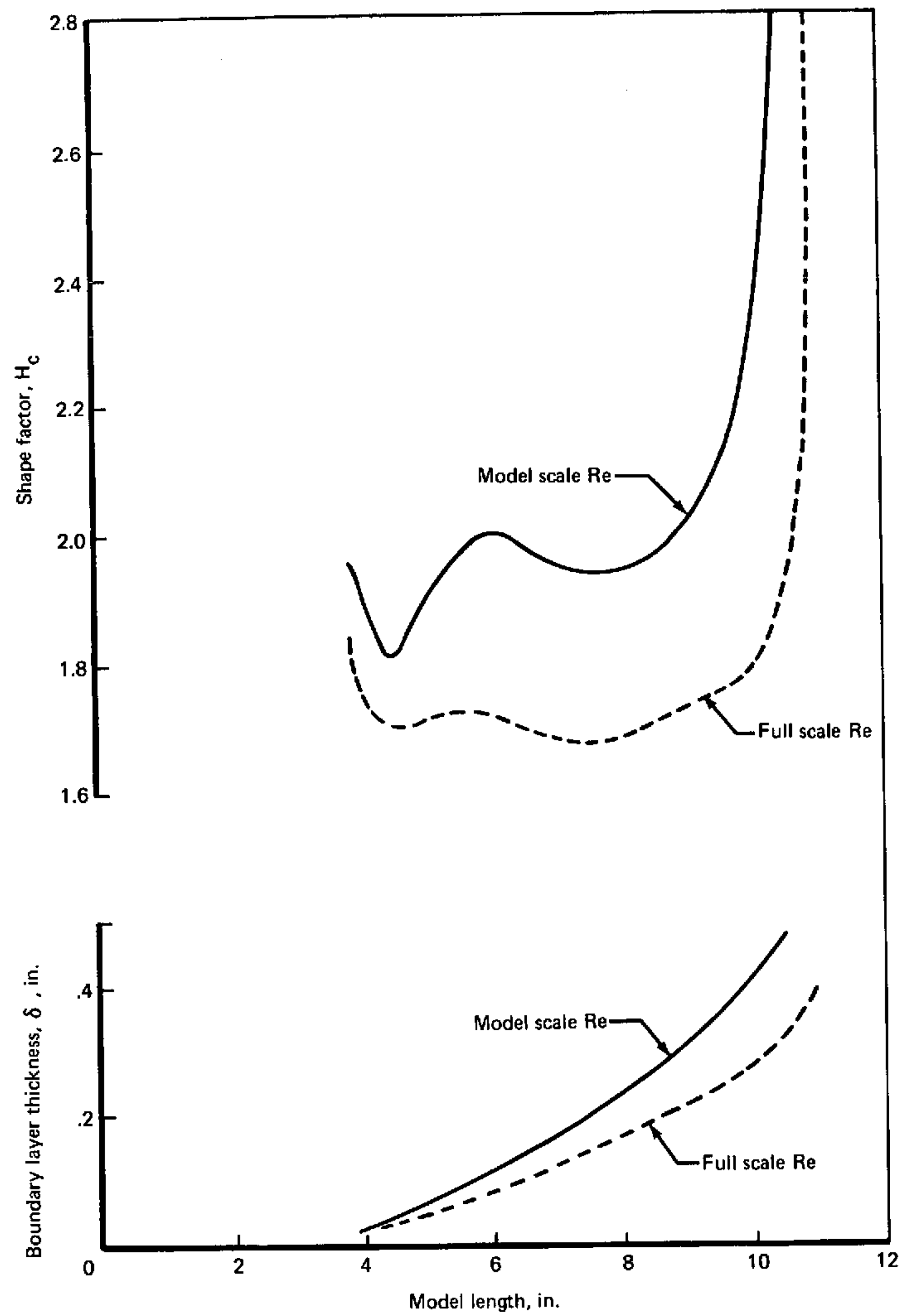

FIGURE B-2.—REYNOLDS NUMBER EFFECT ON BOUNDARY LAYER CHARACTERISICS— MODEL 2, L/D = 1.0, APPROACH CONFIGURATION

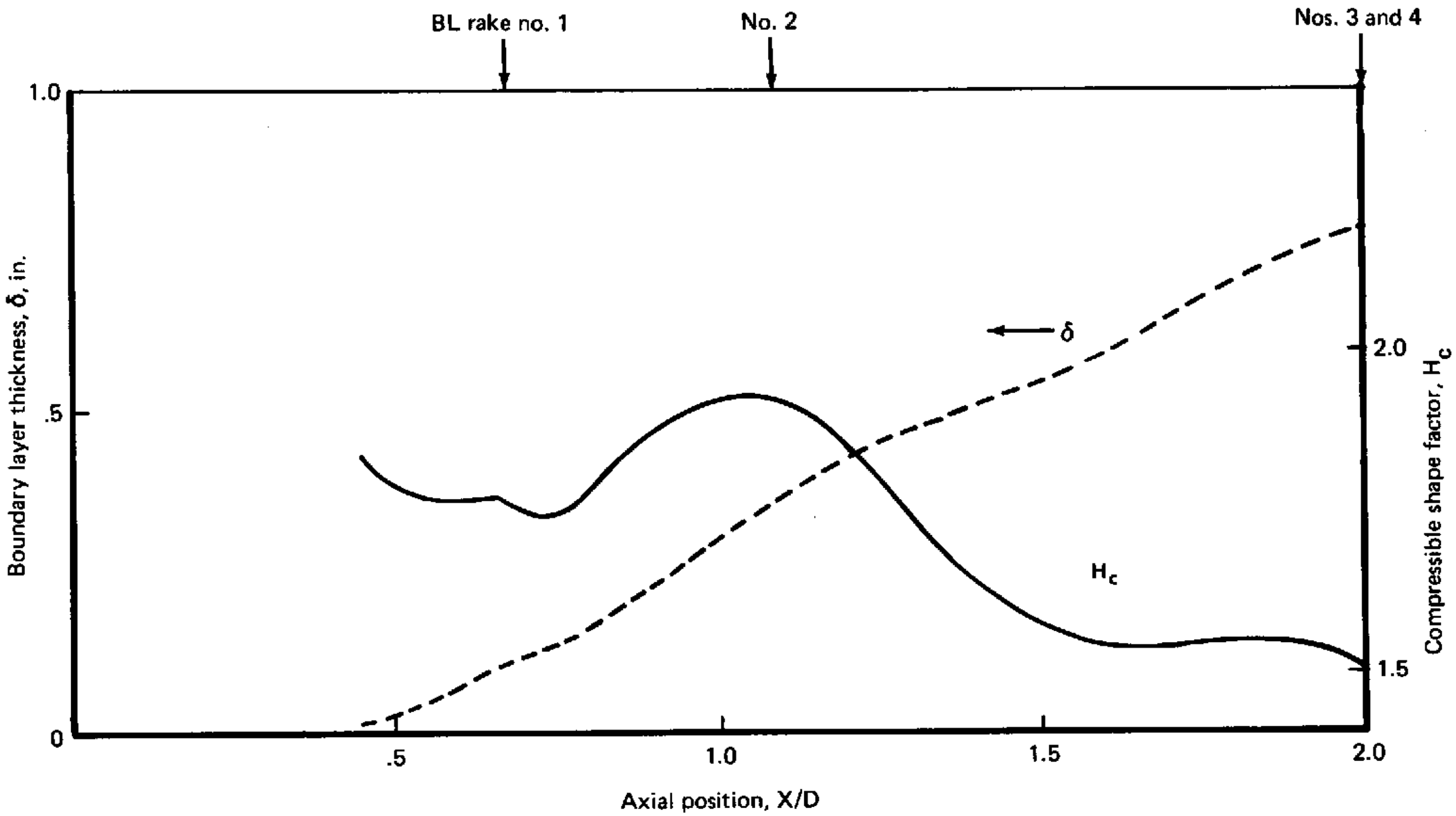

FIGURE B-3.—COWL BOUNDARY LAYER CHARACTERISTICS—MODEL 1, L/D = 2.0, APPRAOCH CONFIGURATION

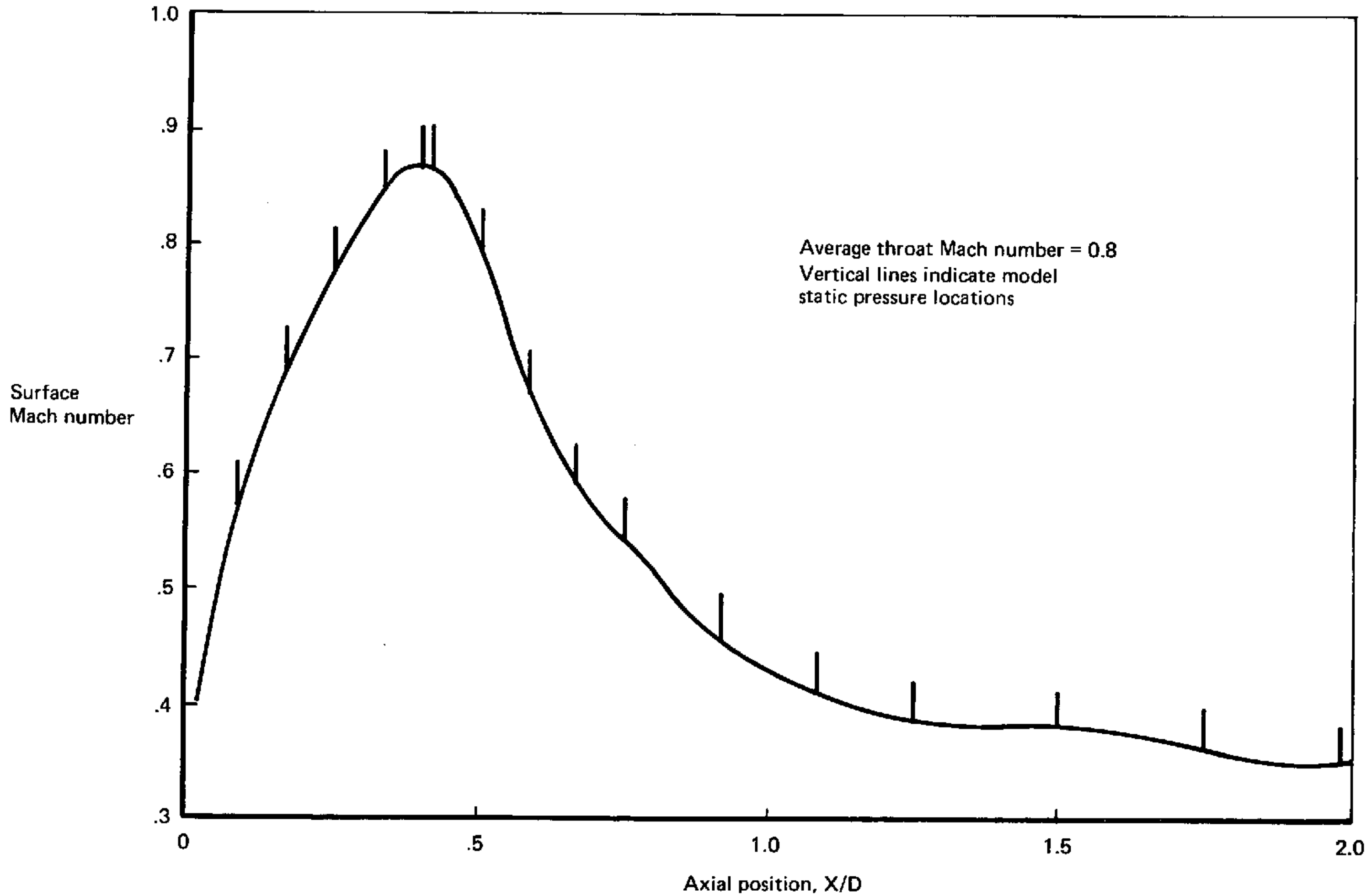

FIGURE B-4.—COWL SURFACE MACH NUMBER DISTRIBUTION—MODEL 1, L/D = 2.0, APPROACH CONFIGURATION

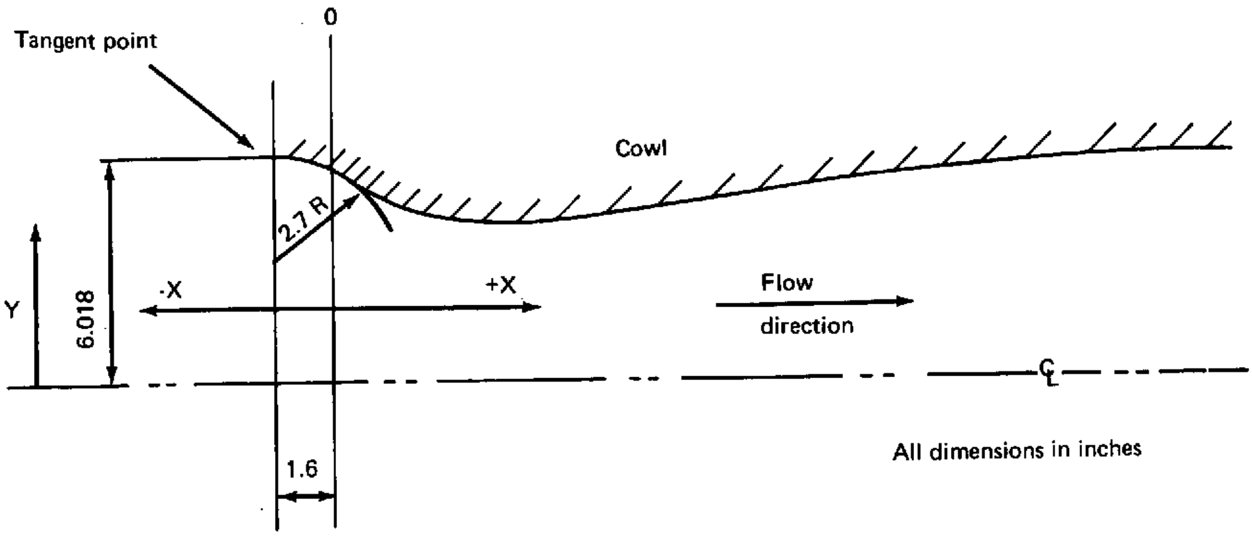

	X	Y
	0	5.686
	0.238	5.494
	0.475	5.092
	0.950	4.868
	1.426	4.713
	1.901	4.596
	2.376	4.506
	2.851	4.437
	3.326	4.386
	3.802	4.351
	4.277	4.330
Throat	4.752	4.323
	5.250	4.332
	6.000	4.385
	7.000	4.500
	8.000	4.638
	9.000	4.772
	10.000	4.914
	12.000	5.172
	14.000	5.380
	16.000	5.551
	18.000	5.720
	20.000	5.865
	22.000	5.970
	24.000	6.018

FIGURE B-5.—MODEL 1, L/D = 2.0, APPROACH CONFIGURATION

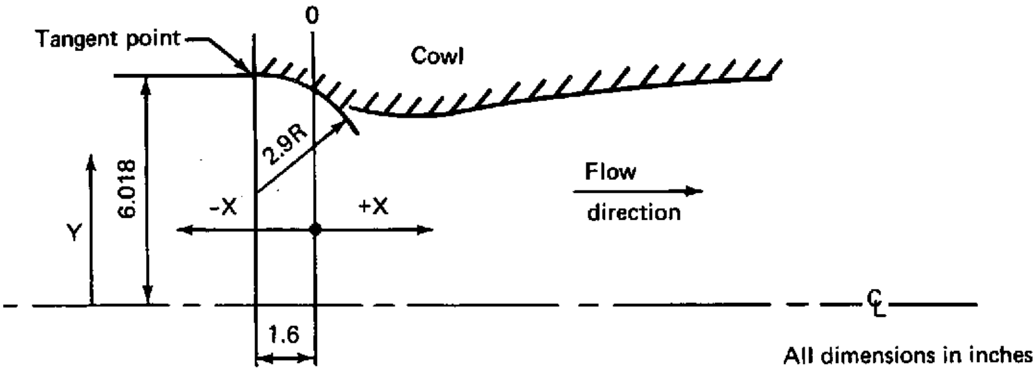

X	Y	X	Y	X	Y	X	Y
0	5.686	5.0041	5.0666	7.1220	5.4734	9.2430	5.8330
0.0281	5.6311	5.0645	5.0784	7.1825	5.4851	9.3090	5.8412
0.2718	5.3678	5.1250	5.0903	7.2429	5.4968	9.3701	5.8494
0.6108	5.2218	5.1855	5.1021	7.3034	5.5085	9.4312	5.8576
0.9654	5.1179	5.2459	5.1140	7.3639	5.5202	9.4923	5.8657
1.3273	5.0425	5.3064	5.1253	7.4244	5.5319	9.5535	5.8730
1.6926	4.9859	5.3669	5.1377	7.4849	5.5436	9.6147	5.8801
2.0599	4.9477	5.4273	5.1495	7.5455	5.5550	9.6759	5.8872
2.4285	4.9165	5.4878	5.1614	7.6061	5.5663	9.7371	5.8943
2.7978	4.8998	5.5483	5.1731	7.6666	5.5776	9.7983	5.9014
3.1675	4.8945	5.6088	5.1847	7.7272	5.5809	9.8535	5.9086
3.1680	4.8940	5.6693	5.1963	7.7878	5.6002	9.9207	5.9157
3.2291	4.8943	5.7298	5.2079	7.8484	5.6115	9.9819	5.9228
3.2907	4.8949	5.7904	5.2195	7.9089	5.6220	10.0000	5.9250
3.6603	4.9042	5.8509	5.2312	7.9695	5.6341	10.0432	5.9292
3.7834	4.9093	5.9114	5.2428	8.0000	5.6400	10.1045	5.9354
3.8449	4.9129	5.9719	5.2544	8.0302	5.6449	10.1658	5.9416
3.9065	4.9164	6.000	5.2600	8.0909	5.6552	10.2271	5.9477
3.9680	4.9199	6.0324	5.2660	8.1517	5.6655	10.2885	5.9531
4.0294	4.9241	6.0930	5.2774	8.2124	5.6758	10.3499	5.9580
4.0909	4.9290	6.1535	5.2889	8.2732	5.6860	10.4000	5.9627
4.1523	4.9339	6.2140	5.3003	8.3339	5.6963	10.5000	5.9710
4.2137	4.9388	6.2746	5.3118	8.3947	5.7066	10.600	5.9792
4.2160	4.9386	6.3351	5.3233	8.4555	5.7169	10.700	5.9863
4.2750	4.9448	6.3957	5.3347	8.5162	5.7269	10.800	5.9920
4.3361	4.9527	6.4562	5.3462	8.5772	5.7360	10.900	5.9975
4.3973	4.9605	6.5167	5.3577	8.6381	5.7452	11.000	6.0020
4.4564	4.9683	6.5773	5.3692	8.6990	5.7544	11.100	6.0050
4.5194	4.9770	6.6378	5.3807	8.7600	5.7636	11.200	6.0075
4.5801	4.9875	6.6983	5.3923	8.8209	5.7728	11.300	6.0096
4.6408	4.9980	6.7589	5.4038	8.8818	5.7820	11.400	6.0115
4.7015	5.0086	6.8194	5.4153	8.9427	5.7312	11.500	6.0130
4.7622	5.0194	6.8799	5.4268	9.000	5.8000	11.600	6.0140
4.8226	5.0312	6.9405	5.4384	9.0037	5.8004	11.700	6.0153
4.8831	5.043	7.000	5.4500	9.0648	5.8085	11.800	6.0160
4.9436	5.0548	7.0010	5.4500	9.1258	5.8167	11.900	6.0172
5.000	5.0680	7.0615	5.4617	9.1869	5.8249	12.000	6.0180

FIGURE B-6.—MODEL 2, L/D = 1.0, TAKEOFF CONFIGURATION

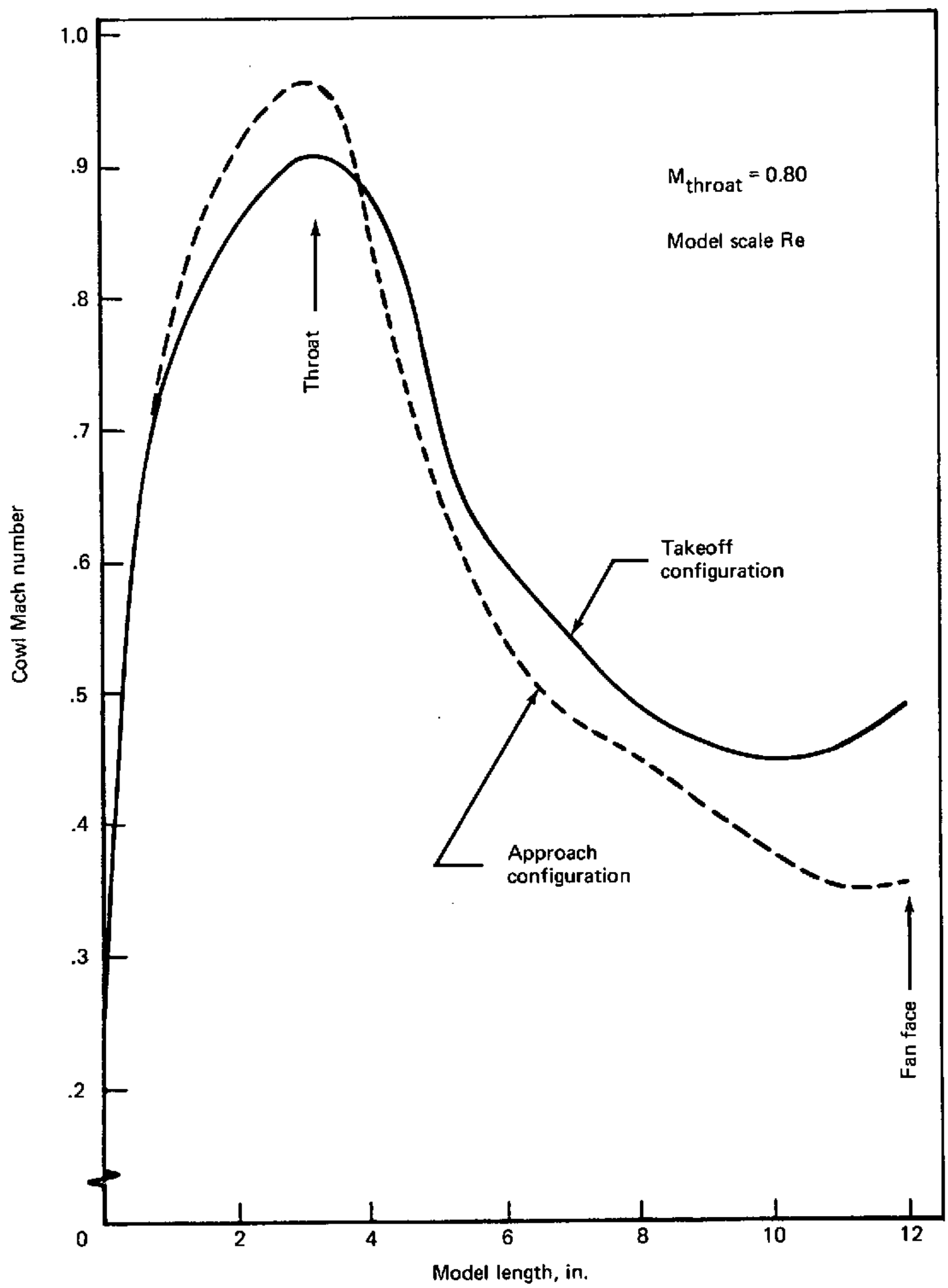

FIGURE B-7.—COWL SURFACE MACH NUMBER VS DISTANCE FROM LIP, MODEL 2, L/D = 1.0

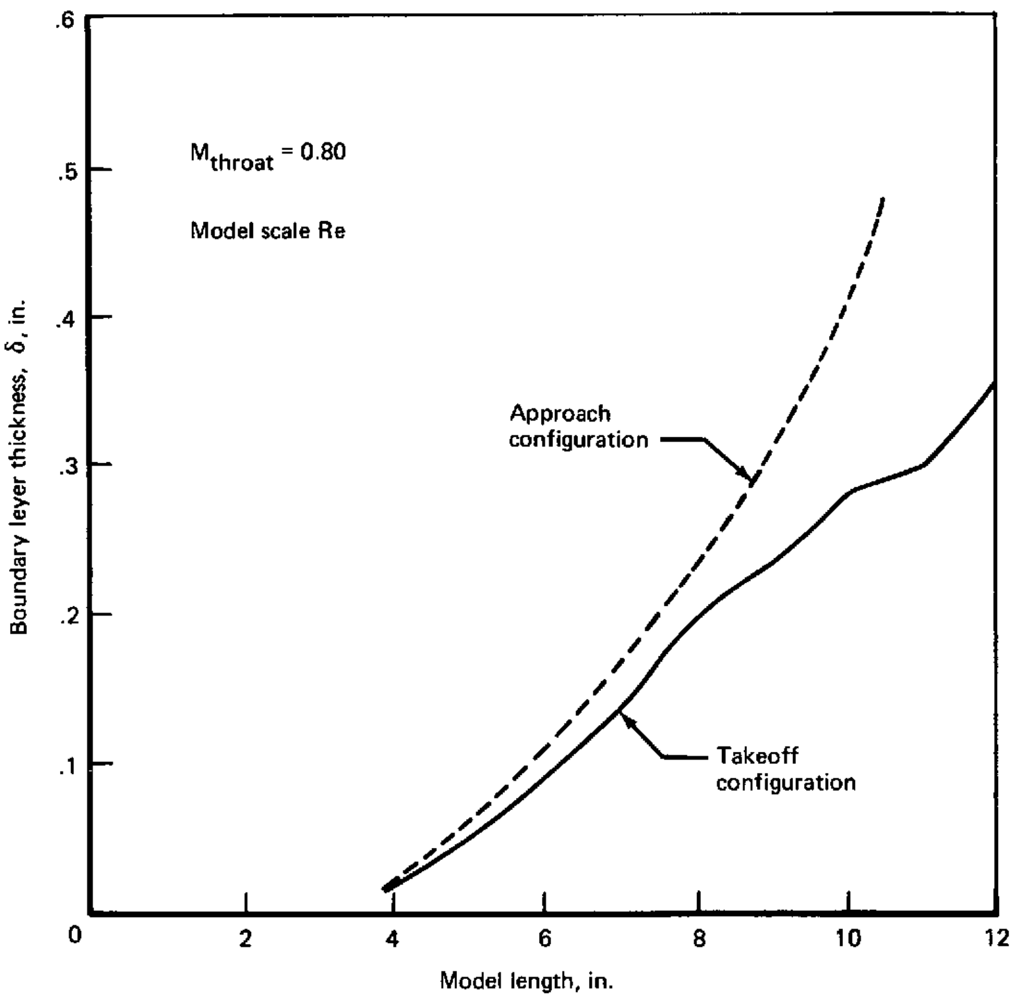

FIGURE B-8.—BOUNDARY LAYER THICKNESS VS DISTANCE FROM LIP, MODEL 2, L/D = 1.0

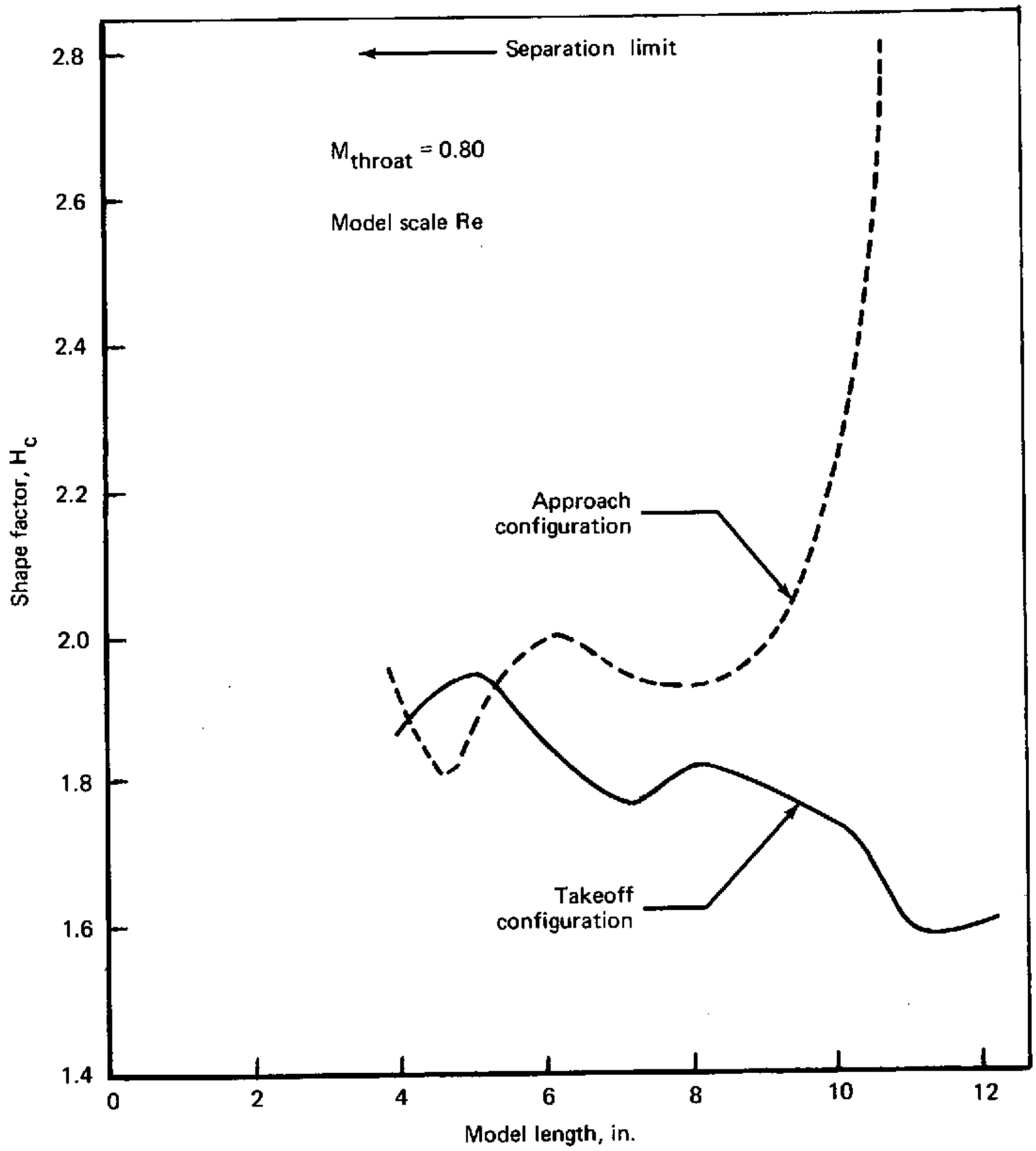

FIGURE B-9.—BOUNDARY LAYER SHAPE FACTOR VS DISTANCE FROM LIP, MODEL 2, L/D = 1.0

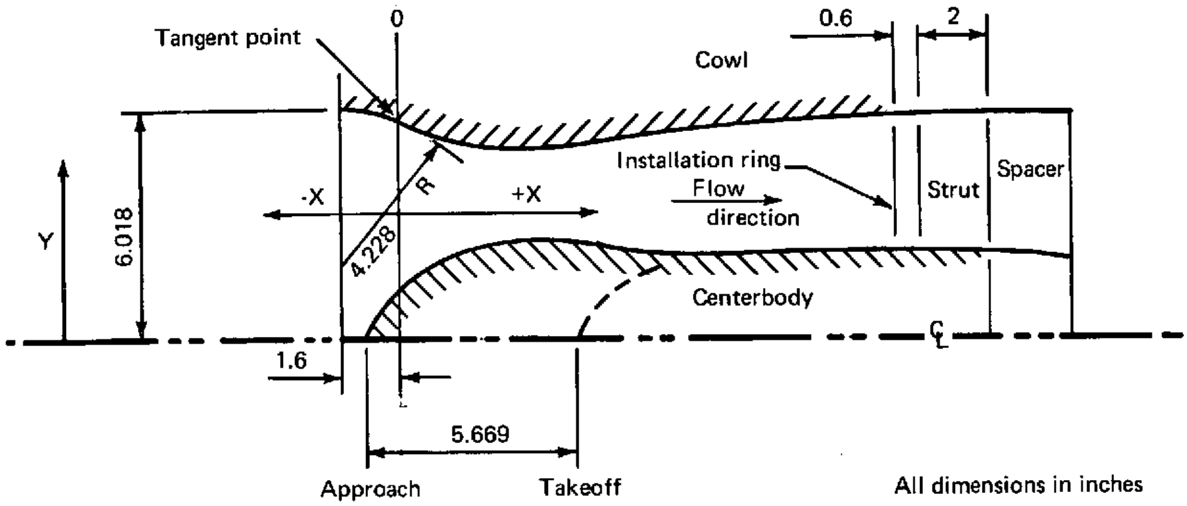

	Centerbody	
	X	Y
	-0.8009	0
	-0.7559	0.3815
	-0.3060	1.1222
	0.1440	1.5071
	0.5939	1.7838
	1.0439	1.9979
	1.4938	2.1681
	1.9438	2.3039
	2.3937	2.4112
	2.8436	2.4938
	3.2936	2.5514
	3.7435	2.5932
	4.1935	2.6128
	4.4185	2.6151
	4.6434	2.6115
	5.0934	2.5858
	5.5433	2.5426
	5.9933	2.4899
	6.4432	2.4364
	6.8931	2.3892
	7.3431	2.3501
	7.7930	2.3197
	8.2429	2.2989
	8.6929	2.2881
	8.9179	2.2868
	15.667	2.2868
Spacer	16.667	2.2868
	17.667	2.1250

Cowl				
X	Y	X	Y	
0	5.9115	10.4927	5.9010	
0.1440	5.6697	10.9430	5.9415	
0.3690	5.5323	11.3930	5.9739	
0.5939	5.4393	11.8420	5.997	
0.8189	5.3678	12.2920	6.0110	
1.0439	5.3097	12.7420	6.0180	
1.4938	5.2215	15.6670	6.0180	Spacer
1.9438	5.1601	17.6670	6.0180	
2.3937	5.1192			
2.8436	5.0956			
3.2836	5.0879			
3.7435	5.0960			
4.1935	5.1190			
4.6434	5.1536			
5.0934	5.1975			
5.5433	5.2485			
5.9933	5.3030			
6.4432	5.3617			
6.8931	5.4233			
7.3431	5.4870			
7.7930	5.5518			
8.2429	5.6166			
8.6929	5.6803			
9.1428	5.7417			
9.5928	5.7998			
10.0328	5.8523			

FIGURE B-10.—MODEL 3, L/D = 1.3, APPROACH AND TAKEOFF CONFIGURATIONS

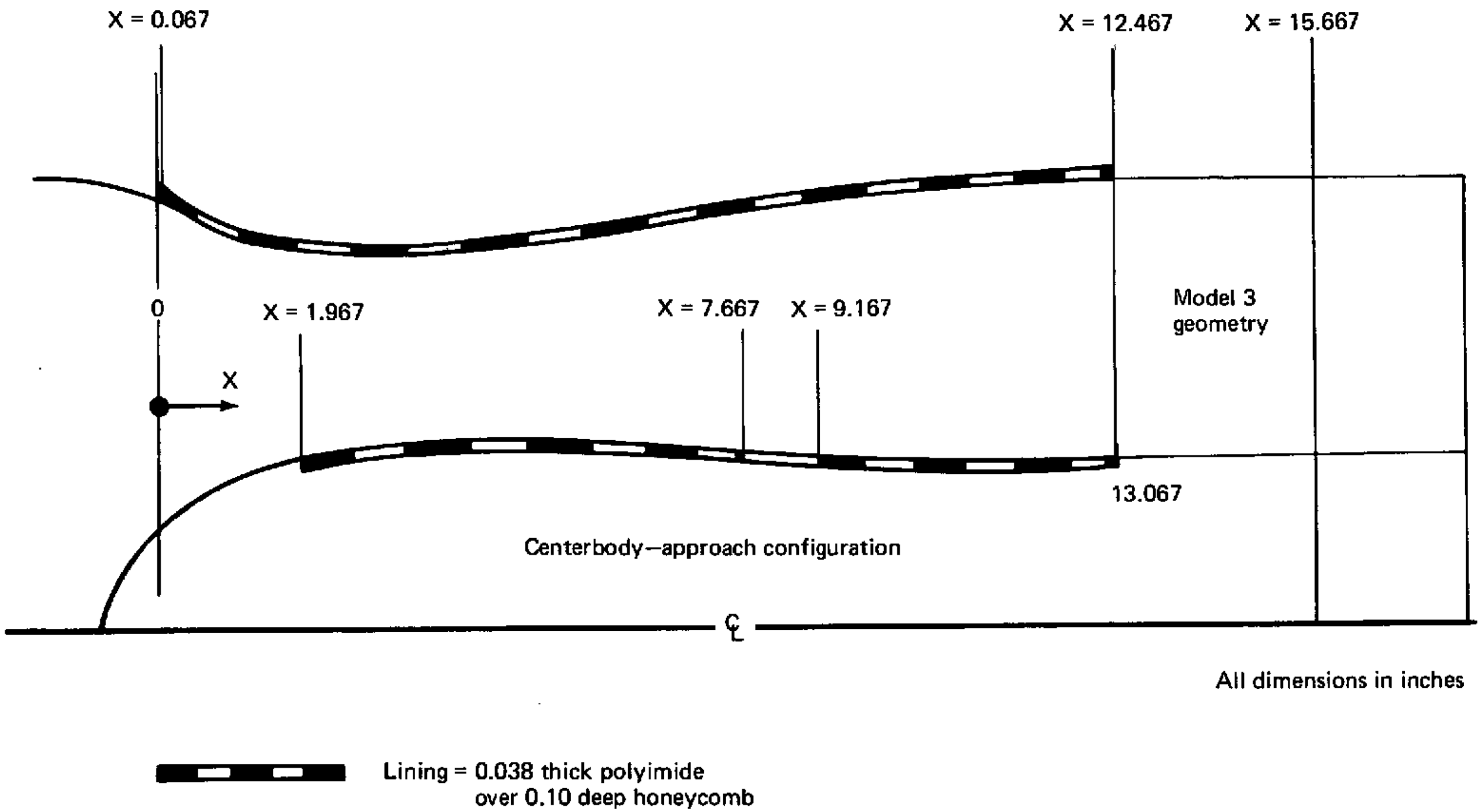

FIGURE B-11.—MODEL 3A, L/D = 1.3, ACOUSTIC LINING DETAILS FOR RUN 101

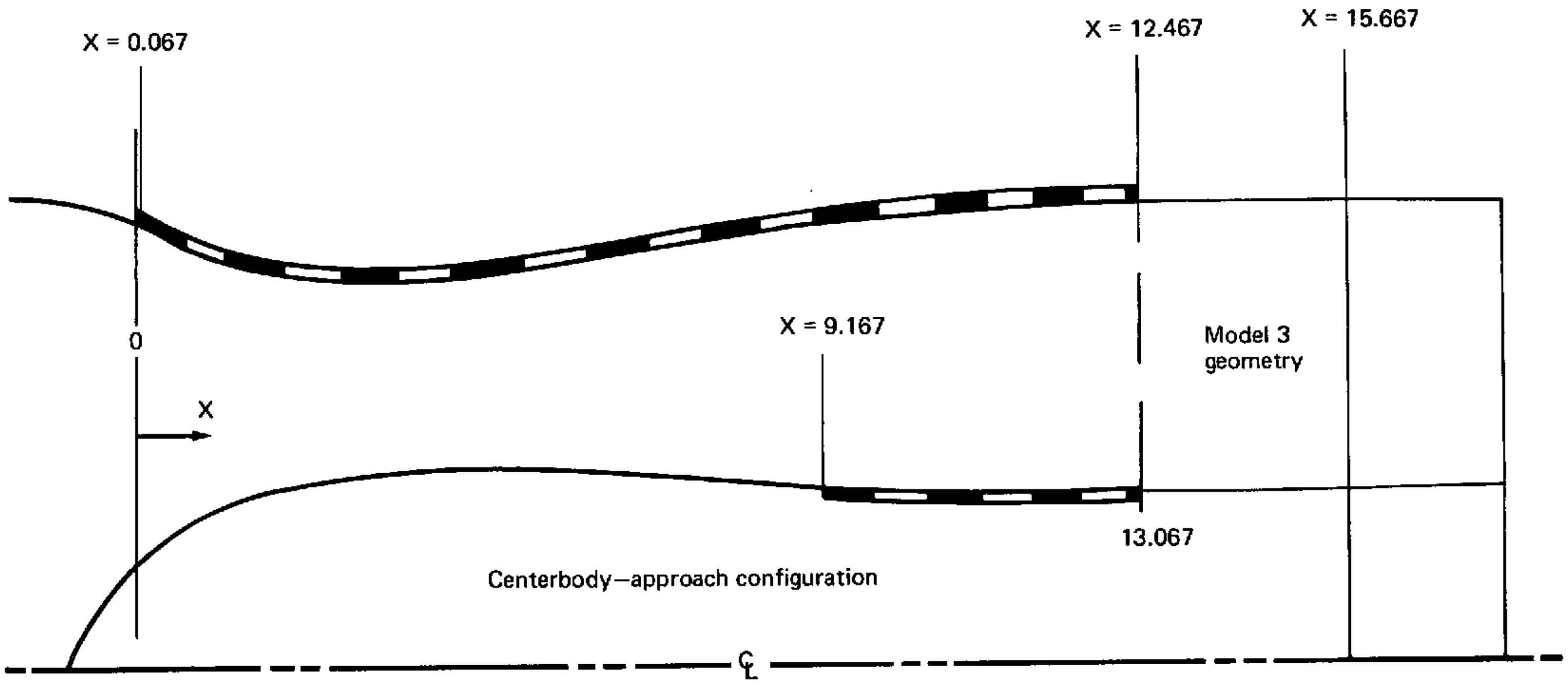

All dimensions in inches

Lining: 0.038 thick polyimide
over 0.10 deep honeycomb

FIGURE B-12.—MODEL 3B, L/D = 1.3, ACOUSTIC LINING DETAILS FOR RUN 102

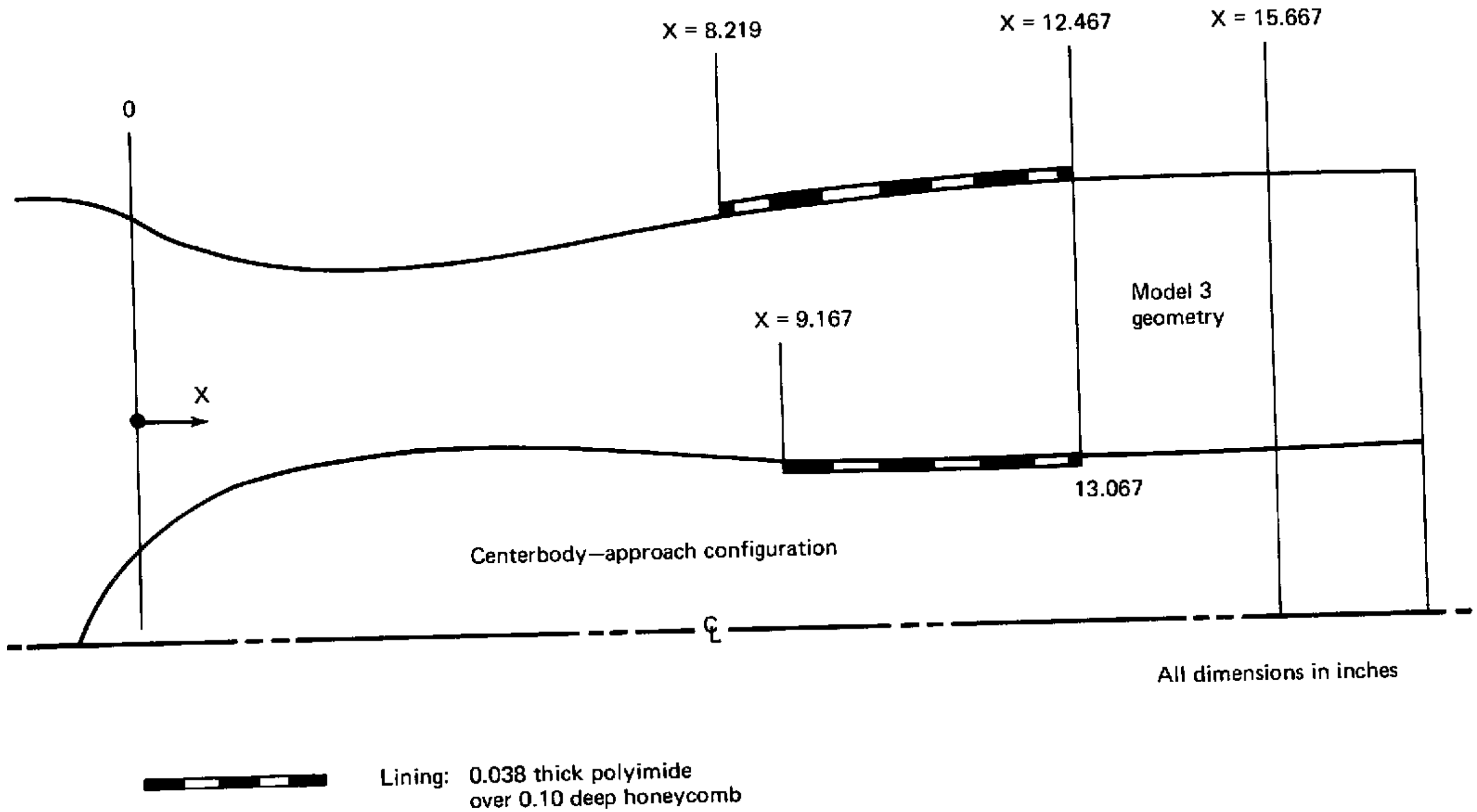

FIGURE B-13.—MODEL 3C, L/D = 1.3, ACOUSTIC LINING DETAILS FOR RUN 10

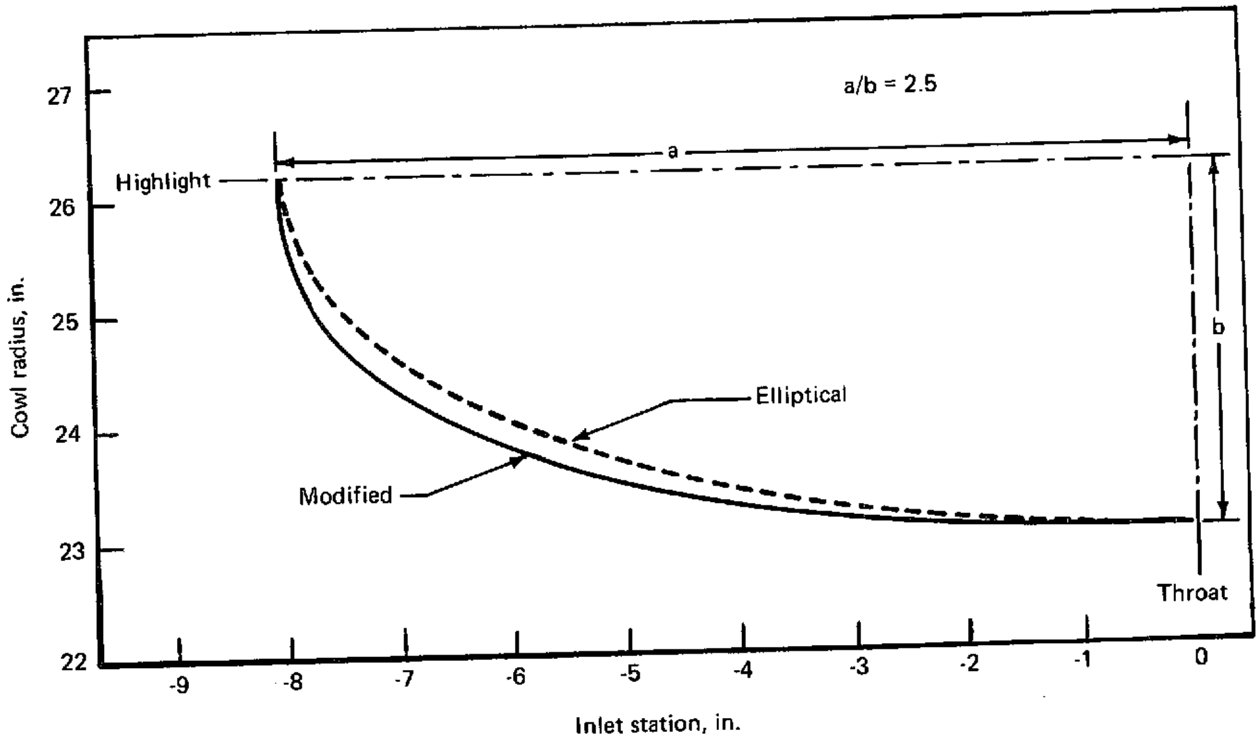

FIGURE B-14.—LIP MODIFICATION, TRANSLATING C/B, L/D = 1.0

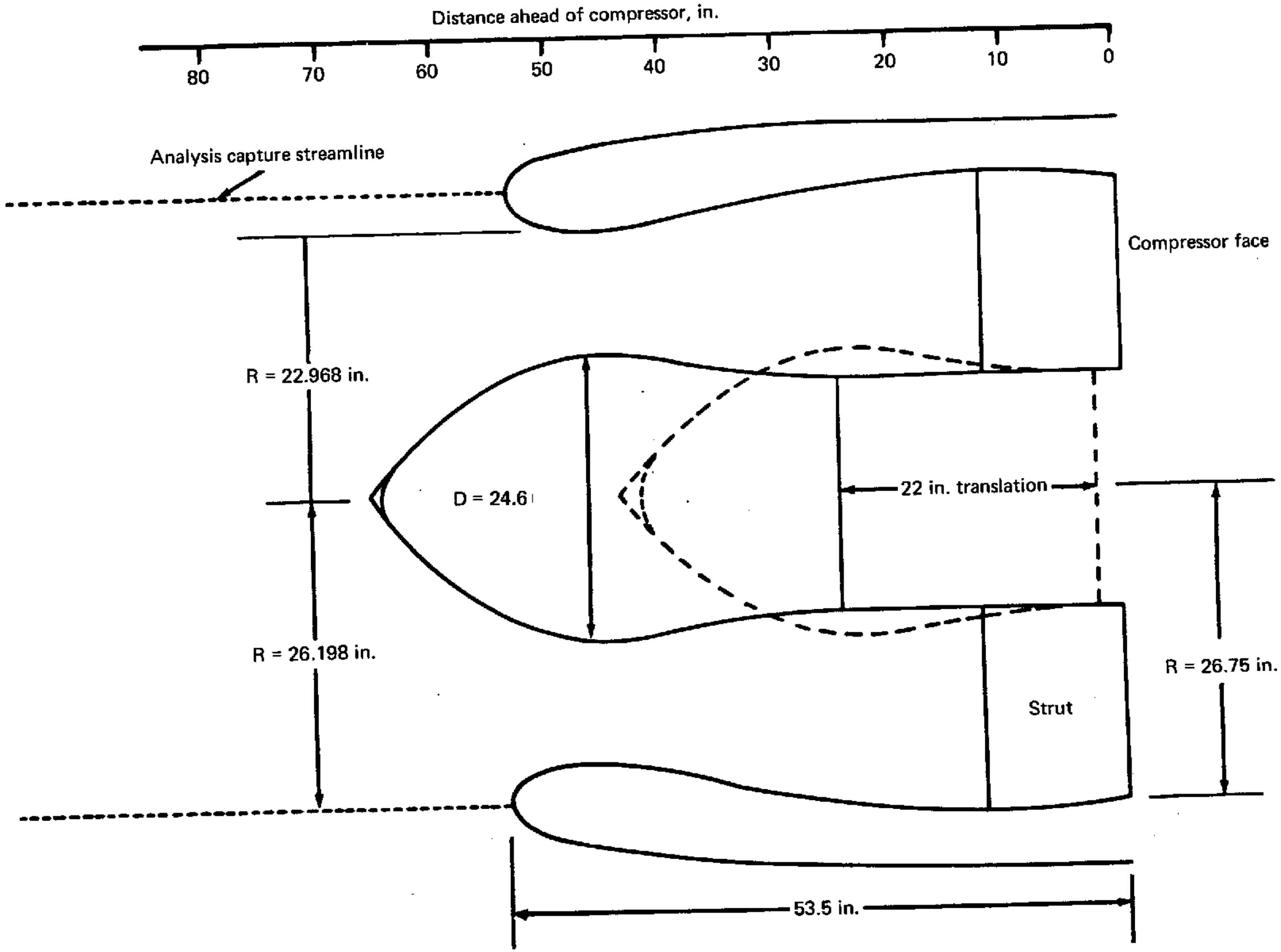

FIGURE B-15.—BASIC INLET DIMENSIONS, FULL SCALE, TRANSLATING C/B, L/D = 1.0

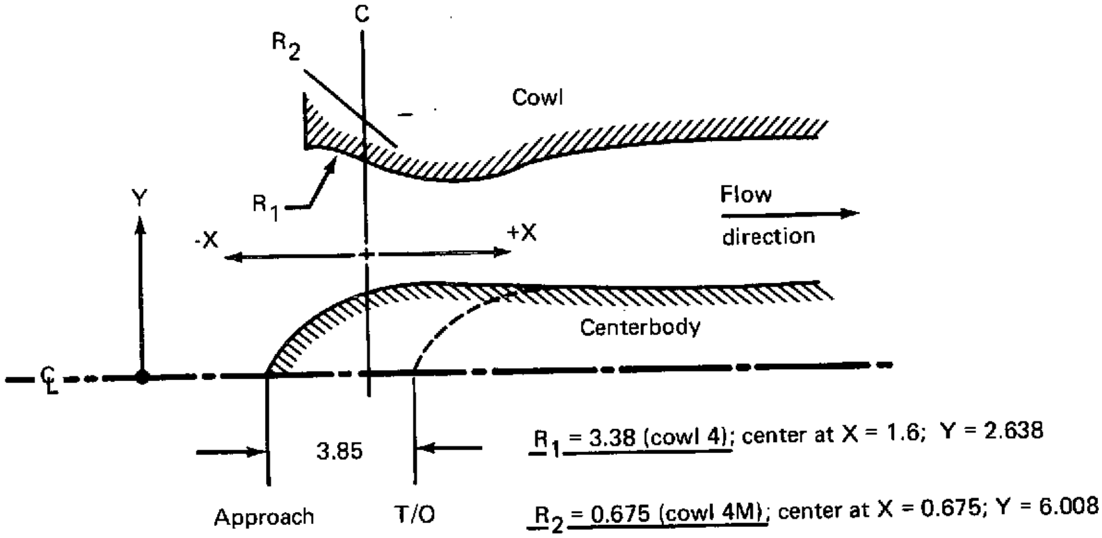

	Centerbody X	Centerbody Y
	-2.694	0
	-2.246	0.519
	-1.567	1.202
	-0.675	1.914
	0	2.312
	0.490	2.520
	0.996	2.670
	1.428	2.743
Throat	1.850	2.767
	2.300	2.723
	2.750	2.642
	3.200	2.563
	3.650	2.496
	4.100	2.439
	4.550	2.383
	5.000	2.339
Straight line	5.550	2.287
Straight line	12.036	2.287

	Cowl 4 X	Cowl 4 Y
	-1.583	6.018
	↕	R_1
	0.274	5.461
	0.500	5.340
	0.950	5.222
	1.400	5.179
	1.850	5.168
	2.300	5.185
	2.750	5.255
	3.200	5.341
	3.650	5.432
	4.100	5.518
	4.550	5.592
	5.000	5.661
	6.012	5.798
	7.025	5.902
	8.037	5.975
	9.050	6.015
Straight line	9.697	6.018
Straight line	12.036	6.018

Cowl 4M X	Cowl 4M Y
0	6.008
↕	R_2
0.274	5.461
0.500	5.340
↓	↓
Same as cowl 4	

All dimensions in inches.

FIGURE B-16.—MODELS 4 AND 4M, L/D = 1.0, APPROACH AND TAKEOFF CONFIGURATIONS

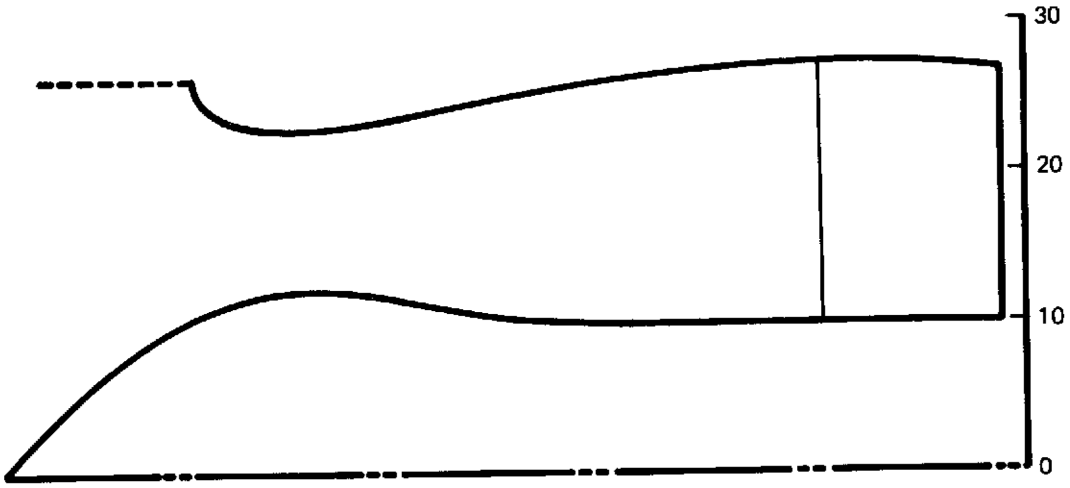

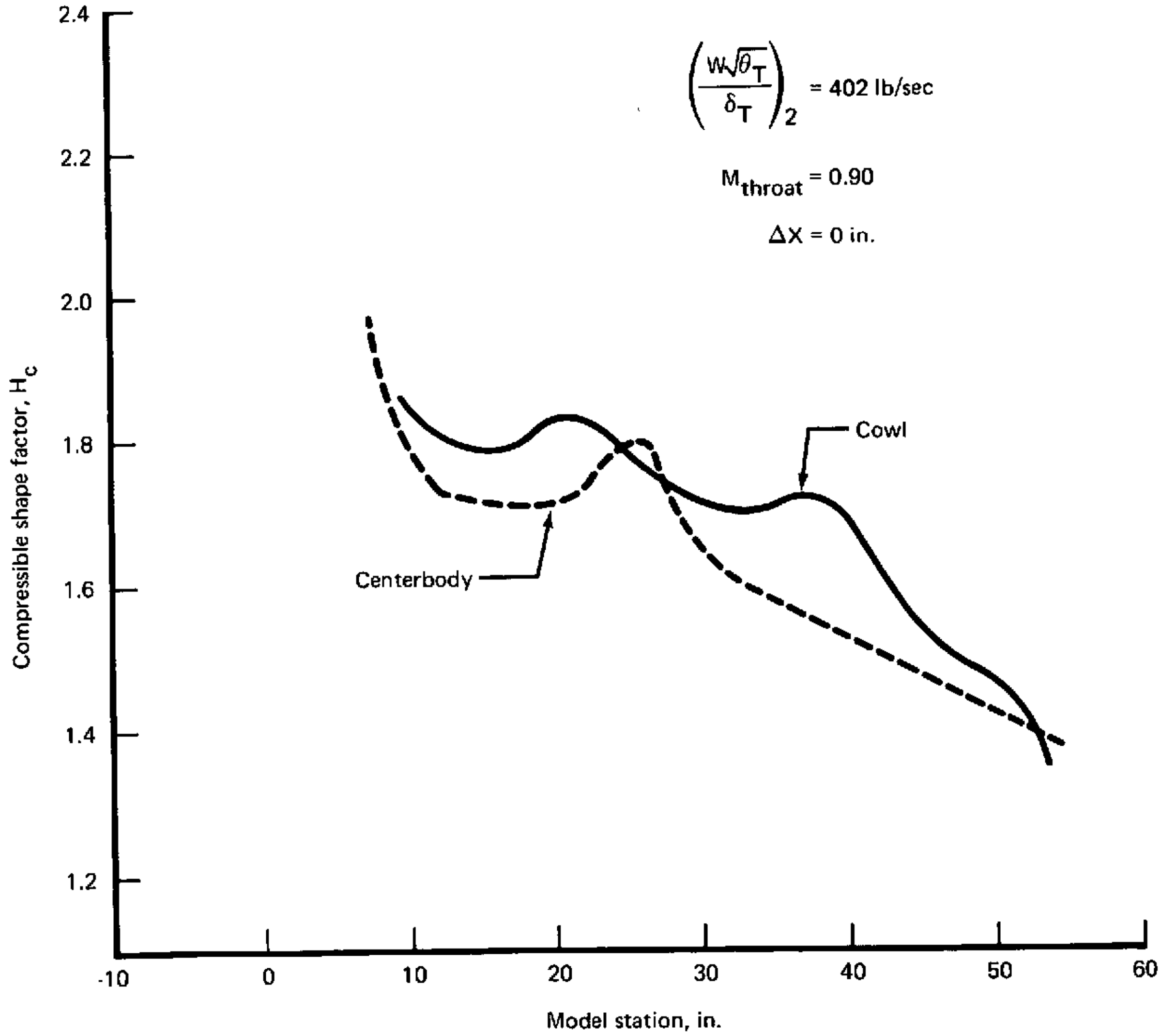

FIGURE B-17.—BOUNDARY LAYER SHAPE FACTOR, APPROACH CONFIGURATION, TRANSLATING C/B INLET (FS), L/D = 1.0

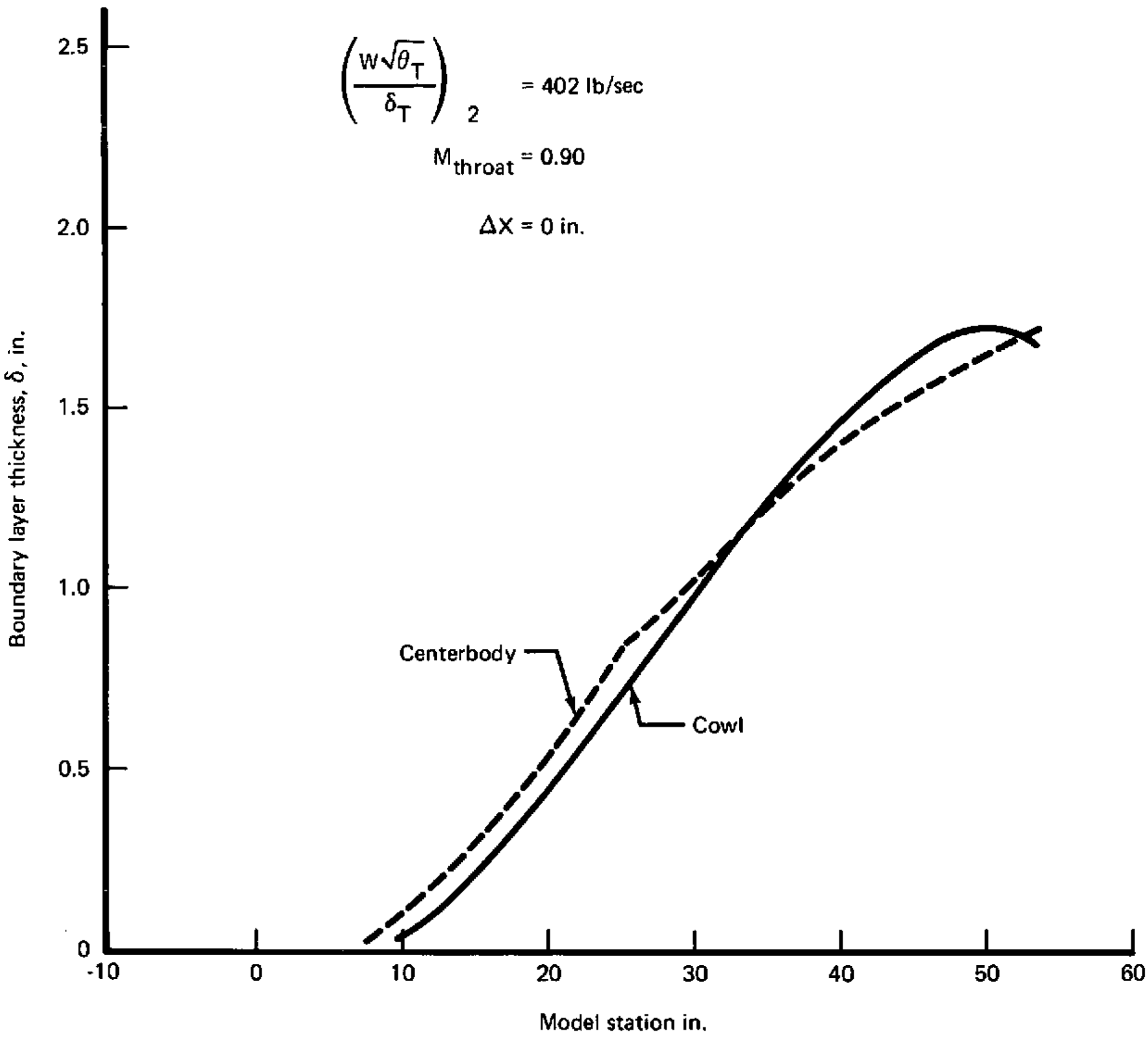

FIGURE B-18.—BOUNDARY LAYER THICKNESS, APPROACH CONFIGURATION TRANSLATING C/B INLET (FS), L/D = 1.0

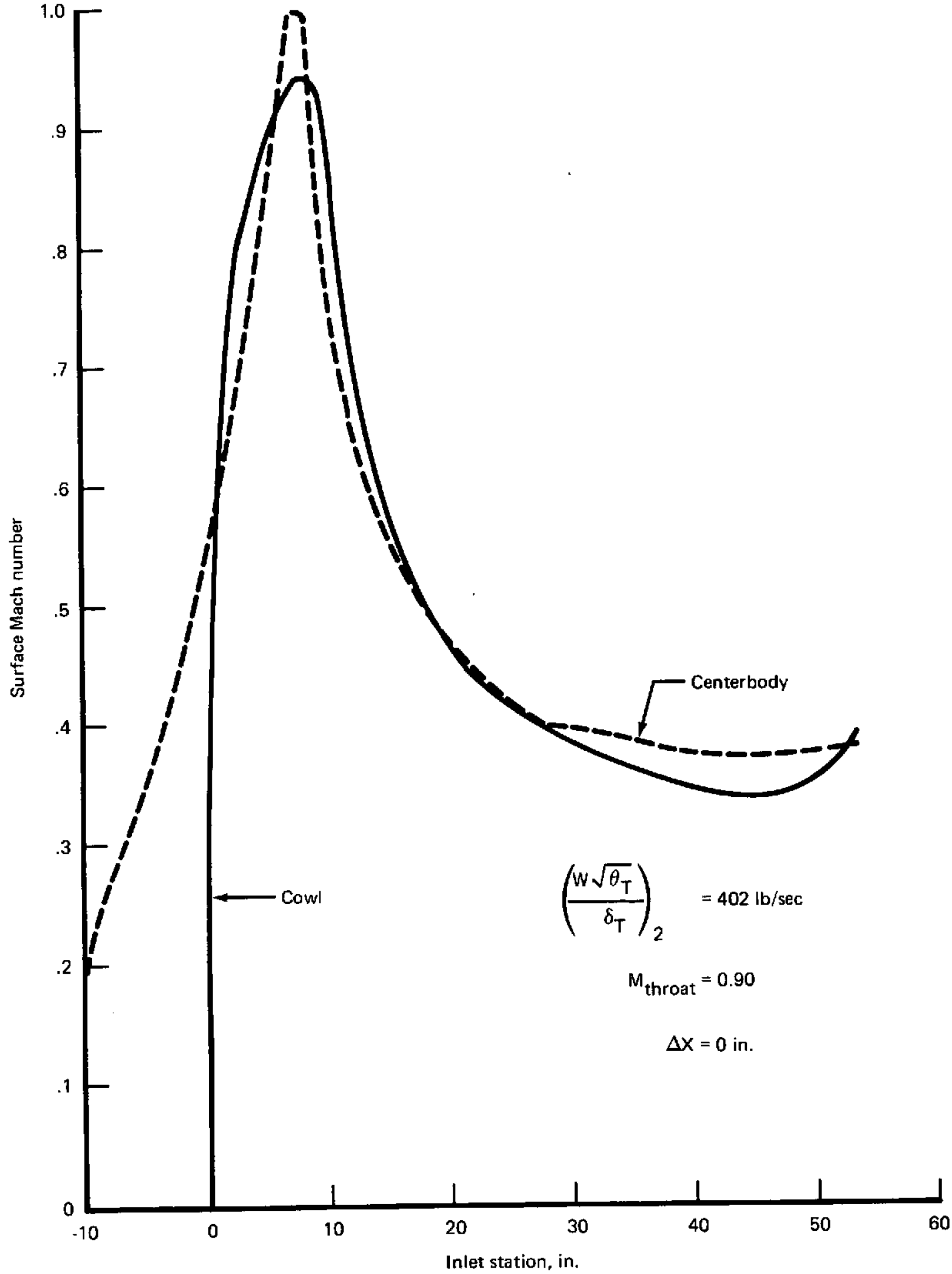

FIGURE B-19.—SURFACE MACH NUMBER DISTRIBUTION, APPROACH CONFIGURATION, TRANSLATING C/B INLET (FS), L/D = 1.0

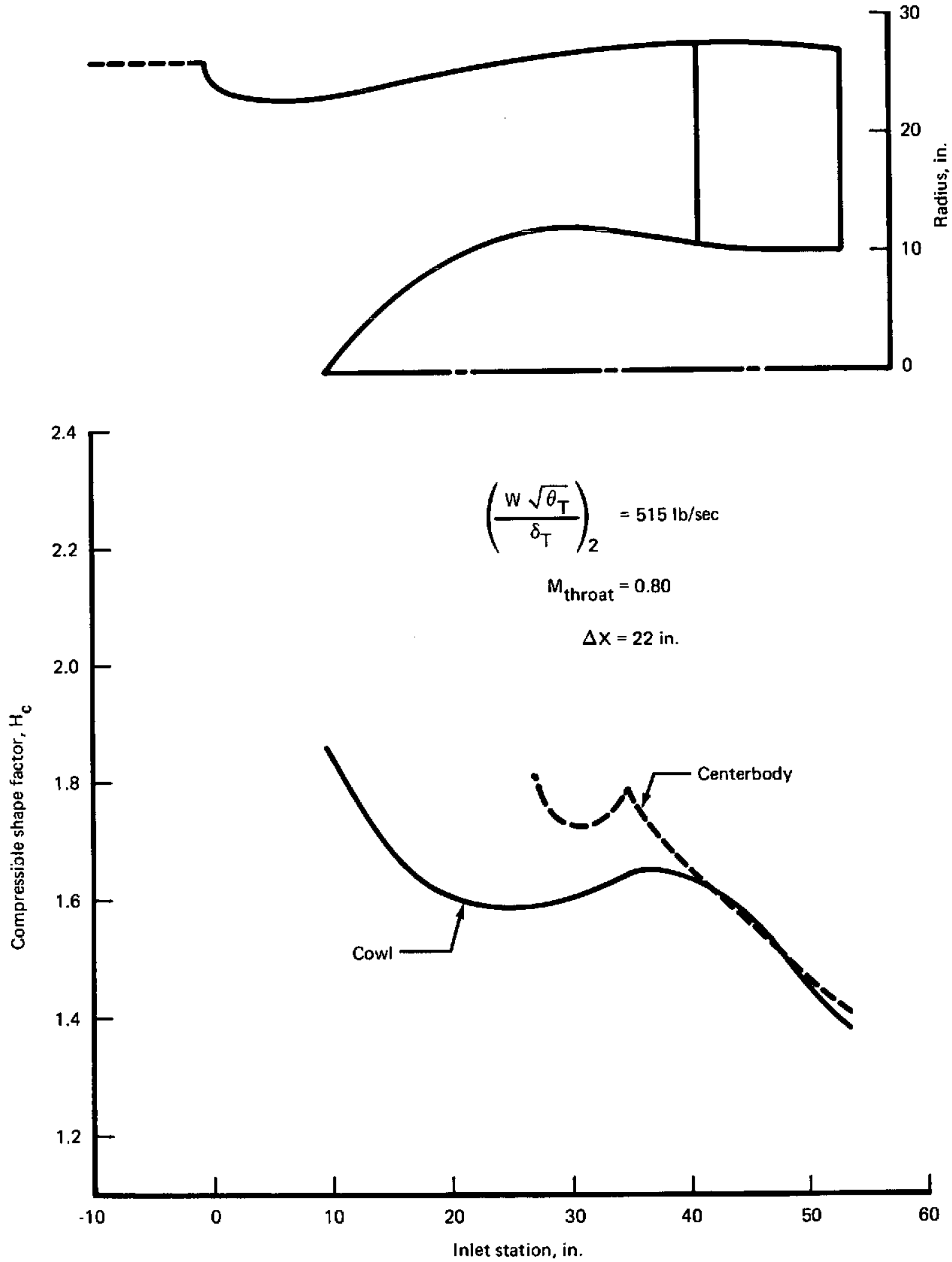

FIGURE B-20.—BOUNDARY LAYER SHAPE FACTOR, TAKEOFF CONFIGURATION, TRANSLATING C/B INLET (FS), L/D = 1.0

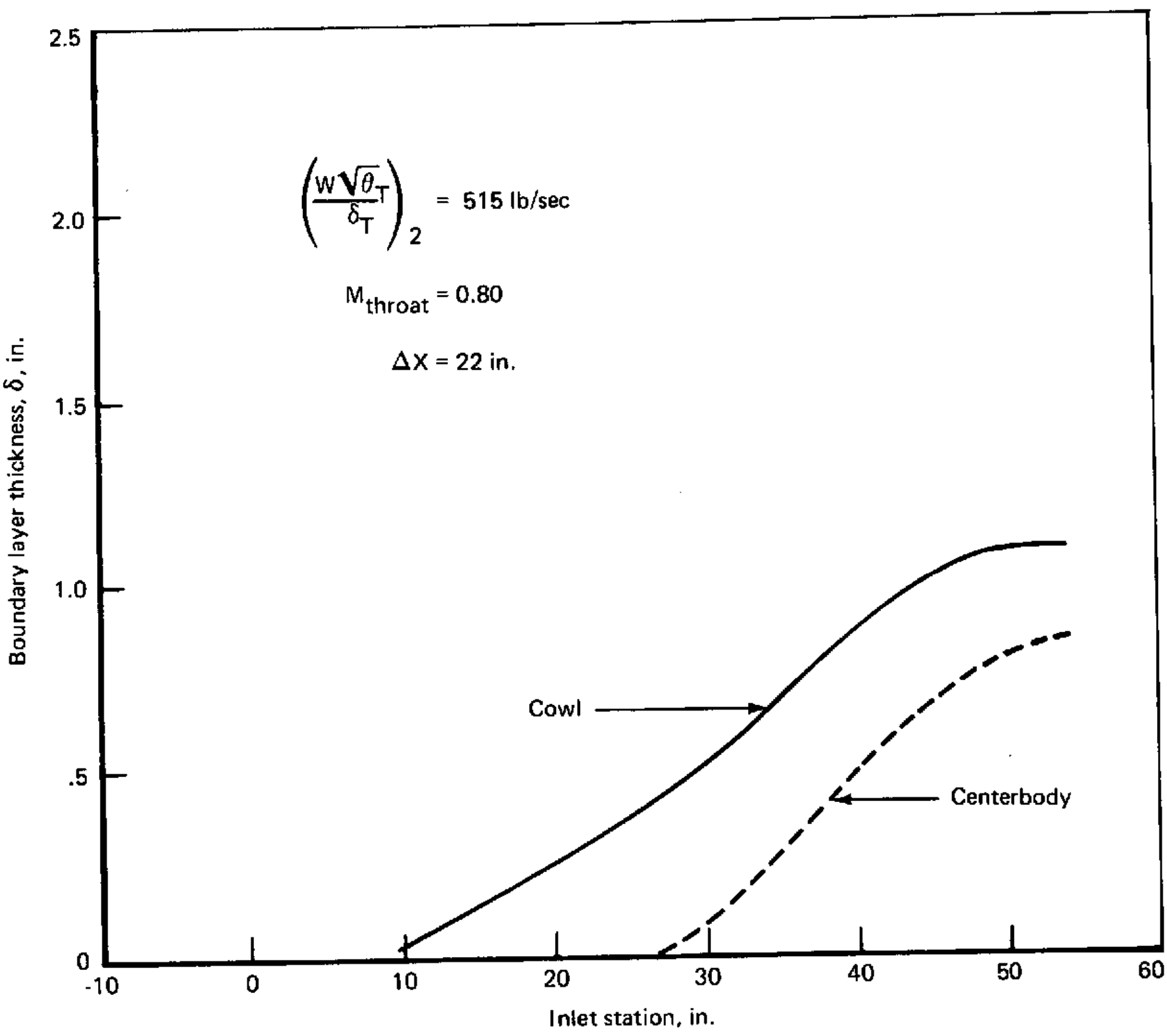

FIGURE B-21.—BOUNDARY LAYER THICKNESS, TAKEOFF CONFIGURATION, TRANSLATING C/B INLET (FS), L/D = 1.0

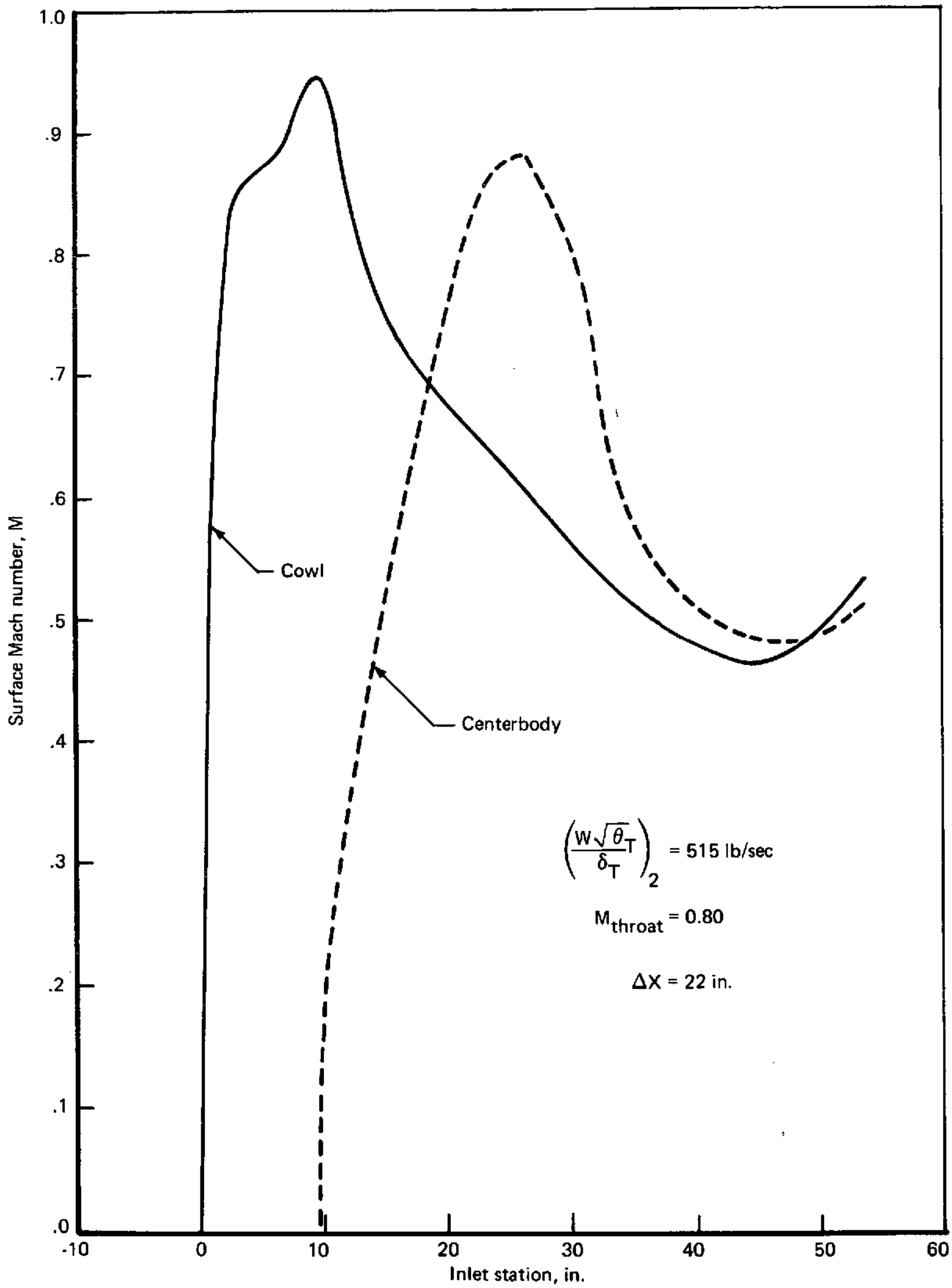

FIGURE B-22.—SURFACE MACH NUMBER DISTRIBUTION, TAKEOFF CONFIGURATION, TRANSLATING C/B, INLET (FS), L/D = 1.0

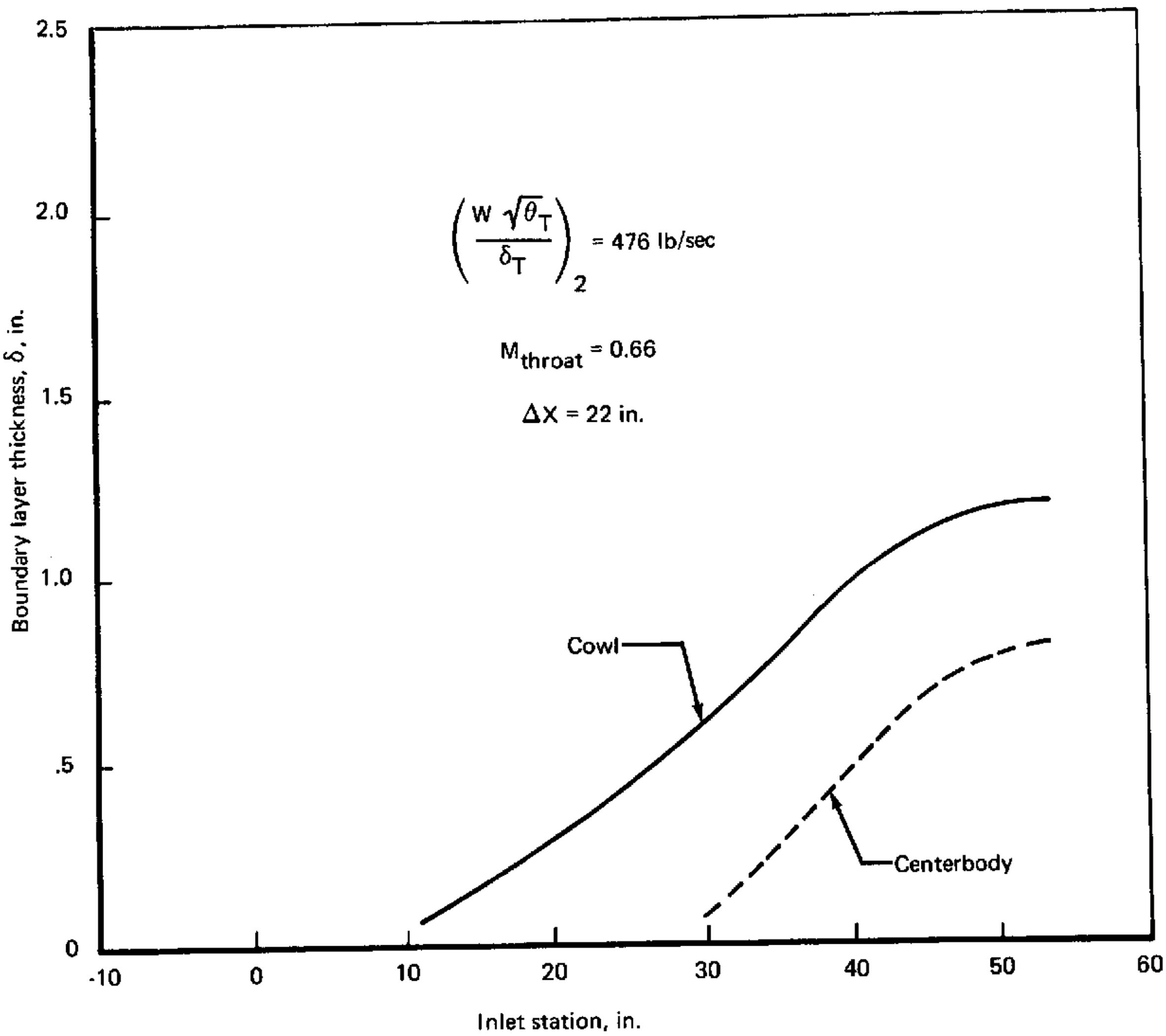

FIGURE B-23.—BOUNDARY LAYER THICKNESS, CRUISE CONFIGURATION, TRANSLATING C/B INLET (FS) L/D = 1.0

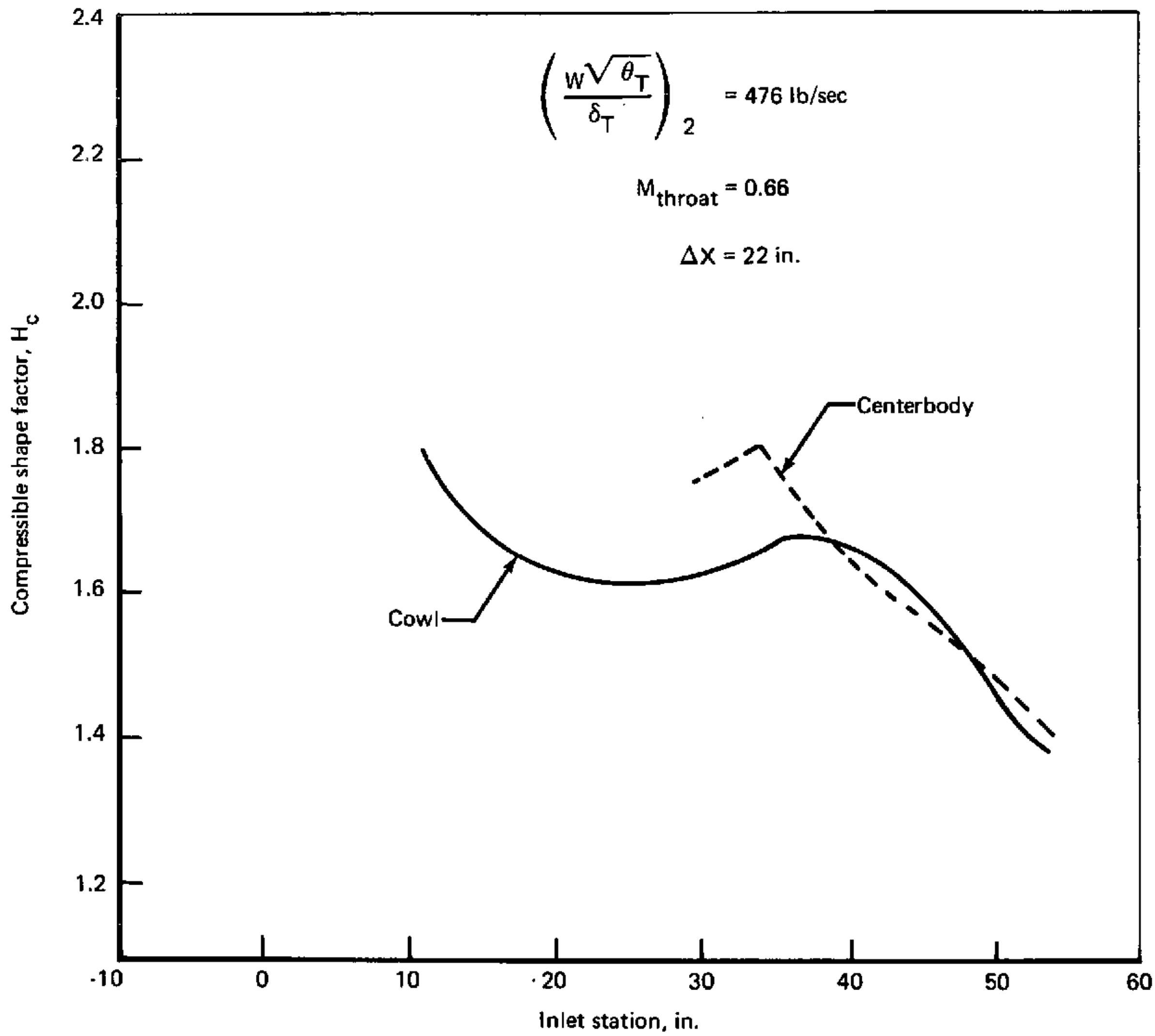

FIGURE B-24.—BOUNDARY LAYER SHAPE FACTOR, CRUISE CONFIGURATION, TRANSLATING C/B INLET (FS), L/D = 1.0

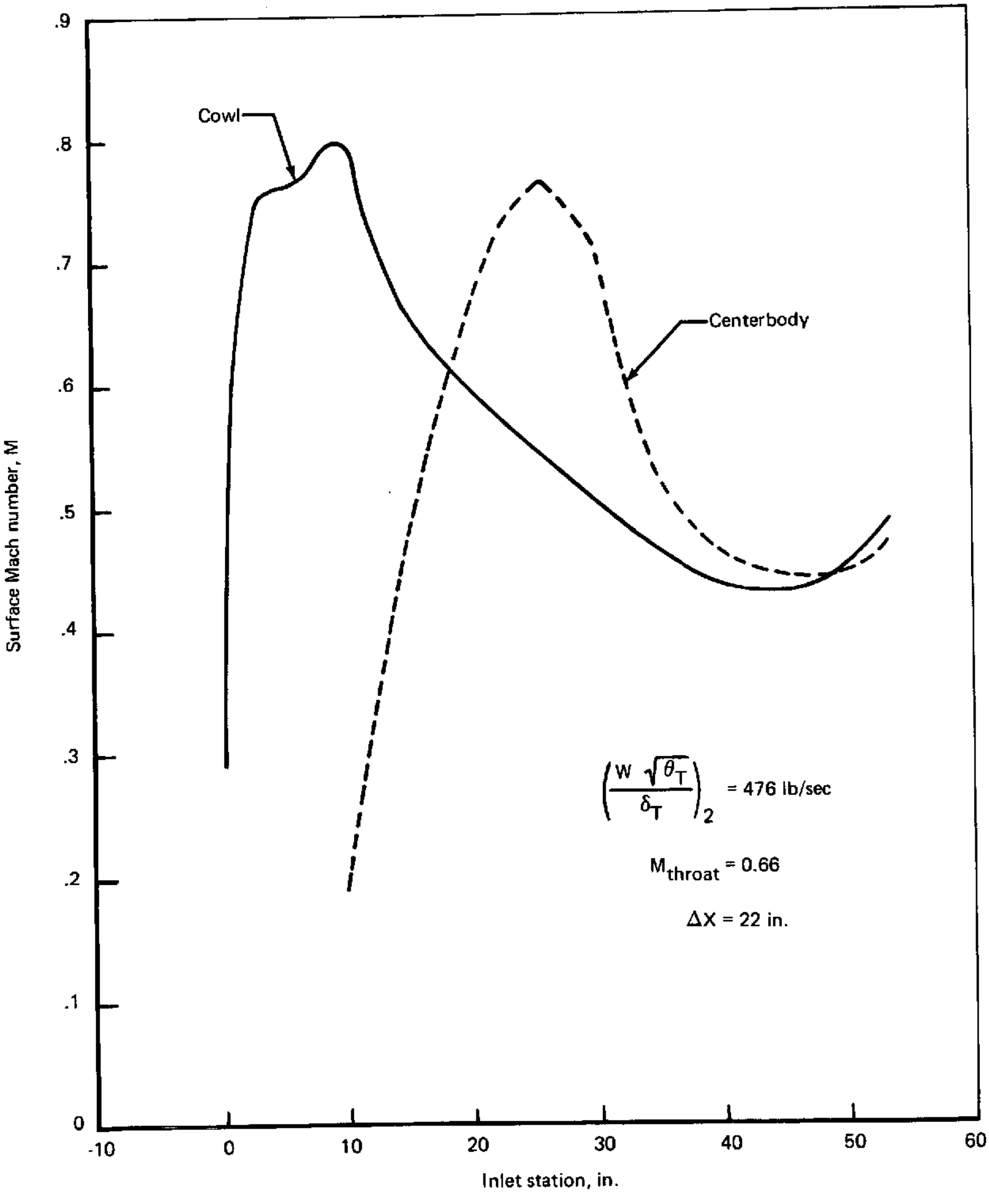

FIGURE B-25.—SURFACE MACH NUMBER DISTRIBUTION, CRUISE CONFIGURATION, TRANSLATING C/S INLET (FS), L/D = 1.0

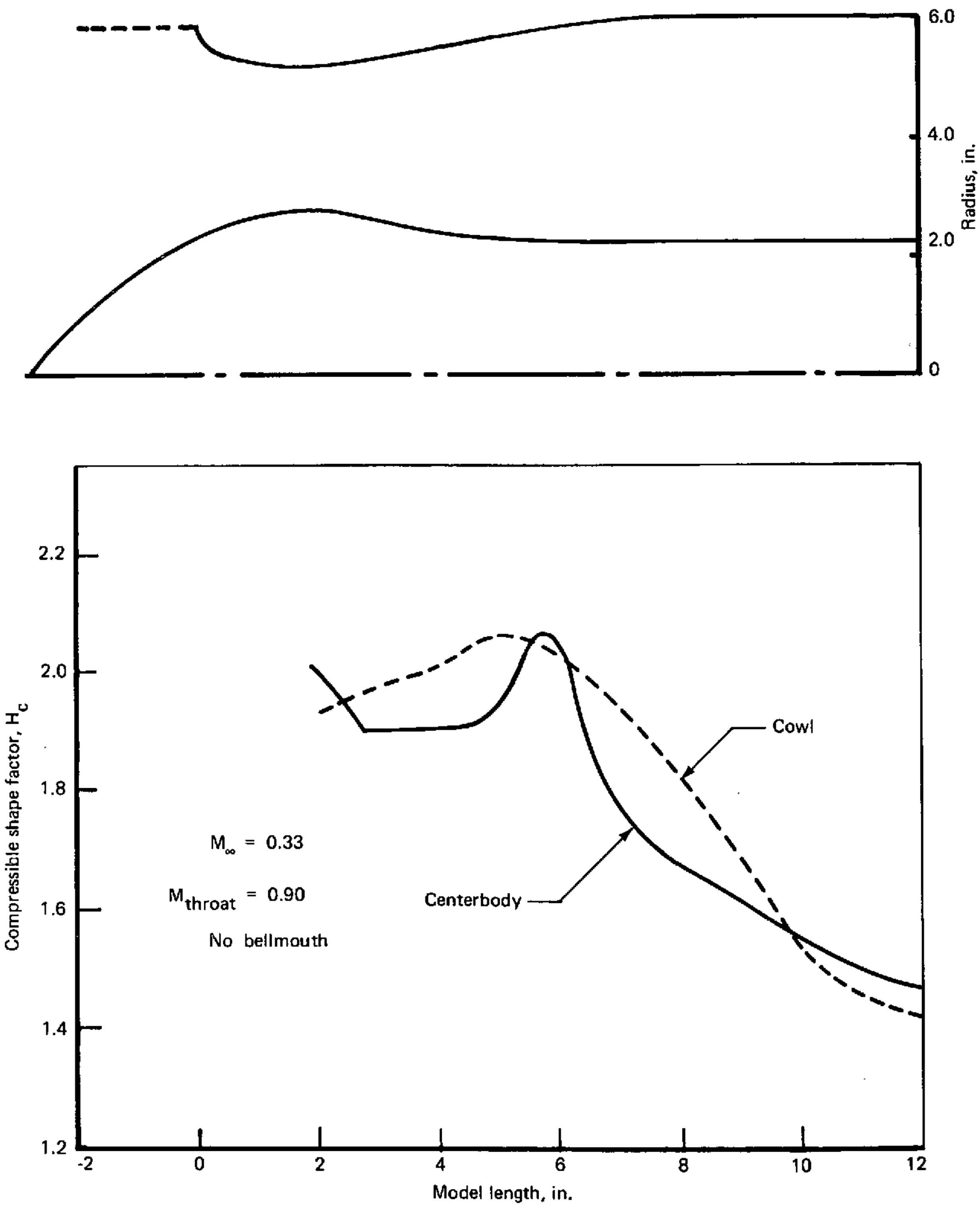

FIGURE B-26.—MODEL-SCALE BOUNDARY LAYER SHAPE FACTOR, APPROACH CONFIGURATION, TRANSLATING C/B INLET, L/D = 1.0

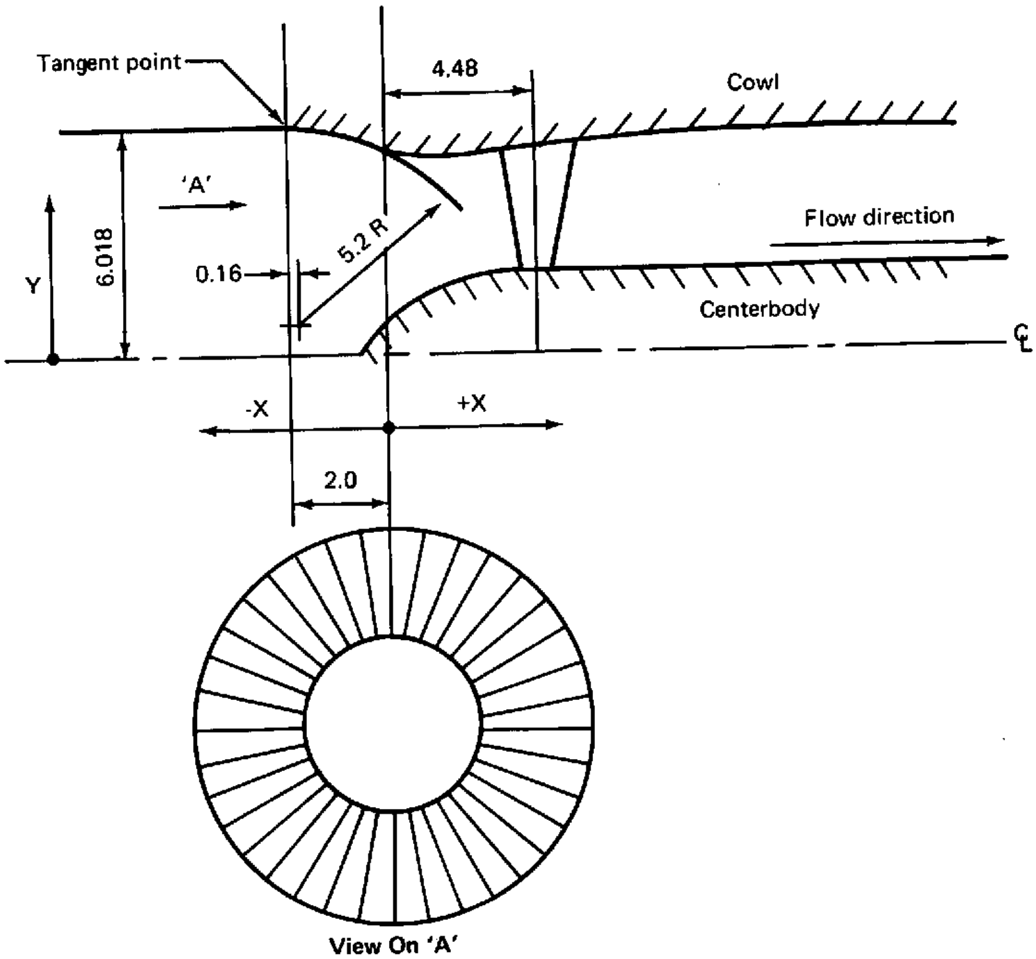

Cowl		Centerbody	
X	Y	X	Y
0	5.45	-0.6	0
0.28	5.37		2:1 Ellipse
0.59	5.31	3.125	2.287
0.88	5.29		Constant
1.88	5.33		
2.88	5.45		
3.88	5.58		
4.78	5.70		
7.40	5.90		
9.65	5.98		
13.10	6.018		

All dimensions in inches

FIGURE B-27.—MODEL 5A, L/D = 1.0, MULTIPASSAGE TYPE I CONFIGURATION

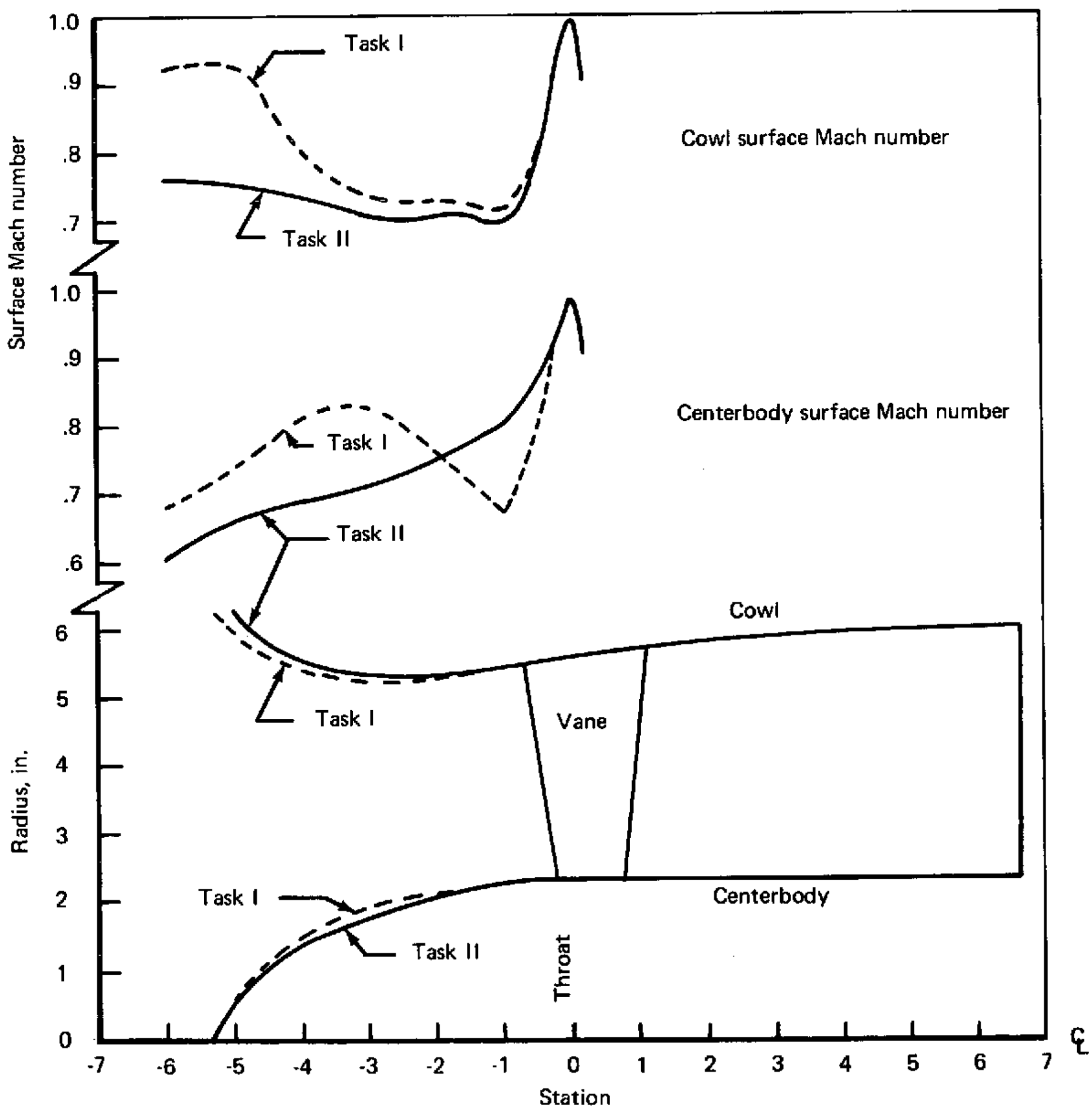

FIGURE B-28.—DESIGN MODIFICATIONS TO RADIAL VANE INLET FOR PHASE II TESTING

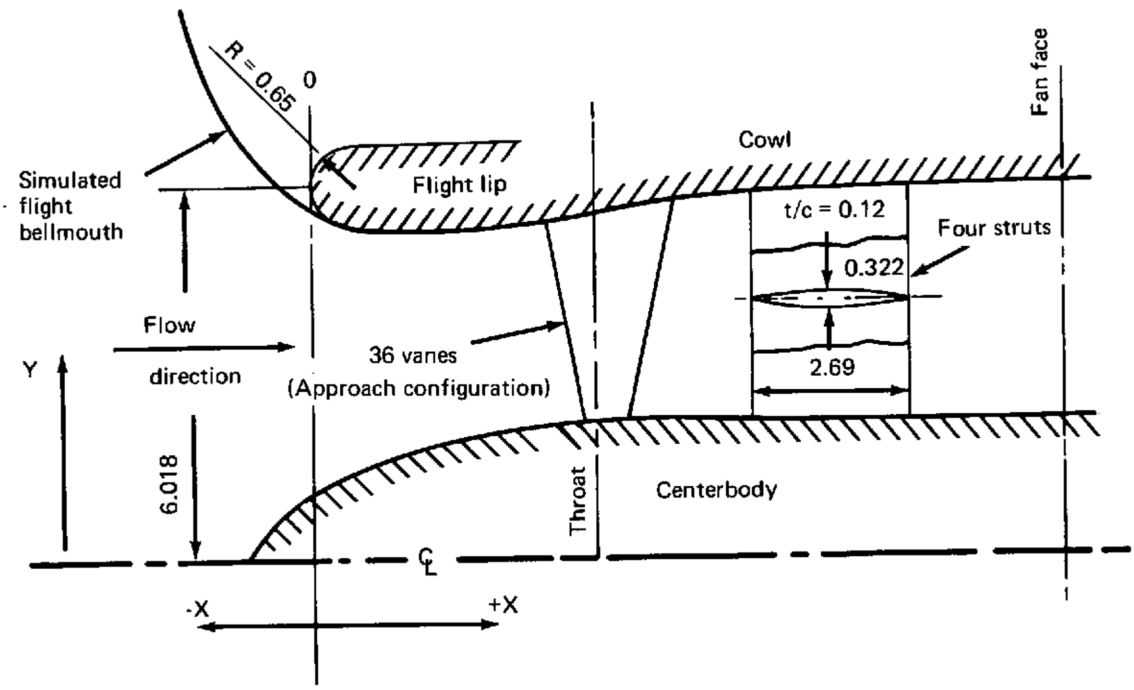

	Cowl		Centerbody	
	X	Y	X	Y
			-0.82	0
			-0.50	0.68
	0	6.018	0	1.10
	0.50	5.400	0.50	1.37
	1.00	5.320	1.00	1.57
	1.50	5.290	1.50	1.75
	2.00	5.290	2.00	1.89
	2.50	5.310	2.50	2.01
	3.00	5.335	3.00	2.12
	3.50	5.370	3.50	2.20
	4.00	5.430	4.00	2.27
Throat	4.50	5.520	4.50	2.28
	5.50	5.710	5.50	2.28
	6.50	5.820	6.50	2.28
	7.50	5.900	7.50	2.28
	8.50	5.930	8.50	2.28
	9.50	5.960	9.50	2.28
	10.50	6.000	10.50	2.28
Fan face	12.036	6.018	12.036	2.28

All dimensions in inches

FIGURE B-29.—MODEL 5B, L/D = 1.0 MULTIPASSAGE TYPE I CONFIGURATION (PHASE II)

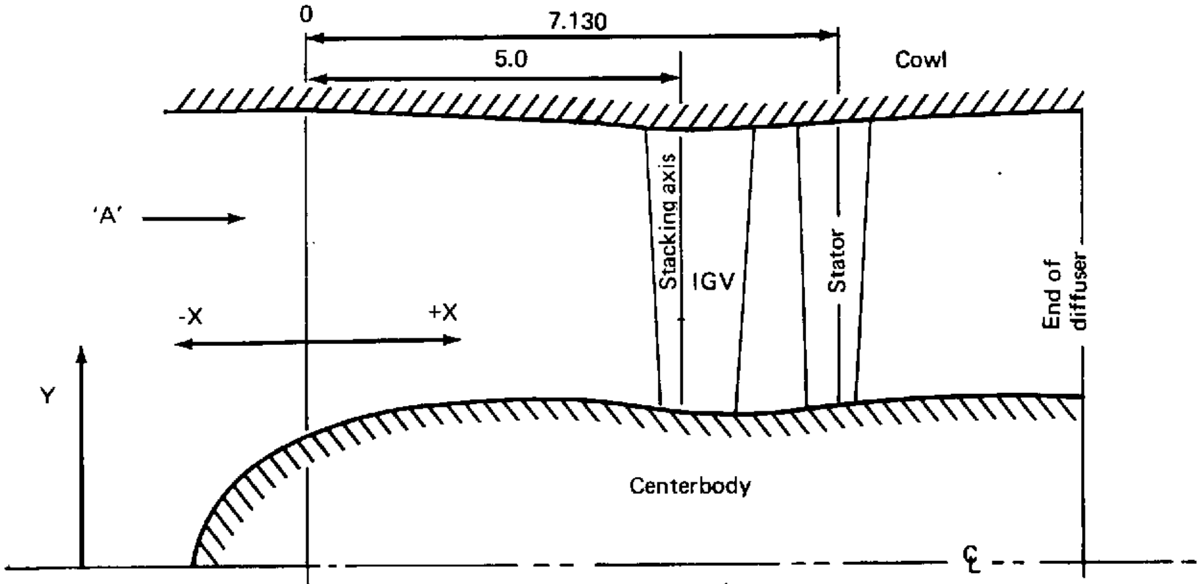

Centerbody	
X	Y
-1.5	0
-0.9	1.215
0	1.800
1.125	2.160
2.250	2.250
3.375	2.182
4.049	2.092
4.274	2.088
4.500	2.083
5.000	2.020
5.400	1.984
5.624	1.980
5.849	1.985
6.074	2.000
6.299	2.025
6.524	2.043
6.749	2.074
7.199	2.124
7.424	2.144
7.649	2.160
8.099	2.191
8.549	2.214
9.00	2.232
10.349	2.252

Cowl	
X	Y
1.125	6.018
2.25	5.950
3.375	5.900
4.049	5.860
4.274	5.849
4.500	5.827
5.000	5.777
5.400	5.750
5.624	5.746
5.849	5.752
6.074	5.773
6.299	5.804
6.524	5.842
6.749	5.874
7.199	5.926
7.424	5.946
7.649	5.959
8.099	5.982
8.549	5.993
9.000	6.007
10.349	6.018

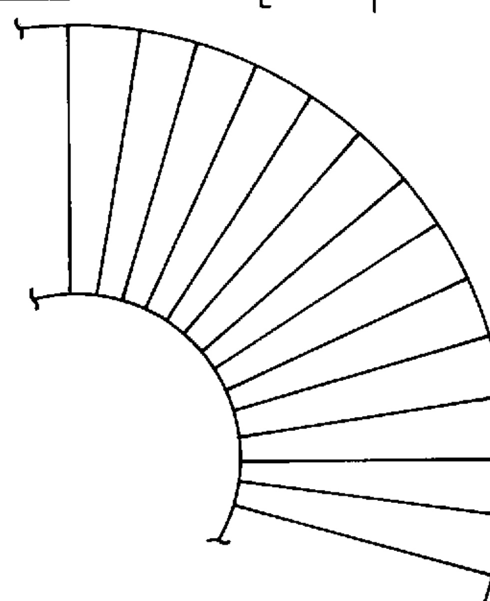

Part View On 'A'

All dimensions in inches

FIGURE B-30.—MODEL 6, L/D = 1.0 MULTIPASSAGE TYPE II CONFIGURATION

Tip section (R = 5.777)
NACA 63-008
Chord = 1.4015
Solidity = 1.66

Hub section (R = 2.02)
NACA 63-004
Chord = 1.05
Solidity = 3.34

θ = blade twist angle

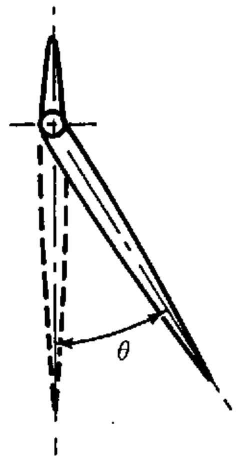

45 Guide Vanes (IGV)

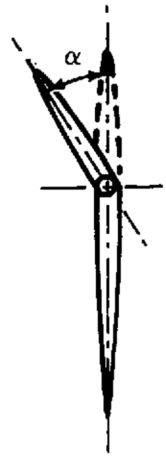

45 Stators

Tip section (R = 5.899)
NACA 64-008
Chord = 0.84
Solidity = 1.0

Hub section (R = 2.099)
NACA 64-004
Chord = 0.607
Solidity = 1.91

α = blade turning angle

All dimensions in inches

NACA 63-008		NACA 64-008		IGV		Stator	
X, % chord	Y, % chord	X, % chord	Y, % chord	Radius	θ, deg	Radius	α, deg
0	0	0	0	1.9797	26.56	2.0742	26.56
0.5	0.664	0.5	0.658	2.5552	30.96	2.5916	30.96
0.75	0.8055	0.75	0.794	3.0391	34.65	3.0505	34.65
1.25	1.023	1.25	1.005	3.4694	36.74	3.4645	36.74
2.50	1.4065	2.50	1.365	3.8620	38.47	3.8559	38.47
5.00	1.9510	5.0	1.875	4.2253	39.58	4.2226	39.58
7.50	2.358	7.5	2.259	4.5646	40.24	4.5714	40.24
10.0	2.686	10.0	2.574	4.8834	40.86	4.9043	40.86
15.0	3.190	15.0	3.069	5.1851	41.37	5.2283	41.37
20.0	3.550	20.0	3.437	5.4719	41.83	5.5500	41.83
25.0	3.797	25.0	3.704	5.7457	42.27	5.8739	42.27
30.0	3.946	30.0	3.884				
35.0	4.000	35.0	3.979				
40.0	3.954	40.0	3.992				
45.0	3.821	45.0	3.883				
50.0	3.609	50.0	3.684				
55.0	3.328	55.0	3.411				
60.0	2.991	60.0	3.081				
65.0	2.608	65.0	3.704				
70.0	2.191	70.0	2.291				
75.0	1.754	75.0	1.854				
80.0	1.313	80.0	1.404				
85.0	0.885	85.0	0.961				
90.0	0.403	90.0	0.550				
95.0	0.176	95.0	0.205				
100.0	0	100.0	0				

FIGURE B-31.—MODEL 6, IGV AND STATOR DETAILS

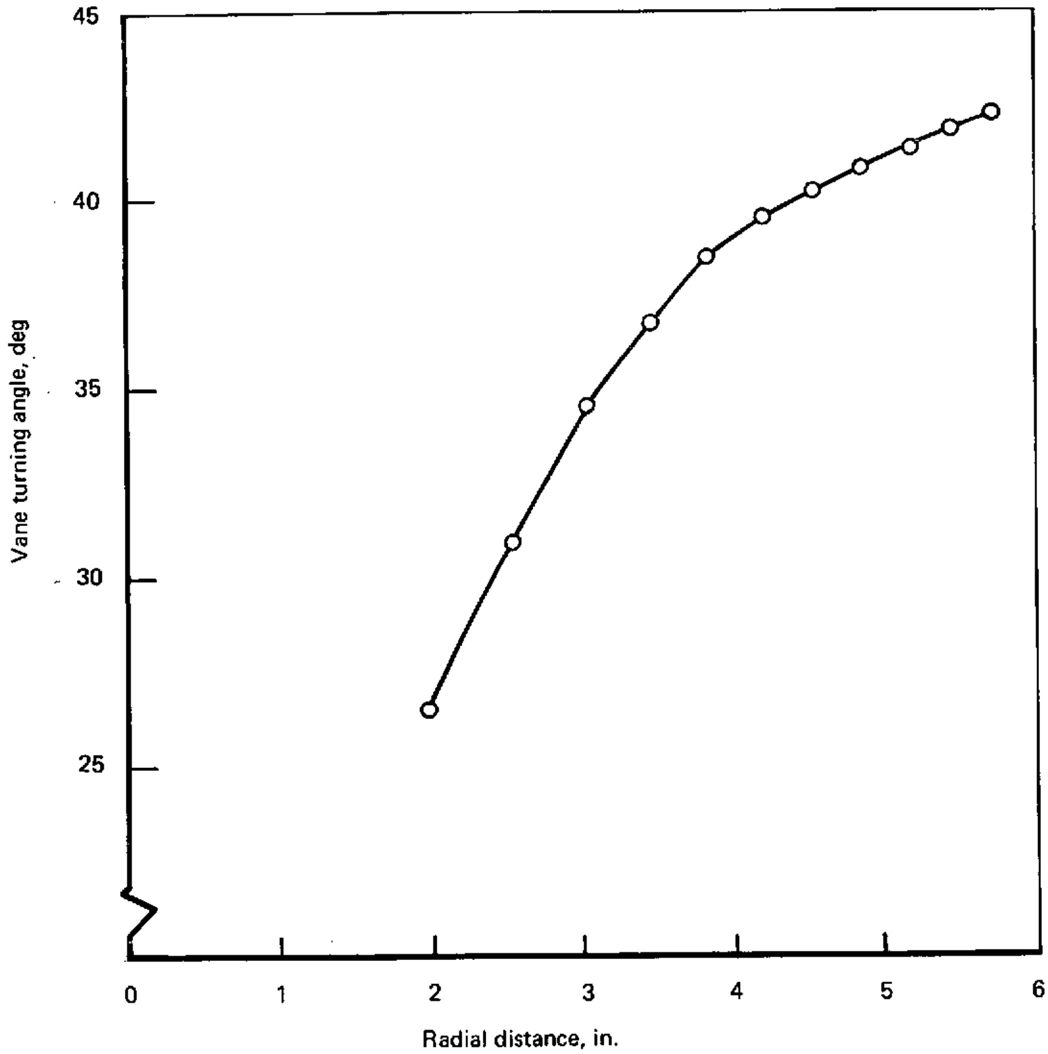

FIGURE B-32.—VANE TURNING ANGLE DISTRIBUTION, DOUBLE ARTICULATED VANE INLET

APPENDIX C

TEST PROCEDURE AND INSTRUMENTATION DETAILS

C.1 TEST APPROACH

A baseline test was followed by test runs to acquire data on six different inlet designs. A long bellmouth and straight-wall duct were installed for a "baseline" noise test against which all sonic inlet models could be compared.

Some of the models were tested under more than one throat area setting or experimental configuration. A new test run number was assigned to each configuration, and thus some inlet models have more than one run number associated with them. This relationship is recorded in table C-1. The design drawing numbers of each model along with some description of sonic inlet hardware are summarized in table C-2.

A range of throat Mach numbers from 0.5 to 1.0 was obtained in the inlet models. This was accomplished with a 12-in. test fan, which took the place of an engine in that it provided both an air suction source and a noise source.

The 12-in. fan rig consisted of a 32-bladed rotor mounted in a housing and discharge case which contained a translating cone to control backpressure on the fan. No inlet guide vanes were installed during these tests, but tandem stators were installed in the fan discharge duct. These two rows of exit stators consisted of 27 blades per row. The leading edge of the first row of stators was located downstream at a distance equal to two true chords of the rotor. The fan face hub-to-tip ratio of the rotor was 0.38.

Drive power for the fan was provided by a turbodrive directly coupled to the fan shaft. Energy for the drive turbine was derived from plant air that was put through a combustion chamber prior to its introduction into the turbine nozzle. Rotational speed of the unit was controlled by manipulating both the fuel flow and air flow to the turbine; desired throat Mach number settings in the test models were obtained by this means. The fan rpm was measured by a magnetic pickup installed near a gear driven by the turbine shaft. This rpm was always recorded on a separate track of the magnetic tape, concurrently with acoustic data, to provide the necessary input for tone tracking during acoustic data analysis. Aerodynamic data were recorded on punched paper tape and reduced to engineering units by a computer, which also performed most of the required calculations.

TABLE C-1.—SONIC INLET TEST MODEL INDEX

Model	L/D	Run	Fig. no.	Description
0	2.0	1	C-1	Baseline configuration: straight, constant-diameter duct with long bellmouth fitted
1	2.0	2	C-2, -3	Fundamental (contracting cowl) inlet; approach configuration with long bellmouth fitted
2	1.0	3	C-4	Fundamental (contracting cowl) inlet; takeoff configuration with long bellmouth fitted
3	1.3	4	C-5	Translating centerbody inlet; approach configuration with long bellmouth fitted
		5	C-6	Takeoff configuration with long bellmouth fitted
3A	1.3	101	C-9	Model 3, approach configuration with acoustic lining added to internal surfaces.
3B	1.3	102	C-10	Model 3, approach configuration with acoustic lining added to internal cowl surface and diffuser section of centerbody only
3C	1.3	10	C-13	Model 3, approach configuration with acoustic lining added to diffuser section only
4	1.0			Translating centerbody inlet; approach configuration
		6	C-7	• Long bellmouth fitted
		8	C-11	• Flight lip fitted
		11	C-14, -15, -16	• Flight lip fitted (part of run) short bellmouth (remainder)
		12	C-17	Takeoff configuration with short bellmouth fitted
5A	1.0	7	C-8	Radial vane inlet; approach configuration with long bellmouth fitted
5B	1.0	13	C-18, -19	Radial vane inlet; approach configuration with long bellmouth fitted
		14	C-18	Takeoff configuration with short bellmouth fitted
6	1.0	9	C-12	Double-articulating vane inlet; approach configuration • Short bellmouth fitted (part of run) • Flight lip fitted (remainder of run)

TABLE C-2.—SONIC INLET CONFIGURATION SUMMARY

Run	Model	L/D	Boeing design drawing	Description
1	0	2.0	–	Baseline, straight pipe inlet
2	1	2.0	5342-1	Fundamental inlet, approach throat
3	2	1.0	5364-4	Fundamental inlet, takeoff throat
4	3	1.3	5364-5	Centerbody inlet, approach thorat
5	3	1.3	5364-5	Centerbody inlet, takeoff throat
6	4	1.0	5364-15	Centerbody inlet, approach throat
7	5A	1.0	5364-16	Radial vane inlet, approach throat, multipassage inlet, type 1
101	3A	1.3	5369-1	Centerbody inlet, approach throat, acoustic lining on cowl and centerbody
102	3B	1.3	5369-1	Centerbody inlet, approach throat, identical to run 101 except removed 5369-3 portion of lined centerbody and installed hardwall portion of 5364-7-1 assembly
8	4	1.0	5364-15-2	Centerbody inlet, approach throat, same as run 6 except installed flight lip instead of bellmouth
9	6	1.0	5364-20	Double-articulating vane inlet, approach throat, multipassage inlet, type 2
10	3C	1.3	5369-1	Centerbody inlet, approach throat, acoustically lined diffuser, hardwall throat
11	[a]4	1.0	5364-31-1	Centerbody inlet, approach throat, same as run 6, except with P_T probes on four struts at diffuser exit, short bellmouth for simulated flight inflow
12	[a]4	1.0	5364-31-1	Centerbody inlet, takeoff throat, same as run 11 except retracted centerbody by 3.85 in., short bellmouth for simulated flight inflow
13	[b]5B	1.0	5364-40A-1	Radial vane inlet, approach throat, rotating P_T rake at diffuser exit, short bellmouth for simulated flight airflow, same as run 7 but with different centerbody
14	[b]5B	1.0	5364-40A-1	Radial vane inlet, takeoff throat, same as run 13 but with vanes removed for takeoff area, short bellmouth for simulated flight inflow

[a] Final inlet concept 1

[b] Final inlet concept 2

C.2 DATA KEYS

During each test run the inlet models were subjected to a range of different operating conditions (and throat Mach numbers), and each different operating condition was assigned a number. A description of the operating parameters for each condition number was compiled in a data key for each test run. These data keys are included in the following pages.

RUN 1 DATA KEY

Baseline 26-in. straight wall inlet, L/D $\approx$ 2.0

CONDITION	REMARKS
1 through 35	Basic aerodynamic data only—to establish fan map. No traverses taken.
36 through 54	Basic aerodynamic far-field noise, and plane 6 wall-mounted Kulite. Points along a selected operating line.
36, 38, 41, 46, 49, 54	Aerodynamic data with plane 6, traverse to establish inlet recovery of bellmouth and straight-wall long inlet.
55	Slow acceleration, with nozzle area as for Condition 54. Recorded far-field noise plus PL 6 Kulite.
56	Slow acceleration, with nozzle area as for Condition 23. Recorded far-field noise on all 10 microphones plus PL 6 Kulite.

RUN 2 DATA KEY

Fundamental approach inlet, Model 1, L/D = 2.0, Dwg. 5342-1,
Test conditions 1 through 7

Full aerodynamic and acoustic data, with boundary layer probes in the inlet and P_S, P_T traverse at the fan face. No near-field noise data.

Run 2 Test Condition	Normalized Throat Average Mach No.	Throat Wall Mach No.	Recovery	Mechanical rpm	Nearest condition from Run 1 Baseline	
					Condition	Mechanical rpm
1	0.517	0.558	0.996	13 920	36	13 910
2	0.667	0.734	0.994	16 590	38	16 350
3	0.798	0.882	0.990	17 920	39	17 780
4	0.860	0.966	0.985	18 760	40-41	18 220-18 690
5	1.000	1.074	0.974	19 210	42	19 190
6	0.972	1.075	0.959	19 580	43	19 620
7	0.951	1.078	0.952	19 950	44	20 040

RUN 2 DATA KEY

Fundamental approach inlet, Model 1, L/D = 2.0, Dwg. 5342-1,
Test conditions 8 through 15

Near-field noise data plus stinger Kulite
and P_S traverses

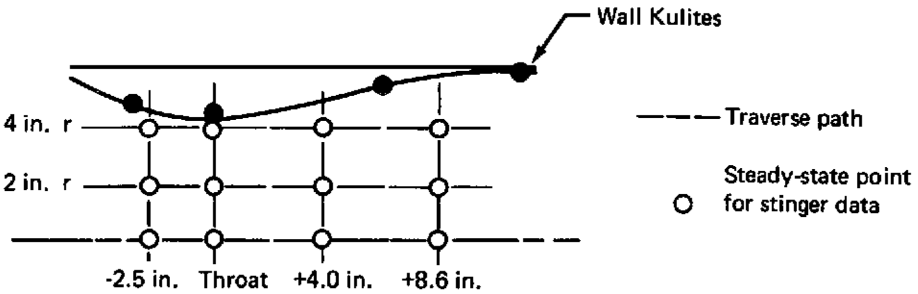

Run 2 Test Condition	Normalized Throat Average Mach No.	Throat Wall Mach No.	Recovery	Mechanical rpm	Nearest condition from Run 1 Baseline: Condition	Nearest condition from Run 1 Baseline: Mechanical rpm
8	Stall margin investigation					
9	Stall margin investigation					
10	≈0.52	0.548		14 250	36	13 910
11	≈0.67	0.725		16 770	38	16 350
12	≈0.80	0.880		18 040	39	17 780
13	≈0.86	0.960		17 950	39-40	17 780-18 220
14	≈0.98	1.053		17 990	40	18 220
* 15	≈0.90	0.933		18 000	40	18 220

* Stinger Kulite steady-state points of symbol O in diagram were taken for condition 15 only. Conditions 10 through 14 have continuous traverses of stinger.

RUN 3 DATA KEY

Fundamental inlet, takeoff throat, Model 2, L/D = 1.0, Dwg. 5364-4

Test conditions 1 through 5

Full aerodynamic data with boundary layer rakes and P_S, P_T traverse at the fan face.

Recorded far-field acoustic data but no near-field acoustic data.

Test conditions 6, 7, and 8

All near-field acoustic data plus midstream stinger traverses. Duct wall Kulites at planes in the inlet: planes 3, 4, 5, and 6, plus stinger Kulite and P_S.

Continuous traverses were taken along three radial paths and three axial paths as shown below. Steady-state data in midstream were taken at the circled locations shown.

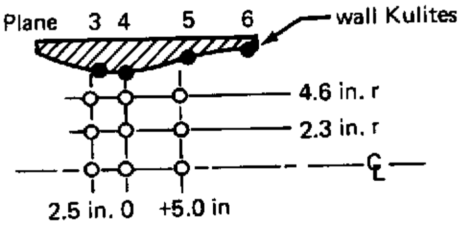

Run 3 Test Condition	Normalized Throat Average Mach No.	Throat Wall Mach No.	Recovery	Mechanical rpm	Nearest condition from Run 1 Baseline	
					Condition No.	Mechanical rpm
1	0.515	0.566	0.997	18 140	40	18 220
2	0.615	0.674	0.996	19 350	43	19 620
3	0.725	0.802	0.994	21 890	46-47	21 040-22 180
4	0.863	0.948	0.990	22 980	47-48	22 180-23 410
5	1.000	1.082	0.986	23 730	48	23 410
6	≈0.72	0.792		22 010	46-47	21 040-22 180
7	≈0.86	0.942		23 050	47-48	22 180-23 410
8	≈1.0	1.066		23 640	48	23 410

RUN 4 DATA KEY

Centerbody inlet, approach throat, Model 3, L/D = 1.3, Dwg. 5364-5

Test conditions 1 through 5

Full aerodynamic data with boundary layer rakes and P_S, P_T traversed at the fan face. Recorded far-field acoustic data, with near-field acoustic data on the duct wall only near the fan face.

Test conditions 6 through 16

A repeat of conditions 1 through 5. The noise data from conditions 6 through 16 supersede those of conditions 1 through 5. Aerodynamic data are supplemental to the previous conditions.

Run 4 Test Condition	Normalized Throat Average Mach No.	Throat Wall Mach No.	Recovery	Mechanical rpm	Nearest condition from Run 1 Baseline	
					Condition No.	Mechanical rpm
1	≈0.50	0.52	0.996	14 940	37	14 350
2	≈0.60	0.62	0.995	16 820	38	16 350
3	≈0.70	0.72	0.992	17 930	39	17 780
4	≈0.82	0.83	0.986	19 160	41	18 690
5	≈0.98	0.91	0.984	19 350	42	19 190
6	0.505	0.52	0.996	14 000	37	14 350
7	0.601	0.62	0.994	15 740	38	16 350
8	0.710	0.72	–	17 190	39	17 780
9	0.823	0.82	0.988	18 340	40	18 220
10	0.853	0.84	0.990	18 390	40	18 220
11	0.905	0.89	0.984	18 870	41	18 690
12	1.00	0.93	0.980	19 210	42	19 190
13	1.00	0.93	–	19 330	42	19 190
14	≈1.00	–	–	19 400	43	19 620
15	≈0.893	0.94	0.966	19 910	43	19 620
16	Decell from 19 800 to 14 000 rpm.					

RUN 5 DATA KEY

Centerbody Inlet, takeoff throat, Model 3, L/D = 1.3, Dwg. 5364-5

Full aerodynamic data with boundary layer rakes and P_S, P_T traverse at the fan face. Recorded far-field acoustic data, with near-field acoustic data on the duct wall only near the fan face.

Run 5 Test Condition	Normalized Throat Average Mach No.	Throat Wall Mach No.[a]	Recovery	Mechanical rpm	Nearest condition from Run 1 Baseline	
					Condition 1	Mechanical rpm
1	0.498	0.527	0.995	17 880	39	17 780
2	0.707	0.727	0.993	22 330	47	22 180
3	0.820	0.820	0.992	23 590	48	23 410
4	0.911	0.886	0.989	24 690	50	24 750
5	0.936	0.900	0.989	24 990	51	25 350
[b]6	1.000	0.985	0.985	25 660	52	26 020
7	0.973	1.113	0.970	25 960	52	26 020
[c]8	$\approx$0.973	1.113	$<$0.970	26 300	53	26 500

[a] Only the P statics on the centerbody give a good indication of throat wall Mach number. In the takeoff mode the outer wall statics, at minimum diameter, are ahead of the aerodynamic choke plane.

[b] A deceleration, condition 6A, was taken with all acoustic data on tape, from 25 600 to 14 000 rpm.

[c] No aerodynamic data are available for condition 8.

RUN 6 DATA KEY

Centerbody inlet, approach throat, Model 4, L/D = 1.0, with standard bellmouth, Dwg. 5364-15

Test conditions 1 through 5

Acoustic data from all far-field microphones, near-field acoustic data at duct wall in planes 6 and 7. Plane 6 aerodynamic traverse.

Test condition 6

Far-field and near-field acoustic data, steady state, plus basic aerodynamic data only, no plane 6 traverse. Also have all acoustic data during deceleration from 21 700 to 14 000 rpm.

Test condition 7

All acoustic data taken during acceleration from 14 000 to 21 700 rpm.

Test condition 8

Reset same condition as condition 6 to obtain plane 6 aerodynamic traverse.

Run 6 Test Condition	Normalized Throat Average Mach No.	Throat Wall Mach No.	Recovery	Mechanical rpm	Nearest condition from Run 1 Baseline	
					Condition No.	Mechanical rpm
1	0.491	0.55	0.997	13 600	36	13 910
2	0.687	0.77	0.995	16 750	38	16 350
3	0.807	0.91	0.990	17 900	39	17 780
4	0.894	1.02	0.985	19 150	42	19 190
5	0.923	1.05	0.968	19 850	43	19 620
6	1.00	1.13	0.900	21 700	46-47	21 040-22 180
7	Accel.			14000-21700		
8	0.898	1.13	0.900	21 700	46-47	21 040-22 180

RUN 7 DATA KEY

Radial vane inlet, approach throat, Model 5A with standard bellmouth, L/D = 1.0, Dwg. 5364-16

Test conditions 1 through 5

Acoustic data from all far-field microphones, near-field acoustic at duct wall in planes 6 and 7. Full acoustic data plus plane 6 aerodynamic traverse.

Test condition 6

Same data as conditions 1 through 5, plus acoustic data of a deceleration from 23 500 to 14 000 rpm.

Run 7 Test Condition	Normalized Throat Average Mach No.	Throat Outerwall Mach No.	Recovery	Mechanical rpm	Nearest condition from run 1 baseline	
					Condition No.	Mechanical rpm
1	0.522	0.481	0.993	14 000	36	13 910
2	0.719	0.640	0.983	17 100	38	16 350
3	0.850	0.763	0.973	18 800	41	18 690
4	0.992	0.940	0.943	21 800	46	21 040
5	1.000	1.050	0.884	23 500	48	23 410
6	0.938	0.881	0.952	20 300	44	20 040

RUN 8 DATA KEY

Centerbody inlet, approach throat Model 4, L/D = 1.0, Dwg. 5364-15-2

Same as Run 6 except installed flight lip instead of standard bellmouth.

Installed boundary layer rake on centerbody in plane 5 in addition to plane 6 rakes.

Run 8 Test Condition	Normalized Throat Average Mach No.	Throat Outerwall Mach No.	Recovery	Mechanical rpm	Nearest condition from run 1 baseline	
					Condition No.	Mechanical rpm
1	0.491	0.537	0.997	13 550	36	13 910
2	0.682	0.750	0.996	16 880	38	16 350
3	0.812	0.833	0.995	18 080	40	18 220
4	0.909	1.054	0.990	18 750	41	18 690
5	1.000	1.071	0.986	19 150	42	19 190
6	0.947	1.069	0.979	19 700	43	19 620
7	Acceleration from 13 500 to 19 700 rpm, plug full open					
8	0.888	1.027	0.990	19 150	42	19 190
9	Plug excursion from 0.00 to 1.03			18 750	41	18 690
10	Acceleration from 13 500 to 21 000 rpm, plug full open					
11	0.947	1.070	0,966	20 050	44	20 040
12		1.079		20 900	46	21 040
13	Plug excursion			15 000		
14	Plug excursion			16 880		

RUN 9 DATA KEY

Double articulating vane inlet, approach throat, Model 6, L/D = 1.0, Dwg. 5364-20

Conditions 1 through 8

Weight flow calibration only, with standard bellmouth

Conditions 9 through 15

Performance and noise data with flight lip bellmouth

Run 9 Test Condition	Normalized Throat Average Mach No.	Recovery	Mechanical rpm	Nearest condition from run 1 baseline	
				Condition No.	Mechanical rpm
1	0.510	0.977	14 600	37	14 350
2	0.573	0.971	16 000	38	16 350
3	0.697	0.957	18 200	40	18 220
4	0.798	0.946	19 650	43	19 620
5	0.891	0.932	20 850	45	20 430
6	0.928	0.924	21 500	46	21 040
7	0.987	0.909	22 500	47	22 180
8	Acceleration 14 500 to 22 500 rpm				
9	0.500	0.976	14 400	37	14 350
10	0.711	0.954	18 300	40	18 220
11	0.822	0.942	19 700	43	19 620
12	0.942	0.928	20 800	45	20 430
13	1.000	0.916	21 700	47	22 180
14	0.942	0.896	23 000	48	23 410
15	Acceleration 14 000 to 23 000 rpm				

RUN 10 DATA KEY

Centerbody inlet, approach throat, Model 3C, L/D = 1.3, Dwg. 5369-1
Acoustic lining in diffuser, hardwall throat

Acquired aerodynamic and acoustic data on all conditions except condition 6 where aerodynamic data are limited.

Run 10 Test Condition	Normalized Throat Average Mach No.	Recovery	Mechanical rpm	Nearest condition from run 1 baseline	
				Condition No.	Mechanical rpm
1	0.520	0.993	14 400	37	14 350
2	0.705	0.990	17 400	39	17 780
3	0.795	0.986	18 400	40	18 220
4	0.938	0.980	19 200	42	19 190
5	0.976	0.964	19 900	44	20 040
6	1.00	0.934	20 480	45	20 430

RUN 11 DATA KEY

Centerbody inlet, approach throat, Model 4, L/D = 1.0, Dwg. 5364-31-1
Final inlet concept 1

Run 11 Test Condition	Normalized Throat Average Mach No.	Recovery	Mechanical rpm	Remarks
1	0.485	0.995	13 650	1, 2
2	0.665	0.992	16 800	1, 2
3	0.765	0.990	18 100	1, 2
4	0.860	0.983	19 100	1, 3
5	0.875	0.974	19 550	1, 2
6	1.000	0.927	21 400	1, 2
7	0.915	0.964	20 200	1, 2
8			19 550	1, 2, 4
9			19 720	1, 2, 5
10	Acceleration from 13 500 to 21 500 rpm. Recorded all acoustic data.			1
11	0.635	0.994	16 920	3, 6, 7
12	0.835	0.965	19 800	3, 6, 7
13	0.965	0.928	20 300	3, 6, 7
14	0.915		19 900	6, 8, As 2 but Aero only
15	0.670	0.998	17 000	9
16	0.990	0.964	20 270	9
17	1.000	0.935	21 500	9
18 A, B, C	0.665	–	17 000	9,10 Blown air, 0, 200, and 300 ft/sec
19	0.915	–	20 100	9, 10 Blown air, 200 ft/sec
19 B	0.915	–	19 800	9, 10 Blown air, 300 ft/sec
20	Noise baseline with rig off and blown air off—all microphones, including near field			
21	Noise baseline with 200 ft/sec blown air. Rig turned off			
22	Noise baseline with 300 ft/sec blown air. Rig turned off			
23	0.665	–	16 800	9, 10 Blown air, 100 ft/sec
24	0.915	–	19 800	9, 10 Blown air, 100 ft/sec
25	Noise baseline with 100 ft/sec blown air. Rig turned off.			

Legend of Remarks Run 11

1. Twenty-eight probe rotating rake at 8 in. from diffuser exit.

2. Full aerodynamic and noise data includes nine-position traverse with four-arm P_T rake, boundary layer rakes, all rig pressures, plus all far-field and near-field microphones.

3. Full acoustic data. Aerodynamic rake at fan inlet set at single position only, 0°.

4. Fan backload increased to near stall.

5. Fan was operated halfway between operating line and stall line.

6. Same configuration as note 1 but with short bellmouth 5364-35 faired to the flight lip.

7. Midstream data taken with stinger probe per section 2.1.1 of coordination sheet INSP-CS-070.

8. Repeat of condition 7 to establish whether bellmouth 5364-35 improved performance over that of flight lip.

9. Same inlet as note 6 but measured diffuser exit pressure with four fixed rakes in the exit plane instead of the rotating rake at 0.75 diameter downstream as on all previous conditions. A check to see if this alters the performance measurements. Recorded all acoustic data.

10. Induced distortion from six crosswind tubes at the inlet lip. Took aerodynamic and acoustic data.

RUN 12 DATA KEY

Centerbody inlet, takeoff throat, Model 4, L/D = 1.0, Dwg. 5364-31-1

Final inlet concept 1

Run 12 Test Condition	Normalized Throat Average Mach No.	Recovery	Mechanical rpm	Remarks
1	0.465	0.998	17 100	1, 2
2	0.640	0.997	21 300	1, 2
3	0.690	0.996	22 230	1, 2
4	0.730	0.994	22 900	1, 2
5	0.780	0.994	23 500	1, 2
6	0.810	0.991	24 000	1, 2
7	0.875	0.979	25 000	1, 2
8	1.000	0.968	26 000	1, 2
9	Decel from 26 000 to 17 000 rpm. Recorded all acoustic data.			1
10	0.630	0.996	23 680	1, 2, 3
11	0.710	0.994	23 680	1, 2, 4
12	0.690	0.996	22 040	1, 5
13	1.000	0.968	25 840	1, 5
14	0.690	–	22 260	2, 6 Blown air, 0 ft/sec
15	0.690	–	22 280	2, 6 Blown air, 100 ft/sec
16	0.690	–	22 280	2, 6 Blown air, 200 ft/sec
17	0.690	–	22 320	2, 6 Blown air, 300 ft/sec
18	0.875	–	25 100	2, 6 Blown air, 0 ft/sec
19	0.875	–	25 100	2, 6 Blown air, 100 ft/sec
20	0.875	–	25 140	2, 6 Blown air, 200 ft/sec
21	0.875	–	25 140	2, 6 Blown air, 250 ft/sec

Legend of Remarks Run 12

1. Centerbody retracted by 3.85 in. from the approach configuration. Short bellmouth 5364-35 was faired to the flight lip. Diffuser exit pressure was measured in the diffuser exit plane by seven elements on each of four fixed struts. Boundary layer was measured at one location on the inner and outer wall in the diffuser exit plane.

2. Recorded full aerodynamic data (but did not use the four-arm rotating rake). Recorded all far-field microphones and the Kulite microphone in outer wall near diffuser exit.

3. The fan was operated very near stall by increasing the backpressure. Same rpm as test condition 5.

4. Fan was operated halfway between operating line and stall line.

5. Stinger probe measurements (noise and static pressure) were taken in midstream.

   Made stinger axial traverses at 3 radii:

   —1/8 in. from throat* outer wall
   —1/8 in. from throat inner wall
   —Midway in the throat passage

   Made radial traverses at four axial locations:

   —In the throat* plan
   —4 in. downstream from the throat
   —5.5 in. downstream from the throat
   —9.0 in. downstream from the throat

   Recorded steady-state data at the 12 locations where the above traverse paths cross.

   *For reference here, the "throat" is taken to mean the geometric throat plane when the centerbody is in the approach position.

6. Induced distortion from six crosswind tubes at the inlet lip. Took aerodynamic and acoustic data. Same configuration of inlet as note 1.

RUN 13 DATA KEY

Radial vane inlet, approach throat, Model 5B, L/D = 1.0, Dwg. 5364-40A-1

Final inlet concept 2

Run 12 Test Condition	Normalized Throat Average Mach No.	Recovery	Mechanical rpm	Remarks
1	0.530	0.989	13 925	1, 2
2	0.735	0.978	17 000	1, 2
3	0.860	0.960	18 700	1, 2
4	0.945	0.927	20 500	1, 2
5	0.960	0.904	21 650	1, 2
6	0.880	0.864	23 680	1, 2
7	1.000	0.917	21 100	1, 2
8	0.979	0.850	20 620	1, 3
9	0.960	0.840	20 620	1, 4
10	Accel from 13 900 to 20 630 rpm. Recorded all acoustic data.			1
11	0.670	0.977	17 140	1, 5
12	1.000	0.934	20 650	1, 5
13	1.000	0.946	20 100	1, 6
14	0.735	0.977	17 230	2, 7 Blown air, 0 ft/sec
15	0.735	0.975	17 230	2, 7 Blown air, 100 ft/sec
16	0.735	0.971	17 230	2, 7 Blown air, 200 ft/sec
17	0.735	0.969	17 230	2, 7 Blown air, 300 ft/sec
18	0.910	0.945	19 820	2, 7 Blown air, 0 ft/sec
19	0.910	0.941	19 820	2, 7 Blown air, 100 ft/sec
20	0.910	0.940	19 770	2, 7 Blown air, 200 ft/sec
21	0.910	0.938	19 770	2, 7 Blown air, 300 ft/sec
22	1.000	0.929	20 710	1, 8
23	0.935	0.939	20 200	1, 8

Legend of Remarks Run 13

1. Short bellmouth 5364-35 was faired to the flight lip. The rotating four-arm rake was installed to measure pressure in the diffuser exit plane.

2. Recorded full aerodynamic and acoustic data.

3. Fan was operated very near stall by increasing the backpressure.

4. Fan was operated halfway between operating line and stall line.

5. Midstream data taken with stinger probe per section 2.1.1. of coordination sheet INSP-CS-070.

6. Recorded aerodynamic data with rotating rake only at 0°. No noise data recorded. This point was run only to verify maximum flow condition.

7. Induced distortion from six crosswind tubes at the inlet lip. Took aerodynamic and acoustic data. Same configuration of inlet as note 1.

8. Recorded full aerodynamic traverse but no acoustic data. This point was run only to verify the maximum flow condition for the inlet.

RUN 14 DATA KEY

Radial vane inlet, takeoff throat, Model 5B, L/D = 1.0, Dwg. 5364-40A-1

Final inlet concept 2

Run 13 Test Condition	Normalized Throat Average Mach No.	Recovery	Mechanical rpm	Remarks
1	0.485	0.997	16 830	1, 2
2	0.670	0.995	20 975	1, 2
3	0.740	0.994	21 970	1, 2
4	0.780	0.993	22 560	1, 2
5	0.840	0.992	23 310	1, 2
6	0.890	0.992	23 690	1, 2
7	0.965	0.968	25 000	1, 2
8	1.000	0.953	25 700	1, 2
9	0.960	0.983	24 400	1, 2
10	0.670	0.995	23 710	1, 2, 3
11	0.780	0.993	23 710	1, 2, 4
12	Accel from 16 000 to 25 700 rpm. Recorded all acoustic data.			1
13	0.670	0.991	21 070	5
14	0.660	0.986	21 070	5
15	0.655	0.983	21 070	5
16	0.650	0.979	21 070	5
17	0.880	0.975	24 430	5, 6
18	0.915	0.960	24 980	5
19	0.885	0.957	24 880	5
20	0.875	0.957	24 850	5
21	0.870	0.957	24 850	5
22	0.670	0.995	20 940	7
23	0.965	0.968	24 900	7

Legend of Remarks Run 14

1. Vanes removed to form the takeoff configuration. Short bellmouth 5364-35 was faired to the flight lip. The rotating four-arm rake was installed to measure pressure in the diffuser exit plane.
2. Recorded full aerodynamic and acoustic data.
3. Fan backload increased to near stall.
4. Fan was operated halfway between operating line and stall line.
5. Same inlet configuration as note 1. Induced distortion from six crosswind tubes at the inlet lip. Recorded full aerodynamic and acoustic data.
6. No further data were taken at this particular rpm because an undesirable fan blade vibration condition existed.
7. Midstream data were taken with stinger probe per section 2.1.1 of coordination sheet INSP-CS-070.

RUN 101 DATA KEY

Centerbody inlet, approach throat, Model 3A, acoustic lining on cowl and centerbody, L/D = 1.3, Dwg. 5369-1

Extensive instrumentation, included boundary layer rakes on inner and outer wall in the diffuser, and at diffuser exit; plus aerodynamic traverse at diffuser exit.

Far-field acoustic data every 10° plus near-field acoustic data in planes 6 and 7.

Run 101 Test Condition	Normalized Throat Average Mach No.	Throat Outerwall Mach No.	Recovery	Mechanical rpm	Nearest condition from run 1 baseline	
					Condition No.	Mechanical rpm
1	0.530	0.54	0.986	14 400	37	14 350
2	0.624	0.61	0.984	15 700	38	16 350
3	0.706	0.71	0.975	17 200	39	17 780
4	0.781	0.77	0.971	18 200	40	18 220
5	0.789	0.78	0.970	18 400	41	18 690
6	Acceleration from 15 000 to 22 000 rpm					
7	0.799	0.79	0.975	18 850	41	18 690
8	0.826	0.81	0.974	19 200	42	19 190
9	0.832	0.82	0.967	19 400	43	19 620
10	0.869	0.83	0.972	19 800	44	20 040
11	0.899	0.87	0.963	20 500	45	20 430
12	1.000	0.88	0.905	21 000	46	21 040

RUN 102 DATA KEY

Centerbody inlet, approach throat, Model 3B, acoustic lining on cowl with hardwall centerbody, L/D = 1.3, Dwg. 5369-1.
Centerbody treated forward portion (5369-3) replaced by hardwall centerbody 5364-7-1.

Extensive instrumentation, including boundary layer rakes on inner and outer wall in the diffuser, and at diffuser exit; plus aerodynamic traverse at diffuser exit.

Far-field acoustic data every 10° plus near-field acoustic data in planes 6 and 7.

Run 102 Test Condition	Normalized Throat Average Mach No.	Throat Outerwall Mach No.	Recovery	Mechanical rpm	Nearest condition from Run 1 Baseline	
					Condition No.	Mechanical rpm
1	1.000	0.86	0.953	19 400	43	19 620
2	0.965	0.88	0.943	19 800	44	20 040

C.3 INSTRUMENTATION DETAILS

Most of the model tests were part of a concept screening process and did not carry the extensive instrumentation that was used on the last four test runs of the program. The last runs were on two of the selected best concepts, which were more completely instrumented for aerodynamic measurements.

A system of "instrumentation planes" was used as an aid in recordkeeping:

- Plane 0 or 1, was always taken immediately upstream of the inlet lip. Ambient conditions.
- Plane 2, was always the measuring plane of the bellmouth (flow measuring standard) when used.
- Plane 3, lip highlight of inlet model.
- Plane 4, was always located at the geometric throat.
- Plane 5, midway in the diffuser section.
- Plane 5.5 or 6.0; either of these planes was taken as the diffuser exit plane.

Due to the many design differences between inlet concepts, the axial positions of the instrumentation planes were changed from the model to another. Figures C-1 through C-19 were included to clarify the geometry and instrumentation for each test run.

The use of static pressure ports, boundary layer total pressure rakes, and traversing probes or rakes for total pressure (P_T) measurement has been indicated on figures C-1 through C-19.

C.4 MICROPHONE CHARACTERISTICS

The microphones used for measuring far-field noise were 1/4-in.-diameter "B&K" condenser microphones, type 4135 + UA 0035 + 2615. Near-field noise both in the flow and on the inlet duct walls was measured with 1/8-in.-diameter "Kulite" high-frequency response transducers (model CPL-070-50A). Throughout the rest of this section the two different types of microphones will be referred to as either the far-field or the near-field microphone.

The microphones were calibrated prior to use during each test. Calibration procedure is described in appendix D of volume III of this report (Boeing document D6-40818).

C.4.1 Frequency Response of Microphones

A typical far-field microphone was tested for its frequency response. The results were plotted on curve 4 of figure C-20. The frequency responses measured by microphones used in the test facility were checked by comparing their measurements against a "standards" microphone of known accuracy. The microphone obtained from Boeing Primary Standards Group came complete with a frequency response curve which was included as curve 1 of figure C-21. The Sonic Inlet Test Group used their equipment in an effort to establish the response curve for the "standards" microphone and found essentially the same results. These are shown in curve 2 of figure C-21.

Frequency response characteristics for two of the facility microphones were presented in curves 2 and 3 of figure C-20. It was noted that there appeared to be microphone resonance at 18 000 Hz on the duct wall microphone (curve 2, fig. C-20). The observed spike at 18 00 Hz, and subsequent drop in dB level, were noted in some of the spectrum plots for this microphone.

C.4.2 Frequency Response of Magnetic Tape and System Analyzer

The frequency response or reproducibility of the magnetic tape system and the subsequent process through the spectrum analyzer was checked as follows. The microphone and preamplifier were removed from the system, and a Gaussian white noise generator was used to feed a signal into the tape conditioning amplifier from which the conditioned signal was then recorded on magnetic tape. The conditioning amplifier was used throughout testing to provide a known gain setting of the signal recorded on tape. The signal level recorded on magnetic tape had to be between 0.1 and 1.0 volt RMS to achieve maximum sensitivity from the tape recording system.

The Gaussian source generator should ideally produce a signal of constant level across the frequency spectrum. Actually, the deviation of ±1.0 dB noted on figures C-22 and C-23 was found to be in error in the Gaussian source generator and not in the magnetic tape or spectrum analyzer system. The recorded white noise was analyzed with a 40-cycle, constant-bandwidth filter in conjunction with a system which performed a 32-second time average of the spectrum. Results shown in figures C-22 and C-23 are the same signal recorded on two separate channels of the magnetic tape. The magnetic tape recorder used during this program had 14 separate channels, each preceded by a separate signal conditioning amplifier. Eleven channels were assigned to microphone signals, and thus all noise data were recorded simultaneously.

C.4.3 Microphone Noise Floor

It was important to determine the noise floor for the noise data acquisition system. This was to eliminate any question that some of the lowest noise levels encountered during test might be equal to or less than the noise floor of the noise measuring system. The fan was shut down (noise source eliminated), and a recording of the signals from all near-field and far-field microphones was put on magnetic tape. The signals from the tape were then put through a spectrum analyzer which used a 40-cycle, constant-bandwidth filter and performed a 32-second time averaging of the spectrum. The spectrum revealed the floor levels for the far-field and near-field microphones. These are plotted on figures C-24 and C-25, respectively.

The microphones were subjected to a decibel level in the upper portion of their range of application when testing them for frequency response. Further investigation was performed on one of the near-field microphones. A test was made to establish the capability of the near-field microphone to measure pure tones that were near the noise floor for the microphone. A near-field microphone was removed from the test facility and examined under laboratory conditions. The electronic noise of the microphone and system was found to be about 75 dB, as shown in figure C-26. A pure tone of 80 dB was fed into the microphone for each of the 13 frequencies (spikes) shown on figure C-26. The results showed that the equipment had the capability of distinguishing discrete tones down to the floor level of the system.

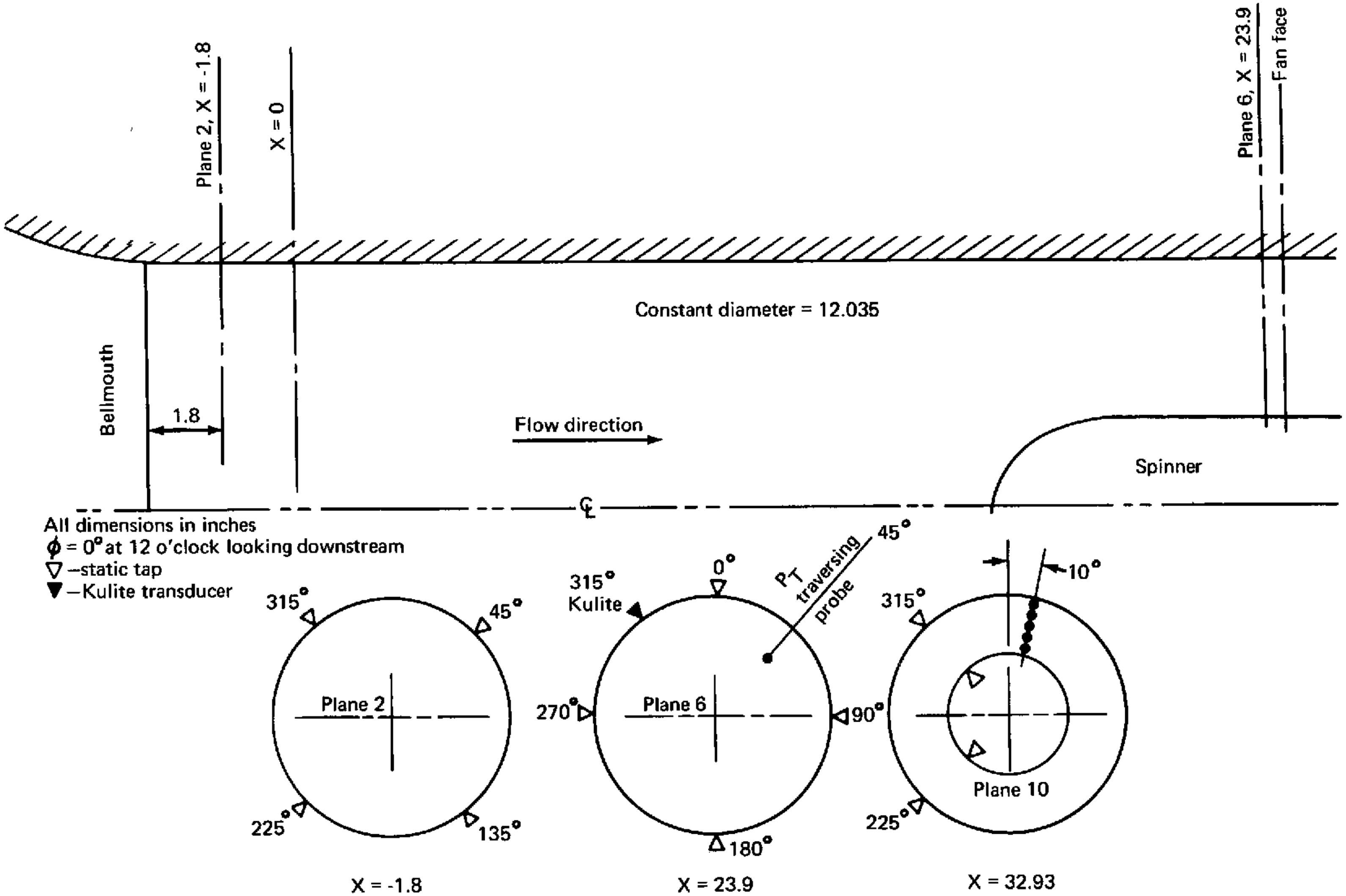

FIGURE C-1.—RUN 1 INSTRUMENTATION—BASELINE MODEL

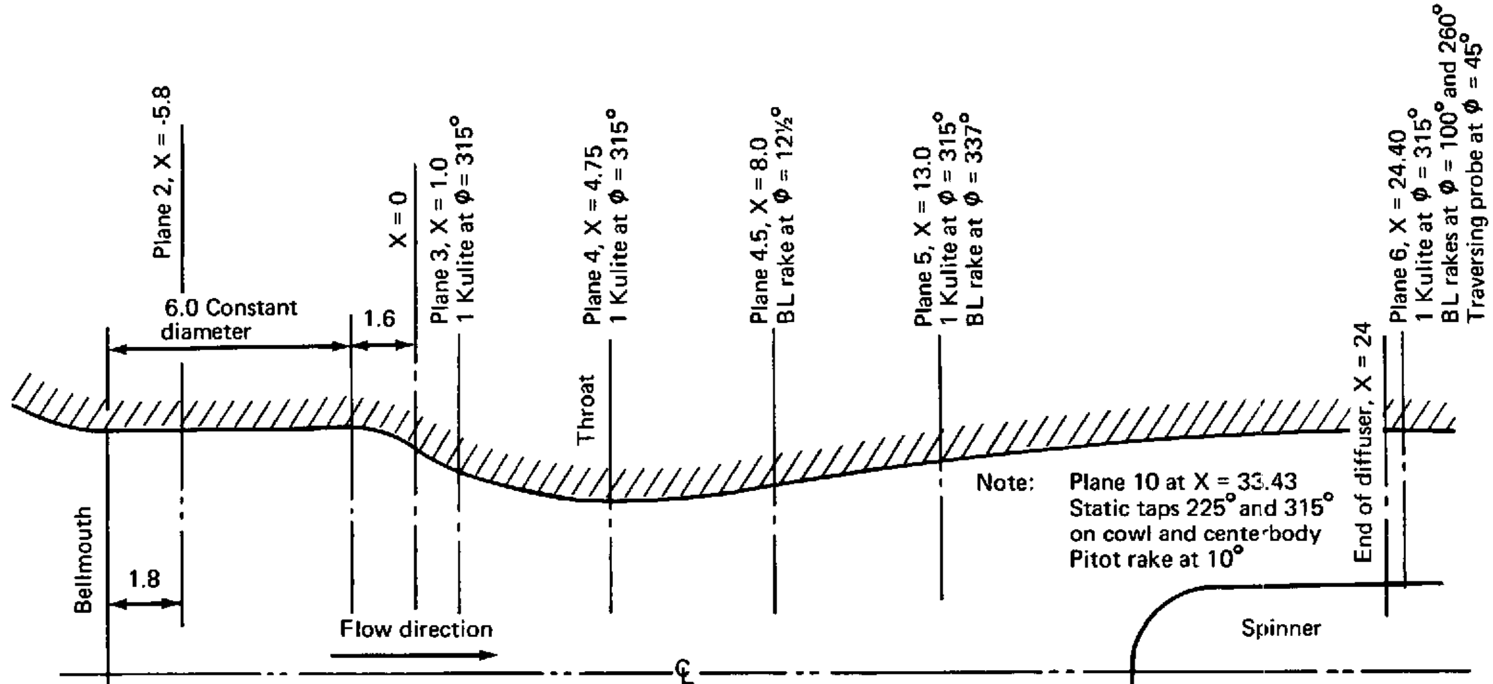

All dimensions in inches
$\phi = 0°$ at 12 o'clock looking downstream

Points of steady static pressure measurement

Longitudinal position, X	-5.8(C)	-1.0(C)	0(C)	1.0(C)	2.0(C)	3.0(C)	4.0(C)	4.75(C)	5.0(C)	6.0(C)	7.0(C)
Angular position, ϕ	0,90,180,270	0	0	0	0	0	0	0,90,180,270	0	0	0

X		8.0(C)	9.0(C)	11.0(C)	13.0(C)	15.0(C)	18.0(C)	21.0(C)	23.8(C)
ϕ		0,90,180,270	0	0	0,90,180,270	0	0	0	0,90,180,270

(C) = cowl only

FIGURE C-2.—RUN 2 INSTRUMENTATION—FUNDAMENTAL INLET, APPROACH, MODEL 1, L/D = 2.0, CONDITIONS 1 THROUGH 7

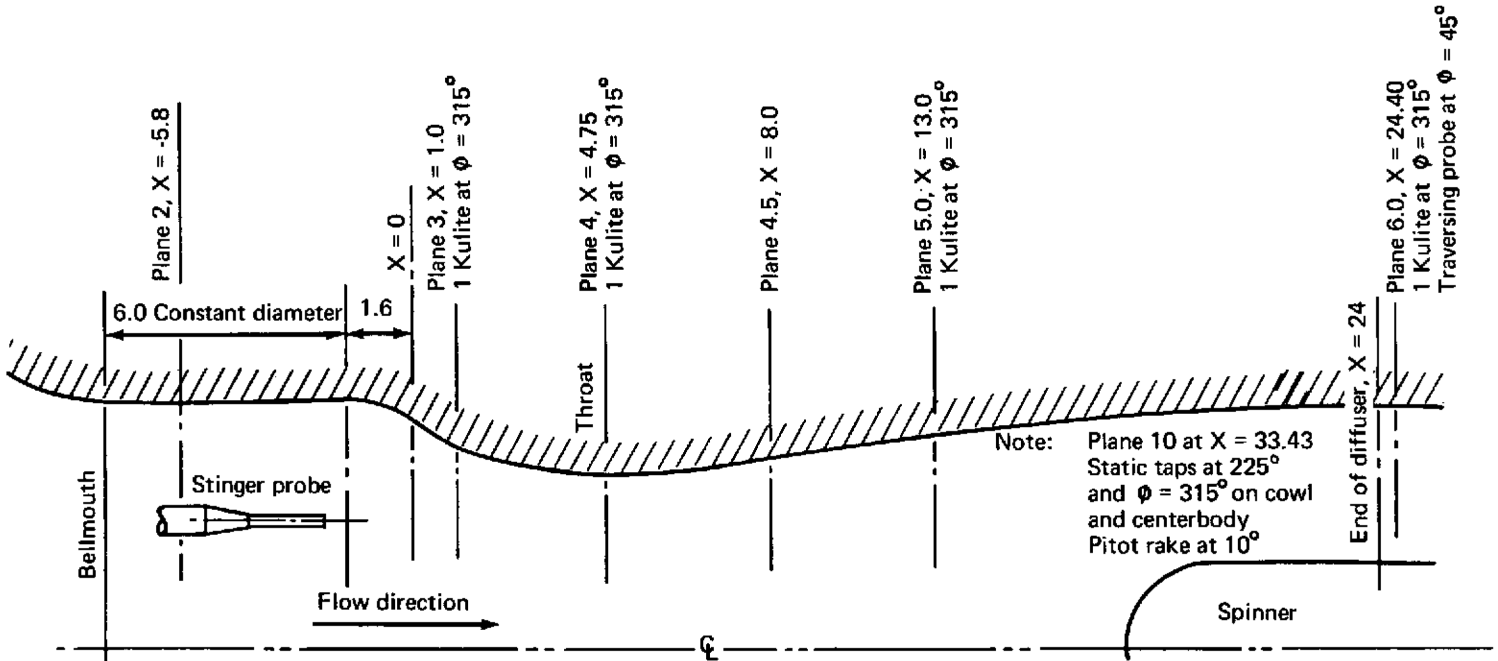

All dimensions in inches
ϕ = 0 at 12 o'clock looking downstream

Points of steady static pressure measurement											
Longitudinal position, X	-5.8(C)	-1.0(C)	0(C)	1.0(C)	2.0(C)	3.0(C)	4.0(C)	4.75(C)	5.0(C)	6.0(C)	7.0(C)
Angular position, ϕ	0,90,180,270	0	0	0	0	0	0	0,90,180,270	0	0	0

X		8.0(C)	9.0(C)	11.0(C)	13.0(C)	15.0(C)	18.0(C)	21.0(C)	23.8(C)
ϕ		0,90,180,270	0	0	0,90,180,270	0	0	0	0,90,180,270

(C) = cowl only

FIGURE C-3.—RUN 2 INSTRUMENTATION—FUNDAMENTAL INLET, APPROACH, MODEL 1, L/D = 2.0, CONDITIONS 8 THROUGH 14

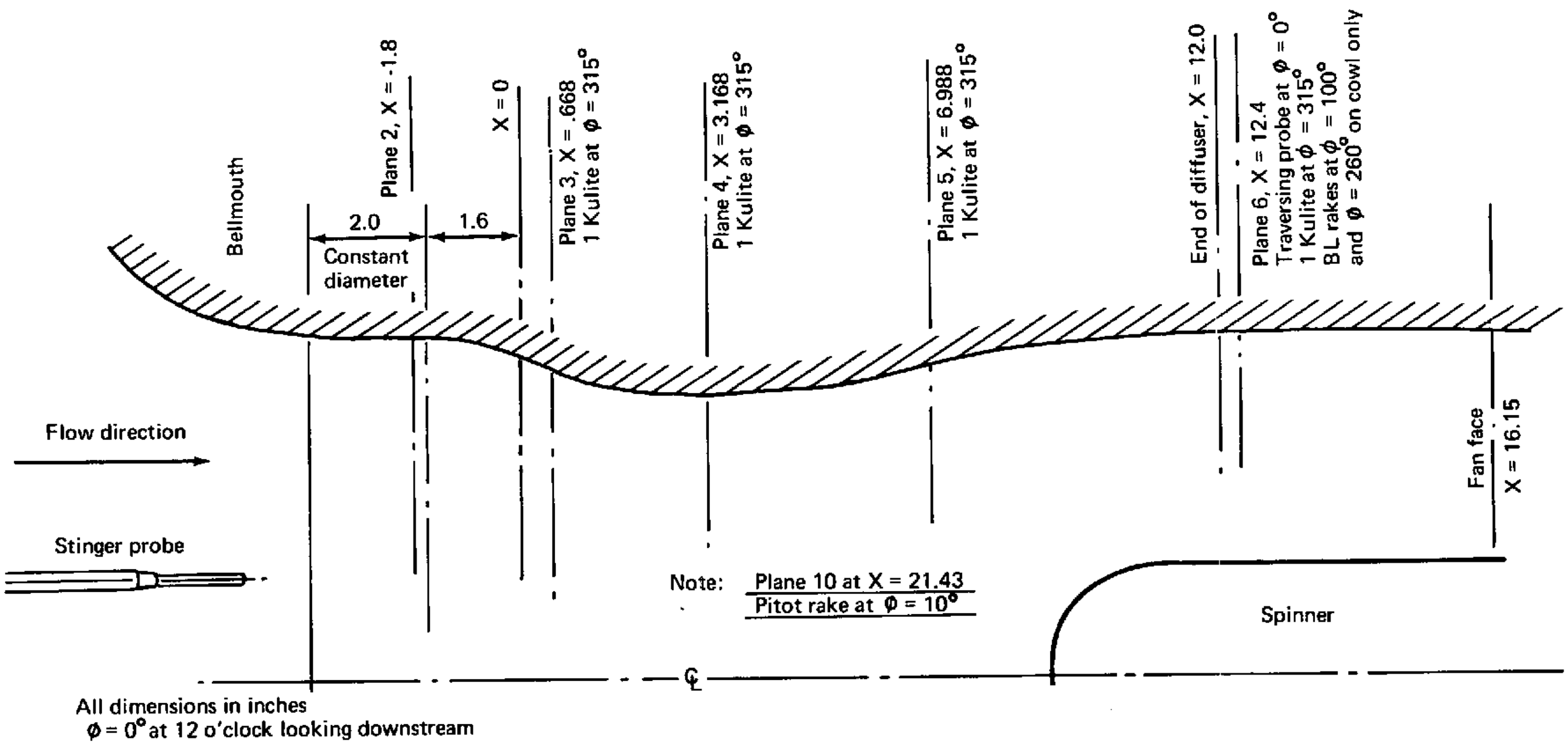

Points of steady static pressure measurement				
Longitudinal position, X	-1.8	3.168	12.4	21.43
Angular position, φ	0,90,180,270	0,45,90,135,180,225,270,315	65,155,245,335	225,315

FIGURE C-4.—RUN 3 INSTRUMENTATION—FUNDAMENTAL INLET, TAKEOFF, MODEL 2, L/D = 1.0

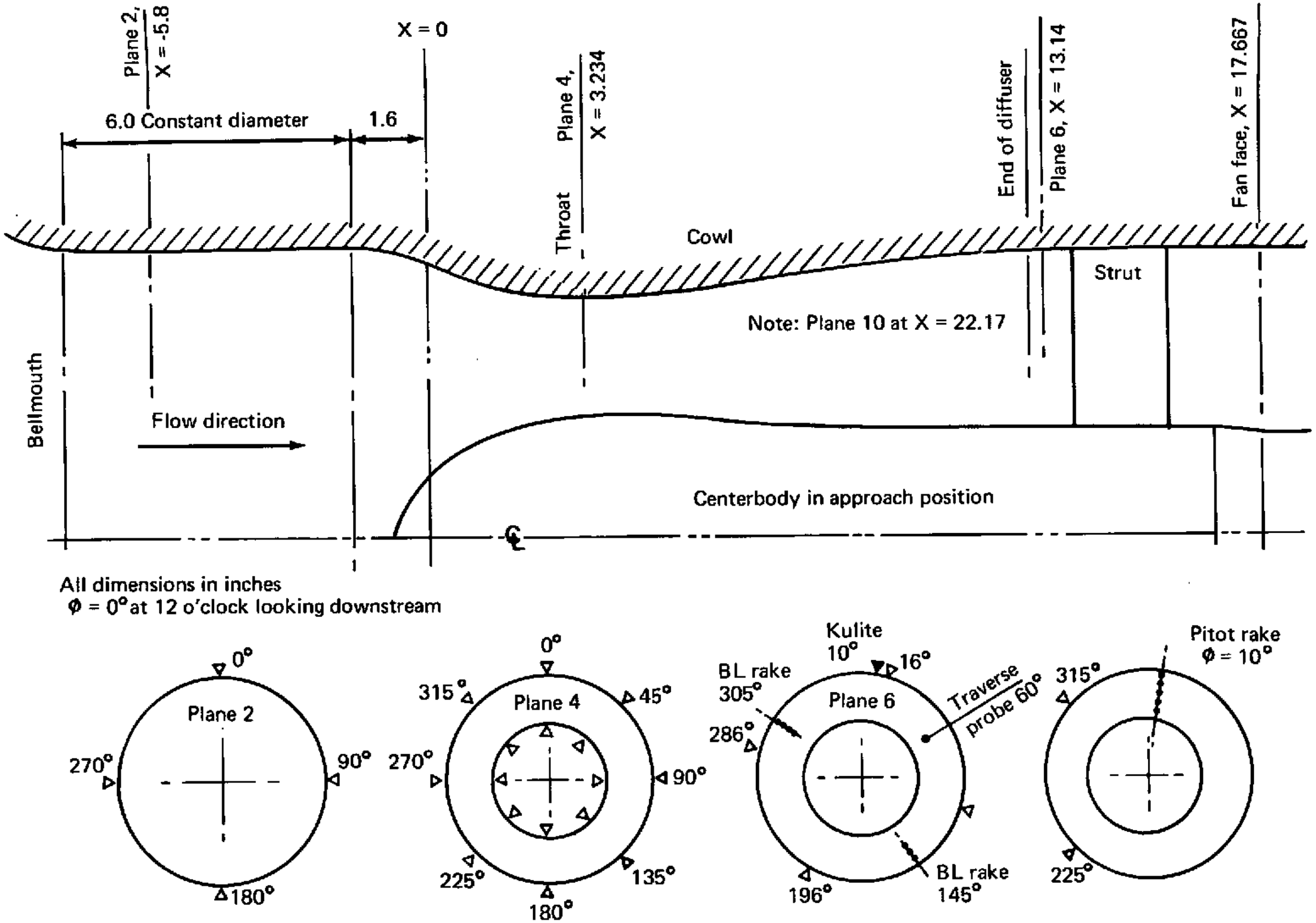

▽ –Static taps
▼ –Kulite transducer

FIGURE C-5.—RUN 4 INSTRUMENTATION—CENTERBODY INLET, APPROACH, MODEL 3, L/D = 1.3

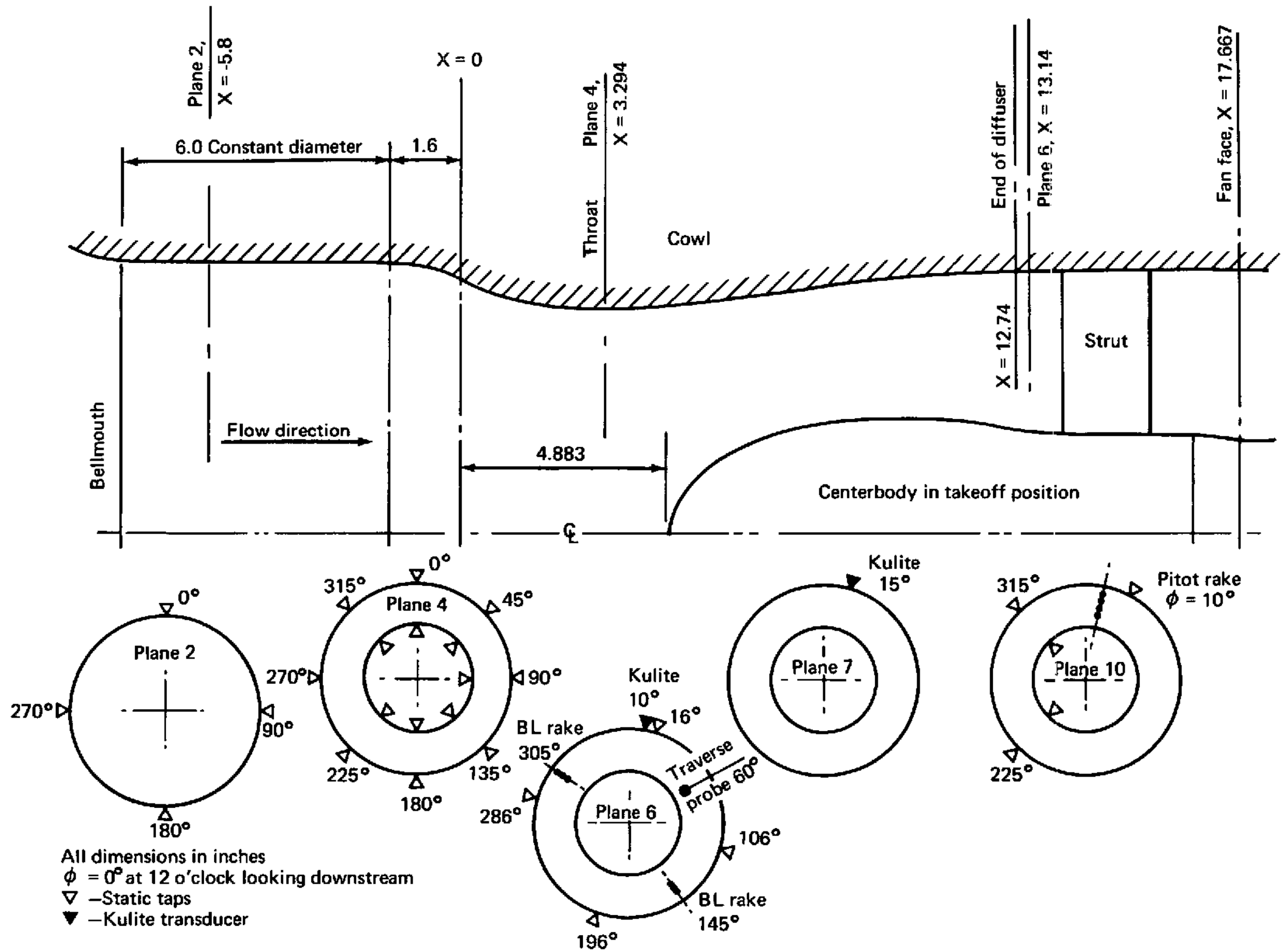

FIGURE C-6.—RUN 5 INSTRUMENTATION—CENTERBODY INLET, TAKEOFF, MODEL 3, L/D = 1.3

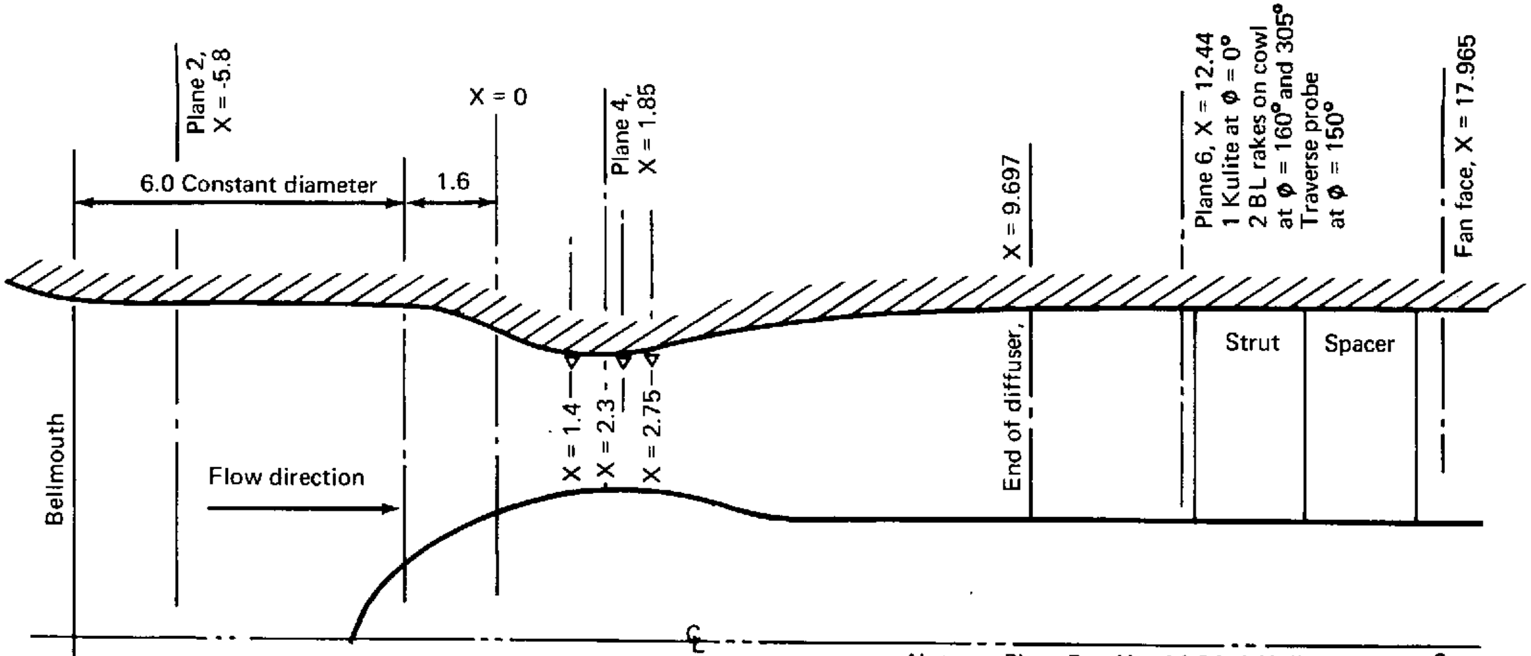

All dimensions in inches
ϕ = 0° at 12 o'clock looking downstream
∇ —Static taps

Note: Plane 7 at X = 14.64, 1 Kulite at ϕ = 10°
Plane 10 at X = 26.45, static taps at ϕ = 225° and 315° on cowl and centerbody, and pitot rake at ϕ = 10°

Points of steady static pressure measurement					
Longitudinal position: X	-5.8(C)	1.4(C)	1.85(C+CB)	2.3(C)	2.75(C)
Angular position: ϕ	0,90,180,270	0	0,45,90,135,180,225,270,315	0	0
X	12.44(C)				
ϕ	30,120,210,300				

(C) = cowl only
(C+CB) = cowl and centerbody

FIGURE C-7.—RUN 6 INSTRUMENTATION—CENTERBODY INLET, APPROACH, MODEL 4, L/D = 1.0

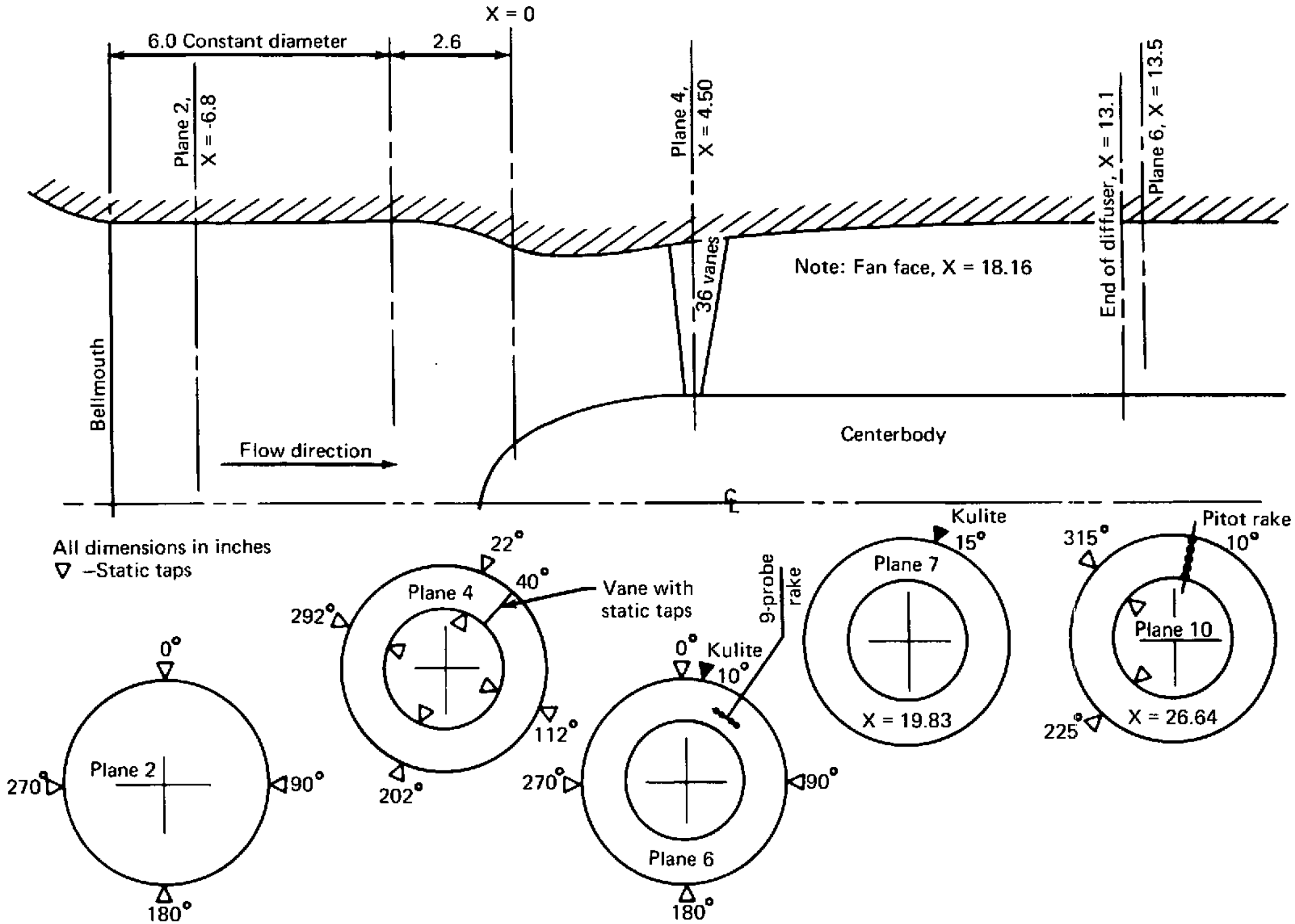

FIGURE C-8.—RUN 7 INSTRUMENTATION—RADIAL VANE INLET, MODEL 5A, L/D = 1.0

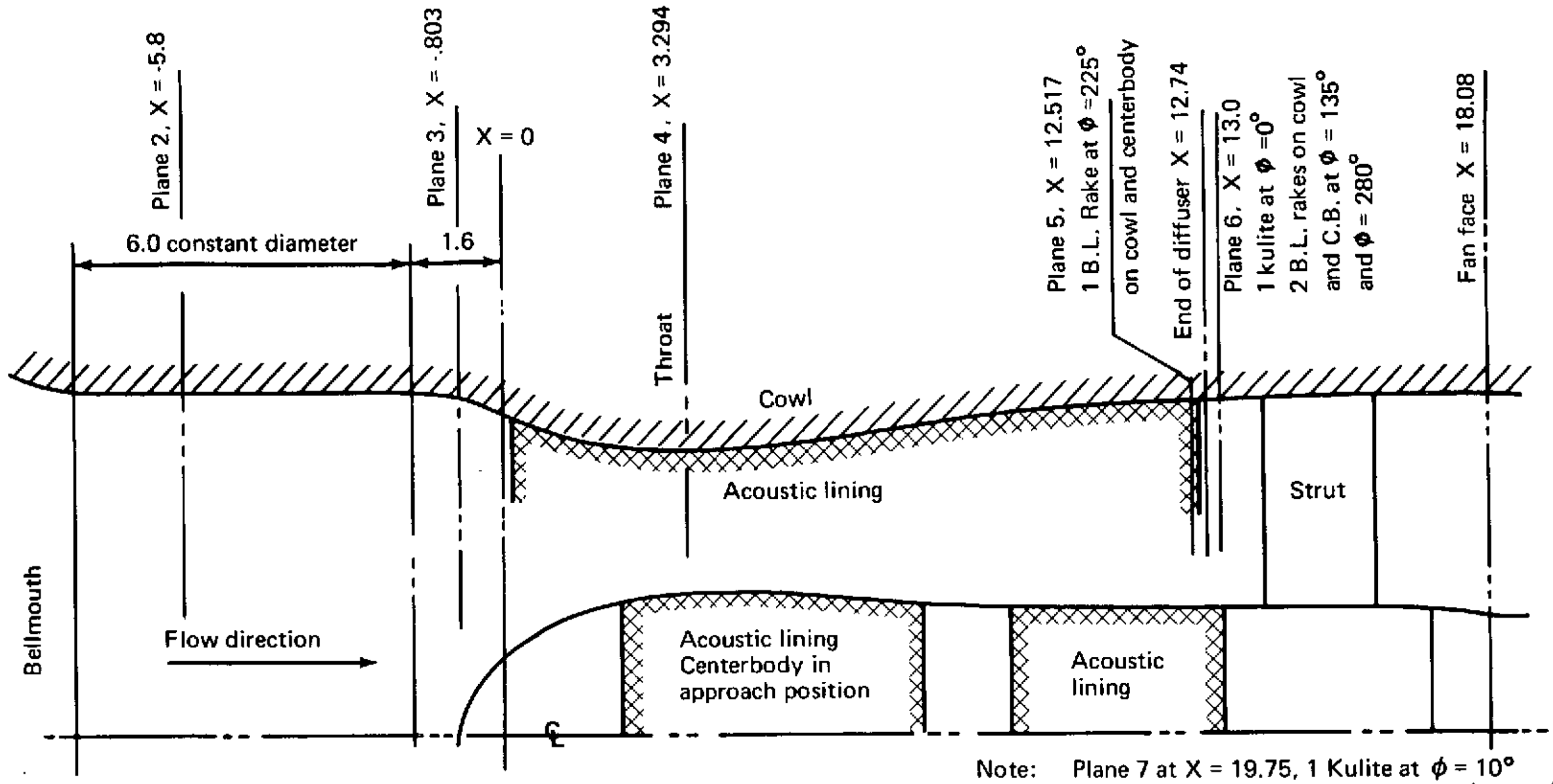

All dimensions in inches
ϕ = 0° at 12 o'clock looking downstream

Note: Plane 7 at X = 19.75, 1 Kulite at ϕ = 10°
Plane 10 at X = 26.56, static taps at ϕ = 225° and 315° on cowl and centerbody, pitot rake at ϕ = 10°

Points of steady static pressure measurement									
Longitudinal position: X	-5.8(C)	-0.803(C)	0.667(C)	1.667(C)	2.667(C)	3.294(C+CB)	4.667(C)	5.667(C)	6.667(C)
Angular position: ϕ	0,90,180,270	45,135,225,315	45	45	45	45,135,225,315	45	45	45

X	7.667(C)	9.667(C)	12.517	13.0(C)	
ϕ	45	45	45(C+CB)	45,135,225,315	

(C) = cowl only
(C+CB) = cowl and centerbody

FIGURE C-9.—RUN 101 INSTRUMENTATION—CENTERBODY INLET, TREATED, MODEL 3A, L/D = 1.3

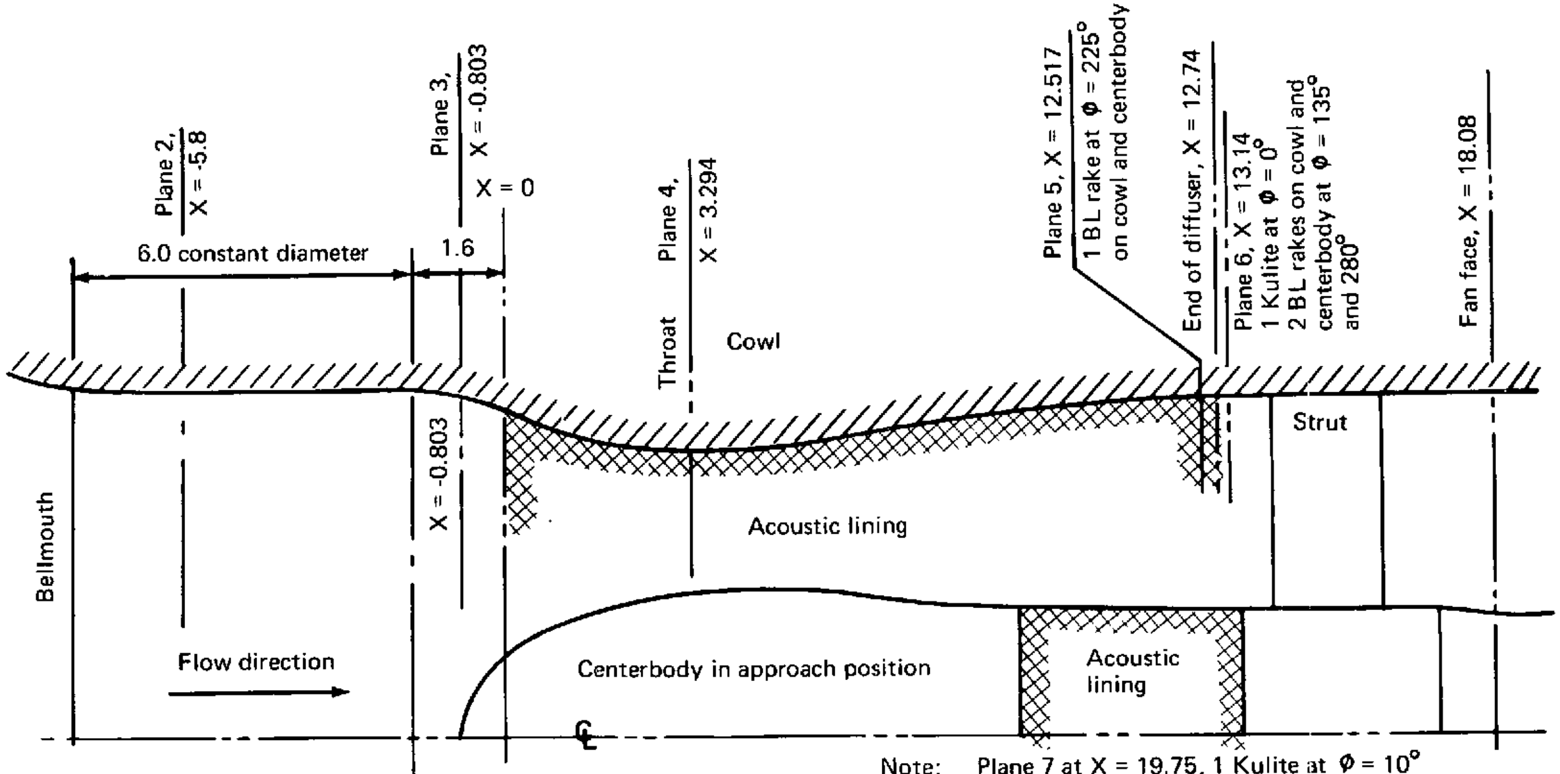

Note: Plane 7 at X = 19.75, 1 Kulite at Φ = 10°
Plane 10 at X = 26.56, static taps at Φ = 225° and 315° on cowl and centerbody, pitot rake at Φ = 10°

All dimensions in inches
Φ = 0° at 12 o'clock looking downstream

Points of steady state pressure measurement

Longitudinal position: X	-5.8(C)	-0.803(C)	0.667(C)	1.667(C)	2.667(C)	3.294(C+CB)	4.667(C)	5.667(C)	6.667(C)
Angular position: Φ°	0,90,180,270	45,135,225,315	45	45	45	45,135,225,315	45	45	45

X	7.667(C)	9.667(C)	12.517	13.14(C)
Φ	45	45	45(C+CB)	45,135,225,315

(C) = Cowl only
(C+CB) = Cowl and centerbody

FIGURE C-10.—RUN 102 INSTRUMENTATION—CENTERBODY INLET, TREATED, MODEL 3B, L/D = 1.3

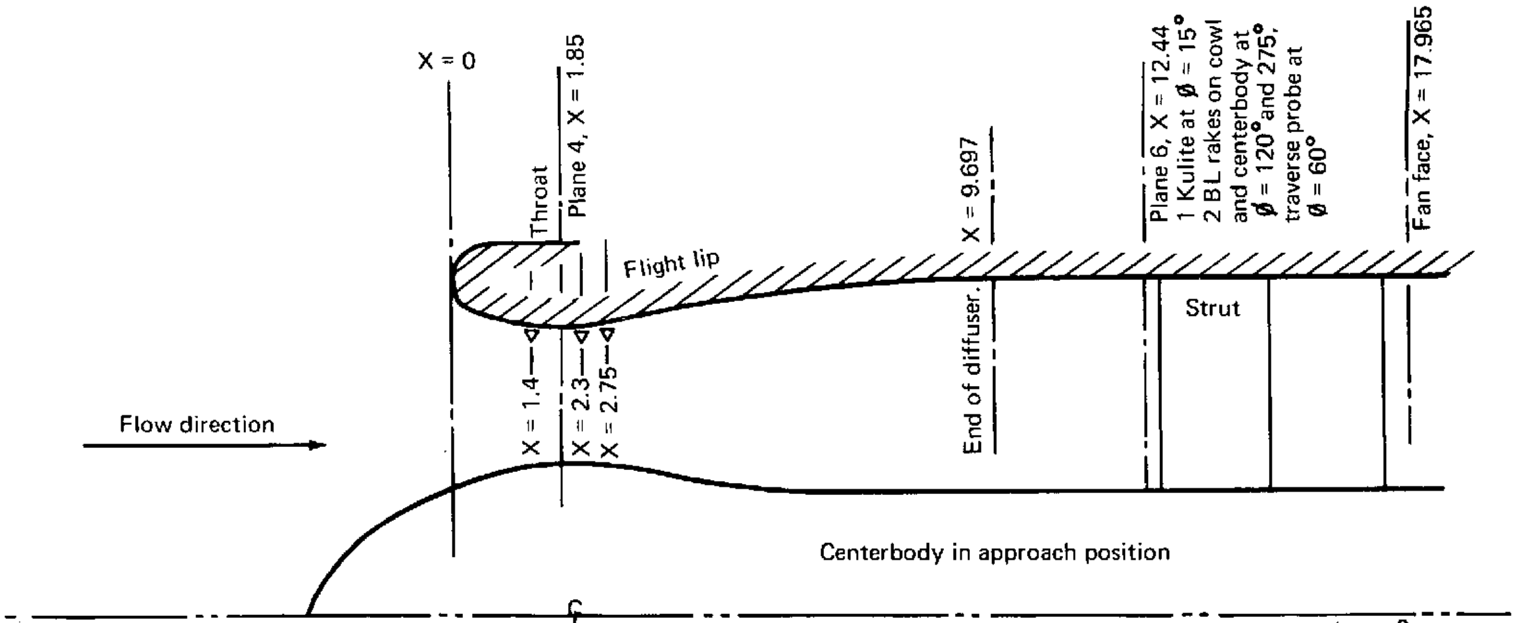

All dimensions in inches
Ø = 0° at 12 o'clock looking downstream

Note: Plane 7 at X = 19.64, 1 Kulite at Ø = 10°
Plane 10 at X = 26.45, static taps at Ø = 225° and 315° on cowl and centerbody, pitot rake at Ø = 10°

	Points of steady static pressure measurement					
Longitudinal pos. X	1.4(C)	1.85(C+CB)	2.3(C)	2.75(C)	25.58(C+CB)	
Angular position: Ø	0	0,45,90,135,180,225,270,315	0	0	225,315	
X						
Ø						

(C) = Cowl only
(C+CB) = Cowl and centerbody

FIGURE C-11.—RUN 8 INSTRUMENTATION—CENTERBODY INLET, FLIGHT LIP, MODEL 4, L/D = 1.0

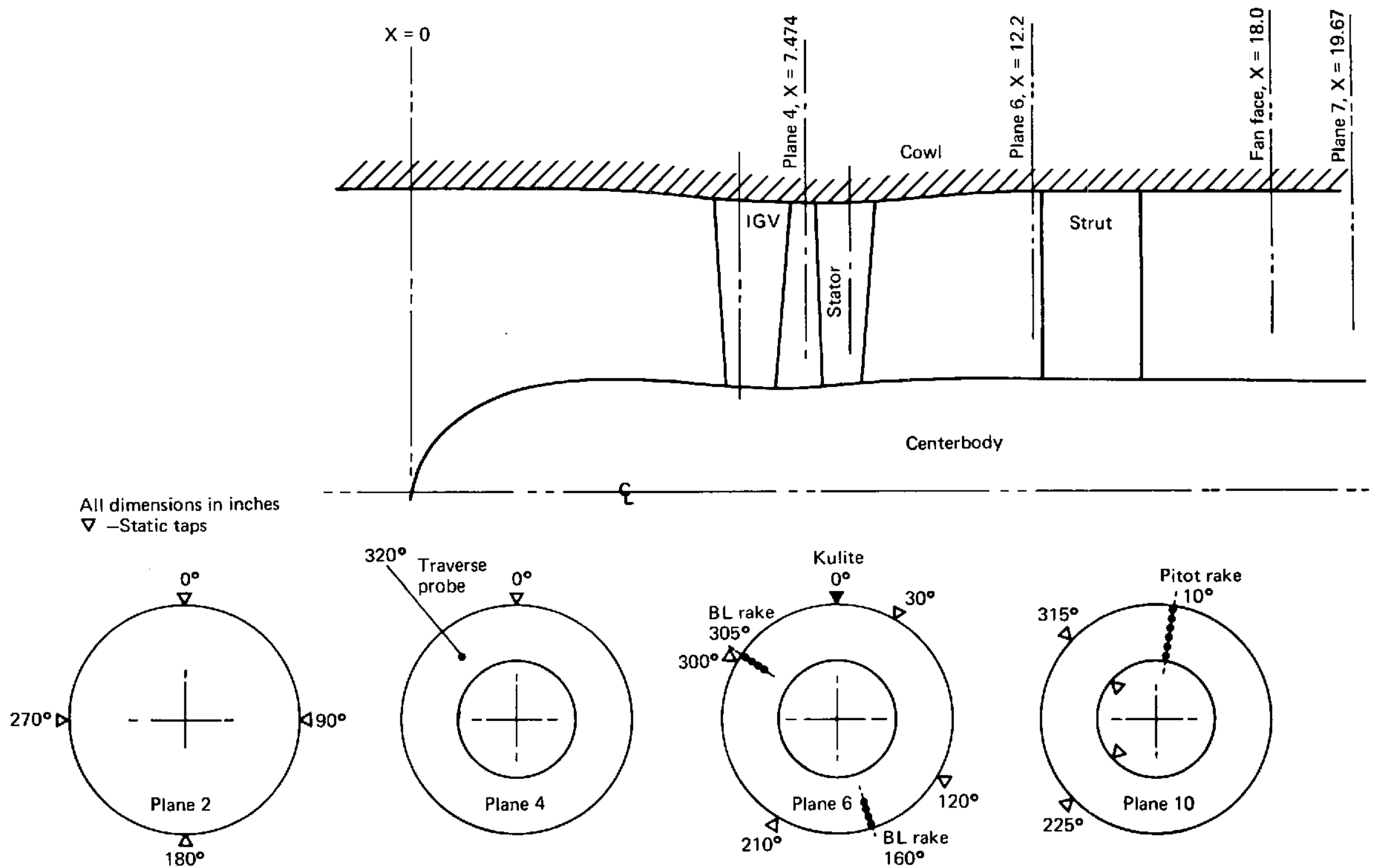

FIGURE C-12.–RUN 9 INSTRUMENTATION–DOUBLE-ARTICULATED VANE INLET, MODEL 6, L/D = 1.0

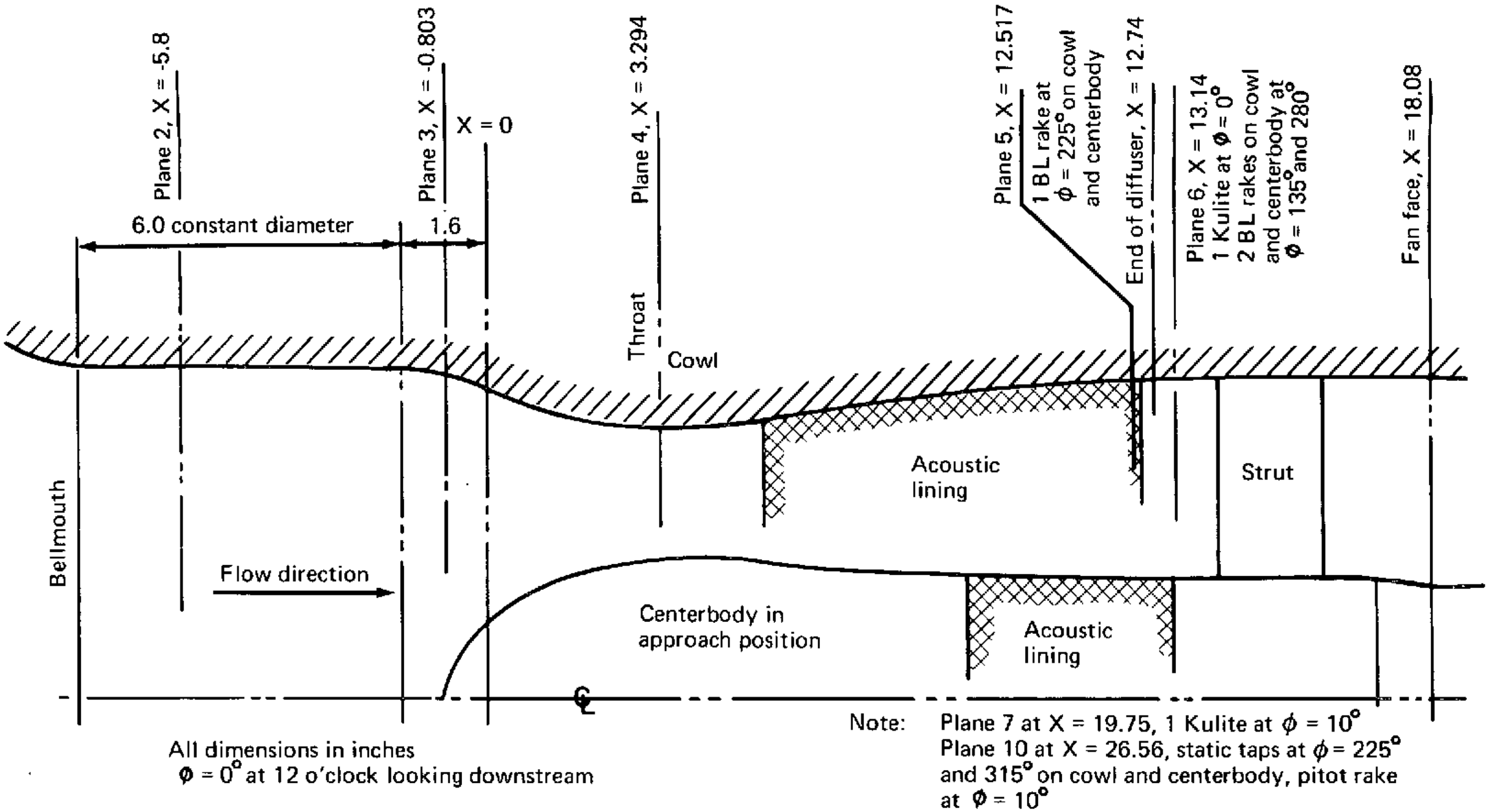

Points of steady static pressure measurement									
Longitudinal position: X	-5.8(C)	-0.803(C)	0.667(C)	1.667(C)	2.667(C)	3.294(C+CB)	4.667(C)	5.667(C)	6.667(C)
Angular position: ϕ°	0,90,180,270	45,135,225,315	45	45	45	45,135,225,315	45	45	45

X	7.667(C)	9.667(C)	12.517 (C+CB)	13.14
ϕ	45	45	45	45,135,225,315

(C) = Cowl only
(C+CB) = Cowl and centerbody

FIGURE C-13.—RUN 10 INSTRUMENTATION—CENTERBODY INLET, TREATED, MODEL 3C, L/D = 1.3

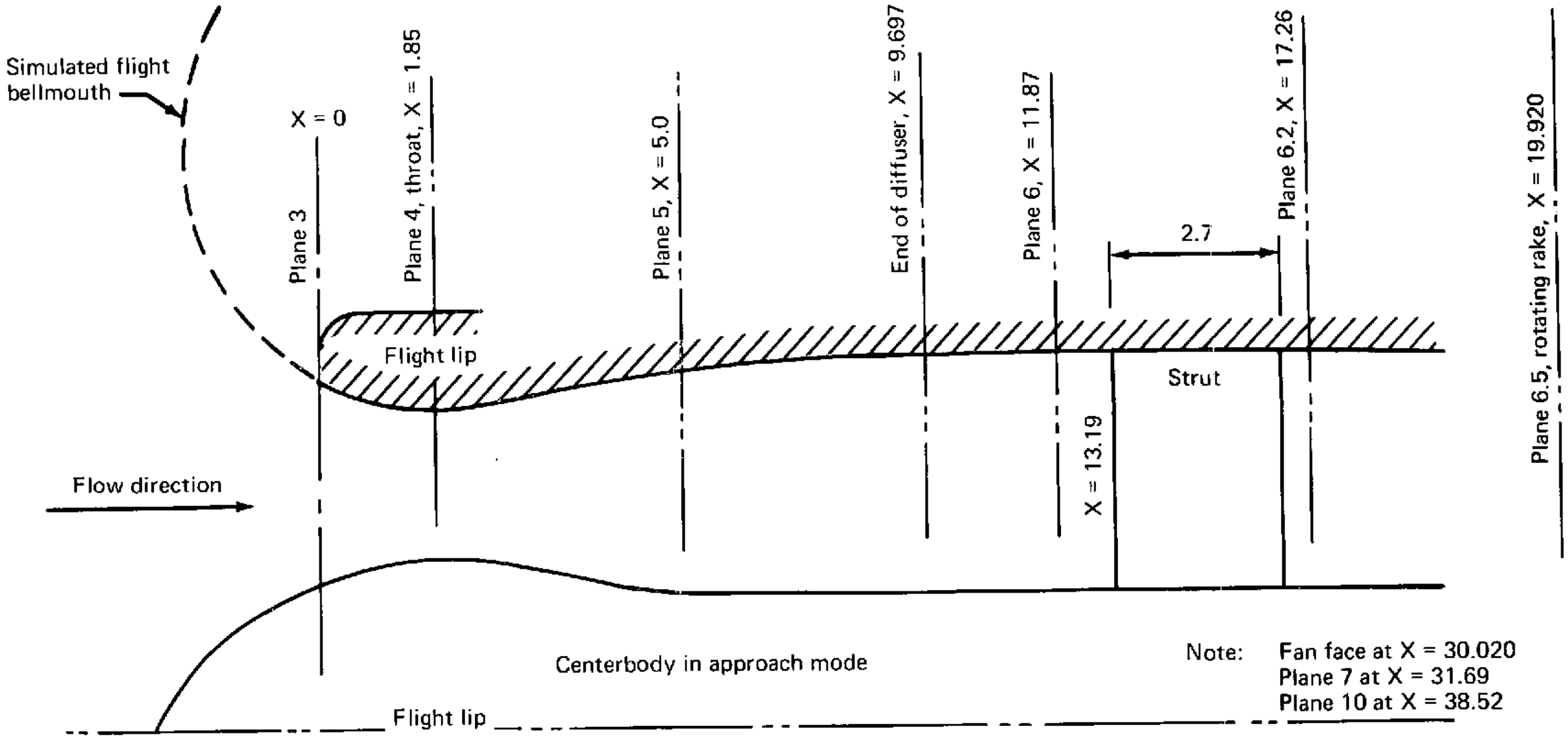

All dimensions in inches
$\phi = 0^\circ$ at 12 o'clock looking downstream

Points of steady static pressure measurement									
Longitudinal position: X	0(C)	0.4(C)	0.9(C)	1.4(C+CB)	1.85(C+CB)	2.3(C+CB)	2.75(C+CB)	3.25(C+CB)	3.75(C)
Angular position: ϕ	0	0	0	0	0,45,90,135,180,225,270,315	0	0	0	0
X	4.25 (C+CB)	5.0(C)	6.0(C)	7.25(C)	9.25(C)	11.87(C+CB)			
ϕ	0	0	0	0	0	0,90,180,270			

(C) = Cowl only
(C+CB) = Cowl and centerbody

FIGURE C-14.—RUN 11 INSTRUMENTATION—CENTERBODY INLET, APPROACH, MODEL 4, L/D = 1.0

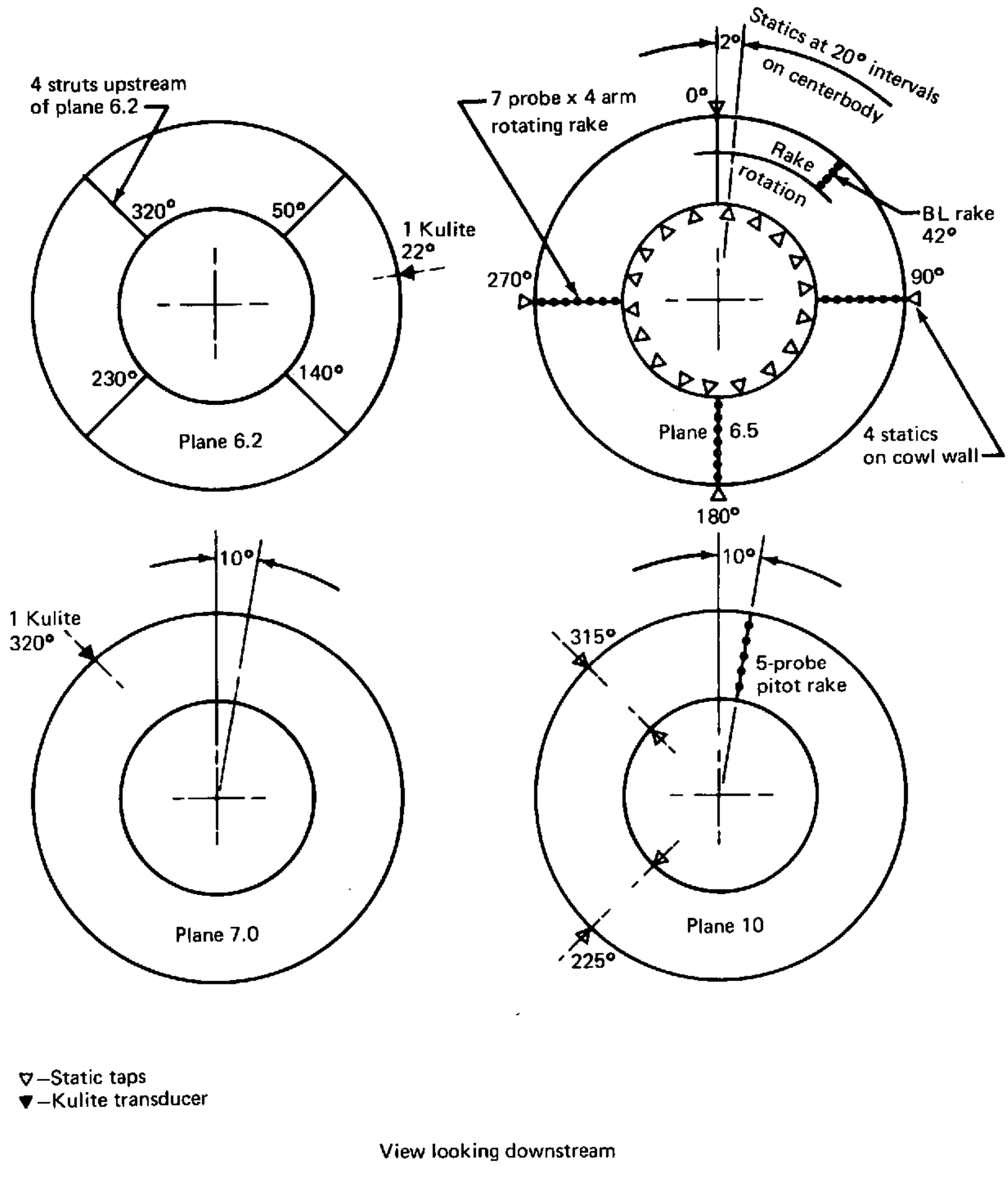

FIGURE C-15.—RUN 11 INSTRUMENTATION—MODEL 4, CONDITIONS 1 THROUGH 14

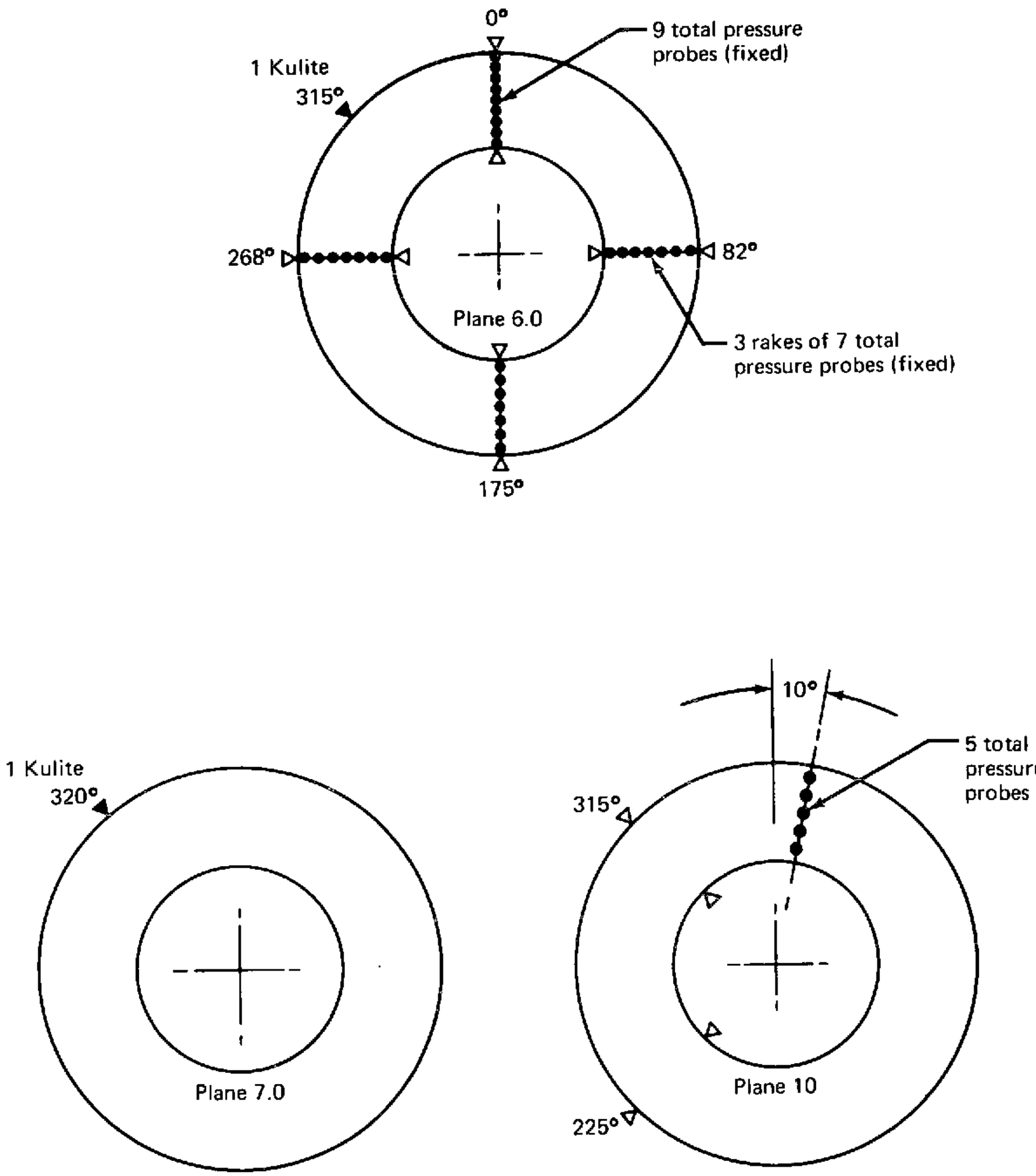

FIGURE C-16.—RUN 11 INSTRUMENTATION—MODEL 4, CONDITIONS 15 AND ON

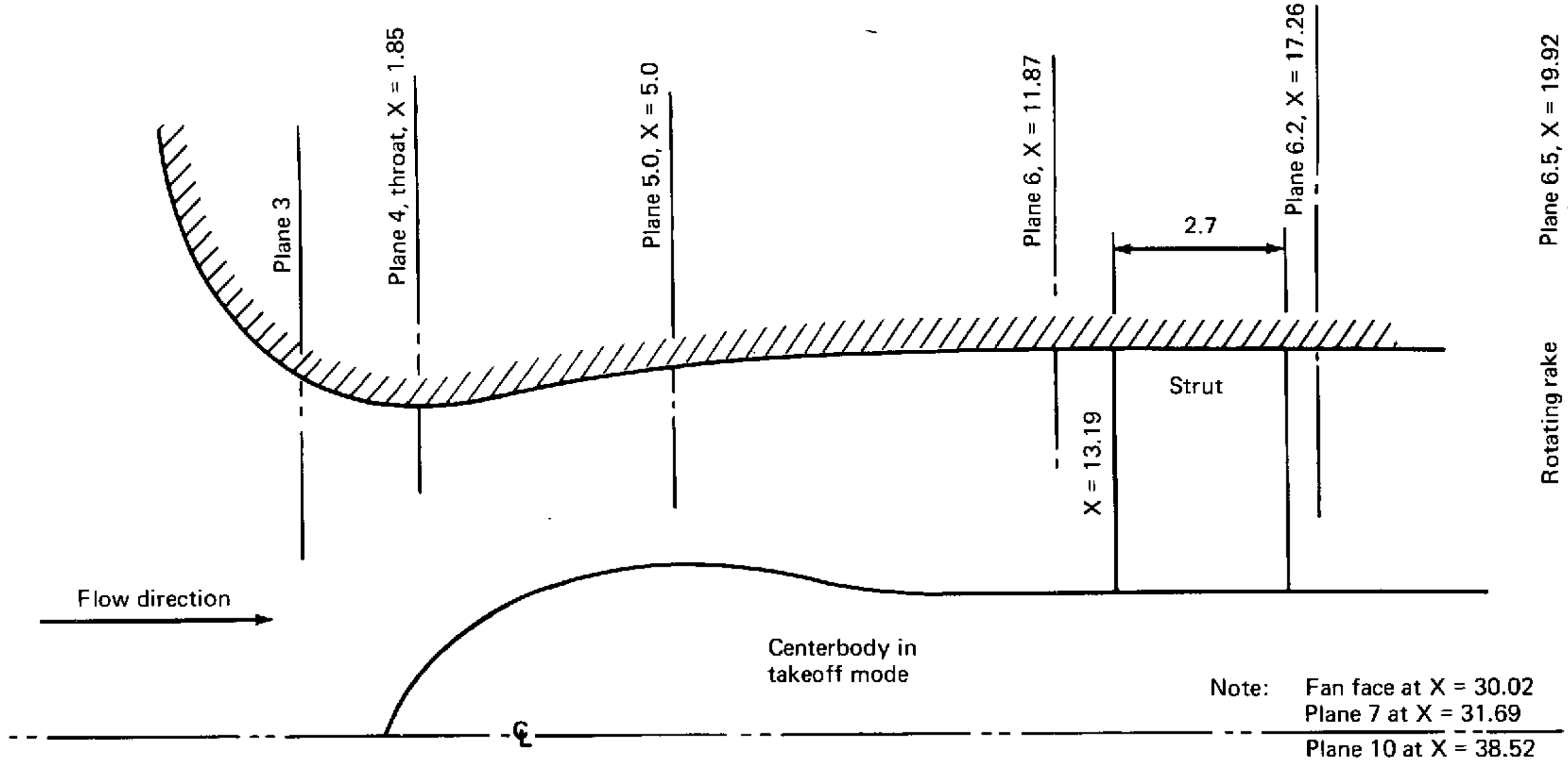

Points of steady static pressure measurement

Longitudinal position: X	0(C)	0.4(C)	0.9(C)	1.4(C)	1.85(C)	2.3(C)	2.75(C)	3.25(C)	3.75(C)	4.25(C)	5.0(C)	5.25(CB)
Angular position: ϕ	0	0	0	0	8 x 45	0	0	0	0	0	0	0

X	5.7(CB)	6.0(C)	6.15(CB)	6.6(CB)	7.1(CB)	7.25(C)	8.1(CB)	9.25(C)	11.87(C+CB)	
ϕ	8 x 45	0	0	0	0	0	0	0	4 x 90	

(C) = Cowl
(CB) = Centerbody
(C+CB) = Cowl and centerbody

FIGURE C-17.—RUN 12 INSTRUMENTATION—CENTERBODY INLET, TAKEOFF, MODEL 4, L/D = 1.0

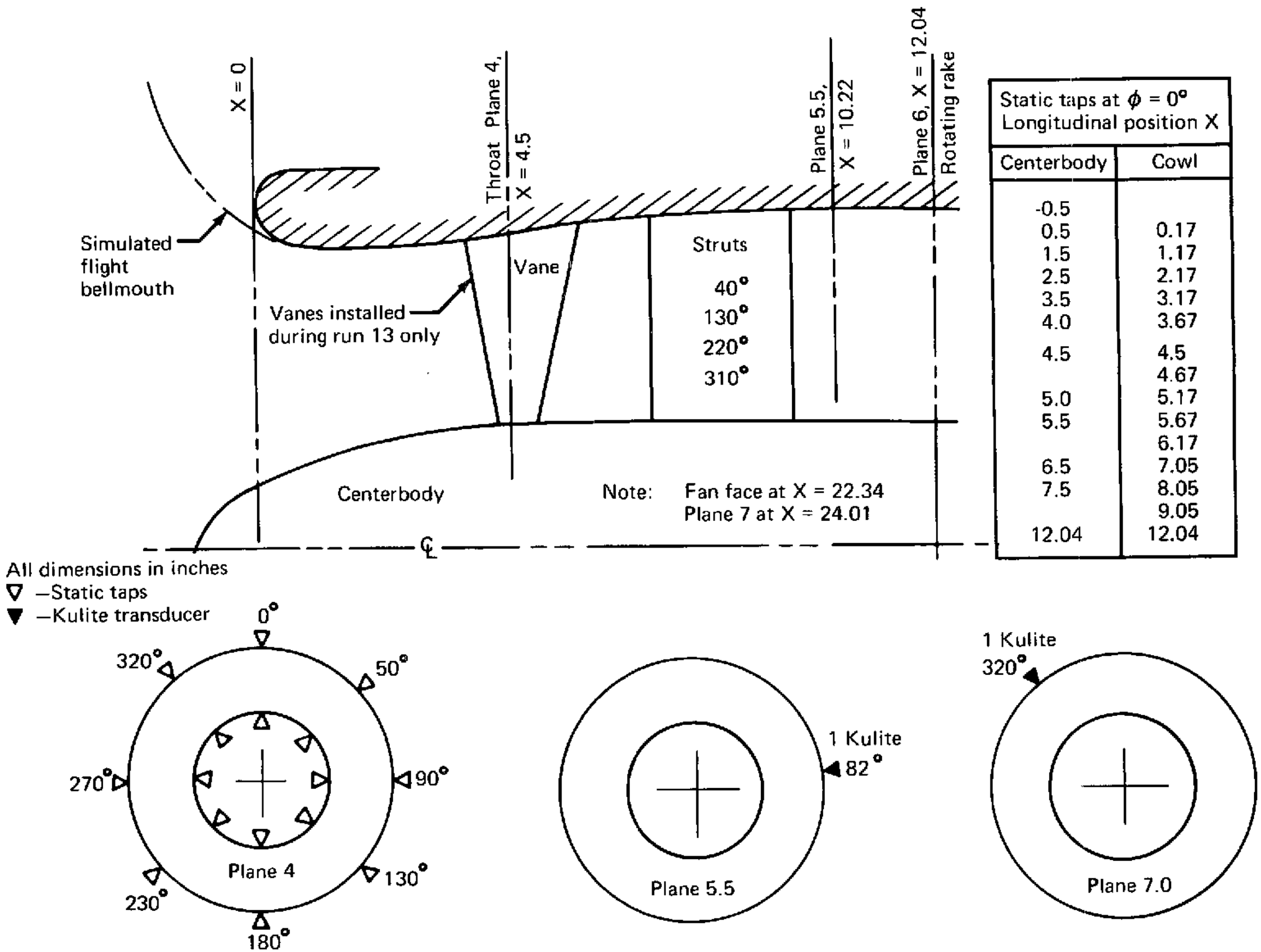

Static taps at $\phi = 0°$ Longitudinal position X	
Centerbody	Cowl
-0.5	
0.5	0.17
1.5	1.17
2.5	2.17
3.5	3.17
4.0	3.67
4.5	4.5
	4.67
5.0	5.17
5.5	5.67
	6.17
6.5	7.05
7.5	8.05
	9.05
12.04	12.04

FIGURE C-18.—RUN 13 AND 14 INSTRUMENTATION—RADIAL VANE INLET, MODEL 5B, L/D = 1.0

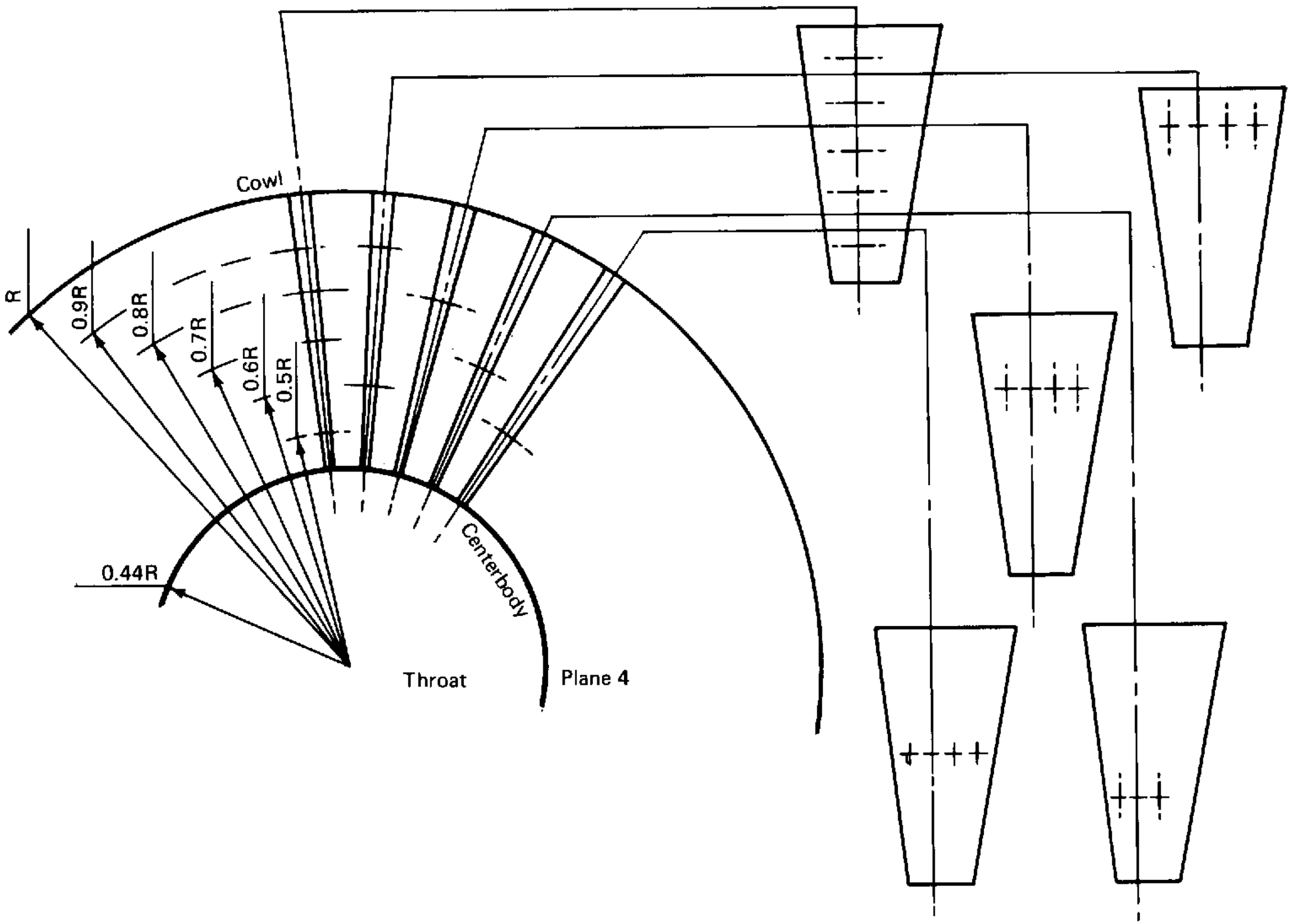

FIGURE C-19.—RUN 13 INSTRUMENTATION—RADIAL VANE INLET, MODEL 5B, L/D = 1.0

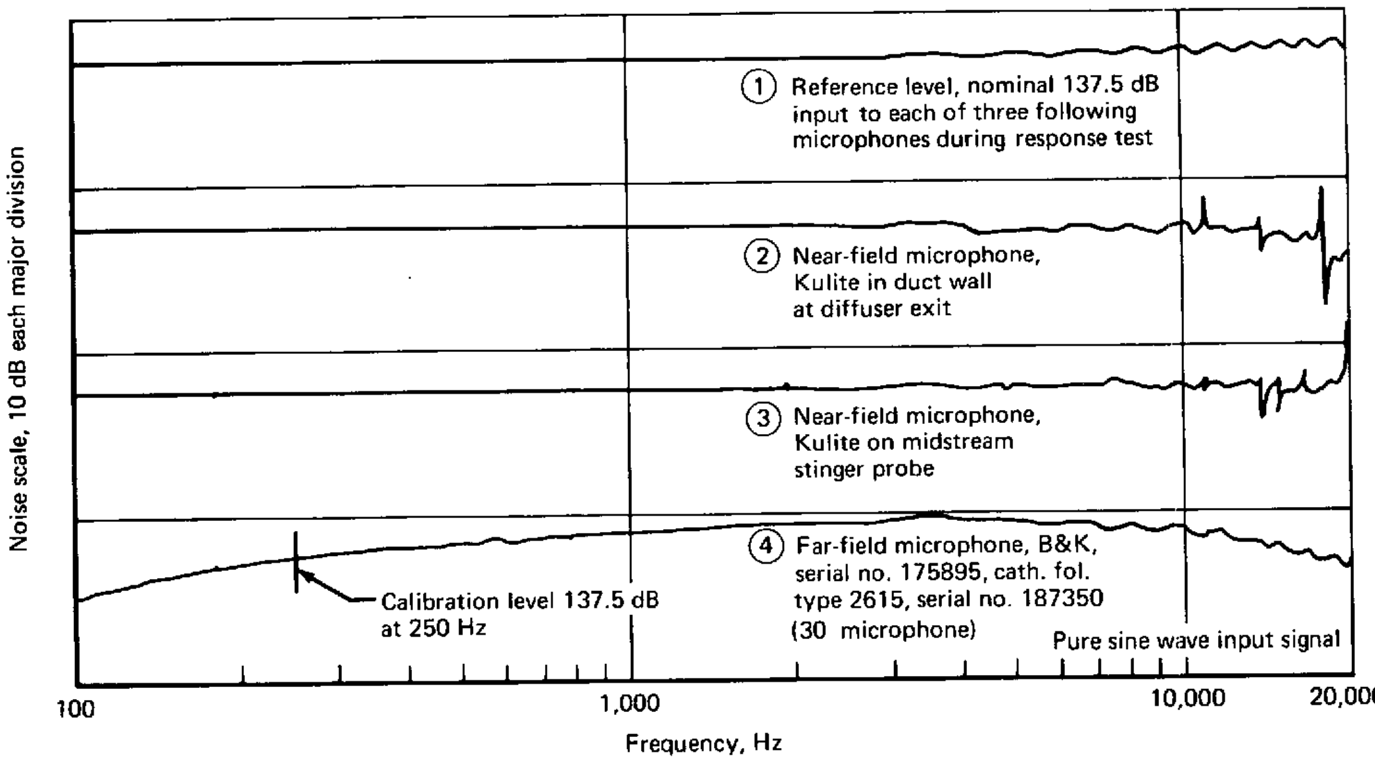

FIGURE C-20.—MICROPHONE FREQUENCY RESPONSE CHARACTERISTICS

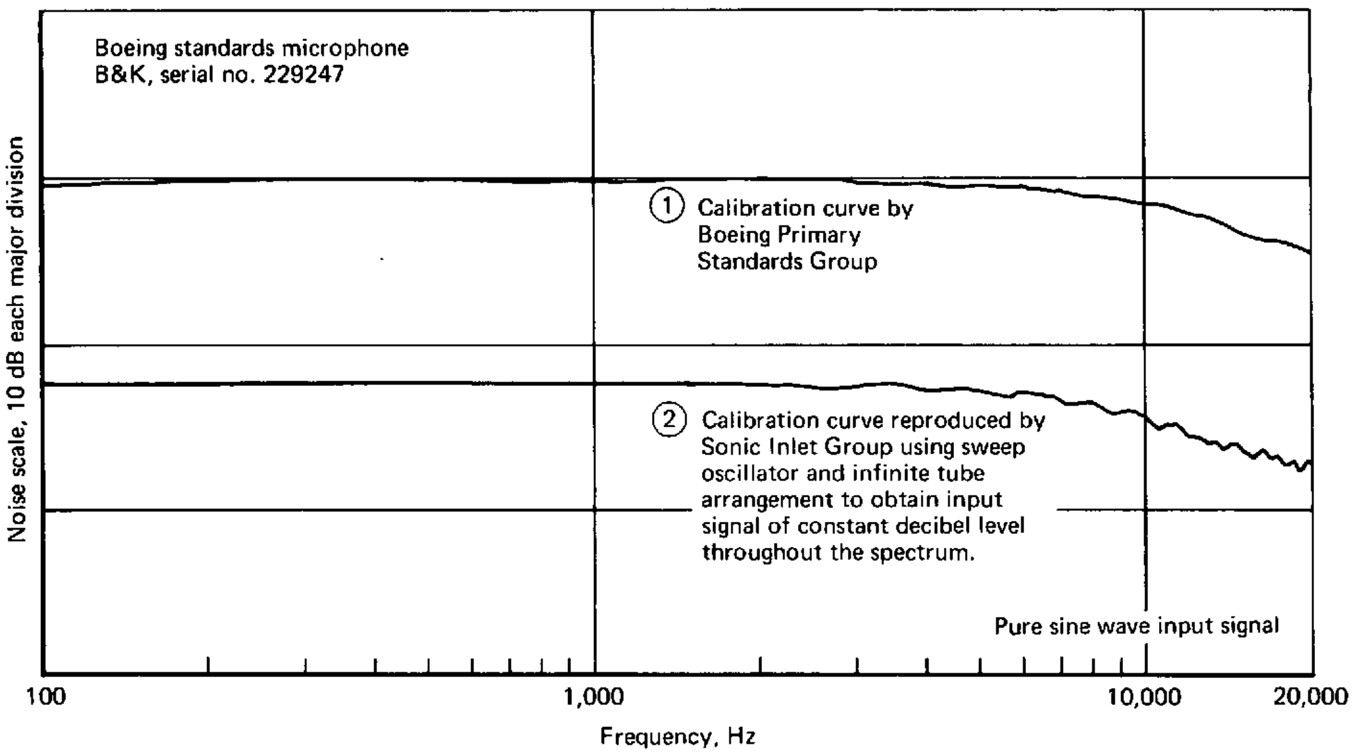

FIGURE C-21.—STANDARD MICROPHONE FREQUENCY RESPONSE CHARACTERISTICS

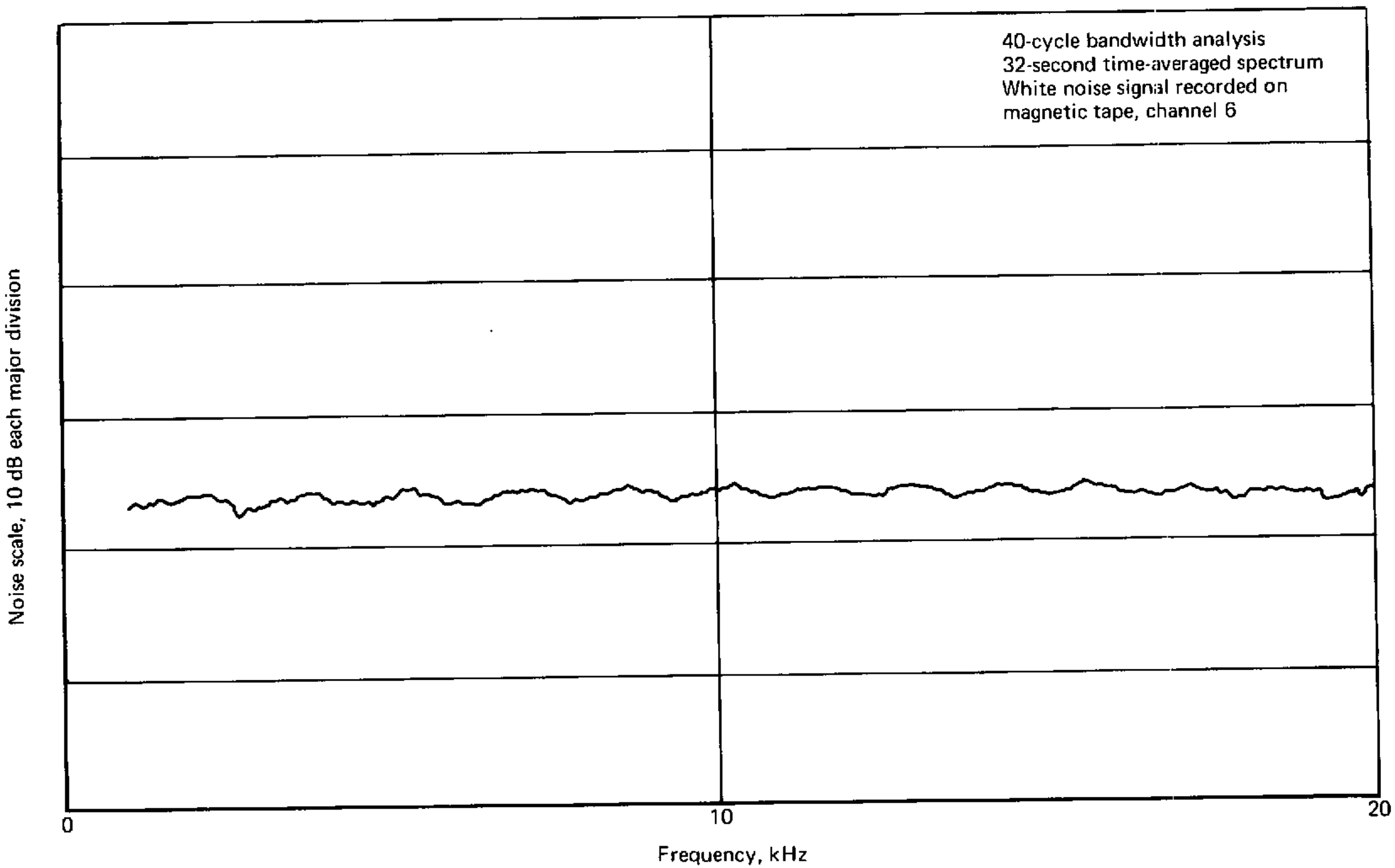

FIGURE C-22.—FREQUENCY RESPONSE—MAGNETIC TAPE SYSTEM AND SPECTRUM ANALYZER

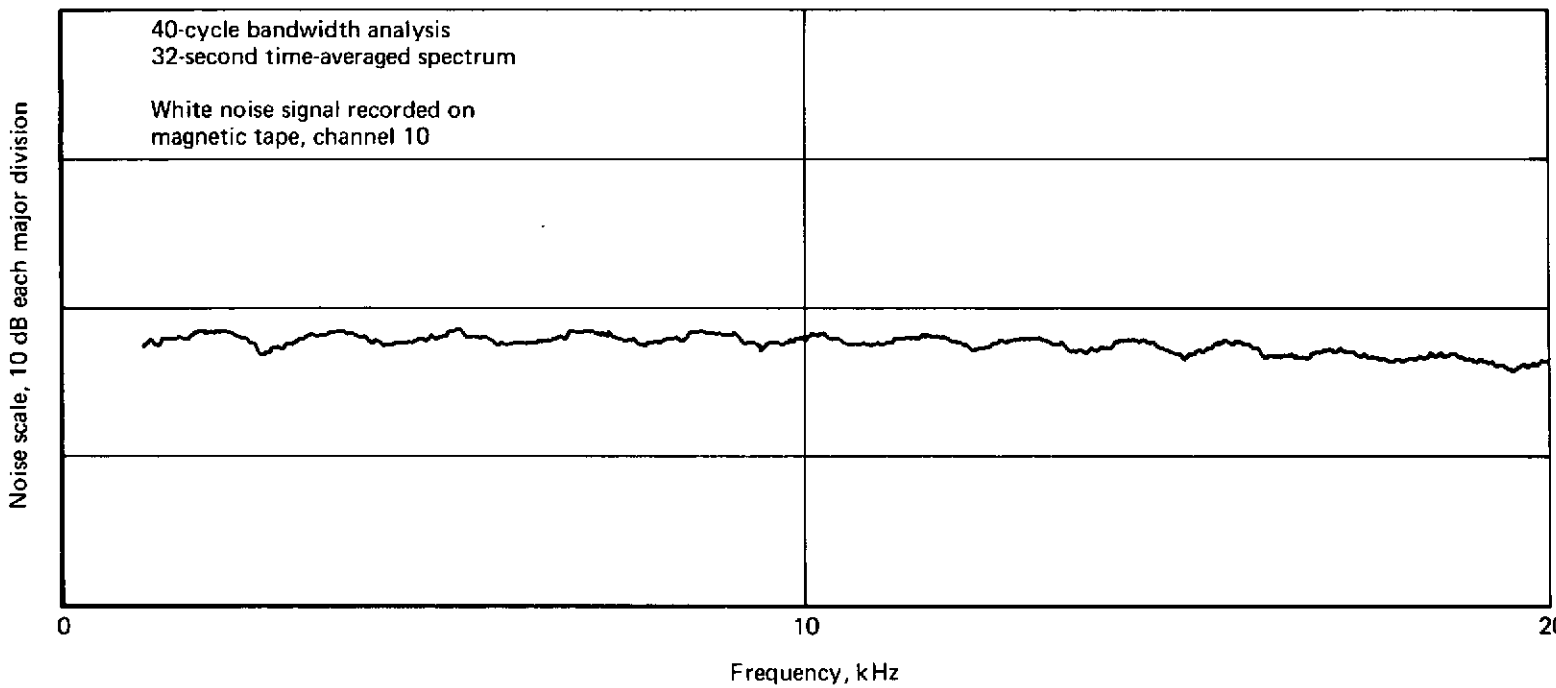

FIGURE C-23.—FREQUENCY RESPONSE—MAGNETIC TAPE SYSTEM AND SPECTRUM ANALYZER

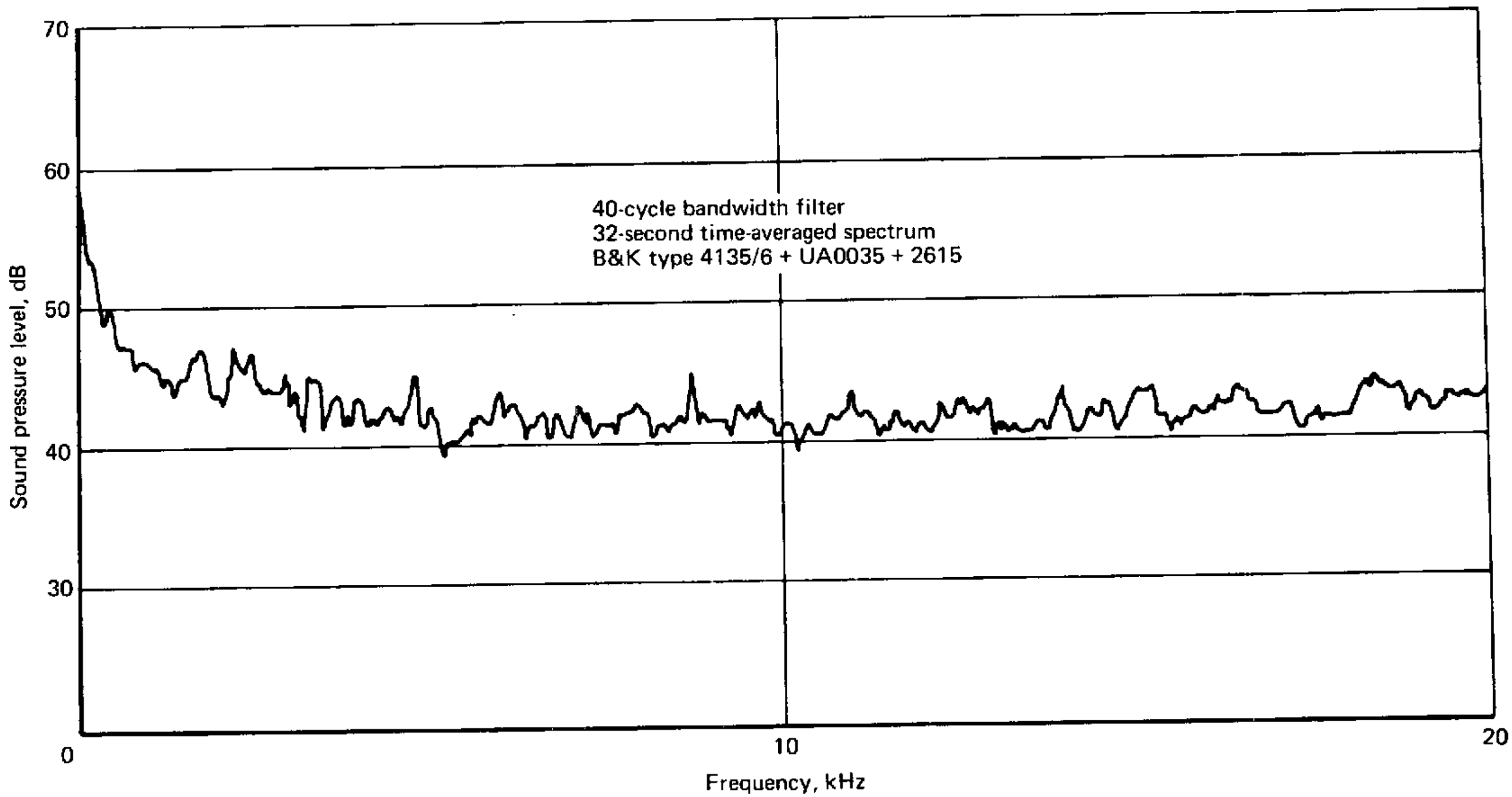

FIGURE C-24.—NOISE FLOOR—FAR-FIELD FORWARD ARC MICROPHONE

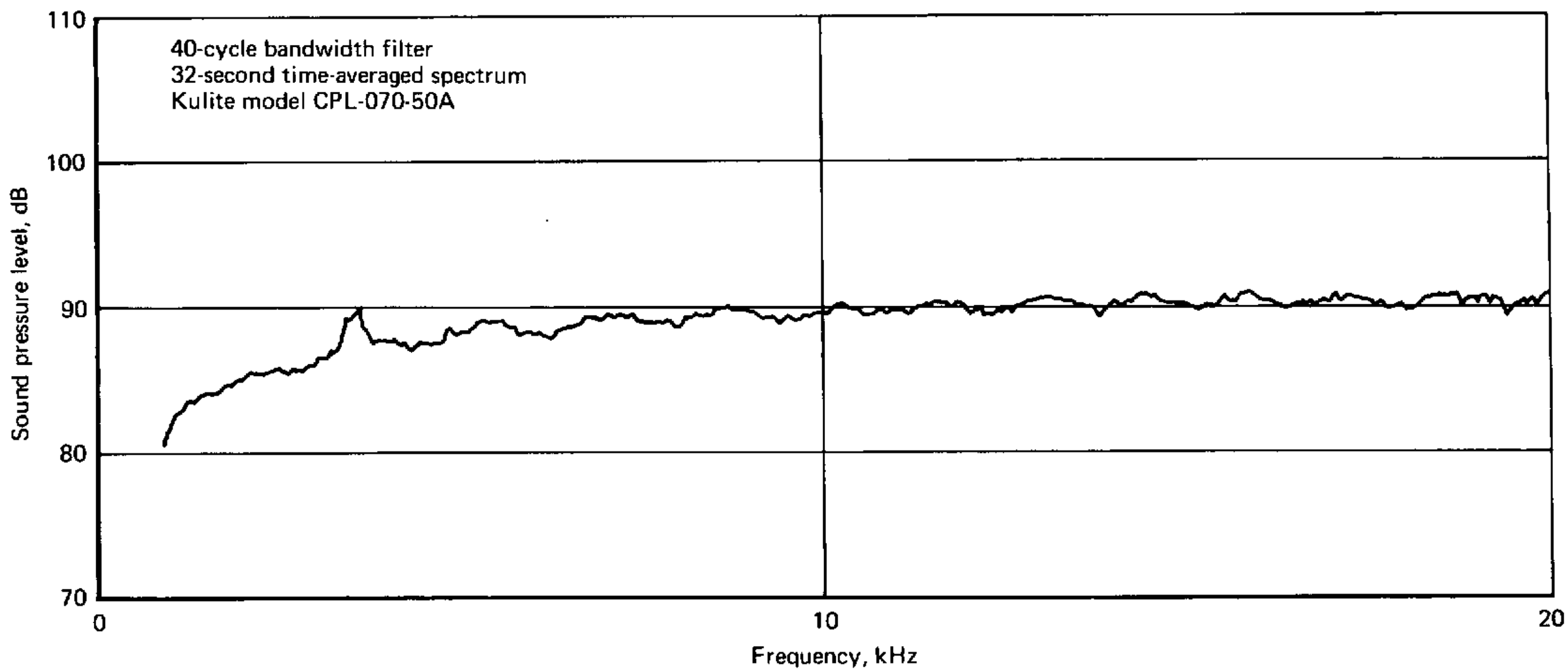

FIGURE C-25.—NOISE FLOOR—NEAR-FIELD MICROPHONE

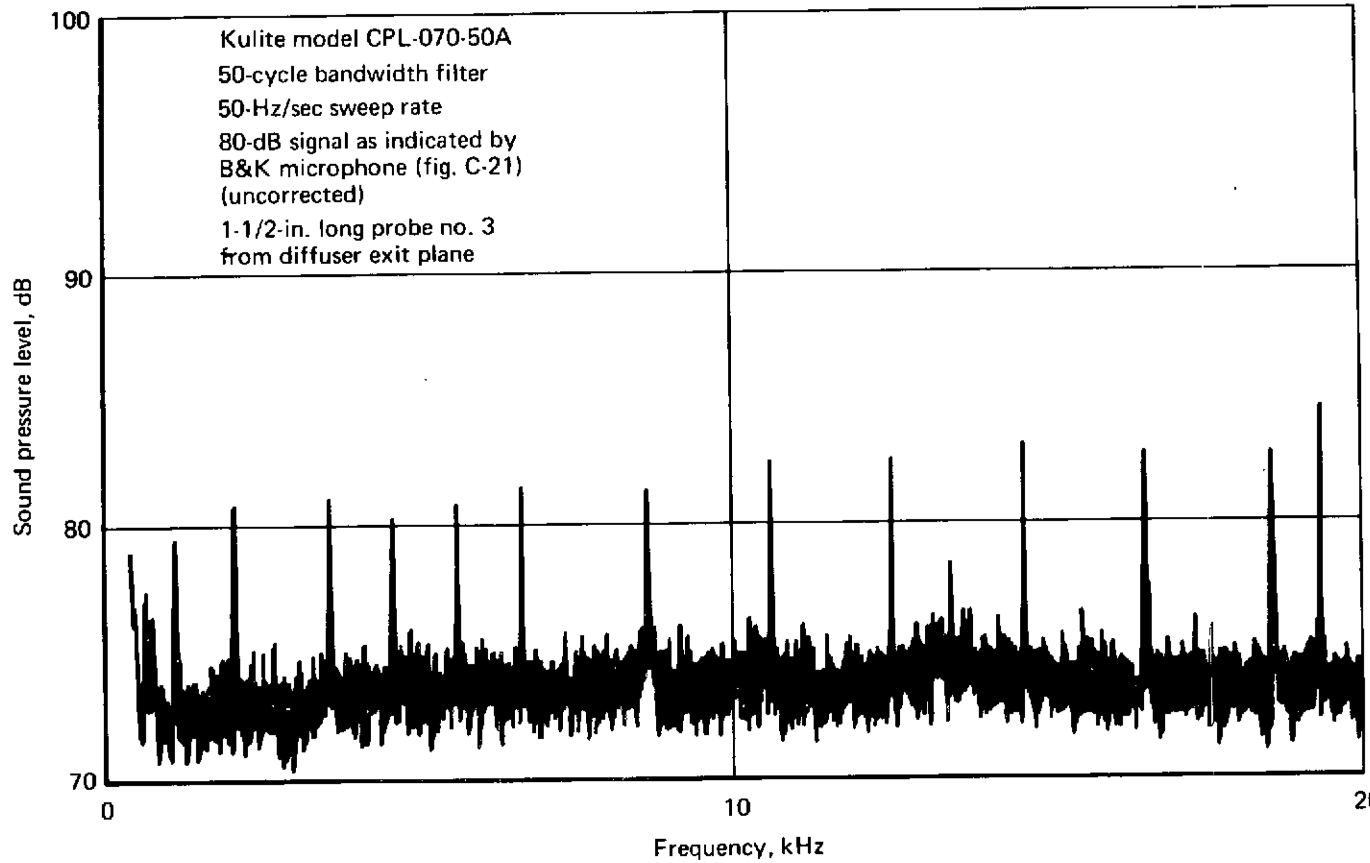

FIGURE C-26.—NEAR-FIELD MICROPHONE SENSITIVITY

APPENDIX D

DATA ANALYSIS PROCEDURE

This appendix summarizes the methods used for handling the data during test and discusses both the aerodynamic data reduction procedure and the methods of acoustic data analysis.

D.1 AERODYNAMIC DATA

All pressure, temperature, and rpm data were recorded in digital form on punched paper tape which was subsequently input to a computer at the test laboratory. This provided aerodynamic data of reduced form within 5 minutes of the event during the course of the test program. The test laboratory computer reduced all parameters to engineering units and performed such calculations as air mass-flow, fan pressure recovery, and inlet distortion.

Inlet recovery was defined as the ratio of average exit pressure from the diffuser divided by ambient pressure in the acoustic chamber. Average exit pressure was calculated in the diffuser exit plane. Total pressure measuring instrumentation was located at several different radii to entirely cover the flow area of the diffuser exit plane. The overall average pressure was calculated from an area-weighted average of all total pressure readings in the exit plane. Each total pressure reading was considered representative of the pressure existing in an area described by an annular ring with the pressure element at the centroid radius. Boundaries of each area ring were determined by the proximity of adjacent pressure elements. The calculation procedure can be summarized as follows:

$$\overline{PT_6} = \frac{\sum_{i=1}^{n} A_i\, PT_i}{\sum_{i=1}^{n} A_i}$$

$$\text{Recovery} = \overline{PT_6}/P_{\text{ambient}}$$

Whenever a multiposition traversing rake was used for complete mapping of total pressure at the diffuser exit plane, the punched paper tape was converted into digital form on a magnectic tape. The format on magnetic tape was made compatible with the CDC 6600. This magnetic tape was then used as input for the 6600, which used the pressure survey data to produce plots of recovery maps for the diffuser exit plane.

Calculations of flow distortion were based on the same flow measurements, which were used to establish inlet total pressure recovery. Distortion in the diffuser exit plane was defined as:

$$\text{Distortion} = \frac{P_{T_{max}} - P_{T_{min}}}{PT_6}$$

Pressure measurements used in calculating distortion were taken at a distance no nearer to the flow duct outer wall than 4% radius, and no nearer than 8% radius to the duct inner wall.

Air flow was measured by a bellmouth with adaptor section, which was bolted on the front of the inlet models. Some models were run with either a short bellmouth or a flight lip. Mass flow for these tests was determined by referring to a flow calibration which correlated mass flow to model throat static pressure. This information was obtained in a prior test where the bellmouth was used as the flow measuring standard.

Table D-1 is a legend of terms used to describe aerodynamic data output. Tables D-2 through D-17 are each a sample of the output from each of the test runs performed during the Sonic Inlet program. A sample for each run was included because the output format is slightly different for each model, as determined by geometry and instrumentation changes.

Bellmouth measured mass flow (WAC) was the first item of the printout. In cases where the model was tested without the standard bellmouth, the computer program used inlet throat area, inlet throat static pressure, and ambient pressure to calculate mass flow. This mass flow printout should be ignored in those cases because there was no information input for throat Mach number gradients; thus, the calculated mass flow was in error. This item was deleted from the output of the latest runs to avoid confusion.

Mass flow was additionally calculated from the total pressure traverses made in the diffuser exit plane. The result was always printed in the data tabulation section covering planes 5.5, 6.0, or 6.5. Refer to table D-17. Highest reliability in this method of calculating mass flow was found in test runs 11 through 14 (tables D-14, -15, -16, and -17) where the four-arm rake was used for pressure measurement. This rake was able to account for nonuniformity of flow in the duct.

Mach number values were printed in the tabulation of data parameters received during test. Wall surface Mach numbers from the throat and forward were calculated with the assumption that ambient total pressure was still valid (i.e., zero losses). The same procedure applied to the region from the throat to the downstream location where the first boundary layer total pressure rake was located. The Mach number in the region of each total pressure element was calculated by referring to the wall static pressure measurement in that axial location.

Static pressure was measured on both the inner and outer walls of the flow annulus in the diffuser exit plane. The average of these values was used in calculation of Mach number at the location of each total pressure element in the diffuser exit plane.

Calculations of throat midstream Mach number could be performed for only those inlets where an inlet stinger probe was used during test. For these limited cases, throat Mach number was calculated for the outer wall, centerbody wall, and midway in the flow stream.

Throat section average Mach number was used as a base parameter in comparing noise, recovery, and distortion between different models. It was hand calculated after concluding the following:

- The area coefficient of each model inlet throat was not known so throat geometric area was used and all were compared on this basis.
- Measured mass flow and geometric throat area were used to calculate the average throat Mach number.

Throat average Mach number, instead of throat wall Mach number, was used for data comparison because it was more indicative of the total mass flow. Mass flow in turn is a prime indicator of engine power setting, and this is primarily where the noise and aerodynamic performance of flight inlets should be judged. By this means, a practical comparison of different inlet models was obtained regardless of the different Mach number gradients in each inlet design. Inlet throat wall Mach number, on the other hand, was less indicative of total mass flow. It was highly dependent on the contours of both the cowl and centerbody, particularly the contours from the throat and forward.

D.2 ACOUSTIC DATA

Far-field forward arc noise was measured every 10° for the segment of 0° through 80° from inlet forward centerline. Near-field noise at the diffuser exit was measured on all inlet test models. The microphone was flush mounted in the duct outer wall. Sixty-second time samples of FM tape recording of the acoustic data were taken during the tests, and all microphones were simultaneously recorded on separate channels of a magnetic tape. A flow diagram of the acoustic data analysis system is shown in figure D-1.

D.2.1 Online Analysis

The overall noise level of each microphone was monitored during test by displaying each signal on an oscilloscope. Quick-look at the far-field noise spectrum was obtained by online analysis of the noise measured by the 30° microphone. A spectrum analyzer which used a filter bandwidth equal to 6% of the filter center frequency was used to obtain these quick-look noise spectra.

D.2.2 Offline Analysis

Acoustic data final results were based on spectrum analysis performed by playback of the multichannel magnetic tape.

D.2.2.1 Narrow Band Spectrum Analysis

Spectrum analysis performed on all near-field noise measurements was done with a 40-cycle constant bandwidth filter. During tape playback the analyzer performed a 32-second time averaging on each 40-cycle bandwidth filter in the spectrum. Output was in the form of 40-cycle bandwidth, 32-second time-averaged spectrum plots.

D.2.2.2 One-Third-Octave Band Spectrum Analysis

Final results of the far-field noise data were obtained from tape playback on a system which provided noise data analysis at 1/3-octave bandwidth. This spectrum analysis was done in the same manner as for narrow band analysis. A 32-second time averaging of the spectrum was obtained.

Output of the 1/3-octave spectrum was in the form of computer punched cards. These were used as input to a computer program which scaled the noise data to full scale and calculated perceived noise level at 500-ft sideline for the angles 10° through 80°. The PNL at 50°, 500-ft sideline, was used for model comparison because this was the location of peak noise level. Output was in the form of sound pressure level in 1/3-octave spectrum plots, tabular printout of 1/3-octave spectra, and printout of perceived noise levels.

D.2.2.3 Perceived Noise Levels

Noise spectra output from the analyzer were of course scale model data as measured by each microphone in its specific location of the test setup. It was considered most beneficial to convert all scale model noise data to full-scale engine data at 500-ft sideline and compare the results of each model on this basis. To be consistent with other accepted means of noise evaluation on new flight hardware concepts, perceived noise levels were required. This made it necessary to convert the data to full scale because most of the scale model frequency spectrum, including the blade passing tone, was at too high a frequency to be compatible with the standard procedure for calculating perceived noise levels.

The diameter and airflow rate of the STF 369C engine were used as specifications for scaling the data since it was an engine being considered for STOL application. The fan diameter ratio was 52/12, engine to scale model. The number of fan blades and specific weight flow were assumed to be the same for both model and full scale.

Details of the noise scaling and PNL calculation program were documented in reference D-1. The major functions of the program are summarized in the following text.

That portion of the scale model 1/3-octave spectrum lying between 2000 and 40 000 Hz was input required by the program. Blade passing tone was calculated for the scale model by referral to the number of fan blades and rpm input. Whenever the blade passing tone fell very nearly on the borderline between two of the 1/3-octave filters, the program was arranged to compute the proper filter to which to assign the blade passing tone. This consisted of calculating the expected rpm error or fluctuation envelope and assigning the blade tone to the filter band of highest sound pressure level only if the rpm could have drifted into that range.

Once the filter band containing the blade passing tone was established, this described the shape of the spectrum for both model and full scale. Since the blade number was the same in both cases, the blade passing tone for full scale was simply that of the model ratioed down by 12/52. That set the filter band which contained blade passing tone for the full-scale engine. The same sound pressure level as for model data was assigned (prior to scaling). This procedure, applied to each filter band of the 2000 to 40 000 Hz input spectrum, reduced the full-scale engine spectrum to cover the 1/3-octave filter bands from 630 Hz through 10 000 Hz. The portion of the full-scale spectrum from 630 Hz down to 50 Hz was assumed to be the same SPL level as for the 630-Hz band. This assumption was necessary because of a phenomenon peculiar to the scale model fan. The 12-in. scale model fan rotor was machined from a forging, and thus the blades were integral with the spool. A rotor vibration existed which created low-frequency noise spikes of high magnitude in the spectrum. The level of these spikes was in many cases comparable in dominance to the blade passing tone. This spectrum peculiarity had never been observed in data from full-scale engines where the fan rotor and blades were manufactured as separate pieces. The high-level spikes at the low end of the spectrum would have introduced error into the perceived noise calculations. Scale model spectra input to the program had to be in keeping with spectra shapes typical of full-scale engines. The spectra were made to conform to full-scale engine data by inserting a command in the program. This took the sound pressure level of the 1/3-octave band at 2500 Hz and assigned the same level to all lower bands. The corresponding region on the full-scale spectrum included the region from the 1/3-octave band at 630 Hz and all lower bands.

Once the frequencies, sound pressure levels, and shape of the spectrum were established, it was converted to full scale by applying the mass flow ratio:

$$SPL_{\text{full scale}} = SPL_{\text{model}} + 10 \log_{10} (W_{\text{full scale}}/W_{\text{model}})$$

Full-scale noise levels were converted to 500-ft sideline values by applying the standard extrapolation inverse square divergence law:

$$SPL_{\text{full scale}} = SPL_{\text{model}} - 20 \log_{10} (R_{\text{full scale}}/R_{\text{model}})$$

where R is the distance from the noise source to a measuring point in far field.

Atmospheric absorption was also taken into account when mathematically constructing the 1/3-octave spectrum (full scale) at 500-ft sideline. At this point in the computer program, the last step was to compute the perceived noise level (PNdB) from the scaled spectrum. These values were calculated for each 10° radial lying between 10° and 80° from inlet forward centerline at a point where they crossed the 500-ft sideline. The standard procedure was followed in calculating perceived noise levels. This can be found in reference D-2.

REFERENCES

D-1 A. R. Errington: A Discussion of the Logical Structure and Solution Algorithm Used In Version B of the 12-Inch Fan Noise Scaling Program (TEE 178B). Boeing Coordination Sheet AME P-M-427, October 2, 1972.

D-2 Definitions and Procedures for Computing the Perceived Noise Level of Aircraft Noise. ARP 865, The Society of Automotive Engineers, October 15, 1964.

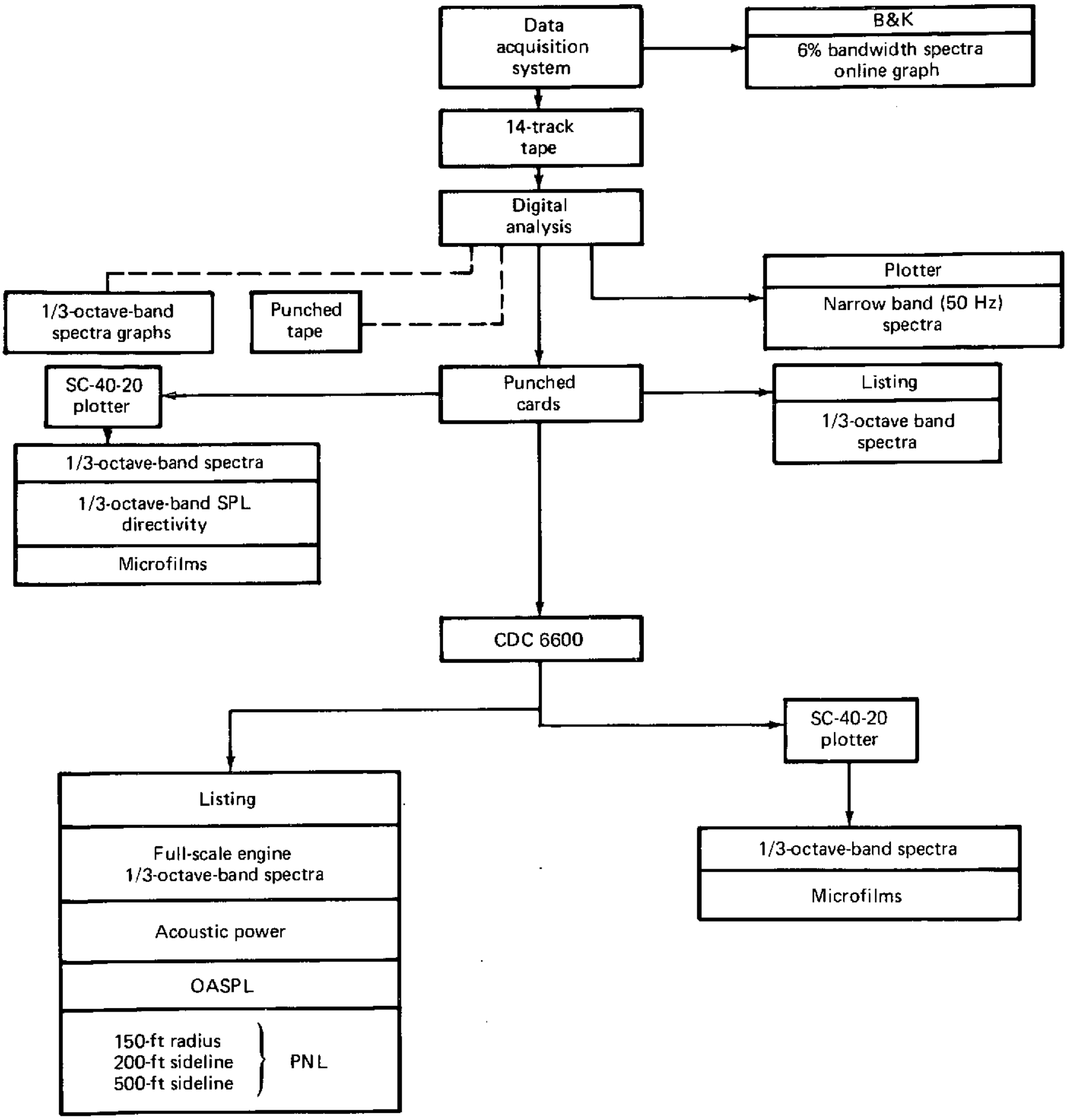

FIGURE D-1.—ACOUSTIC DATA ANALYSIS SYSTEM

TABLE D-1.–LEGEND FOR AERODYNAMIC DATA PRINTOUT

Term	Description
WAC	Inlet airflow $W\sqrt{\theta}/\delta$ lb/sec. Note: where flight lip inlets were tested, this airflow was not used. Refer to corresponding airflow calculation run and plot of $W\sqrt{\theta}/\delta$ versus inlet duct wall static.
FPR	Fan pressure ratio–inlet lip to stator discharge.
M6	Calculated from P_{S6} average and P_{T1}. Plane 6 Mach number.
N1	Fan mechanical rpm.
PTAMBO	Ambient pressure in the acoustic chamber, i.e., pressure at the inlet of the test vehicle, psia.
PLUG POS	Fan backload plug position, in.–0.0 was full open; 3.00 was point of maximum closure.
FAN TIP MR	Relative Mach number of air to fan blade tip. Based on P_{S6} average and P_T near the outer wall in plane 6.
N1C	Corrected fan rpm, $N/\sqrt{\theta}$.
TAMB ACOUSTIC TAMB AC CH	Ambient temperature in acoustic chamber, °R.
RH	Relative humidity in acoustic chamber, %.
FAN TIP M	Mach number of fan blade tip.
FAN TIP FPS	Fan tip speed, ft/sec.
PLANE 1	Ambient or inlet conditions to fan.
PT12Ø	Ambient pressure in acoustic chamber at 20° microphone location, psia.
PT1W	Ambient pressure in acoustic chamber at wall near test vehicle inlet, psia.
PT1	Ambient pressure in acoustic chamber (=PTAMBO) = average of PT12Ø and PT1W, psia.
TT1.1 through TT1.3	Temperature, °R, at three places on the inlet bellmouth when used.
AVG TT1	Temperature, °R, average of three bellmouth temperatures.
TT12Ø	Temperature, °R, in acoustic chamber at location of 20° microphone.
TT1W	Temperature, °R, in acoustic chamber on wall adjacent to test vehicle inlet.
TT1	Average of TT12Ø and TT1W, °R.
PLANE 2	Plane of bellmouth throat statics when standard bellmouth was used.
PS2.1-PS2.4	Four bellmouth throat statics spaced at 90° in the throat plane, psia.
BSBM	Average pressure, bellmouth throat wall statics (average of PS2.1-PS2.4.), psia.
PSBM/PT1	P_S/P_T for bellmouth throat.
AVG M2	Bellmouth throat Mach number based on P_{SBM} and P_{T1}.
PLANE 3	Ahead of throat plane. Usually the starting point for a string of cowl statics located along an axial line. Specific inlet detail drawing must be consulted for exact location of these statics.

TABLE D-1.–CONCLUDED

Term	Description
PLANE 4	The number 4 or 400 indicates the geometric throat plane.
PLANE 5	Intermediate measuring plane approximately midway in the diffuser.
PLANE 6	Diffuser exit plane.
M6	Mach number in plane 6. The value printed under the plane 6 section was calculated based on P_S wall average in plane 6 and the P_T measured in plane 6 with the traverse probe inserted to position 1. Differs from M6 printed out in summary group at heading. There P_{T1} was used, assuming zero loss.
FAN TIP MR	Mach number relative to the fan blade tip. The value printed under the plane 6 section was calculated based on P_S wall average in plane 6, and the P_T in plane 6 with the traverse probe inserted to position 1 (i.e., near fan blade tip).
PS6.1-PS6.4	Four static pressures spaced at 90° in plane 6.
PLANE 6 TRAV	Radial traverse with P_S, P_T wedge probe.
OBS PS-A and OBS PS-B	Two observed static pressures on the wedge probe.
OBS PS/PT	Observed value of P_S/P_T for the probe.
TRUE PS	Obtained from Mach number correction for the probe.
TRUE PT	Same as measured P_T. No correction required.
WCOR 6	Incremental weight flow corrected to local conditions.
M	Local Mach number.
PT/PT1	Recovery. Local pressure compared to ambient pressure.
WCOR 2	Plane 6 weight flow calculation corrected to plane 2.
PL6 FPR	Pressure ratio from fan face to stator exit.
MB or MB4	Mach number, M. Throat section average Mach number calculated based on bellmouth weight flow measurement and inlet throat area. P_S/P_T corresponding to this M was sometimes printed out.
PLANE 6 ROTATING RAKE	(Used only in runs 11, 12, 13, and 14) The rotating rake had four arms approximately equally spaced around the circumference. Each arm carried total pressure elements at seven different radii. The rake was set at a new circumferential position in 10° increments to cover the full 360° of the inlet duct. Only readings from the four arms set at the first position were printed out during test. Airflow and total pressure recovery were printed out based on the pressure data from the first position of the rake.
PLANE 10	
PT10.1-PT10.5	Total pressure at center of five equal area increments downstream from the stators, psia.
PS	Two places on duct inner wall and two places on duct outer wall downstream from the stators.

TABLE D-2.–RUN 1, SAMPLE AERODYNAMIC DATA TABULATION

```
PROG C-T
TEST NO.   2274                               DATE     11972

RUN NO./COND NO.      1.041

MAP NO/CONFIG NO.     6.001

WAC     20.028        PTAMBO          14.545    TAMB ACOUSTIC        510.67
FPR     1.1884        PLUG POS         2.40     RH                      87%
M       0.402         FAN TIP MR       0.982    FAN TIP M             0.896
N1      18650         N1C             18798     FAN TIP FPS           976.5

PLANE 1:
PT120       14.550    PT1W  14.540     PT1   14.545
PAMB-PT1     0.016

TT1.1    51.33F    511.02R
TT1.2    50.64F    510.33R
TT1.3    50.64F    510.33R      BMTT1    510.56R
TT120    50.99F    510.67R
TT1W     51.33F    511.02R      TT1      510.85R

PLANE 2:
PS2.1-PS2.4       13.557    13.556    13.558    13.560
PSBM              13.558
PSBM/PT1           0.932
WCOR2             20.028       AVG M2   0.402

PLANE 6:
PS6.1-PS6.4       13.000    13.027    13.018    13.026
AVG PS6           13.018

PLANE 10:
PT10.1-PT10.5       17.435  - 17.435    17.275    17.045    17.185
AVG PT10            17.285
PSO10.1-PSO10.2 15.627    15.675
PSI10.1-PSI10.2 15.281    15.278

701.78 @ 03.86
*
```

TABLE D-2.–CONCLUDED

PROG C-T
TEST NO. 2274 DATE 11972

RUN NO./COND NO. 1.041

MAP NO/CONFIG NO. 6.001

WAC	20.115	PTAMBO	14.540	TAMB ACOUSTIC	509.98
FPR	1.1865	PLUG POS	2.40	RH	87%
M	0.396	FAN TIP MR	0.982	FAN TIP M	0.898
N1	18690	N1C	18855	FAN TIP FPS	978.6

PLANE 1:
PT120 14.550 PT1W 14.530 PT1 14.540
PAMB-PT1 0.004

TT1.1	49.95F	509.64R		
TT1.2	50.30F	509.98R		
TT1.3	49.61F	509.29R	BMTT1	509.64R
TT120	50.30F	509.98R		
TT1W	50.99F	510.67R	TT1	510.33R

PLANE 2:
PS2.1-PS2.4 13.546 13.544 13.542 13.543
PSBM 13.544
PSBM/PT1 0.932
WCOR2 20.115 AVG M2 0.396

PLANE 6:
PS6.1-PS6.4 13.017 13.066 13.059 13.059
AVG PS6 13.050

PLANE 10:
PT10.1-PT10.5 17.422 17.372 17.212 17.022 17.142
AVG PT10 17.252
PSO10.1-PSO10.2 15.594 15.650
PSI10.1-PSI10.2 15.269 15.261

PLANE 6-TRAVERSE:

RADIUS	OBS PS-A	OBS PS-B	OBS PS-AVG	OBS PS/PT	TRUE PS/PT	TRUE PS	TRUE PT	WCOR6	M	REC PT/PT1
5.885	12.961	13.122	13.042	0.916	0.916	13.030	14.232	1.957	0.358	0.979
5.609	13.129	13.106	13.118	0.908	0.906	13.094	14.451	2.052	0.378	0.994
5.319	13.089	13.047	13.068	0.903	0.901	13.038	14.472	2.101	0.389	0.995
5.012	13.148	12.934	13.041	0.900	0.897	13.005	14.497	2.136	0.397	0.997
4.685	13.178	13.060	13.119	0.904	0.902	13.090	14.517	2.094	0.388	0.999
4.334	13.143	13.151	13.147	0.906	0.904	13.120	14.519	2.075	0.383	0.999
3.951	13.213	13.021	13.117	0.904	0.902	13.088	14.509	2.090	0.387	0.998
3.527	13.232	13.045	13.139	0.905	0.903	13.111	14.519	2.081	0.385	0.999
3.045	13.193	13.190	13.192	0.909	0.907	13.170	14.514	2.039	0.376	0.998
2.470	13.292	13.290	13.291	0.916	0.915	13.278	14.517	1.966	0.360	0.999

AVG PT= 14.474 AVG PS= 13.102
AVG PT6/PT1= 0.996 WCOR6= 20.586
W= 20.492 MR= 0.9764
M= 0.385

TABLE D-3.–RUN 2, SAMPLE AERODYNAMIC DATA TABULATION

PROG CI
TEST NO. 2274 DATE 20472

RUN NO./COND NO. 2.003

MAP NO/CONFIG NO. 39.002

WAC	18.969	PTAMBO	14.690	TAMB ACOUSTIC	496.53
FPR	1.1740	PLUG POS	2.40	RH	75%
M6	0.394	FAN TIP MR	0.955	FAN TIP M	0.870
N1	17920	N1C	18259	FAN TIP FPS	938.3

PLANE 1:
PT120 14.700 PT1W 14.680 PT1 14.690
PAMB-PT1 0.017

TT1.1	40.29F	499.98R		
TT1.2	39.60F	499.29R		
TT1.3	39.95F	499.63R	BMTT1	499.63R
TT120	36.84F	496.53R		
TT1W	38.57F	498.25R	TT1	497.39R

PLANE 2:

PS2.1-PS2.4	13.808	13.806	13.800	13.799
PSBM	13.803			
PSBM/PT1	0.940			
WCOR2	18.969	AVG M2	0.300	

	PSIA	M	PS/PT
PS 201	14.128	0.237	0.962
PS 202	13.961	0.271	0.950
PS 300	11.652	0.585	0.793
PS 301	10.744	0.684	0.731
PS 302	9.787	0.784	0.666
PS 303	9.113	0.855	0.620
PS 400	8.860	0.882	0.603
PS 401	8.881	0.879	0.605
PS 402	9.777	0.785	0.666
PS 403	10.698	0.689	0.728
PS 450	11.382	0.615	0.775
PS 451	11.791	0.569	0.803
PS 452	12.411	0.497	0.845
PS 500	12.767	0.452	0.869
PS 501	12.982	0.424	0.884
PS 502	13.131	0.404	0.894
PS 503	13.195	0.395	0.898
PS 600	13.158	0.400	0.896
PS 600	13.158	0.400	0.896

NO STINGER PROBE

PLANE 4:

PS4.1-PS4.4	8.860	8.916	8.893	8.850
AVG PS4	8.880			

TABLE D-3.—CONTINUED

PROG CI
TEST NO. 2274 DATE 20472

RUN NO./COND NO. 2.003

PLANE 4.5:

PS45.1-PS45.4	11.382	11.391	11.371	11.390
AVG PS45	11.384			

B/L PROBE

PORT	B/L-PT	PS/PT	M	PT/PT1
1	12.654	0.900	0.392	0.862
2	13.589	0.838	0.510	0.925
3	14.252	0.799	0.576	0.970
4	14.473	0.787	0.596	0.985
5	14.524	0.784	0.600	0.989

AVG PT 13.775 AVG M 0.529 REC 0.938

PLANE 5:

PS5.1-PS5.4	12.767	12.753	12.794	12.787
AVG PS5	12.775			

B/L PROBE

PORT	B/L-PT	PS/PT	M	PT/PT1
1	13.130	0.973	0.198	0.894
2	13.249	0.964	0.229	0.902
3	13.397	0.954	0.262	0.912
4	13.782	0.927	0.331	0.938
5	13.780	0.927	0.331	0.938
6	13.932	0.917	0.354	0.949
7	14.123	0.905	0.381	0.962

AVG PT 13.720 AVG M 0.321 REC 0.934

PLANE 6:

PS6.1-PS6.4	13.158	13.185	13.230	13.226
AVG PS6	13.200			

B/L PROBE

PORT	B/L-PT	PS/PT	M	PT/PT1
1	13.894	0.950	0.272	0.946
2	13.958	0.946	0.284	0.950
3	14.035	0.941	0.297	0.956
4	14.118	0.935	0.312	0.961
5	14.205	0.929	0.326	0.967
6	14.280	0.924	0.337	0.972
7	14.351	0.920	0.348	0.977
8	14.420	0.915	0.358	0.982
9	14.428	0.915	0.359	0.982

PROBE 1:
AVG PT 14.202 AVG M 0.325 REC 0.967

TABLE D-3.—CONTINUED

PROG C1
TEST NO. 2274 DATE 20472

RUN NO./COND NO. 2.003

PLANE 6 CONT'D

B/L PROBE

PORT	B/L-PT	PS/PT	M	PT/PT1
1	14.003	0.943	0.292	0.953
2	14.099	0.936	0.308	0.960
3	14.198	0.930	0.324	0.967
4	14.304	0.923	0.341	0.974
5	14.402	0.917	0.355	0.980
6	14.491	0.911	0.368	0.987
7	14.561	0.907	0.377	0.991
8	14.572	0.906	0.379	0.992
9	14.581	0.905	0.380	0.993

PROBE 2:
AVG PT 14.365 AVG M 0.350 REC 0.978

PLANE 10:					
PT10.1-PT10.5	17.460	17.400	17.300	17.010	17.060
AVG PT10	17.246				
PS10.1T-PS10.2T	15.667	15.702			
PS10.1H-PS10.2H	15.376	15.361			

TABLE D-3.—CONCLUDED

```
PROG C1-T
TEST NO.   2274                      DATE    20472

RUN NO./COND NO.      2.003

MAP NO/CONFIG NO.   39.002

WAC     19.017        PTAMBO        14.690    TAMB ACOUSTIC      496.87
FPR     1.1732        PLUG POS       2.40     RH                    75%
M6      0.395         FAN TIP MR     0.957    FAN TIP M           0.872
N1      17960         N1C           18297     FAN TIP FPS        940.4

PLANE 1:
PT120      14.700    PT1W  14.680    PT1  14.690
PAMB-PT1   0.018

TT1.1   40.29F   499.98R
TT1.2   39.60F   499.29R
TT1.3   40.29F   499.98R     BMTT1   499.75R
TT120   37.19F   496.87R
TT1W    38.91F   498.60R     TT1     497.74R

PLANE 2:
PS2.1-PS2.4      13.812    13.800    13.791    13.791
PSBM             13.799
PSBM/PT1          0.939
WCOR2            19.017     AVG M2   0.300

PLANE 6:
 S.1-PS6.4       13.179    13.137    13.226    13.232
AVG PS6          13.194

PLANE 10:
PT10.1-PT10.5     17.510    17.430    17.200    16.960    17.070
AVG PT10          17.234
PS10.1T-PS10.2T 15.662    15.699
PS10.1H-PS10.2H 15.372    15.360
```

PLANE 6-TRAVERSE:

RADIUS	OBS PS-A	OBS PS-B	OBS PS-AVG	OBS PS/PT	TRUE PS/PT	TRUE PS	TRUE PT	WCOR6	M	REC PT/PT1
5.885	13.184	13.049	13.117	0.933	0.933	13.122	14.059	1.757	0.316	0.957
5.609	13.235	13.042	13.139	0.921	0.921	13.133	14.261	1.900	0.345	0.971
5.319	13.189	13.124	13.157	0.912	0.911	13.139	14.429	2.007	0.369	0.982
5.012	13.212	13.130	13.171	0.901	0.899	13.138	14.612	2.118	0.393	0.995
4.685	13.277	13.219	13.248	0.903	0.901	13.217	14.670	2.101	0.389	0.999
4.334	13.273	13.204	13.239	0.902	0.899	13.205	14.684	2.116	0.393	1.003
3.951	13.192	13.258	13.225	0.900	0.898	13.190	14.690	2.129	0.396	1.000
3.527	13.315	13.157	13.236	0.901	0.899	13.202	14.692	2.123	0.394	1.000
3.045	13.221	13.371	13.296	0.905	0.903	13.268	14.694	2.082	0.385	1.000
2.470	13.351	13.436	13.394	0.912	0.910	13.375	14.693	2.010	0.369	1.000

```
AVG PT=         14.547    AVG PS=      13.198
AVG PT6/PT1=  0.990     WCOR6=       20.335
               20.138     MR=           0.9304
                0.335
```

TABLE D-4.—RUN 3, SAMPLE AERODYNAMIC DATA TABULATION

```
PROG CI-B
TEST NO.   2274                          DATE    30272

RUN NO./COND NO.      3.004

MAP NO/CONFIG NO.    43.003

WAC    24.939    PTAMBO      14.665    TAMB ACOUSTIC   501.70
FPR    1.2538    PLUG POS     1.00     RH                 83%
MS     0.505     FAN TIP MR   1.231    FAN TIP M        1.122
N1     22930     N1C         23339     FAN TIP FPS      1203

PLANE 1:
PT120      14.660    PT1W  14.670    PT1  14.665


TT1.1     42.71F    502.38R
TT1.2     43.40F    503.08R
TT1.3     43.40F    503.08R    BMTT1    502.85R
TT120     42.02F    501.73R
TT1W      43.05F    502.74R    TT1      502.22R

PLANE 2:
PS2.1-PS2.4      13.041 13.043 13.041 13.040
PS2M             13.041
PS2M/PT1          0.889
WCOR2            24.939   AVG M2  0.413

NO STINGER PROBE

PLANE 4:
         PS4.1-PS4.8    8.231   8.107   8.410   8.170   8.241   8.092   8.331
AVG PS4           8.221    M4    0.943


PLANE 6:
PS6.1-PS6.4  12.290 12.293 12.353 12.341
AVG PS6      12.319


PLANE 10:
PT10.1-PT10.5   18.625 18.435 18.435 18.305 18.085
AVG PT10          18.337
PS10.1T-PS10.2T 15.792 15.762
PS10.1H-PS10.2H 15.253 15.173
```

TABLE D4.–CONCLUDED

PROG C1-3
TEST NO. 2274 DATE 30272

RUN NO./COND NO. 3.004

B/L PROBE

PORT	B/L-PT	PS/PT	M	PT/PT1
1	13.611	0.905	0.330	0.928
2	13.956	0.873	0.426	0.952
3	14.223	0.865	0.458	0.973
4	14.421	0.854	0.477	0.983
5	14.513	0.849	0.490	0.990
6	14.570	0.846	0.496	0.994
7	14.606	0.844	0.499	0.996
8	14.625	0.842	0.501	0.997
9	14.651	0.841	0.504	0.999

PROBE 1:
AVG PT 14.350 AVG M 0.472 REC 0.979

B/L PROBE

PORT	B/L-PT	PS/PT	M	PT/PT1
1	13.593	0.906	0.373	0.927
2	13.927	0.885	0.422	0.950
3	14.303	0.861	0.467	0.975
4	14.495	0.853	0.488	0.990
5	14.531	0.845	0.497	0.994
6	14.622	0.843	0.501	0.997
7	14.646	0.841	0.503	0.999
8	14.659	0.840	0.505	1.000
9	14.669	0.840	0.506	1.000

PROBE 2:
AVG PT 14.379 AVG M 0.475 REC 0.981

PLANE 6-TRAVERSE:

RADIUS	OBS PS-A	OBS PS-B	OBS PS-AVG	OBS PS/PT	TRUE PS/PT	TRUE PS	TRUE PT	WCORG	M	REC PT/PTI
5.885	12.433	12.453	12.443	0.909	0.910	12.465	13.700	2.015	0.370	0.934
5.609	12.426	12.415	12.421	0.873	0.873	12.424	14.230	2.338	0.445	0.972
5.319	12.343	12.468	12.405	0.846	0.845	12.334	14.660	2.540	0.497	1.000
5.312	12.339	12.284	12.312	0.840	0.837	12.232	14.659	2.584	0.509	1.000
4.635	12.199	12.295	12.247	0.836	0.833	12.212	14.659	2.614	0.513	1.000
4.334	12.196	12.291	12.244	0.834	0.832	12.206	14.677	2.623	0.520	1.001
3.951	12.114	12.105	12.110	0.825	0.821	12.055	14.679	2.684	0.538	1.001
3.527	12.015	12.035	12.025	0.820	0.816	11.960	14.658	2.714	0.547	1.000
3.345	11.892	11.997	11.945	0.815	0.809	11.865	14.662	2.751	0.558	1.000
2.470	11.742	11.925	11.834	0.811	0.805	11.794	14.647	2.772	0.565	0.999

AVG PT 14.523 AVG PS 12.165
AVG PT/PTI 0.998 WCORG 25.633
WCORR 25.335 PL 6 FPR 1.266

TABLE D-5.—RUN 4, SAMPLE AERODYNAMIC DATA TABULATION

```
PROG C1-C
TEST NO.   2274                         DATE    31572

  N NO./COND NO.       4.009

MAP NO/CONFIG.NO.    40.003

WAC    19.931    PTAMBO      14.860    TAMB ACOUSTIC  518.95
FPR    1.1401    PLUG POS     0.00     RH                78%
M6     0.416     FAN TIP MR   0.968    FAN TIP M       0.874
N1     18340     N1C         18309     FAN TIP FPS    960.3

PLANE 1:
PT120      14.860   PT1W  14.860   PT1  14.860


TT1.1     60.99F   520.68R
TT1.2     60.65F   520.33R
TT1.3     60.65F   520.33R    BMTT1    520.45R
TT120     59.27F   518.95R
TT1W      59.27F   518.95R    TT1      518.95R

PLANE 2:
PS2.1-PS2.4    13.869 13.862 13.856 13.861
PSBM           13.862
PSBM/PT1        0.933
WCOR2          19.931   AVG M2  0.317

  ANE 4:
  4.1-PS4.8(O)    9.550  9.472  9.485  9.723  9.424  9.503  9.515  9.468
AVG PS4        9.518    M4   0.824
PS4.9-PS4.16(I)  9.679  9.322  9.918  9.445  9.584  9.602  9.685  9.611
AVG PS4          9.606    M4   0.815


PLANE 6:
PS6.1-PS6.4  13.175 13.178 13.216 13.195
AVG PS6      13.191


AP PL6 FPR  1.239

PLANE 10:
PT10.1-PT10.5  17.010 17.030 17.030 16.840 16.800
AVG PT10       16.942
PS10.1T-PS10.2T 15.184 15.193
PS10.1H-PS10.2H 14.874 14.846
```

TABLE D-5.–CONCLUDED

PROG C1-C
TEST NO. 2274 DATE 31572

RUN NO./COND NO. 4.009

B/L PROBE

PORT	B/L-PT	PS/PT	M	PT/PT1
1	13.827	0.954	0.260	0.931
2	14.175	0.931	0.322	0.954
3	14.474	0.911	0.367	0.974
4	14.697	0.898	0.396	0.989
5	14.789	0.892	0.408	0.995
6	14.826	0.890	0.412	0.998
7	14.848	0.889	0.415	0.999
8	14.856	0.888	0.416	1.000
9	14.863	0.888	0.417	1.000

PROBE 1:
AVG PT 14.585 AVG M 0.382 REC 0.982

B/L PROBE

PORT	B/L-PT	PS/PT	M	PT/PT1
1	13.749	0.960	0.244	0.925
2	13.998	0.942	0.293	0.942
3	14.357	0.919	0.350	0.966
4	14.881	0.887	0.419	1.002
5	14.725	0.896	0.400	0.991
6	14.793	0.892	0.408	0.996
7	14.832	0.889	0.413	0.998
8	14.850	0.888	0.415	0.999
9	14.861	0.888	0.416	1.000

PROBE 2:
AVG PT 14.552 AVG M 0.377 REC 0.979

PLANE 6-TRAVERSE:

RADIUS	OBS PS-A	OBS PS-B	OBS PS-AVG	OBS PS/PT	TRUE PS/PT	TRUE PS	TRUE PT	WCOR6	M	REC PT/PT1
5.885	13.300	13.270	13.285	0.972	0.973	13.300	13.675	1.152	0.200	0.920
5.609	13.241	13.331	13.286	0.916	0.917	13.306	14.505	1.938	0.353	0.976
5.319	13.243	13.332	13.288	0.899	0.900	13.303	14.787	2.113	0.392	0.995
5.012	13.252	13.333	13.293	0.895	0.896	13.307	14.849	2.145	0.399	0.999
4.685	13.235	13.229	13.232	0.891	0.891	13.244	14.860	2.188	0.409	1.000
4.334	13.173	13.100	13.139	0.884	0.885	13.143	14.857	2.242	0.422	1.000
3.951	13.096	13.064	13.080	0.880	0.881	13.087	14.860	2.277	0.430	1.000
3.527	13.078	13.051	13.065	0.880	0.880	13.071	14.856	2.284	0.432	1.000
3.045	13.045	13.050	13.048	0.878	0.879	13.054	14.857	2.294	0.434	1.000
2.470	13.031	13.018	13.025	0.890	0.891	13.036	14.635	2.193	0.410	0.985

AVG PT	14.674	AVG PS	13.186
AVG PT/PT1	0.988	WCOR6	20.824
WCOR2	20.571	PL 6 FPR	1.155

TABLE D-6.—RUN 5, SAMPLE AERODYNAMIC DATA TABULATION

```
PROG C1-C
TEST NO.   2274                          DATE    32072

RUN NO./COND NO.      5.003

MAP NO/CONFIG NO.   48.000

WAC    25.419    PTAMBO       14.805    TAMB ACOUSTIC   508.95
FPR    1.2413    PLUG POS      0.00     RH                 68%
M6     0.558     FAN TIP MR   1.277     FAN TIP M        1.149
N1     23590     N1C          23769     FAN TIP FPS      1235

PLANE 1:
PT120      14.810   PT1W  14.800   PT1  14.805


TT1.1     50.99F   510.67R
TT1.2     51.33F   511.02R
TT1.3     51.33F   511.02R    BMTT1    510.90R
TT120     49.26F   508.95R
TT1W      49.61F   509.29R    TT1      509.12R

PLANE 2:
PS2.1-PS2.4     13.086 13.089 13.089 13.103
PSBM            13.092
PSBM/PT1         0.884
WCOR2           25.419   AVG M2  0.423

PLANE 4:
PS4.1-PS4.8(O)    9.563   9.510   9.516   9.573   9.478   9.538   9.535   9.524
AVG PS4         9.530    M4    0.819
PS4.9-PS4.16(I)   9.582   9.218   9.735   9.359   9.520   9.539   9.587   9.616
AVG PS4         9.520    M4    0.820


PLANE 6:
PS6.1-PS6.4   11.948 11.934 12.038 12.023
AVG PS6       11.986


AP PL6 FPR  1.346

PLANE 10:
PT10.1-PT10.5  18.535 18.735 18.435 18.235 17.945
AVG PT10       18.377
PS10.1T-PS10.2T 15.557 15.550
PS10.1H-PS10.2H 14.998 14.981
```

TABLE D-6.–CONCLUDED

PROG C1-C
TEST NO. 2274 DATE 32072

RUN NO./COND NO. 5.003

B/L PROBE

PORT	B/L-PT	PS/PT	M	PT/PT1
1	13.943	0.860	0.470	0.942
2	14.654	0.818	0.544	0.990
3	14.789	0.811	0.556	0.999
4	14.811	0.809	0.558	1.001
5	14.815	0.809	0.559	1.001
6	14.816	0.809	0.559	1.001
7	14.815	0.809	0.559	1.001
8	14.816	0.809	0.559	1.001
9	14.815	0.809	0.559	1.001

PROBE 1:
AVG PT 14.671 AVG M 0.545 REC 0.991

B/L PROBE

PORT	B/L-PT	PS/PT	M	PT/PT1
1	13.682	0.876	0.439	0.924
2	14.427	0.831	0.522	0.975
3	14.730	0.814	0.551	0.995
4	14.783	0.811	0.556	0.999
5	14.801	0.810	0.557	1.000
6	14.809	0.809	0.558	1.000
7	14.812	0.809	0.558	1.001
8	14.813	0.809	0.559	1.001
9	14.815	0.809	0.559	1.001

PROBE 2:
AVG PT 14.601 AVG M 0.539 REC 0.986

PLANE 6-TRAVERSE:

RADIUS	OBS PS-A	OBS PS-B	OBS PS-AVG	OBS PS/PT	TRUE PS/PT	TRUE PS	TRUE PT	WCOR6	M	REC PT/PT1
5.885	12.142	12.208	12.175	0.892	0.893	12.187	13.655	2.178	0.407	0.922
5.609	12.063	12.385	12.224	0.831	0.828	12.180	14.720	2.648	0.527	0.994
5.319	12.321	12.133	12.227	0.828	0.824	12.177	14.776	2.667	0.533	0.998
5.012	12.091	12.153	12.122	0.819	0.815	12.054	14.798	2.722	0.549	1.000
4.685	12.083	11.999	12.041	0.814	0.808	11.958	14.798	2.757	0.560	1.000
4.334	11.885	11.997	11.941	0.807	0.800	11.837	14.797	2.799	0.574	1.000
3.951	11.900	11.893	11.897	0.804	0.796	11.781	14.805	2.820	0.581	1.000
3.527	11.827	11.929	11.878	0.802	0.794	11.758	14.804	2.828	0.583	1.000
3.045	11.844	11.902	11.873	0.802	0.794	11.752	14.803	2.830	0.584	1.000
2.470	11.892	11.983	11.938	0.807	0.800	11.832	14.799	2.801	0.575	1.000

AVG PT 14.6755 AVG PS 11.9514
AVG PT/PT1 0.9915 WCOR6 27.0482
WCOR2 26.8179 PL 6 FPR 1.2522

TABLE D-7.—RUN 6, SAMPLE AERODYNAMIC DATA TABULATION

```
PROG C1-D
TEST NO.   2274                          DATE    32372

RUN NO./COND NO.      6.003

MAP NO/CONFIG NO.     0.004

WAC    19.954    PTAMBO        14.800    TAMB AC CH    511.36
FPR    1.1381    PLUG POS       0.00     RH               60%
M6     0.384     FAN TIP MR     0.939    FAN TIP M      0.857
N1     17910     N1C           18010     FAN TIP FPS   937.8

PLANE 1:
PT120      14.800   PT1W  14.800   PT1   14.800


TT1.1     53.40F   513.09R
TT1.2     52.37F   512.05R
TT1.3     54.09F   513.78R    BMTT1    512.97R
TT120     51.68F   511.36R
TT1W      52.37F   512.05R    TT1      511.71R

PLANE 2:
PS2.1-PS2.4    13.801 13.808 13.798 13.807
PSBM           13.804
PSBM/PT1        0.933
WCOR2          19.954    AVG M2  0.317

PLANE 4:
PS4.1-PS4.8(O)   8.921 10.146  8.889   8.714   8.741   8.594   8.568   8.624
AVG PS4        8.900    M4    0.884
PS4.9-PS4.16(I)  8.470  8.446  8.580   8.602   8.820   8.755   8.473   8.500
AVG PS4        8.531    M4    0.918
        303     400     401     402
 PS    9.759   8.921   9.310  11.012
PS/PT  0.659   0.603   0.643   0.744
  M    0.795   0.882   0.821   0.664

PLANE 6:
PS6.1-PS6.4   13.341 13.360 13.480 13.298
AVG PS6       13.370


AP PL6 FPR  1.185

PLANE 10:
PT10.1-PT10.5  16.910 16.930 16.940 16.670 16.770
AVG PT10       16.844
PS10.1T-PS10.2T 15.118 15.121
PS10.1H-PS10.2H 14.818 14.794
```

TABLE D-7.—CONCLUDED

PROG C1-D
TEST NO. 2274 DATE 32372

RUN NO./COND NO. 6.003

B/L PROBE

PORT	B/L-PT	PS/PT	M	PT/PT1
1	14.280	0.936	0.308	0.965
2	14.462	0.925	0.337	0.977
3	14.609	0.915	0.358	0.987
4	14.713	0.909	0.372	0.994
5	14.762	0.906	0.379	0.998
6	14.783	0.905	0.382	0.999
7	14.792	0.904	0.383	1.000
8	14.794	0.904	0.383	1.000
9	14.794	0.904	0.383	1.000

PROBE 1:
AVG PT 14.660 AVG M 0.365 REC 0.991

B/L PROBE

PORT	B/L-PT	PS/PT	M	PT/PT1
1	14.242	0.939	0.302	0.962
2	14.397	0.929	0.327	0.973
3	14.580	0.917	0.354	0.985
4	14.693	0.910	0.370	0.993
5	14.753	0.906	0.378	0.997
6	14.780	0.905	0.381	0.999
7	14.792	0.904	0.383	1.000
8	14.797	0.904	0.384	1.000
9	14.799	0.904	0.384	1.000

PROBE 2:
AVG PT 14.644 AVG M 0.363 REC 0.990

PLANE 6-TRAV:

RADIUS	OBS PS-A	OBS PS-B	OBS PS-AVG	OBS PS/PT	TRUE PS/PT	TRUE PS	TRUE PT	WCOR6	M	REC PT/PT1
5.885	13.355	13.359	13.357	0.940	0.941	13.379	14.215	1.658	0.296	0.961
5.609	13.213	13.033	13.123	0.910	0.912	13.142	14.416	1.997	0.366	0.974
5.319	13.376	13.378	13.377	0.905	0.907	13.395	14.775	2.047	0.377	0.998
5.012	13.362	13.349	13.356	0.902	0.903	13.372	14.808	2.081	0.385	1.000
4.685	13.315	13.245	13.280	0.897	0.898	13.295	14.800	2.125	0.395	1.000
4.334	13.243	13.241	13.242	0.895	0.896	13.256	14.799	2.148	0.400	1.000
3.951	13.135	13.263	13.199	0.892	0.893	13.212	14.795	2.173	0.405	1.000
3.527	13.145	13.265	13.205	0.892	0.893	13.218	14.798	2.171	0.405	1.000
3.045	13.136	13.259	13.198	0.892	0.893	13.210	14.802	2.178	0.407	1.000
2.470	13.213	13.033	13.123	0.910	0.912	13.142	14.416	1.997	0.366	0.974

AVG PT 14.6624 AVG PS 13.2619
AVG PT/PT1 0.9905 WCOR6 20.5743
WCOR2 20.3789 PL 6 FPR 1.1523 MB 0.8104 PS/PT 0.6493
NOTE: DATA FROM TRAV RADIUS 2.470 SUBSTITUTED FOR DATA AT RADIUS 5.609

TABLE D-8.–RUN 7, SAMPLE AERODYNAMIC DATA TABULATION

```
PROG CI-E
TEST NO.   2274                        DATE    40372

RUN NO./COND NO.       7.002

MAP NO/CONFIG NO.      0.305

WAC    18.170    PTAMBO       14.705    TAMB AC CH   523.44
FPR    1.1175    PLUG POS     0.00      RH               60%
M6     0.384     FAN TIP MR   0.895*    FAN TIP M     0.803
N1     17070     N1C          16972     FAN TIP FPS  893.8
```

* Use P_{T1} and P_S to get M_R here.

```
PLANE 1:
PT120      14.710   PT1W  14.700   PT1   14.705


TT1.1     65.13F   524.32R
TT1.2     64.44F   524.13R
TT1.3     65.43F   525.16R     BMTT1    524.70R
TT120     63.75F   523.44R
TT1W      63.75F   523.44R     TT1      523.44R

PLANE 2:
PS2.1-PS2.4      13.904 13.890 13.895 13.893
PSBM             13.896
PSBM/PT1          0.945
WCOR2            18.170   AVG M2  0.286

PLANE 4:
PS4.1-PS4.4(O)  11.255  11.232 11.247 11.131
AVG PS4         11.166   M4    0.640
PS4.5-PS4.8(I)   9.221   9.796  9.651   9.377
AVG PS4          9.511   M4    0.814
VANE STATICS:
   RAD    PS      PS/PT1     M
  1.104 10.757   0.732   0.684
  1.643 10.463   0.711   0.715
  2.192 10.172   0.692   0.745
  2.736  9.890   0.673   0.775
  3.280  9.633   0.655   0.802


PLANE 6:
PS6.1-PS6.4   13.300 13.266 13.273 13.287
AVG PS6       13.282
M6     0.307       FAN TIP MR   0.860
```

Uses P_S wall plane 6 and P_T rake at rad 1 to get M_R

```
PLANE 10:
PT10.1-PT10.5   16.525 16.565 16.525 16.335 16.215
AVG PT10        16.433
PS10.1T-PS10.2T 14.969 14.969
PS10.1H-PS10.2H 14.713 14.693
```

TABLE D-8.–CONCLUDED

PROG CI-E
TEST NO. 2274 DATE 40372

RUN NO./COND NO. 7.002

PL6 RAKE TRAV:

RAD	NO. 1	2	3	4	5	6	7	8	9
1 PT	14.158	14.167	14.130	14.192	14.191	14.186	14.172	14.164	14.167
PT/PTI	0.963	0.964	0.964	0.965	0.965	0.965	0.964	0.963	0.964
M	0.304	0.305	0.307	0.309	0.309	0.308	0.306	0.305	0.305
2 PT	14.247	14.251	14.277	14.271	14.276	14.277	14.277	14.275	14.275
PT/PTI	0.969	0.969	0.971	0.970	0.971	0.971	0.971	0.971	0.971
M	0.317	0.318	0.322	0.321	0.322	0.322	0.322	0.322	0.322
3 PT	14.384	14.380	14.407	14.379	14.372	14.369	14.378	14.384	14.392
PT/PTI	0.978	0.978	0.980	0.978	0.977	0.977	0.978	0.978	0.979
M	0.340	0.339	0.343	0.339	0.338	0.337	0.339	0.340	0.341
4 PT	14.658	14.481	14.496	14.434	14.416	14.419	14.468	14.494	14.507
PT/PTI	0.997	0.985	0.986	0.982	0.981	0.981	0.984	0.986	0.987
M	0.379	0.354	0.356	0.348	0.345	0.345	0.352	0.356	0.358
5 PT	14.686	14.567	14.568	14.486	14.457	14.459	14.534	14.579	14.591
PT/PTI	0.999	0.991	0.991	0.985	0.983	0.983	0.988	0.992	0.992
M	0.382	0.366	0.366	0.354	0.350	0.350	0.361	0.367	0.369
6 PT	14.686	14.567	14.568	14.486	14.457	14.459	14.534	14.579	14.591
PT/PTI	0.999	0.991	0.991	0.985	0.983	0.983	0.988	0.992	0.992
M	0.382	0.366	0.366	0.354	0.350	0.350	0.361	0.367	0.369
7 PT	14.626	14.652	14.623	14.503	14.480	14.501	14.615	14.665	14.638
PT/PTI	0.994	0.996	0.994	0.986	0.984	0.986	0.994	0.997	0.995
M	0.373	0.376	0.373	0.357	0.353	0.356	0.371	0.378	0.375
8 PT	14.690	14.646	14.629	14.518	14.484	14.497	14.605	14.660	14.615
PT/PTI	0.999	0.996	0.995	0.987	0.985	0.986	0.993	0.997	0.994
M	0.382	0.376	0.374	0.359	0.354	0.356	0.371	0.378	0.372
9 PT	14.546	14.612	14.606	14.508	14.477	14.485	14.570	14.589	14.520
PT/PTI	0.990	0.994	0.994	0.987	0.985	0.985	0.991	0.993	0.988
M	0.363	0.373	0.372	0.358	0.354	0.355	0.367	0.369	0.360
10 PT	14.427	14.468	14.436	14.370	14.336	14.329	14.352	14.315	14.240
PT/PTI	0.982	0.984	0.982	0.978	0.975	0.975	0.976	0.974	0.969
M	0.347	0.353	0.348	0.338	0.333	0.332	0.335	0.330	0.318
AVG REC	0.987	0.985	0.985	0.980	0.979	0.979	0.983	0.984	0.983

MB 0.684 PS/PT 0.732

Uses outer wall P_S average of 4 for all Mach number calculations on this page.

TABLE D-9.—RUN 101, SAMPLE AERODYNAMIC DATA TABULATION

```
PROG C2-A
TEST NO.   2290                              DATE    41772

RUN NO./COND NO.    101.005      MAP NO/CONFIG NO.     5.001

VAC    19.128    PTAMBO       14.905    TAMB AC CH    509.64
FPR    1.1363    PLUG POS      0.00     RH               65%
M6     0.473     FAN TIP MR   1.009     FAN TIP M      0.888
N1     18350     N1C          18512     FAN TIP FPS    960.8

PLANE 1:
PT120       14.900     PT1W    14.910     PT1     14.905
TT1.1-TT1.3    510.673 509.293 508.948  BMTT1   509.638
TT120   509.638
TT1W    509.633    TT1   509.633

PLANE 2:
PS2.1-PS2.4      14.033   13.986   13.971   13.961
PS2M             13.989
PS2M/PT1          0.939
AVG M2       0.302

PLANE 3:
PS3.1-PS3.4      14.115   14.095   14.075   14.105
  PS/PT1          0.947    0.946    0.944    0.946
  AVG M3          0.283
          301             302                  303
          OUT        IN        OUT        IN        OUT
  PS     12.795    11.333    11.327    10.628    10.511
PS/PT     0.859     0.792     0.760     0.713     0.705
  M       0.472     0.587     0.639     0.712     0.724

PLANE 4 (THROAT):
PS4.1-PS4.4(O)   10.109    9.958    9.884   10.085
PS4 AVG   10.009   PS4A/PT1    0.672
M4          0.776

PS4.1-PS4.4(I)   10.058   10.134   10.071   10.057
PS4 AVG   10.080   PS4A/PT1    0.676
M4          0.769
              401                  402                  403
          IN        OUT        IN        OUT        IN        OUT
  PS     9.894    10.136    10.927    10.991    11.804    11.849
PS/PT    0.664     0.683     0.733     0.738     0.792     0.795
  M      0.738     0.758     0.631     0.674     0.587     0.582
```

PROG C2-A
TEST NO. 2200 DATE 41772

RUN NO./COND NO. 101.005

PLANE 5:

OUTER B/L RAKE PS 12.304

PR	PT	PS/PT	PT/PT1	M
1	12.849	0.958	0.862	0.250
2	13.135	0.937	0.881	0.307
3	13.471	0.913	0.904	0.362
4	13.884	0.886	0.932	0.419
5	14.279	0.862	0.958	0.466
6	14.551	0.846	0.976	0.496
7	14.805	0.831	0.993	0.521
AV	14.031	0.877	0.941	0.437

INNER B/L RAKE PS 12.304

PR	PT	PS/PT	PT/PT1	M
1	12.336	0.997	0.828	0.061
2	12.430	0.990	0.834	0.121
3	12.577	0.978	0.844	0.177
4	12.683	0.970	0.851	0.209
5	12.890	0.955	0.865	0.259
6	13.094	0.940	0.879	0.300
7	13.495	0.912	0.906	0.366
AV	12.930	0.943	0.871	0.278

501

	IN	OUT
PS	12.605	12.662
PS/PT	0.846	0.850
M	0.495	0.483

PLANE 10:

PT10.1-PT10.5 17.205 17.245 17.155 16.635 16.445

AVG PT10 16.937

	10.1 IN	10.1 OUT	10.2 IN	10.2 OUT
PS	15.216	14.930	15.230	14.914
PS/PT	0.898	0.882	0.899	0.881
M	0.394	0.423	0.393	0.430

PROG C2-A
TEST NO. 2290 DATE 41772

N NO./COND NO. 101.005

PLANE 6:
M6 0.183 FAN TIP MR 0.890
PS6.1-PS6.4 12.78 12.79 12.78 12.65

OUTER NO.1 B/L RAKE PS 12.747

PR	PT	PS/PT	PT/PT1	M
1	13.240	0.963	0.888	0.234
2	13.487	0.945	0.905	0.285
3	13.860	0.920	0.930	0.343
4	14.309	0.891	0.960	0.410
5	14.591	0.874	0.979	0.444
6	14.736	0.865	0.989	0.460
7	14.836	0.861	0.993	0.468
8	14.833	0.859	0.995	0.470
9	14.859	0.858	0.997	0.473
AV	14.392	0.891	0.960	0.409

OUTER NO.2 B/L RAKE PS 12.747

PR	PT	PS/PT	PT/PT1	M
1	12.936	0.985	0.868	0.145
2	13.027	0.979	0.874	0.177
	13.400	0.951	0.899	0.267
4	13.714	0.930	0.920	0.325
5	14.064	0.906	0.944	0.373
6	14.347	0.889	0.963	0.415
7	14.531	0.877	0.975	0.437
8	14.672	0.869	0.984	0.453
9	14.835	0.861	0.993	0.467
AV	13.936	0.912	0.938	0.357

AVG RAKES 1&2

PR	PT	PS/PT	PT/PT1	M
1	13.088	0.974	0.878	0.195
2	13.257	0.962	0.890	0.237
3	13.630	0.935	0.915	0.311
4	14.011	0.910	0.940	0.370
5	14.327	0.890	0.961	0.412
6	14.541	0.877	0.976	0.438
7	14.663	0.869	0.984	0.452
8	14.752	0.864	0.990	0.462
9	14.732	0.860	0.995	0.470
AV	14.144	0.901	0.949	0.338

TABLE D-9.–CONTINUED

PROG C2-A
TEST NO. 2290 DATE 41772

RUN NO./COND NO. 101.005

INNER NO.1
PS6.1-PS6.4 12.669 12.692 12.691 12.676

B/L RAKE PS 12.682

PR	PT	PS/PT	PT/PT1	M
1	13.244	0.958	0.889	0.250
2	13.270	0.956	0.890	0.255
3	13.675	0.927	0.917	0.330
4	13.867	0.915	0.930	0.360
5	14.026	0.904	0.941	0.392
6	14.153	0.896	0.950	0.403
7	14.234	0.893	0.958	0.416
8	14.325	0.885	0.961	0.421
9	14.505	0.874	0.973	0.442
AV	14.059	0.902	0.943	0.387

INNER NO.2 B/L RAKE PS 12.682

PR	PT	PS/PT	PT/PT1	M
1	13.366	0.949	0.897	0.275
2	13.632	0.930	0.915	0.323
3	13.893	0.913	0.932	0.363
4	14.103	0.899	0.946	0.393
5	14.276	0.888	0.958	0.415
6	14.407	0.880	0.967	0.431
7	14.514	0.874	0.974	0.443
8	14.590	0.869	0.979	0.452
9	14.699	0.863	0.986	0.464
AV	14.232	0.890	0.958	0.416

AVG RAKES 1&2

PR	PT	PS/PT	PT/PT1	M
1	13.305	0.953	0.893	0.263
2	13.451	0.943	0.903	0.291
3	13.784	0.920	0.925	0.347
4	13.985	0.907	0.938	0.376
5	14.151	0.896	0.950	0.399
6	14.232	0.888	0.958	0.416
7	14.399	0.881	0.966	0.430
8	14.457	0.877	0.970	0.437
9	14.602	0.869	0.980	0.453
AV	14.170	0.895	0.951	0.401

TABLE D-9.–CONCLUDED

PROG C2-A
TEST NO. 2290 DATE 41772

RUN NO./COND NO. 101.005|
TRAV:

RADIUS	OBS PS-A	OBS PS-B	OBS PS-AVG	OBS PS/PT	TRUE PS/PT	TRUE PS	TRUE PT	WCORS	M	REC PT/PTI
5.883	12.823	12.832	12.830	0.933	0.934	12.832	13.047	0.879	0.155	0.875
5.619	12.836	12.811	12.824	0.944	0.944	12.825	13.588	1.585	0.289	0.912
5.336	12.860	12.896	12.878	0.915	0.915	12.863	14.071	1.923	0.360	0.944
5.037	12.881	12.909	12.895	0.878	0.875	12.853	14.695	2.273	0.442	0.966
4.719	12.864	12.838	12.851	0.867	0.863	12.797	14.832	2.361	0.464	0.996
4.379	12.810	12.798	12.804	0.861	0.857	12.743	14.873	2.405	0.476	0.999
4.010	12.751	12.712	12.732	0.856	0.851	12.664	14.882	2.442	0.486	0.999
3.602	12.659	12.666	12.663	0.850	0.845	12.583	14.891	2.479	0.496	0.999
3.143	12.605	12.675	12.640	0.853	0.843	12.547	14.880	2.492	0.500	0.999
2.604	12.540	12.714	12.627	0.858	0.853	12.563	14.722	2.425	0.482	0.988

AVG PT	14.4486	AVG PS	12.7279
AVG PT/PTI	0.9696	WCOR6	21.2644
WCOR2	20.6181	PL6 FPR	0.0000

TABLE D-10.—RUN 102, SAMPLE AERODYNAMIC DATA TABULATION

```
PROG C2-A
TEST NO.   22ØØ                          DATE    42472

RUN NO./COND NO.   1Ø2.ØØ1      MAP NO/CONFIG NO.    1.ØØ2

WAC    19.934    PTAMBO      14.695    TAMB AC CH   515.35
FPR    1.14Ø5    PLUG POS     Ø.ØØ     RH              75%
M6     Ø.543     FAN TIP MR  1.Ø86     FAN TIP M     Ø.933
N1     1937Ø     NIC         19423     FAN TIP FPS  1Ø14

PLANE 1:
PT12Ø        14.73Ø   PT1W   14.69Ø   PT1   14.695
TT1.1-TT1.3   516.533 515.5Ø3 515.5Ø3  3MTT1  515.843
TT12Ø  515.343
TT1W   516.533   TT1  516.193

PLANE 2:
PS2.1-PS2.4     13.749  13.71Ø  13.691  13.631
PS2M            13.7Ø8
PS2M/PT1         Ø.933
AVG M2       Ø.317

PLANE 3:
PS3.1-PS3.4     13.845  13.815  13.8Ø5  13.825
  PS/PT1         Ø.942   Ø.94Ø   Ø.94Ø   Ø.941
  AVG M3         Ø.297
        3Ø1          3Ø2               3Ø3
        OUT      IN      OUT       IN      OUT
  PS   12.41Ø  12.131  1Ø.761    9.971   9.753
PS/PT   Ø.845   Ø.826   Ø.732    Ø.679   Ø.664
  M     Ø.497   Ø.531   Ø.682    Ø.766   Ø.788

PLANE 4 (THROAT):
PS4.1-PS4.4(O)    9.172   9.Ø12   8.855   9.Ø86
PS4 AVG    9.Ø31   PS4A/PT1    Ø.615
M4         Ø.864

PS4.1-PS4.4(I)    9.165   9.15Ø   9.Ø66   9.157
PS4 AVG    9.135   PS4A/PT1    Ø.622
M4         Ø.853
            4Ø1                 4Ø2                 4Ø3
        IN       OUT       IN       OUT       IN       OUT
  PS    8.762    9.471   1Ø.1Ø2   1Ø.385   11.344   11.Ø27
PS/PT   Ø.596    Ø.645    Ø.688    Ø.7Ø7    Ø.772    Ø.75Ø
  M     Ø.892    Ø.813    Ø.752    Ø.722    Ø.62Ø    Ø.654
```

TABLE D-10.–CONTINUED

PROG C2-A
TEST NO. 2290 DATE 42472

RUN NO./COND NO. 102.001

PLANE 5:
OUTER B/L RAKE PS 11.434

PR	PT	PS/PT	PT/PT1	M
1	11.563	0.979	0.727	0.127
2	11.651	0.981	0.793	0.164
3	11.730	0.971	0.802	0.207
4	11.977	0.955	0.815	0.253
5	12.249	0.934	0.834	0.315
6	12.574	0.909	0.856	0.371
7	13.298	0.860	0.905	0.470
AV	12.404	0.922	0.844	0.343

INNER B/L RAKE PS 11.435

PR	PT	PS/PT	PT/PT1	M
1	13.099	0.877	0.891	0.438
2	13.725	0.837	0.934	0.511
3	14.234	0.804	0.972	0.567
4	14.559	0.789	0.991	0.592
5	14.657	0.784	0.993	0.601
6	14.676	0.783	0.999	0.602
7	14.680	0.782	0.999	0.603
AV	14.331	0.802	0.975	0.571

	501	
	IN	OUT
PS	11.337	11.355
PS/PT	0.806	0.807
M	0.565	0.563

PLANE 10:
PT10.1-PT10.5 16.905 16.885 16.965 16.555 16.435
AVG PT10 16.759

	10.1		10.2	
	IN	OUT	IN	OUT
PS	15.013	14.723	15.039	14.696
PS/PT	0.896	0.879	0.897	0.877
M	0.399	0.434	0.396	0.437

TABLE D-10.—CONTINUED

PROG C2-A
TEST NO. 2290 DATE 42472

RUN NO./COND NO. 102.ØØ1

PLANE 6:
M6 Ø.165 FAN TIP MP Ø.928
PS6.1-PS6.4 12.Ø2 11.94 12.Ø2 11.96

OUTER NO.1 B/L RAKE PS 11.985

PR	PT	PS/PT	PT/PT1	M
1	12.Ø32	Ø.996	Ø.819	Ø.Ø75
2	12.122	Ø.989	Ø.825	Ø.123
3	12.295	Ø.975	Ø.837	Ø.191
4	12.545	Ø.955	Ø.854	Ø.256
5	12.844	Ø.933	Ø.874	Ø.316
6	13.261	Ø.9Ø4	Ø.9Ø3	Ø.383
7	13.515	Ø.887	Ø.92Ø	Ø.413
8	13.752	Ø.872	Ø.936	Ø.448
9	14.161	Ø.846	Ø.964	Ø.494
AV	13.Ø44	Ø.919	Ø.888	Ø.35Ø

OUTER NO.2 B/L RAKE PS 11.985

PR	PT	PS/PT	PT/PT1	M
1	12.197	Ø.983	Ø.83Ø	Ø.158
2	12.233	Ø.976	Ø.836	Ø.188
3	12.671	Ø.945	Ø.862	Ø.283
4	13.Ø65	Ø.917	Ø.889	Ø.353
5	13.543	Ø.885	Ø.922	Ø.422
6	13.953	Ø.859	Ø.95Ø	Ø.471
7	14.226	Ø.843	Ø.968	Ø.5Ø1
8	14.399	Ø.832	Ø.98Ø	Ø.519
9	14.568	Ø.823	Ø.991	Ø.536
AV	13.495	Ø.888	Ø.918	Ø.415

AVG RAKES 1&2

PR	PT	PS/PT	PT/PT1	M
1	12.114	Ø.989	Ø.824	Ø.124
2	12.2Ø2	Ø.982	Ø.83Ø	Ø.16Ø
3	12.483	Ø.96Ø	Ø.85Ø	Ø.242
4	12.8Ø5	Ø.936	Ø.871	Ø.3Ø9
5	13.193	Ø.9Ø9	Ø.898	Ø.373
6	13.6Ø7	Ø.881	Ø.926	Ø.43Ø
7	13.879	Ø.864	Ø.944	Ø.462
8	14.Ø75	Ø.852	Ø.958	Ø.485
9	14.364	Ø.834	Ø.978	Ø.515
AV	13.269	Ø.9Ø3	Ø.9Ø3	Ø.384

TABLE D-10.–CONTINUED

PROG C2-A
TEST NO. 2290 DATE 42472

RUN NO./COND NO. 102.001

INNER NO.1
PS6.1-PS6.4 11.926 11.936 11.937 11.951

B/L RAKE PS 11.923

PR	PT	PS/PT	PT/PT1	M
1	13.460	0.836	0.915	0.429
2	14.211	0.839	0.967	0.507
3	14.563	0.819	0.991	0.543
4	14.653	0.814	0.997	0.551
5	14.675	0.813	0.999	0.553
6	14.675	0.812	0.999	0.553
7	14.679	0.812	0.999	0.553
8	14.678	0.812	0.999	0.553
9	14.674	0.813	0.999	0.553
AV	14.505	0.822	0.987	0.537

INNER NO.2 B/L RAKE PS 11.923

PR	PT	PS/PT	PT/PT1	M
1	13.353	0.892	0.939	0.407
2	14.231	0.833	0.969	0.509
3	14.617	0.816	0.995	0.548
4	14.670	0.813	0.998	0.553
5	14.677	0.812	0.999	0.553
6	14.679	0.812	0.999	0.553
7	14.680	0.812	0.999	0.553
8	14.680	0.812	0.999	0.553
9	14.680	0.812	0.999	0.553
AV	14.504	0.822	0.987	0.537

AVG RAKES 1&2

PR	PT	PS/PT	PT/PT1	M
1	13.411	0.889	0.913	0.414
2	14.221	0.838	0.968	0.508
3	14.592	0.817	0.993	0.545
4	14.661	0.813	0.998	0.552
5	14.676	0.812	0.999	0.553
6	14.678	0.812	0.999	0.553
7	14.679	0.812	0.999	0.553
8	14.679	0.812	0.999	0.553
9	14.677	0.812	0.999	0.553
AV	14.504	0.822	0.987	0.537

TABLE D-10.–CONCLUDED

PROG C2-A
TEST NO. 2200 DATE 42472

RUN NO./COND NO. 102.001
TRAV:

RADIUS	OBS PS-A	OBS PS-B	OBS PS-AVG	OBS PS/PT	TRUE PS/PT	TRUE PS	TRUE PT	WCORS	M	REC PT/PTI
5.888	12.151	12.067	12.109	0.991	0.991	12.108	12.215	0.643	0.112	0.831
5.619	12.108	11.976	12.042	0.953	0.953	12.045	12.643	1.462	0.264	0.860
5.336	12.192	12.122	12.157	0.897	0.895	12.135	13.555	2.134	0.421	0.923
5.037	12.158	12.095	12.127	0.874	0.871	12.084	13.870	2.292	0.448	0.944
4.719	12.218	12.224	12.221	0.838	0.832	12.123	14.578	2.564	0.524	0.992
4.379	12.154	12.200	12.177	0.835	0.823	12.075	14.581	2.534	0.526	0.992
4.019	12.101	12.178	12.140	0.823	0.820	12.025	14.662	2.530	0.540	0.993
3.602	12.059	12.059	12.059	0.822	0.813	11.932	14.675	2.568	0.552	0.999
3.143	11.997	12.022	12.010	0.818	0.809	11.873	14.678	2.590	0.559	0.999
2.604	11.996	11.920	11.958	0.817	0.807	11.819	14.640	2.699	0.562	0.996

AVG PT	14.0397	AVG PS	12.0218
AVG PT/PTI	0.9533	WCOR6	22.3423
WCOR2	21.2996	PL6 FPR	0.0000

TABLE D-11.—RUN 8, SAMPLE AERODYNAMIC DATA TABULATION

```
PROG C2-B
TEST NO.   2274                          DATE    50272

RUN NO./COND NO.     8.003     MAP NO/CONFIG NO.    3.006

WAC    19.770    PTAMBO        14.830    TAMB AC CH    525.51
FPR    1.1370    PLUG POS       0.00     RH               65%
M6     0.400     FAN TIP MR    0.945     FAN TIP M      0.856
N1     18090     N1C           17966     FAN TIP FPS   947.2

PLANE 1:
PT120       14.830    PT1W    14.830    PT1    14.830
TT1.1-TT1.3    525.508 525.853 526.198   AVGTT1   525.853
TT120  525.508
TT1W   526.198    TT1  525.853

PLANE 4 (THROAT):
PS4.1-PS4.8(O)   9.000  9.009  8.980  8.929   8.873   8.817   8.855   8.929
PS4 AVG  8.924   PS4A/PT1  0.602
M4        0.884
PS4.1-PS4.8(I)   8.366  8.704  8.580  8.671   8.621   8.589 14.918   8.841
PS4 AVG  9.411   PS4A/PT1  0.635
M4        0.833

OUTER     303      400      401      402
  PS     8.812    9.000    9.378   10.724
PS/PT    0.594    0.607    0.632    0.723
  M      0.895    0.876    0.836    0.697

PLANE 5:
INNER B/L RAKE  PS   13.242
PR    PT        PS/PT     PT/PT1      M
 1   13.949     0.949     0.941     0.274
 2   14.090     0.940     0.950     0.299
 3   14.239     0.930     0.960     0.324
 4   14.385     0.921     0.970     0.346
 5   14.540     0.911     0.981     0.368
 6   14.643     0.904     0.987     0.382
 7   14.782     0.896     0.997     0.400

AV  14.481     0.915     0.977     0.360

INNER    501
  PS    13.311
PS/PT    0.898
  M      0.396


PLANE 10:
PT10.1-PT10.5   16.920   16.990   17.020   16.670   16.710
AVG PT10        16.862
            10.1              10.2
        IN       OUT       IN       OUT
  PS   14.828   14.842   14.840   14.848
PS/PT   0.879    0.880    0.880    0.881
  M     0.433    0.431    0.431    0.430
```

PROG C2-B
TEST NO. 2274 DATE 50272

RUN NO./COND NO. 8.003

PLANE 6:
M6 0.333 FAN TIP MR 0.915
PS6.1-PS6.4 13.29 13.28 13.25 13.33

OUTER NO.1 B/L RAKE PS 13.285

PR	PT	PS/PT	PT/PT1	M
1	14.359	0.925	0.968	0.335
2	14.529	0.914	0.980	0.360
3	14.641	0.907	0.987	0.375
4	14.732	0.902	0.993	0.387
5	14.780	0.899	0.997	0.393
6	14.926	0.890	1.007	0.411
7	14.819	0.897	0.999	0.398
8	14.825	0.896	1.000	0.399
9	14.829	0.896	1.000	0.400
AV	14.707	0.903	0.992	0.384

OUTER NO.2 B/L RAKE PS 13.285

PR	PT	PS/PT	PT/PT1	M
1	14.350	0.926	0.968	0.334
2	14.461	0.919	0.975	0.350
	14.574	0.912	0.983	0.366
4	14.655	0.907	0.988	0.377
5	14.718	0.903	0.993	0.385
6	14.764	0.900	0.996	0.391
7	14.795	0.898	0.998	0.395
8	14.810	0.897	0.999	0.397
9	14.825	0.896	1.000	0.399
AV	14.662	0.906	0.989	0.378

AVG RAKES 1&2

PR	PT	PS/PT	PT/PT1	M
1	14.354	0.926	0.968	0.335
2	14.495	0.917	0.978	0.355
3	14.607	0.910	0.985	0.371
4	14.693	0.904	0.991	0.382
5	14.749	0.901	0.995	0.389
6	14.845	0.895	1.001	0.402
7	14.807	0.897	0.999	0.397
8	14.817	0.897	0.999	0.398
9	14.827	0.896	1.000	0.399
AV	14.684	0.905	0.990	0.381

PROG C2-B
TEST NO. 2274 DATE 50272

RUN NO./COND NO. 8.003

INNER NO.1
PS6.1-PS6.4 13.306 13.246 13.303 13.301

B/L RAKE PS 13.289

PR	PT	PS/PT	PT/PT1	M
1	14.188	0.937	0.957	0.307
2	14.479	0.918	0.976	0.352
3	14.660	0.907	0.989	0.377
4	14.770	0.900	0.996	0.392
5	14.835	0.896	1.000	0.400
6	14.823	0.897	1.000	0.398
7	14.828	0.896	1.000	0.399
8	14.832	0.896	1.000	0.399
9	14.830	0.896	1.000	0.399
AV	14.719	0.903	0.993	0.385

INNER NO.2 B/L RAKE PS 13.289

PR	PT	PS/PT	PT/PT1	M
1	14.204	0.936	0.958	0.310
2	14.531	0.915	0.980	0.360
3	14.698	0.904	0.991	0.382
4	14.787	0.899	0.997	0.394
5	14.817	0.897	0.999	0.397
6	14.825	0.896	1.000	0.398
7	14.828	0.896	1.000	0.399
8	14.828	0.896	1.000	0.399
9	14.829	0.896	1.000	0.399
AV	14.727	0.902	0.993	0.386

AVG RAKES 1&2

PR	PT	PS/PT	PT/PT1	M
1	14.196	0.936	0.957	0.309
2	14.505	0.916	0.978	0.356
3	14.679	0.905	0.990	0.380
4	14.778	0.899	0.997	0.393
5	14.826	0.896	1.000	0.399
6	14.824	0.897	1.000	0.398
7	14.828	0.896	1.000	0.399
8	14.830	0.896	1.000	0.399
9	14.829	0.896	1.000	0.399
AV	14.723	0.903	0.993	0.385

TABLE D-11.–CONCLUDED

PROG C2-B
TEST NO. 2274 DATE 50272

RUN NO./COND NO. 8.003

PLANE 6
TRAV:

RADIUS	OBS PS-A	OBS PS-B	OBS PS-AVG	OBS PS/PT	TRUE PS/PT	TRUE PS	TRUE PT	WCOR6	M	REC PT/PTI
5.888	13.372	13.381	13.377	0.933	0.933	13.375	14.342	1.726	0.317	0.967
5.619	13.400	13.364	13.382	0.907	0.906	13.366	14.753	2.006	0.378	0.995
5.336	13.387	13.348	13.368	0.907	0.906	13.351	14.745	2.011	0.379	0.995
5.037	13.337	13.344	13.341	0.901	0.899	13.320	14.811	2.068	0.392	0.999
4.719	13.294	13.264	13.279	0.896	0.894	13.254	14.820	2.112	0.403	1.000
4.379	13.289	13.197	13.243	0.893	0.891	13.216	14.827	2.138	0.409	1.000
4.010	13.259	13.133	13.196	0.890	0.888	13.166	14.821	2.163	0.415	1.000
3.602	13.255	13.117	13.186	0.890	0.888	13.156	14.821	2.169	0.416	1.000
3.143	13.221	13.130	13.176	0.889	0.887	13.145	14.821	2.176	0.418	1.000
2.604	13.186	13.171	13.179	0.892	0.890	13.150	14.784	2.154	0.413	0.997

AVG PT 14.7545 AVG PS 13.2498
AVG PT/PTI 0.9952 WCOR6 20.7240
WCOR2 20.6241 PL6 FPR 1.1413 MB6 0.3719 MB4 0.7998

TABLE D-12.—RUN 9, SAMPLE AERODYNAMIC DATA TABULATION

PROG C2-C
TEST NO. 2274   DATE 51772

RUN NO./COND NO. 9.011   MAP NO/CONFIG NO. 0.008

WAC	22.678	PTAMBO	14.690	TAMB AC CH	515.85
FPR	1.1411	PLUG POS	0.00	RH	80%
M6	0.523	FAN TIP MR	1.082	FAN TIP M	0.947
N1	19630	N1C	19664	FAN TIP FPS	1028

PLANE 1:
PT120 14.690   PT1W 14.690   PT1 14.690
TT1.1-TT1.3 515.503 516.538 518.608   AVGTT1 516.883
TT120 515.848
TT1W 519.988   TT1 517.918

PLANE 2:
PS2.1-PS2.4 13.422 13.361 13.364 13.370
PSBM 13.379
PSBM/PT1 0.911
AVG M2 0.368

PLANE 3&4:
COWL STATICS:

	301	302	303	304	400	401	402
PS	12.935	12.504	12.012	9.642	10.237	10.720	10.835
-/PT	0.881	0.851	0.818	0.656	0.697	0.730	0.738
M	0.430	0.485	0.544	0.800	0.737	0.686	0.674

	403	404	405	406	407	408	409	410
PS	10.725	11.285	11.558	12.090	11.893	11.714	12.026	12.300
PS/PT	0.730	0.768	0.787	0.823	0.810	0.798	0.819	0.837
M	0.686	0.626	0.596	0.535	0.558	0.578	0.542	0.510

PLANE 10:
PT10.1-PT10.5 17.040 17.260 16.980 16.550 15.980
AVG PT10 16.762

	10.1		10.2	
	IN	OUT	IN	OUT
PS	14.698	14.692	14.697	14.696
PS/PT	0.877	0.877	0.877	0.877
M	0.437	0.438	0.438	0.438

TABLE D-12.–CONTINUED

PROG C2-C
TEST NO. 2274 DATE 51772

RUN NO./COND NO. 9.011

PLANE 6:
M6 0.398 FAN TIP MR 1.018
PS6.1-PS6.4 12.22 12.16 12.15 12.23

OUTER NO.1 B/L RAKE PS 12.189

PR	PT	PS/PT	PT/PT1	M
1	13.556	0.899	0.923	0.393
2	13.689	0.891	0.932	0.411
3	13.759	0.886	0.937	0.420
4	13.827	0.882	0.941	0.428
5	13.902	0.877	0.946	0.438
6	14.008	0.870	0.954	0.450
7	13.971	0.873	0.951	0.446
8	13.961	0.873	0.950	0.445
9	14.049	0.868	0.956	0.455
AV	13.863	0.879	0.944	0.433

OUTER NO.2 B/L RAKE PS 12.189

PR	PT	PS/PT	PT/PT1	M
1	13.738	0.887	0.935	0.417
2	13.784	0.884	0.938	0.423
3	13.881	0.878	0.945	0.435
4	13.836	0.881	0.942	0.430
5	13.852	0.880	0.943	0.432
6	13.816	0.882	0.941	0.427
7	13.826	0.882	0.941	0.428
8	13.847	0.880	0.943	0.431
9	14.090	0.865	0.959	0.460
AV	13.879	0.878	0.945	0.435

AVG RAKES 1&2

PR	PT	PS/PT	PT/PT1	M
1	13.647	0.893	0.929	0.405
2	13.736	0.887	0.935	0.417
3	13.820	0.882	0.941	0.428
4	13.831	0.881	0.942	0.429
5	13.877	0.878	0.945	0.435
6	13.912	0.876	0.947	0.439
7	13.898	0.877	0.946	0.437
8	13.904	0.877	0.947	0.438
9	14.069	0.866	0.958	0.458
AV	13.871	0.879	0.944	0.434

TABLE D-12.–CONCLUDED

PROG C2-C
TEST NO. 2274 DATE 51772

RUN NO./COND NO. 9.011

PLANE 6 RAKE TRAV:

RAD NO.	1	2	3	4	5	6	7	8	9PRB
TEST NO.	2274								
1 PT	13.599	13.658	13.831	13.943	13.952	13.925	13.792	13.771	13.807
PT/PT1	0.926	0.930	0.942	0.949	0.950	0.948	0.939	0.938	0.940
M	0.399	0.407	0.430	0.443	0.444	0.441	0.425	0.422	0.42B
TEST NO.	2274								
2 PT	13.659	13.714	13.938	14.041	14.034	13.980	13.796	13.772	13.880
PT/PT1	0.930	0.934	0.949	0.956	0.956	0.952	0.940	0.938	0.945
M	0.408	0.415	0.443	0.455	0.455	0.448	0.426	0.423	0.43B
TEST NO.	2274								
3 PT	13.674	13.777	14.015	14.039	13.978	13.894	13.731	13.806	13.985
PT/PT1	0.931	0.938	0.954	0.956	0.952	0.946	0.935	0.940	0.952
M	0.410	0.423	0.452	0.455	0.448	0.437	0.417	0.427	0.44B
TEST NO.	2274								
4 PT	13.641	13.797	14.005	13.951	13.865	13.786	13.710	13.873	14.013
PT/PT1	0.929	0.939	0.953	0.950	0.944	0.939	0.933	0.944	0.954
M	0.405	0.425	0.450	0.444	0.433	0.423	0.414	0.434	0.45B
TEST NO.	2274								
5 PT	13.656	13.845	14.013	13.877	13.773	13.714	13.755	13.996	14.036
PT/PT1	0.930	0.943	0.954	0.945	0.938	0.934	0.937	0.953	0.956
M	0.408	0.432	0.452	0.436	0.423	0.416	0.421	0.450	0.45B
TEST NO.	2274								
6 PT	13.658	13.900	14.181	13.919	13.737	13.648	13.734	14.113	14.175
PT/PT1	0.930	0.946	0.965	0.948	0.935	0.929	0.935	0.961	0.965
M	0.408	0.438	0.471	0.441	0.418	0.406	0.418	0.463	0.47B
TEST NO.	2274								
7 PT	13.662	13.848	14.210	13.970	13.753	13.638	13.731	14.158	14.131
PT/PT1	0.930	0.943	0.968	0.951	0.937	0.929	0.935	0.964	0.962
M	0.409	0.433	0.475	0.447	0.421	0.406	0.418	0.469	0.46B
TEST NO.	2274								
8 PT	13.656	13.760	14.011	13.853	13.698	13.624	13.722	14.004	13.884
PT/PT1	0.930	0.937	0.955	0.944	0.933	0.928	0.935	0.954	0.946
M	0.409	0.422	0.453	0.434	0.414	0.404	0.417	0.452	0.43B
TEST NO.	2274								
9 PT	13.707	13.745	13.798	13.744	13.695	13.677	13.686	13.846	13.764
PT/PT1	0.934	0.936	0.940	0.936	0.933	0.931	0.932	0.943	0.937
M	0.415	0.420	0.426	0.420	0.413	0.411	0.412	0.432	0.42B
TEST NO.	2274								
10 PT	13.832	13.725	13.806	13.722	13.654	13.666	13.709	13.744	13.826
PT/PT1	0.942	0.934	0.940	0.934	0.930	0.930	0.933	0.936	0.941
M	0.430	0.417	0.427	0.416	0.407	0.409	0.415	0.419	0.429
AVG REC	0.931	0.938	0.952	0.947	0.941	0.937	0.935	0.947	0.950

MB6 0.440

TABLE D-13.—RUN 10, SAMPLE AERODYNAMIC DATA TABULATION

```
PROG C2-A
TEST NO.   2290                         DATE     53072

RUN NO./COND NO.     10.003      MAP NO/CONFIG NO.     0.010

WAC    19.483     PTAMBO       14.710     TAMB AC CH    532.41
FPR    1.1356     PLUG POS      0.00      RH               55%
M6     0.409      FAN TIP MR    0.955     FAN TIP M      0.863
N1     18370      N1C          18095      FAN TIP FPS   961.9

PLANE 1:
PT120        14.710   PT1W    14.710    PT1     14.710
TT1.1-TT1.3    535.168 535.168 533.443  BMTT1   534.593
TT123   532.408
TT1W    533.098    TT1   532.753

PLANE 2:
PS2.1-PS2.4      13.825   13.746   13.760   13.747
PSBM             13.770
PSBM/PT1          0.936
AVG M2        0.309

PLANE 3:
PS3.1-PS3.4      13.890   13.870   13.860   13.890
  PS/PT1          0.944    0.943    0.942    0.944
  AVG M3          0.290
        301            302               303
        OUT       IN       OUT      IN       OUT
  PS   12.185   11.725   11.016   10.414   10.203
PS/PT   0.828    0.797    0.749    0.708    0.694
  M     0.526    0.579    0.656    0.720    0.742

PLANE 4 (THROAT):
PS4.1-PS4.4(O)    9.778    9.416    9.657    9.209
PS4 AVG    9.515   PS4A/PT1    0.647
M4         0.814

PS4.1-PS4.4(I)    9.800    9.670    9.598    9.707
PS4 AVG    9.694   PS4A/PT1    0.659
M4         0.796
          401                402                403
         IN      OUT      IN      OUT      IN      OUT
  PS    9.710   10.472   10.971   11.086   12.229   12.088
PS/PT   0.660    0.712    0.746    0.754    0.831    0.822
  M     0.794    0.714    0.661    0.649    0.521    0.537
```

TABLE D-13.–CONTINUED

PROG C2-A.
TEST NO. 2290 DATE 53072

RUN NO./COND NO. 10.003

PLANE 5:
OUTER B/L RAKE PS 12.598

PR	PT	PS/PT	PT/PT1	M
1	12.921	0.975	0.878	0.191
2	13.119	0.960	0.892	0.241
3	13.402	0.940	0.911	0.299
4	13.780	0.914	0.937	0.360
5	14.166	0.889	0.963	0.413
6	14.432	0.873	0.981	0.445
7	14.655	0.860	0.996	0.470
AV	13.948	0.903	0.948	0.384

INNER B/L RAKE PS 12.526

PR	PT	PS/PT	PT/PT1	M
1	13.359	0.938	0.908	0.305
2	13.703	0.914	0.932	0.361
3	14.082	0.890	0.957	0.413
4	14.370	0.872	0.977	0.447
5	14.555	0.861	0.990	0.468
6	14.652	0.855	0.996	0.479
7	14.704	0.852	1.000	0.484
AV	14.323	0.875	0.974	0.442

	501	
	IN	OUT
PS	12.807	12.940
PS/PT	0.871	0.880
M	0.449	0.432

PLANE 10:
PT10.1-PT10.5 16.830 16.880 16.880 16.460 16.420
AVG PT10 16.704

	10.1		10.2	
	IN	OUT	IN	OUT
PS	15.073	14.723	14.732	14.709
PS/PT	0.902	0.882	0.882	0.881
M	0.386	0.429	0.428	0.430

PROG C2-A
TEST NO. 2290 DATE 53072

RUN NO./COND NO. 10.003

PLANE 6:
M6 0.224 FAN TIP MR 0.882
PS6.1-PS6.4 12.96 13.46 13.00 13.01

OUTER NO.1 B/L RAKE PS 13.108

PR	PT	PS/PT	PT/PT1	M
1	13.451	0.975	0.915	0.193
2	13.716	0.956	0.933	0.255
3	14.035	0.934	0.954	0.314
4	14.325	0.915	0.974	0.359
5	14.577	0.899	0.991	0.393
6	14.655	0.895	0.996	0.403
7	14.686	0.893	0.998	0.406
8	14.698	0.892	0.999	0.408
9	14.707	0.891	1.000	0.409
AV	14.309	0.916	0.973	0.356

OUTER NO.2 B/L RAKE PS 13.108

PR	PT	PS/PT	PT/PT1	M
1	13.412	0.977	0.912	0.181
2	13.660	0.960	0.929	0.244
3	14.108	0.929	0.959	0.326
4	14.448	0.907	0.982	0.376
5	14.622	0.897	0.994	0.398
6	14.632	0.896	0.995	0.400
7	14.702	0.892	1.000	0.408
8	14.705	0.891	1.000	0.409
9	14.710	0.891	1.000	0.409
AV	14.320	0.915	0.974	0.358

AVG RAKES 1&2

PR	PT	PS/PT	PT/PT1	M
1	13.431	0.976	0.913	0.187
2	13.688	0.958	0.931	0.250
3	14.071	0.932	0.957	0.320
4	14.386	0.911	0.978	0.367
5	14.599	0.898	0.993	0.396
6	14.643	0.895	0.996	0.401
7	14.694	0.892	0.999	0.407
8	14.701	0.892	1.000	0.408
9	14.703	0.891	1.000	0.409
AV	14.314	0.916	0.973	0.357

TABLE D-13.—CONTINUED

PROG C2-A
TEST NO. 2290 DATE 53072

RUN NO./COND NO. 10.003

INNER NO.1
PS6.1-PS6.4 12.838 12.868 12.851 12.877

B/L RAKE PS 12.859

PR	PT	PS/PT	PT/PT1	M
1	13.793	0.932	0.938	0.318
2	14.277	0.901	0.971	0.390
3	14.574	0.882	0.991	0.427
4	14.671	0.877	0.997	0.438
5	14.699	0.875	0.999	0.441
6	14.708	0.874	1.000	0.442
7	14.710	0.874	1.000	0.443
8	14.710	0.874	1.000	0.443
9	14.710	0.874	1.000	0.443
AV	14.568	0.883	0.990	0.426

INNER NO.2 B/L RAKE PS 12.859

PR	PT	PS/PT	PT/PT1	M
1	13.669	0.941	0.929	0.297
2	14.176	0.907	0.964	0.376
3	14.444	0.890	0.982	0.411
4	14.679	0.876	0.998	0.439
5	14.705	0.875	1.000	0.442
6	14.709	0.874	1.000	0.443
7	14.710	0.874	1.000	0.443
8	14.710	0.874	1.000	0.443
9	14.711	0.874	1.000	0.443
AV	14.539	0.885	0.988	0.423

AVG RAKES 1&2

PR	PT	PS/PT	PT/PT1	M
1	13.731	0.937	0.934	0.308
2	14.226	0.904	0.967	0.383
3	14.509	0.886	0.986	0.419
4	14.675	0.876	0.998	0.439
5	14.702	0.875	1.000	0.442
6	14.708	0.874	1.000	0.443
7	14.710	0.874	1.000	0.443
8	14.710	0.874	1.000	0.443
9	14.710	0.874	1.000	0.443
AV	14.553	0.884	0.989	0.424

TABLE D-13.—CONCLUDED

PROG C2-A
TEST NO. 2290 DATE 53072

RUN NO./COND NO. 10.003
TRAV:

RADIUS	OBS PS-A	OBS PS-B	OBS PS-AVG	OBS PS/PT	TRUE PS/PT	TRUE PS	TRUE PT	WCOR6	M	REC PT/PTI
5.888	13.039	13.019	13.029	0.960	0.960	13.033	13.572	1.346	0.241	0.923
5.619	13.070	13.044	13.057	0.920	0.920	13.050	14.191	1.871	0.348	0.965
5.336	13.084	13.075	13.080	0.901	0.900	13.059	14.514	2.064	0.391	0.987
5.037	13.033	13.091	13.062	0.890	0.888	13.032	14.684	2.171	0.417	0.998
4.719	13.042	12.941	12.992	0.884	0.882	12.956	14.699	2.220	0.429	0.999
4.379	12.927	12.939	12.933	0.830	0.877	12.893	14.704	2.256	0.437	1.000
4.010	12.851	12.878	12.865	0.875	0.872	12.820	14.701	2.293	0.447	1.000
3.602	12.842	12.808	12.825	0.872	0.869	12.778	14.704	2.316	0.453	1.000
3.143	12.812	12.804	12.808	0.871	0.868	12.759	14.705	2.325	0.455	1.000
2.604	12.791	12.790	12.791	0.881	0.879	12.753	14.518	2.244	0.434	0.987

AVG PT	14.4992	AVG PS	12.9133
AVG PT/PTI	0.9857	WCOR6	21.1043
WCOR2	20.8025	PL6 FPR	0.0000

TABLE D-14.—RUN 11, SAMPLE AERODYNAMIC DATA TABULATION

M
PROG D1-1B
TEST NO. 2307 DATE 80172

RUN NO./COND NO. 11.012 MAP NO/CONFIG NO. 0.001

WAC	20.310	PTAMBO	14.820	TAMB AC CH	525.16
FPR	1.1488	PLUG POS	2.50	RH	65%
M6	0.340	FAN TIP MR	0.988	FAN TIP M	0.927
N1	19690	N1C	19543	FAN TIP FPS	1031

PLANE 1:
PT120 14.820 PT1W 14.820 PT1 14.820
TT1.1-TT1.3 528.613 525.508 525.508 AVGTT1 526.543
TT120 525.163
TT1W 524.818 TT1 524.991

DUCT STATICS:

OUTER

PR	PS	PS/PT1	M
301	10.751	0.726	0.693
302	8.134	0.549	0.967
303	7.928	0.535	0.989
400	7.768	0.524	1.007
401	8.528	0.576	0.925
402	10.027	0.677	0.769
403	10.494	0.708	0.720
PR	PS	PS/PT6.5	M
404	10.810	0.756	0.645
405	11.115	0.778	0.611
500	11.484	0.803	0.568
501	11.889	0.832	0.520
502	12.264	0.858	0.473
503	12.619	0.883	0.426
600	12.652	0.885	0.422

INNER

PR	PS	PS/PT1	M
303	8.546	0.577	0.923
400	7.768	0.524	1.007
401	8.250	0.557	0.954
402	9.788	0.661	0.793
403	10.356	0.699	0.734
PR	PS	PS/PT6.5	M
405	11.141	0.779	0.608
600	12.640	0.884	0.423

PLANE 4 (THROAT):

OUTER

ANG	PS	PS/PT1	M
0	7.768	0.524	1.007
45	7.170	0.484	1.074
90	7.225	0.488	1.067
135	7.077	0.478	1.084
180	7.125	0.481	1.079
225	7.133	0.485	1.072
270	7.179	0.485	1.073
315	7.235	0.488	1.066
AVG	7.245	0.489	1.065
STG	10.879	0.734	0.680

TABLE D-14.—CONTINUED

PROG D1-1B
TEST NO. 2307 DATE 80172

RUN NO./COND NO. 11.012
PLANE 4 CONT:
INNER

ANG	PS	PS/PT1	M
0	7.628	0.515	1.022
45	7.868	0.531	0.996
90	6.960	0.470	1.098
135	8.069	0.545	0.974
180	6.869	0.464	1.108
225	8.605	0.581	0.917
270	7.112	0.480	1.080
315	8.369	0.565	0.942
AVG	7.685	0.519	1.016

PLANE 6:
OUTER

ANG	PS	PS/PT6.5	M
0	12.652	0.885	0.422
90	12.603	0.882	0.428
180	12.580	0.880	0.431
270	12.633	0.884	0.424
AVG	12.617	0.883	0.426

INNER

ANG	PS	PS/PT6.5	M
0	12.640	0.884	0.423
90	12.644	0.885	0.423
180	12.627	0.883	0.425
270	12.636	0.884	0.424
AVG	12.637	0.884	0.424

PLANE 6.5:
INNER

ANG	PS	PS/PT6.5	M
0	12.829	0.897	0.396
20	12.672	0.887	0.419
40	12.666	0.886	0.420
60	12.679	0.887	0.418
80	12.723	0.890	0.412
100	12.697	0.888	0.415
120	12.650	0.885	0.422
140	12.660	0.886	0.420
160	12.693	0.888	0.416
180	12.715	0.890	0.413
200	12.696	0.888	0.415
220	12.650	0.885	0.422
240	12.643	0.884	0.423
260	12.759	0.893	0.406
280	12.690	0.888	0.416
300	12.653	0.885	0.421
320	12.642	0.884	0.423
340	12.667	0.886	0.419
AVG	12.688	0.888	0.416

TABLE D-14.—CONCLUDED

PROG D1-1B
TEST NO. 2307 DATE 80172

RUN NO./COND.NO. 11.012
PLANE 6.5 CONT:
OUTER

ANG	PS	PS/PT6.5	M
0	12.845	0.899	0.394
82	12.840	0.898	0.395
175	12.842	0.898	0.395
268	12.841	0.898	0.395
AVG	12.842	0.898	0.395

RAD	ANG-40 REC	43 REC	136 REC	229 REC	RAD AVG REC	RAD AVG M	PL6.5 WACR	RING AVG PT6.5
5.828	0.939	0.937	0.939	0.942	0.939	0.354	2.681	13.917
5.417	0.956	0.966	0.958	0.975	0.964	0.404	3.120	14.283
4.987	0.967	0.985	0.977	0.991	0.980	0.433	3.208	14.517
4.508	0.972	0.990	0.987	0.987	0.984	0.440	3.330	14.581
3.967	0.973	0.986	0.981	0.973	0.978	0.431	3.220	14.499
3.347	0.981	0.973	0.960	0.952	0.967	0.409	3.066	14.324
2.567	0.945	0.942	0.932	0.928	0.937	0.348	2.302	13.881
AVG	0.962	0.969	0.962	0.964	TOTAL	WAC	20.186	

PT 6.5 AVG 14.296 REBAR 0.965

DISTORTION: 0.065

B/L RAKE-ANG 3

RADIUS	PT	PT/PT1	PS/PT	M
5.978	13.522	0.913	0.936	0.309
5.818	13.873	0.936	0.913	0.364
5.678	13.996	0.944	0.905	0.382
5.518	14.104	0.952	0.898	0.396
5.377	14.226	0.960	0.890	0.412

B/L PS 12.658

PLANE 10:
PT10.1-PT10.2 17.315 17.234 17.095 16.799 16.686
AVG PT10 17.026

INNER
PS 14.827 14.842

OUTER
PS 15.192 15.198

TABLE D-15.—RUN 12, SAMPLE AERODYNAMIC DATA TABULATION

PROG D2-2
TEST NO. 2307 DATE 81472

RUN NO./COND NO. 12.006 MAP NO/CONFIG NO. 0.002

		PTAMBO	14.665	TAMB AC CH	531.03
FPR	1.2372	PLUG POS	0.00	RH	51%
M6	0.525	FAN TIP MR	1.256	FAN TIP M	1.141
N1	23990	N1C	23689	FAN TIP FPS	1256

PLANE 1:
PT120 14.670 PT1W 14.660 PT1 14.665
TT1.1-TT1.3 531.028 532.408 532.408 AVGTT1 531.948
TT120 531.028
TT1W 532.063 TT1 531.546

DUCT STATICS 45 DEG:
OUTER

PR	PS	PS/PT1	M
301	10.001	0.682	0.760
302	7.740	0.528	1.001
303	8.272	0.564	0.943
400	8.057	0.550	0.966
401	6.637	0.453	1.128
402	8.107	0.553	0.961
403	8.842	0.603	0.882
PR	PS	PS/PT6	M
404	9.307	0.640	0.824
405	9.866	0.679	0.765
500	10.227	0.704	0.727
501	10.812	0.744	0.664
502	11.320	0.779	0.609
503	11.776	0.810	0.557
600	11.717	0.806	0.564

INNER

PR	PS	PS/PT1	M
303	7.879	0.537	0.936
400	8.057	0.550	0.966
401	10.056	0.686	0.754
402	9.987	0.681	0.762
403	10.184	0.695	0.741
PR	PS	PS/PT6	M
405	11.126	0.766	0.630
600	11.846	0.815	0.549

PLANE 4 (THROAT):
OUTER

ANG	PS	PS/PT1	M
45	8.057	0.550	0.966
90	8.048	0.549	0.967
135	8.057	0.550	0.966
180	7.989	0.545	0.973
225	8.032	0.548	0.969
270	8.017	0.547	0.970
315	8.045	0.549	0.967
360	8.047	0.549	0.967
AVG	8.037	0.548	0.968

PROG D2-2
TEST NO. 2307 DATE 81472

RUN NO./COND NO. 12.006
PLANE 4 CONT:
INNER

ANG	PS	PS/PT1	M
45	9.565	0.652	0.806
90	8.039	0.548	0.968
135	9.756	0.665	0.786
180	8.775	0.598	0.889
225	10.300	0.702	0.729
270	8.497	0.580	0.919
315	10.142	0.692	0.745
360	8.197	0.559	0.951
AVG	9.159	0.625	0.848

PLANE 6:
OUTER

ANG	PS	PS/PT6	M
45	11.717	0.806	0.564
135	11.702	0.805	0.565
225	11.633	0.800	0.573
315	11.741	0.808	0.561
AVG	11.698	0.805	0.566

INNER

ANG	PS	PS/PT6	M
45	11.846	0.815	0.549
135	11.791	0.811	0.555
225	11.722	0.807	0.563
315	11.733	0.811	0.556
AVG	11.786	0.811	0.556

RAD	ANG 0 REC	90 REC	180 REC	270 REC	RAD AVG REC	RAD AVG M	PL6 WACR	RING AVG PT6
5.830	0.965	0.962	0.977	0.945	0.963	0.520	3.623	14.115
5.437	0.997	0.999	0.995	0.999	0.998	0.569	3.850	14.629
5.015	0.997	1.000	1.000	1.000	0.999	0.572	3.860	14.653
4.552	0.998	1.000	1.000	1.000	0.999	0.572	3.861	14.655
4.036	0.998	1.000	0.999	1.000	0.999	0.572	3.861	14.655
3.444	0.993	1.000	0.997	0.999	0.999	0.571	3.856	14.643
2.727	0.998	0.994	0.960	0.975	0.932	0.547	3.753	14.394
AVG	0.993	0.994	0.990	0.988	TOTAL WAC		26.426	

PT 6 AVG 14.535 REBAR 0.991

DISTORTION: 0.056

TABLE D-15.—CONCLUDED

PROG D2-2
TEST NO. 2307 DATE 81472

RUN NO./COND NO. 12.006
PLANE 6 CONT:
OUTER
B/L RAKE-ANG 25

RADIUS	PT	PT/PT1	PS/PT	M
5.898	13.977	0.953	0.837	0.511
5.778	14.360	0.979	0.815	0.549
5.658	14.581	0.994	0.802	0.570
5.538	14.642	0.999	0.799	0.576
5.417	14.659	1.000	0.798	0.577
5.297	14.663	1.000	0.798	0.577
5.177	14.666	1.000	0.798	0.578
5.058	14.664	1.000	0.798	0.578
4.817	14.665	1.000	0.798	0.578

B/L PS 11.698

INNER
B/L RAKE-ANG 0

RADIUS	PT	PT/PT1	PS/PT	M
3.085	14.640	0.998	0.805	0.565
2.727	14.627	0.998	0.806	0.564
2.506	14.360	0.979	0.821	0.539

PLANE 10:
PT10.1-PT10.2 18.282 18.239 18.042 17.898 18.255
AVG PT10 18.143

INNER
PS 14.765 14.802

OUTER
PS 15.372 15.376

TABLE D-16.—RUN 13, SAMPLE AERODYNAMIC DATA TABULATION

PROG D3-1
TEST NO. 2307 DATE 91172

RUN NO./COND NO. 13.003 MAP NO/CONFIG NO. 0.003

		PTAMBO	14.750	TAMB AC CH	518.61
FPR	1.1279	PLUG POS	0.00	RH	77%
M6	0.317	FAN TIP MR	0.933	FAN TIP M	0.878
N1	18610	N1C	18525	FAN TIP FPS	974.4

PLANE 1:
PT120 14.750 PT1W 14.750 PT1 14.750
TT1.1-TT1.3 532.753 518.953 518.608 AVGTT1 523.438
TT120 518.608
TT1W 519.988 TT1 519.298

DUCT STATICS 0 DEG:
OUTER

PR	PS	PS/PT1	M
301	14.734	0.999	0.039
302	12.096	0.820	0.540
303	12.262	0.831	0.521
304	12.294	0.834	0.517
305	11.696	0.793	0.585
400	10.060	0.682	0.760
401	10.614	0.720	0.702
402	11.400	0.773	0.618
403	12.270	0.832	0.520
PR	**PS**	**PS/PT6**	**M**
404	12.636	0.895	0.402
405	12.692	0.899	0.394
501	12.706	0.900	0.392
502	12.780	0.905	0.381
600	12.973	0.919	0.351

INNER

PR	PS	PS/PT1	M
300	14.372	0.974	0.193
301	13.643	0.925	0.336
302	13.086	0.887	0.417
303	12.633	0.857	0.476
304	12.362	0.838	0.509
305	12.314	0.835	0.515
400	10.211	0.692	0.744
401	10.754	0.729	0.687
402	11.110	0.753	0.649
403	0.001	0.000	8.518
PR	**PS**	**PS/PT6**	**M**
404	12.100	0.857	0.476
405	12.356	0.875	0.442

PROG D3-1
TEST NO. 2307 DATE 91172

RUN NO./COND NO. 13.003
PLANE 4 (THROAT):
OUTER

ANG	PS	PS/PT1	M
0	10.060	0.682	0.760
45	9.981	0.677	0.768
90	10.069	0.683	0.759
135	10.270	0.696	0.738
180	10.007	0.679	0.766
225	10.270	0.696	0.738
270	10.206	0.692	0.745
315	10.403	0.705	0.724
AVG	10.158	0.689	0.750

INNER

ANG	PS	PS/PT1	M
0	10.211	0.692	0.744
45	8.070	0.547	0.970
90	8.147	0.552	0.961
135	8.842	0.600	0.887
180	7.830	0.531	0.996
225	8.088	0.548	0.968
270	8.244	0.559	0.951
315	9.585	0.650	0.810
AVG	8.627	0.585	0.910

VANE STATICS:

RAD	355	1	2	3	4	ANG
4.896	0.607	0.684	0.616	0.692	0.778	5
4.352	0.573	0.622	0.575	0.622	0.829	15
3.808	0.558	0.641	0.554	0.603	0.748	25
3.263	0.557	0.630	0.535	0.590		35
2.720	0.587					

PLANE 6:
OUTER

ANG	PS	PS/PT6	M
0	12.983	0.919	0.349
90	12.966	0.918	0.352
180	12.969	0.918	0.352
270	12.963	0.918	0.353
AVG	12.970	0.918	0.351

INNER

ANG	PS	PS/PT6	M
0	12.797	0.906	0.378
90	12.793	0.906	0.379
180	12.793	0.906	0.379
270	12.808	0.907	0.377
AVG	12.798	0.906	0.378

TABLE D-16.–CONCLUDED

PROG D3-1
TEST NO. 2307 DATE 91172

RUN NO./COND NO. 13.003
PLANE 6 CONT:
ROT RAKE

RAD	ANG- 0 REC	82 REC	175 REC	268 REC	RAD AVG REC	RAD AVG M	PL6 WACR	RING AVG PT6
5.828	0.943	0.949	0.948	0.947	0.947	0.341	2.598	13.962
5.417	0.961	0.961	0.961	0.958	0.960	0.370	2.904	14.164
4.987	0.981	0.978	0.981	0.972	0.978	0.405	3.042	14.423
4.508	0.980	0.979	0.980	0.983	0.980	0.409	3.144	14.459
3.967	0.968	0.974	0.968	0.975	0.971	0.392	2.986	14.324
3.347	0.938	0.967	0.955	0.947	0.952	0.352	2.705	14.035
2.567	0.901	0.934	0.915	0.915	0.916	0.262	1.786	13.513
AVG	0.953	0.963	0.958	0.957	TOTAL WAC		18.353	

PT 6 AVG 14.126 REBAR 0.958

DISTORTION: 0.087

B/L RAKE-ANG 42

RADIUS	PT	PT/PT1	PS/PT	M
5.978	13.646	0.925	0.938	0.303
5.818	13.903	0.943	0.921	0.345
5.678	13.995	0.949	0.915	0.359
5.518	14.074	0.954	0.910	0.370
5.377	14.149	0.959	0.905	0.381

B/L PS 12.802

PLANE 10:
PT10.1-PT10.5 16.795 16.791 16.672 16.441 16.486
AVG PT10 16.637

Inner

P_S 14.746 14.757

P_S 15.056 15.070

TABLE D-17.—RUN 14, SAMPLE AERODYNAMIC DATA TABULATION

PROG D4-1
TEST NO. 2307 DATE 92072

RUN NO./COND NO. 14.005 MAP NO/CONFIG NO. 0.004

		PTAMBO	14.765	TAMB AC CH	519.64
FPR	1.2358	PLUG POS	0.00	RH	66%
M6	0.419	FAN TIP MR	1.189	FAN TIP M	1.113
N1	23320	N1C	23312	FAN TIP FPS	1221

PLANE 1:
PT120 14.760 PT1W 14.770 PT1 14.765
TT1.1-TT1.3 516.883 520.678 519.643 AVGTT1 519.068
TT120 519.643
TT1W 519.988 TT1 519.816

DUCT STATICS 0 DEG:

OUTER

PR	PS	PS/PT1	M
301	10.240	0.694	0.742
302	8.923	0.604	0.880
303	8.811	0.597	0.892
304	8.730	0.591	0.900
305	8.744	0.592	0.899
400	10.451	0.708	0.720
401	10.674	0.723	0.697
402	11.128	0.754	0.649
403	11.608	0.786	0.597
PR	PS	PS/PT6	M
404	11.762	0.802	0.570
405	11.829	0.807	0.562
501	14.346	0.979	0.176 OUT
502	12.109	0.826	0.530
600	12.434	0.848	0.491

INNER

PR	PS	PS/PT1	M
300	14.059	0.952	0.266
301	12.489	0.846	0.495
302	11.032	0.747	0.659
303	9.641	0.653	0.805
304	8.591	0.582	0.915
305	8.771	0.594	0.896
400	10.042	0.680	0.763
401	10.529	0.713	0.712
402	10.813	0.732	0.682
403	0.002	0.000	7.662
PR	PS	PS/PT6	M
404	11.295	0.771	0.622
405	11.296	0.771	0.622

TABLE D-17.—CONTINUED

PROG D4-1
TEST NO. 2307 DATE 92072

RUN NO./COND NO. 14.005
PLANE 4 (THROAT):
OUTER

ANG	PS	PS/PT1	M
0	10.451	0.708	0.720
45	10.450	0.708	0.720
90	10.450	0.708	0.720
135	10.504	0.712	0.715
180	10.410	0.705	0.725
225	10.414	0.705	0.724
270	10.413	0.705	0.724
315	10.508	0.712	0.714
AVG	10.450	0.708	0.720

INNER

ANG	PS	PS/PT1	M
0	10.042	0.680	0.763
45	10.211	0.692	0.745
90	10.180	0.690	0.749
135	10.291	0.697	0.737
180	9.907	0.671	0.777
225	10.237	0.693	0.743
270	10.239	0.694	0.743
315	10.017	0.679	0.766
AVG	10.141	0.687	0.753

PLANE 6:
OUTER

ANG	PS	PS/PT6	M
0	12.437	0.848	0.491
90	12.353	0.843	0.501
180	12.429	0.848	0.492
270	12.408	0.846	0.494
AVG	12.407	0.846	0.494

INNER

ANG	PS	PS/PT6	M
0	12.102	0.826	0.531
90	12.104	0.826	0.531
180	12.098	0.825	0.531
270	12.160	0.830	0.524
AVG	12.116	0.827	0.529

TABLE D-17.—CONCLUDED

PROG D4-1
TEST NO. 2307 DATE 92072

RUN NO./COND NO. 14.005
PLANE 6 CONT:
ROT RAKE

RAD	ANG- 0 REC	82 REC	175 REC	268 REC	RAD AVG REC	RAD AVG M	PL6 WACR	RING AVG PT6
5.828	0.948	0.953	0.956	0.961	0.955	0.451	3.266	14.094
5.417	0.991	0.995	0.999	0.999	0.996	0.517	3.759	14.709
4.987	1.000	1.000	1.000	1.000	1.000	0.522	3.687	14.767
4.508	1.000	1.000	1.000	1.000	1.000	0.522	3.778	14.768
3.967	1.000	1.000	1.000	1.000	1.000	0.522	3.716	14.768
3.347	1.000	1.000	1.000	1.000	1.000	0.522	3.685	14.768
2.567	1.000	0.999	0.998	1.000	0.999	0.521	3.159	14.754
AVG	0.991	0.993	0.994	0.994		TOTAL WAC	24.873	

PT 6 AVG 14.661 REBAR 0.993

DISTORTION: 0.053

B/L RAKE-ANG 42

RADIUS	PT	PT/PT1	PS/PT	M
5.978	13.798	0.935	0.883	0.426
5.818	14.237	0.964	0.855	0.478
5.678	14.386	0.974	0.847	0.494
5.518	14.400	0.975	0.846	0.495
5.377	14.554	0.986	0.837	0.511

B/L PS 12.177

PLANE 10:
PT10.1-PT10.5 18.380 18.506 18.218 17.913 18.216
AVG PT10 18.247

INNER
PS 14.867 14.905

OUTER
PS 15.486 15.478

APPENDIX E

CONCEPT SCREENING—DATA ANALYSIS

C-3.

SUMMARY

This appendix contains a review of past work in the development of sonic inlet as a means of inlet noise reduction for jet aircraft. The study was undertaken so as to utilize past experience to the greatest extent possible in the initial stages of configuration decisions and to identify technology areas where most of the effort should be expanded. Results of this review were reported in Boeing document D6-40573.

A brief description of each of the past sonic inlet studies is presented in this appendix. A tabulation of these studies, including key data presentation, is also presented to facilitate cross-reference in data interpretation.

Considerable effort has been spent on sonic inlet technology by various investigators in the past 10 years. Most of this work, however, was directed toward development of a specific configuration rather than toward activity contributing to a configuration selection or the establishment of a design technology base. Due to the large variation in configurations, as well as in test and measurement techniques, scatter in the existing data is large enough on any parameter that it makes the drawing of any specific conclusion uncertain. The data survey, however, shows some general trends with respect to sonic inlet performance and noise reduction potential. These trends are as follows:

- Substantial discrete frequency noise reduction can be realized for a nominal sonic inlet throat Mach number less than 1.0.
- Sonic inlet concepts are more effective in reducing discrete frequency noise than broadband noise.
- The broadband noise reduction is frequency dependent. The amount of noise reduction is lower for broadband noise at low frequencies.
- The sonic inlet is effective in noise reduction at all inlet angles.

E.1 INTRODUCTION

Inlet noise radiation from a jet aircraft at takeoff and landing approach represents a large part of the total noise annoyance in the airport community. An inlet noise reduction device has been the subject of study for more than a decade. Because an acoustic wave propagates at sonic speed relative to that of air, noise radiated upstream in an engine inlet may be blocked by creating a sonic flow in the inlet. This so-called "sonic inlet" has been the subject of investigation at Boeing and elsewhere.

E.2 SURVEY OF PAST SONIC INLET WORK

In this section, a brief description of each of the reports reviewed is presented. In addition, a tabulation of these reports, including the key data presentation, is included to facilitate cross-referencing for data interpretation (see table E-1).

Investigations of the sonic inlet as a means of inlet noise suppression were first reported in 1960 and 1961.

Results of a series of model sonic inlet tests were reported in reference E-1. The inlet model was of a translating centerbody type. The inlet throat area could be adjusted by properly positioning the centerbody. The air supply was from plant air which passed through the model inlet and exited through a diffuser. The noise source was a single-frequency air siren located at the exit of the diffuser. One microphone serving as a monitor was located immediately in front of the siren. Another microphone was located in front of the inlet model in the flow duct. Representative results showed a noise reduction of 35 dB at a nominal inlet throat Mach number of 0.9.

In reference E-2, experimental results on the reduction of compressor noise by means of a completely choked inlet were reported. A "sonic block silencer," consisting of a contoured duct and centerbody, provided an aerodynamic throat in the silencer. The tests were performed on turbojets of different thrust ranges with the silencer installed. The microphone was located 20 in. in front of the inlet plane. The acoustic measurement of a 160 lb/sec flow jet engine installation demonstrated 16 dB in discrete frequency noise reduction. Subsequent tests on a Bristol Olympus 6 jet engine showed a 12 dB discrete frequency noise reduction. However, background noise associated with the tests may have impaired measurement of the true compressor inlet noise reduction.

In reference E-3, noise measurements were made on an Avon engine fitted with a conventional inlet and a sonic inlet with a center bullet designed to choke the inlet flow. Microphones were positioned along an arc of 50-ft radius at 10° and 90° from the inlet axis. At a 10° angle, a reduction of 28 dB in overall sound pressure level was observed. One-third-octave band spectrum analysis showed a reduction of discrete frequency noise of nearly 40 dB. However, a much smaller reduction of discrete frequency noise, 10 dB, was observed at a 90° angle.

Reference E-4 reports the results of a centerbody-type axisymmetric supersonic inlet test using a J-75 afterburning turbojet engine. The test was set up in an open field. Acoustic instrumentation

TABLE E-1.—SUMMARY OF PREVIOUS SONIC INLET WORK

Test ID	Configuration	Test setup	Location of noise measurement	Noise source	Discrete frequency noise vs $M_{℄}$	Discrete frequency noise vs W/W*	Overall vs $M_{℄}$	Overall vs W/W*	PNL $M_{℄}$	PNL W/W*	Broadband vs $M_{℄}$	Broadband vs W/W*	Directivity	Narrow band spectrum	P_{T_2}/P_{T_1} vs $M_{℄}$	P_{T_2}/P_{T_1} vs W/W*	Distortion vs $M_{℄}$	Distortion vs W/W*	P_{T_2}/P_{T_1} vs rpm
D6-5980 Maestrello, L. 1960	Model center-plug-type sonic inlet in connection with a flow duct	Open field	Upstream and downstream in the flow duct	Siren	X	—	—	—	—	—	—	—	—	—	X	—	—	—	—
Noise Control Shock Vibration Welliver, A 1961	Sonic inlet with screw-type compressor and Olympus-6 turbojet	Open field and indoors	150 ft, 15° off engine axis; 6-in. and 20-in. in front of the inlet plane	Compressor	High inlet throat Mach no.	—	—	—	—	—	High inlet throat Mach no.	—	—	1/3 octave band	Level of recovery quoted	—	—	—	—
T6-3173 McKaig, M. 1964	SST inlet on J-75 engine	Open field	10° to 160° at 10° interval on 200-ft radius arc for far field, 0° to 90° on 25-ft radius arc for near field	Compressor	Near field	—	—	—	For choked and unchoked cond.		—	—	X	X	—	—	—	—	—
NASA TND-2615 Copeland, W.L. 1965	34-in. OD rotor in duct, HD = 24 in., no stator	Driven by motor, TS = 980 ft/sec, open field tests	30° to 105° at 15° interval on 60-ft radius and sweeping boom -30° to 105°	Free rotor in duct	Overall for two inlet lengths. Fan fundamental for two inlet lengths								Overall fan fundamental	0°, 45°, 90°	—	—	—	—	—
NASA TND-3929 Cawthorn, J.M. 1967	SST inlet with Viper 8 engine (turbojet)	Rig test open field	0° to 90° at 15° interval on 25-ft radius	Compressor	—	—	—	—	—	—	—	—	Overall and discrete frequency noise for two rpms one choked, one unchoked	1/3 octave band spectrum	—	—	—	—	X
D6A10155-1 Sawhill, R.H. 1966	5-in. inlet, SST type, with ejector	Model in 9- by 9-ft tunnel	20° from inlet ℄ at 20-ft radius	Siren	X	—	—	—	—	—	—	—	—	For tunnel speed 0, 100, and 150 kn	—	—	—	—	—

TABLE E-1.—Continued

Test ID	Configuration	Test setup	Location of noise measurement	Noise source	Discrete frequency noise vs $M_{\mathbb{C}}$	Discrete frequency noise vs W/W*	Overall vs $M_{\mathbb{C}}$	Overall vs W/W*	PNL vs $M_{\mathbb{C}}$	PNL vs W/W*	Broadband vs $M_{\mathbb{C}}$	Broadband vs W/W*	Directivity	Narrow band spectrum	P_{T_2}/P_{T_1} vs $M_{\mathbb{C}}$	P_{T_2}/P_{T_1} vs W/W*	Distortion vs $M_{\mathbb{C}}$	Distortion vs W/W*	P_{T_2}/P_{T_1} vs rpm
D6A10378-1 Andersson, A.O. 1966	5-in. inlet, SST type, with ejector Two-inlet centerbody	Model in test arena, inlet wrapped with acoustic material	0°-90° at 10° interval, radius not specified	Siren	—	X	—	—	—	—	—	—	Data at 0°, 30°, 60°, and 90° from inlet axis	—	—	—	—	—	—
D6-60120-5 The Boeing Company 1969	Mechanized sonic inlet, eight sides JT3D-3B engine	With long treated duct	10° to 140° at 10° interval on 200-ft-radius horizontal arc, 20° to 130° at 10° interval on 75-ft-radius vertical arc	Compressor	X	—	—	—	—	—	—	—	X	X	X	—	—	—	X
D6-23469, D6-22752 Higgins, C.C. Bosch, J.C. 1969	(1) Eight-side adjustable sonic inlet JT3D engine, 750 in ^{2} throat angle	Rig test with 3/4 length duct and directionalizer	10° to 140° at 10° interval on 200-ft-radius horizontal arc, 20° to 130° at 10° interval on 75-ft-radius vertical arc	JT3D-3B turbofan engine	Horiz and vert plane	—	Horiz and vert plane	—	—	—	—	—	Discrete frequency, overall, PNL vertical and horizontal planes	X	X	—	X	—	X
	(2) 900 in ^{2} throat area	As above	As above	As above	As above	—	As above	—	—	—	—	—	As above	X	X	—	X	—	X
D6-23461TN D6-60120-5 Smith, J.N. The Boeing Company 1969	Five-door 928 in ^{2} JT3D-3B engine	Rig test with directionalizer	10° to 140° at 10° interval on 200-ft-radius horizontal arc, 20° to 130° at 10° interval on 75-ft radius vertical arc	JT3D-3B turbofan engine	X	—	—	—	X	—	—	—	Discrete frequency	X	—	—	—	—	—
ASME J. of Engr for Power Smith, M.J. House, M.Z 1967	Full-scale compressor	—	—	Compressor	—	—	—	—	—	—	X	—	—	—	—	—	—	—	—
General Electric TR D6-68-7 Smith, E.B 1968	Model cascade	Test rig	In cascade flow duct	Warble tone generator	X	X	—	—	—	—	—	—	—	—	X	X	—	—	—

TABLE E-1.—Concluded

Test ID	Configuration	Test setup	Location of noise measurement	Noise source	Discrete frequency noise vs		Overall vs		PNL		Broadband vs		Directivity	Narrow band spectrum	P_{T_2}/P_{T_1} vs		Distortion vs		P_{T_2}/P_{T_1} vs rpm
					$M_{\mathrm{C\!\!\!L}}$	W/W*	$M_{\mathrm{C\!\!\!L}}$	W/W*	$M_{\mathrm{C\!\!\!L}}$	W/W*	$M_{\mathrm{C\!\!\!L}}$	W/W*			$M_{\mathrm{C\!\!\!L}}$	W/W*	$M_{\mathrm{C\!\!\!L}}$	W/W*	
D6-23276 Schaut, L.A. 1969	Model grid inlet, horizontal and vertical grids, simulated approach and cruise conditions	In test cell, acoustic and performance tests in different cells	Mic mounted on boom sweeping horizontally (-20° to 80°)	Compressor	—	—	Acoustic power reduction on a 70° arc	—	—	—	—	—	Overall	For various rpm	X	—	Grid wake decay	—	—
NASA TND-5692 Putnam, T V 1970	XB-70 Airplane	Ground static test	0° to 90° at 10° interval at 240-ft radius	Compressor	—	—	—	At two A/A*	—	—	—	—	Overall at two A/A*	At 0° for two A/A*	For two A/A*	—	For two A/A*	—	—
D6-40208 Anderson, R., et al., 1972	(1) Grid inlet, 12-in. model	Model in anechoic chamber	0° to 80° inlet quadrant 10° interval at 10-ft radius	Fan	(in terms of rpm)		—	—	—	X	—	—	X	—	—	X	—	X	—
	(2) Radial vane inlet, 12-in. model	As above	As above	Fan	(in terms of rpm)		—	—	—	X	—	—	X	—	—	X	—	X	—
NASA TND-4682 Chestnutt, D. 1968	Three-stage compressor 12-in., TD 6 in. HD IGV, two sets, 0.12 and 0.06 t/c (uncambered)	Motor-driven inlet in anechoic chamber	Mic 0°, 15°, 30°, and 90° from ℄, on 10-ft-radius arc also mounted on boom sweeping horizontally	Compressor	(1) Narrow band spectrum compare fan tone at 80% and 98% speed (2) Overall vs angle (3) Overall vs angle (4) Overall vs rpm (5) Overall vs IGV to fan spacing								} 0.12 IGV 0° stagger } 0.06 IGV 15° stagger	X	—	—	—	—	—

$M_{\mathrm{C\!\!\!L}}$ Maximum flow Mach number near inlet throat
W/W* Ratio of inlet flow to sonic flow
A/A* Ratio of flow area to sonic flow area
X Data available
— Data not available

included microphones positioned on 200- and on 25-ft-radius arcs for far-field and near-field noise measurements, respectively. Typical results showed a reduction of 15 PNdB at angles of 20° and 30° measured from the inlet axis. Test results of sonic inlets with acoustically treated inlet guide vanes were also presented. Approximately 5 PNdB noise reduction was observed for the acoustic treatment at an unchoked operation.

In 1965, an investigation was conducted (ref. E-5) of the effects of duct length and duct acoustic treatment on the noise radiation of a rotor in an annular duct. The test setup included a rotor having tip and hub diameters of 34 and 20 in., respectively. The centerbody was of the same length as the inlet duct. The length of both the inlet duct and centerbody could be changed so that the effect of duct length could be investigated. Typical results showed that increasing the inlet duct length from 4 to 16 ft reduced the overall noise by 7 dB and rotor discrete frequency noise by 10 dB measured at an angle 20° from the inlet axis.

An investigation was reported in 1967 (ref. E-6) on the inlet noise reduction and associated performance level of an axisymmetric external-internal compression SST inlet with a Viper 8 turbojet engine. Tests were made for a range of inlet flow areas by translating the inlet centerbody. The noise measurements were taken on both a 25- and a 70-ft-radius circle from 0° to 90° from the inlet axis at 15° intervals. The inlet performance and flow conditions were measured by using total pressure rakes at the exit plane of the inlet and static pressure measurements on the cowl wall and centerbody. Acoustic data were presented for two engine operating conditions—choked and unchoked inlet flows. Reductions were observed of 2 to 5 dB in overall sound pressure level and 2 to 20 dB in the noise level of the fundamental blade passage frequency. The smaller reductions occurred from the 45° to the 90° angles, and the larger reductions from 0° to 45° angles.

In 1966, a series of model SST inlet tests were conducted to investigate the effectiveness of choked flow for inlet noise reduction. Reference E-7 reports on a 5-in. SST model inlet test conducted in a 9- by 9-ft wind tunnel. The tunnel speed was varied from 0 to 150 kn to simulate flight speed. The purpose of the tests was to study the effects of inlet flow Mach number and flight speed on inlet noise suppression. Inlet flow was induced by an air ejector and an air siren was used as noise source. The microphone was placed 20 ft forward of the inlet at 20° from the inlet axis. Narrow band spectrum analysis was made on the noise measurement for various tunnel speeds. The reduction in discrete frequency noise at zero tunnel speed was 33 dB when the inlet flow was increased from 0.63 to 1.0.

Reference E-8 reports on a model SST inlet test conducted outdoors. Inlet flow was induced by an ejector. A motor-driven air siren was used as noise source. The inlet and the ejector air supply lines were wrapped in acoustic material to minimize noise from other sources than the inlet opening. Microphones were placed at 10° intervals from 0° to 90° from the inlet axis. Two centerbodies of different sized were tested. Typical results showed 20-dB noise reduction at 95% maximum inlet air flow ($M \sim 0.77$).

In May 1967, a development program under a NASA contract was undertaken at Boeing to develop an engine nacelle modification for the Boeing 707 airplane to reduce noise during landing approach. The nacelle modification included both inlet and fan duct. Acoustic treatment was the sole means for reducing fan discharge noise, whereas both acoustic treatment and the sonic flow concept were explored to reduce the engine inlet noise. The sonic inlet development was reported in reference E-9. The sonic inlet program started with the design and test of a full-scale, five-sided contracting cowl wall inlet. The final configuration was an eight-sided, contracting cowl wall inlet to provide sonic flow at various landing approach power settings. A full-scale, eight-sided adjustable throat area inlet was constructed and tested. This inlet was then modified and mechanized including a programmed inlet throat area schedule as a function of engine speed. This mechanized sonic inlet was then tested for acoustic and flow performance. In parallel to the full-scale tests, 1/9-scale-model tests were also conducted to provide preliminary information that would influence full-scale-model decisions.

Test results of the five-door, contracting cowl wall sonic inlet were reported in reference E-10. The inlet flow quality of the eight-sided, adjustable sonic inlet was reported in references E-11 and E-12, and the acoustic measurements in reference E-13. The results of model sonic inlet tests were presented in reference E-14.

Additional investigation of noise reduction due to cascade flow Mach number was reported in 1968 (ref. E-15). Two sets of cascades were placed in a flow duct to create a local increase in Mach number. The stagger angle could be varied because the exhaust duct was moveable. A warble tone generator was used as a noise source and was positioned at the exit of the exhaust duct. Noise data upstream and downstream of the cascade were analyzed. The noise reduction was defined as the difference in transmission loss between any velocity and the zero velocity case. No definite trend in the data can be found as a result of stagger angle. A line faired through each set of data was found to fit approximately the following equation:

$$NR = -10 \log_{10}\left(\frac{1}{1 - M_2}\right)^{x_f}$$

where NR is the noise reduction (dB), M_2 is the flow Mach number in the cascade, and x_f is a correlation exponent as function of frequency. Typical values of x_f are 2 for 8000 Hz, 1.5 for 5000 Hz, and 1.0 for 2000 Hz.

An investigation was made in 1969 (ref. E-16) of the acoustic and internal flow characteristics of a model grid inlet. The preliminary configuration of the grid inlet consisted of an inlet duct in which two rows of two-dimensional airfoils were embedded. The rear airfoils could be translated into alignment with the front ones to reduce the inlet flow areas. The flow Mach number between the airfoils was maintained at a transonic level to reduce the inlet noise radiation. This model inlet was tested with a T-50 engine. Acoustic measurements were made using a microphone mounted on a boom sweeping horizontally in the inlet quadrant. Overall noise levels and narrow band spectrum were obtained. Inlet performance instrumentation included static and total pressure probes upstream and downstream of the airfoil grid. Typical acoustic results showed a 13-dB overall noise reduction at a nominal grid throat Mach number of 0.9.

A series of tests were reported in 1970 (ref. E-17) on an XB-70 supersonic airplane to determine the noise reduction and performance level of a two-dimensional supersonic inlet. The tests were performed at Edwards Air Force Base, California. Microphones were placed on a horizontal arc of 240-ft radius at 10° intervals at angles 0° to 90° from the inlet axis. Typical inlet performance instrumentation included static pressure probes in the vicinity of the inlet throat and total pressure probes near the engine compressor face. Acoustic and performance measurements were obtained at unchoked and choked inlet operations for 87% and 100% military power, respectively. Typical results showed a 2- to 5-dB decrease in overall sound pressure level when the inlet was choked at military power.

To evaluate the potential application of the sonic inlet concept to a STOL airplane, a series of model sonic inlet tests were conducted in 1971 and are reported in reference E-18. Two types of sonic inlet concepts were tested. The first configuration was a grid inlet with two rows of parallel vanes (or airfoils) in the inlet duct. One row of the vanes could be translated into alignment with the other to form the inlet throat. The second configuration was a radial vane inlet. Radial vanes were placed in the inlet duct to provide the sonic throat. The inlets were tested on a 12-in.-diameter fan test rig. Acoustic measurements were made in an anechoic chamber. Microphones were positioned on a horizontal arc of 10-ft radius at 10° intervals at angles from 0° to 80° in the inlet quadrant. Instrumentation was also installed to measure the inlet flow performance and fan operating characteristics. Typical results showed that for the grid inlet to attain a 27-PNdB noise reduction the inlet recovery was reduced to 92.8%, and for the radial vane inlet the noise reduction was 22.5 PNdB for the same inlet recovery.

An experiment using choked inlet guide vanes (IGV) as a means of reduction of compressor noise radiated through the inlet was reported in reference E-19. The compressor used was a three-stage transonic axial flow compressor with hub and tip diameters of 6 and 12 in., respectively. The design speed was 24 850 rpm, which corresponds to a tip speed of 1300 ft/sec. Two sets of IGVs were used. They were uncambered, tapered, and of 0.12 and 0.06 thickness to chord ratio. The inlet assembly was tested in an anechoic chamber. Acoustic instrumentation included microphones located on a 10-ft radius arc at 0°, 15°, 30°, 45°, and 90° from the inlet axis. A horizontally sweeping boom was also used for noise measurement. Pressures and temperatures were measured to determine compressor performance. Typical noise data included overall SPL and 1/10 octave band spectra. Reduction of the overall noise level of 25 to 30 dB and 36 dB in the first-stage blade passage frequency noise level was reported.

E.3 DATA ANALYSIS

E.3.1 Flow Mach Number Effect on Sonic Inlet Noise Reduction

The application of the sonic inlet as an inlet noise attenuation device is based upon the fact that sound waves propagate at sonic speed relative to the flow and cannot propagate upstream when flow velocity is greater than or equal to the sonic speed. The propagation of an acoustic wave through the transonic flow in the inlet throat region is highly complex. Analytical solutions are yet to be developed which would describe quantitatively the wave propagation phenomenon. However, some semi-empirical correlations of the noise reduction upstream of a flow channel with subsonic to transonic flows have been developed. Based upon acoustic power reduction of broadband noise associated with fan operation, M. J. T. Smith (ref. E-20) arrived at the formula

$$dB = -10 \log_{10} \left(\frac{1}{1 - M_n} \right) \tag{A}$$

where M_n is the flow Mach number in the channel. Using a set of blade cascades in a flow duct and a warble tone generator as noise source downstream of the cascade, E. B. Smith (ref. E-15) measured the noise intensity (acoustic power) upstream and downstream of the cascade and from the results obtained the formula

$$dB = -10 \log_{10} \left(\frac{1}{1 - M_n} \right)^{x_f} \tag{B}$$

where M_n is the cascade channel flow Mach number and x_f is a correlation exponent as a function of frequency.

In arriving at equation (A), a simple explanation was that if there were no flow through the channel, an equal split of the acoustic energy between the forward and rearward propagation would result. The reason for the unbalanced practical result is that the airflow through the fan blade passage convects a greater portion of the noise in the downstream direction. The frequency-dependent function, x_f, in equation (B) expresses the effectiveness of reduction of sound intensity at various wavelengths.

The reduction of discrete frequency noise from existing data is plotted against flow Mach number in the channel in figure E-1. The noise reduction is either measured at an angle from the inlet axis where maximum reduction occurs or as specified. The flow Mach number is either based on measured data at the inlet centerline or deduced from inlet mass flow. Equation (A) is also superposed in this figure for comparison. The results show that at a flow Mach number of 0.5 the reduction of discrete frequency noise is an average of 2.5 dB. At flow Mach 0.7 the reduction is 18 dB. According to equation (A), however, the respective noise reductions would be 3 and 5.2 dB. From this observation, it can be concluded that sonic inlet acoustic performance is encouraging as far as discrete frequency noise is concerned. The data points on figure E-1 show a fairly linear relationship between $M_{\mathbb{C}}$ and ΔdB between $0.5 \leqslant M_{\mathbb{C}} \leqslant 0.75$. The curves

$$-\Delta dB_{f_o} = 74.7 * M - 34 \quad 0.5 \leqslant M \leqslant 0.75$$

$$-\Delta dB_{f_o} = -130.6M + 343.3M - 186.2M^2 \quad 0.75 \leqslant M \leqslant 0.9$$

represent the trend of the test data.

In figure E-2 the reduction in overall noise level is plotted against the flow Mach number. Four sets of data from Boeing tests of a full-scale, eight-sided sonic inlet with adjustable throat are shown here. These results indicate a maximum overall noise reduction at flow Mach numbers between 0.7 and 0.8. It is not obvious at this time why the noise reduction effectiveness drops off at M = 0.9. Comparison with the noise reduction calculated by equation (A) shows that test data furnishes encouraging noise reduction between M = 0.7 and 0.8. A comparison of figures E-1 and E-2 shows that at $M < 0.6$ the sonic inlet is equally effective in reducing discrete frequency noise and overall noise, although the reduction is limited to below 10 dB on the average. At $M > 0.6$ it can be seen that the reduction in overall noise is less than that of the discrete frequency noise, indicating that the sonic inlet at high flow Mach numbers is not quite as effective on broadband noise as it is with discrete frequency noise.

From the 1/3 octave band spectrum analysis of a 12-in. model grid inlet, pure tone and broadband noise reductions are compared as a function of Mach number for different frequencies. Selected results are shown in figure E-3. The reduction of the noise level associated with the fan fundamental frequency was 25 dB at a nominal grid flow Mach number of 0.825, whereas reductions of broadband noise with center frequencies 4 kHz and 20 kHz were 12 and 17 dB, respectively. More reduction of discrete frequency noise is seen here in comparison to broadband noise reduction.

From the above analysis, one is inclined to suggest that in evaluating sonic inlet applicability the characteristics of the noise source in hand should be considered. If the noise is tone dominated, one may expect that the noise reduction capability would follow that shown in figure E-1. On the other hand, should the noise source be dominated by broadband noise, one would expect the noise reduction capability to follow that shown in figure E-2 or equation (A). Frequency spectra of fan discrete noise reduction and broadband noise reduction for typical sonic inlet configurations and flow Mach numbers would be of value to practical sonic inlet designers. Inlet PNL reduction is plotted in figure E-4 against nominal inlet throat Mach number.

E.3.2 Directivity Pattern of Noise Reduction

Acoustic results in references E-4 and E-6 indicate that sonic inlet noise reduction deteriorates as the angle measured from the inlet axis becomes large. The reduction of fan discrete frequency noise is plotted against angle measured from the inlet axis on figure E-5. A sonic inlet typical for subsonic aircraft application, such as a contracting cowl wall type (eight-sided, adjustable) with acoustically treated fan duct demonstrates two peaks of noise attenuation at $\theta_{max} = 30°$ and 110°. The respective amount of noise reduction is 24 dB and 21 dB. The inlet throat flow Mach number is $M_{\mathfrak{C}} = 0.8$. The directivity pattern of fan discrete frequency noise reduction of an 11% grid inlet is that as the angle measured from the inlet axis increases, the noise reduction increases until the angle reaches 70 where a maximum noise reduction exists. Note that the test setup for the grid inlet excludes the power source driving the fan from the anechoic chamber, and the noise measurements register only the inlet noise. These results suggest that the sonic inlet for subsonic aircraft application is effective in reducing inlet noise radiation at all angles in the forward arc. Inlet PNL reduction directivity is shown in figure E-6.

E.3.3 Sonic Inlet Total Pressure Recovery

Inlet total pressure recovery is plotted in figure E-7 against inlet noise reduction for contracting cowl wall, radial vane, and grid sonic inlets. For the contracting cowl wall sonic inlets, due to the large semiconical angle in the inlet diffuser, tangential blowing boundary layer control flow was introduced. The inlet total pressure recovery increased as the blowing flow was increased. At 18-dB fan tone reduction, inlet total pressure ratio increased from 88.5% to 99.5% as the blowing flow increased from 4 to 12 lb/sec. In the low noise reduction region, enough blowing was introduced so that the inlet total pressure recovery exceeded 1.0, as can be seen in the case of the eight-sided adjustable sonic inlet. In the high noise reduction region, the inlet total pressure recovery decreased at a higher rate than for the low noise reduction. No boundary layer control flow was introduced in the radial vane inlets. The inlet total pressure recovery decreased at approximately a constant rate for the range of noise reduction tested.

E.3.4 Results of a Recent Boeing Sonic Inlet Program

In 1971, Boeing conducted a series of model sonic inlet tests to investigate the feasibility of the sonic inlet for STOL application. After preliminary studies, attention was focused on two types of inlet, the grid and the radial vane inlets. The basic idea for both types is to insert a series of airfoils into the inlet duct to reduce the inlet flow areas such that sonic flows may be obtained at both takeoff and landing approach power settings. The grid inlet uses two rows of parallel vanes (airfoils), one of which can be translated into alignment with the other to form the minimum inlet throat area. The radial vane inlet uses radially inserted vanes of a designated taper to give equal "blockage" at various radial positions.

A grid inlet with airfoils of 11% and 17% thickness-to-chord ratio was tested. The inlet consisted of a bellmouth section, a 13-in. circular duct section which housed the airfoil grid, and straight circular ducts of four different lengths. A photograph of the airfoil grid is shown in figure E-8. The inlet was connected to a 12-in.-diameter fan driven by a 900-hp gas turbine, and the inlet section set up to protrude into an anechoic chamber for noise measurements. Near-field and far-field noise measurements were made. Microphones were located on the inside duct walls upstream and downstream of the airfoil grid to measure the near-field noise level. For far-field noise measurement, microphones were located on a 10-ft arc centered at the bellmouth section, from 0° to 80° from the inlet centerline at 10° intervals. Inlet flow instruments included temperature and pressure probes which permitted the measurement of: bellmouth total temperatures, the anechoic chamber total pressure, vane surface static pressure, total pressure at the fan face, boundary layer velocity profile at the fan face, and total pressure downstream of the fan. One-third octave band noise data were obtained for all the test conditions. Selected 80-Hz bandwidth spectra were also obtained. Typical acoustic results were expressed in PNL reduction at a 500-ft sideline. Inlet flow results included the inlet total pressure recovery (see fig. E-9).

Test configurations for the radial vane inlet included three inlet cowls, one for a typical approach power setting, and two for takeoff power settings. A set of 36 radial vanes with linear taper ratio and constant thickness ratio were inserted into the inlet cowl to provide the sonic flow. The vanes were inserted radially into the approach cowl. For takeoff cowl 1, the vanes were either in a radial position at the rear end of the inlet or swept 30° near the cowl minimum flow area. A photograph of the radial vanes is shown in figure E-10.

The acoustic instrumentation is similar to that of the grid inlet. However, the inlet flow instruments were tailored for the radial vane inlet. Measurements included vane surface velocities and cowl wall surface velocities. Typical results are shown in figure E-11.

REFERENCES

E-1 Maestrello, L.: The Design and Evaluation of an Aerodynamic Inlet Noise Suppressor. Boeing document D6-5980, 1960.

E-2 Sobell III, J. A.; and Welliver, A. D.: Sonic Block Silencing for Axial and Screw-Type Compressor. Report of the Curtiss-Wright Corp. Also: Noise Control Shock Vibration. Vol. 7, no. 5, September-October 1961, pp. 9-11.

E-3 Greatrex, F. B.: "By-Pass Engine Noise," Transactions of the Society of Automotive Engineers. Vol. 60, 1961, pp. 312-324.

E-4 McKaig, M. B.: J-75 Inlet Noise Suppression Test. Boeing document T6-3173, 1964.

E-5 Copeland, W. L.: Inlet Noise Studies for an Axial-Flow Single-Stage Compressor. NASA TND-2615, 1965.

E-6 Cawthorn, J. M.; Morris, G. J.; and Hayes, C.: Measurement of Performance, Inlet Flow Characteristics, and Radiated Noise for a Turbojet Engine Having Choked Inlet Flow. NASA TND-3929, 1967.

E-7 Sawhill, R. H.: Investigation of Inlet Airflow Choking as a Means of Suppressing Compressor Noise-5" Inlet Model. Boeing document D6A-10155-1, 1966.

E-8 Andersson, A. O.: An Acoustic Evaluation on the Effect of Choking Using a Model Supersonic Inlet. Boeing document D6A-10378-1 TN, 1966.

E-9 Study and Development of Turbofan Nacelle Modifications to Minimize Fan-Compressor Noise Radiation, Vol. V—Sonic Inlet Development. Boeing document D6-60120-5, 1969.

E-10 Smith, J. N.: Full-Scale Tests of a Five-Door Sonic Throat Inlet at Tulalip—JT 3D-3B Engine. Boeing document D6-23461TN, 1968.

E-11 Smith, J. N.; and Higgins, C. C.: Inlet and Engine Performance with Eight-Segment Adjustable Boilerplate Sonic Inlet—JT3D-3B Engine. Boeing document D6-23469, 1969.

E-12 Higgins, C. C.; and Lupkes, W. R.: Full Scale Model Tests of an Eight-Sided Contracting Cowl Sonic Throat Inlet. Boeing document D6-22745, 1969.

E-13 Bosch, J. C.: Acoustic Study of a Boilerplate Sonic Inlet for a JT3D Turbofan Engine Nacelle. Boeing document D6-22752, 1969.

E-14 Wise, W. H.: Summary Report—Model Tests of Sonic Throat Inlets for Turbofan Engine Inlet Noise Attenuation. Boeing document D6-23468, 1968.

E-15 Smith, E. B., et. al.: Study and Tests to Reduce Compressor Sounds of Jet Aircraft. General Electric Company technical report DS-68-7, contract FA65WA-1236 to FAA, 1968.

E-16 Schaut, L. A.: Results of an Experimental Investigation of Total Pressure Performance and Noise Reduction of an Airfoil Grid Inlet. Boeing document D6-23276, 1969.

E-17 Putnam, T. W.; and Smith, R. H.: XB-70 Compressor-Noise Reduction and Propulsion-System Performance for Choked Inlet Flow. NASA TND-5692, 1970.

E-18 Anderson, R.; DeStafanis, P.; Farquhar, B. W.; Giarda, G.; Shuehle, A.; and VanDuine, A. A.: Boeing/Aeritalia Sonic Inlet Feasibility Study. Boeing document D6-40208, 1972.

E-19 Chestnutt, D.: Noise Reduction by Means of Inlet-Guide-Vane Choking in an Axial-Flow-Compressor. NASA TND-4682, 1968.

E-20 Smith, M. J. T.; and House, M. E.: "Internally Generated Noise From Gas Turbine Engines, Measurement and Prediction," Transactions of ASME, Journal of Engineering for Power. 1967.

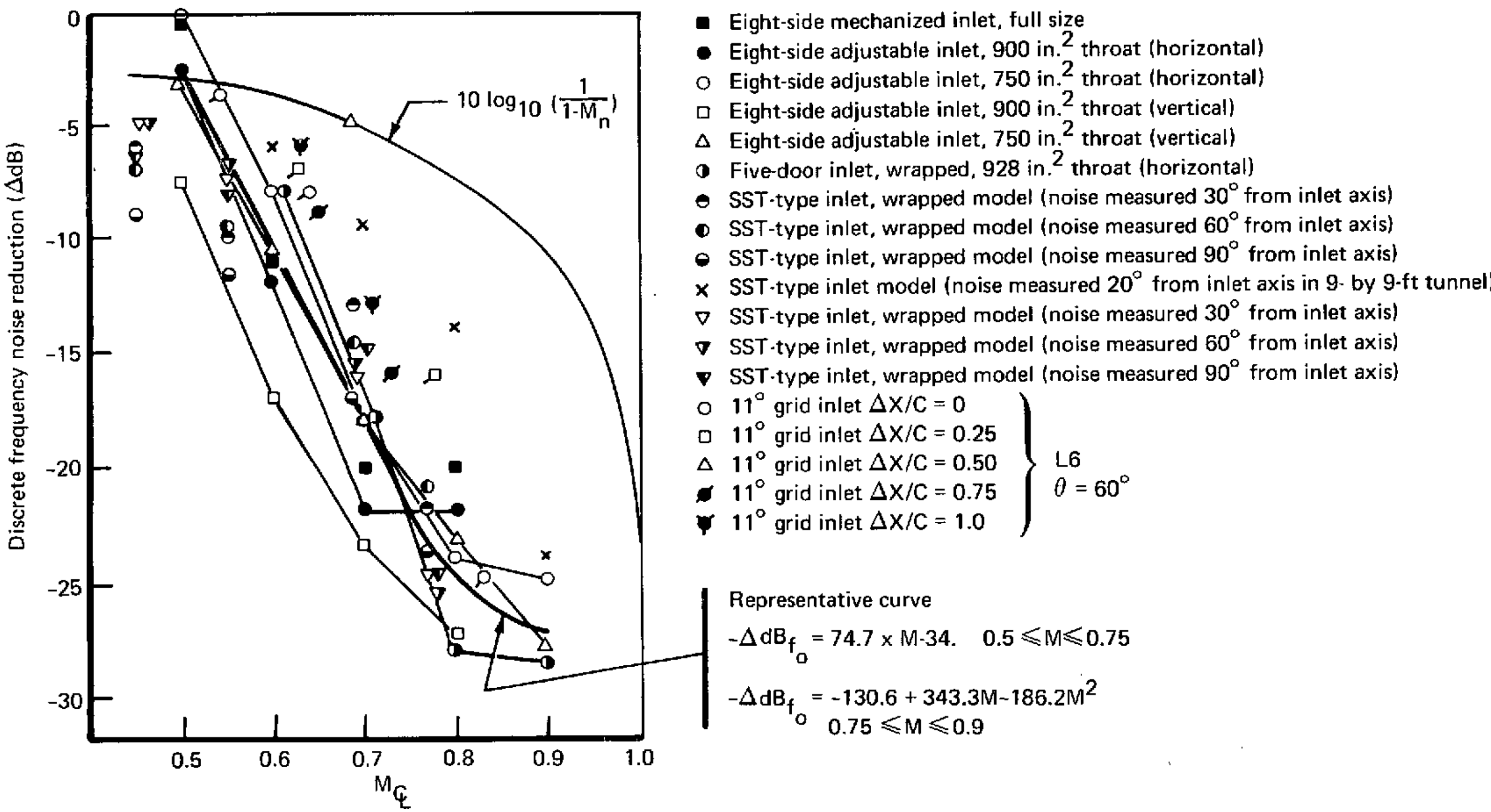

FIGURE E-1.—DISCRETE FREQUENCY NOISE REDUCTION VS FLOW MACH NUMBER

● Eight-side adjustable, 900 in.^{2} throat (horizontal)
⊙ Eight-side adjustable, 750 in.^{2} throat (horizontal)
⊡ Eight-side adjustable, 900 in.^{2} throat (vertical)
△ Eight-side adjustable, 750 in.^{2} throat (vertical)
⊗ XB-70 ground test data (20° from inlet centerline)
⊕ SST-type inlet with viper-8 engine (30° from inlet axis)

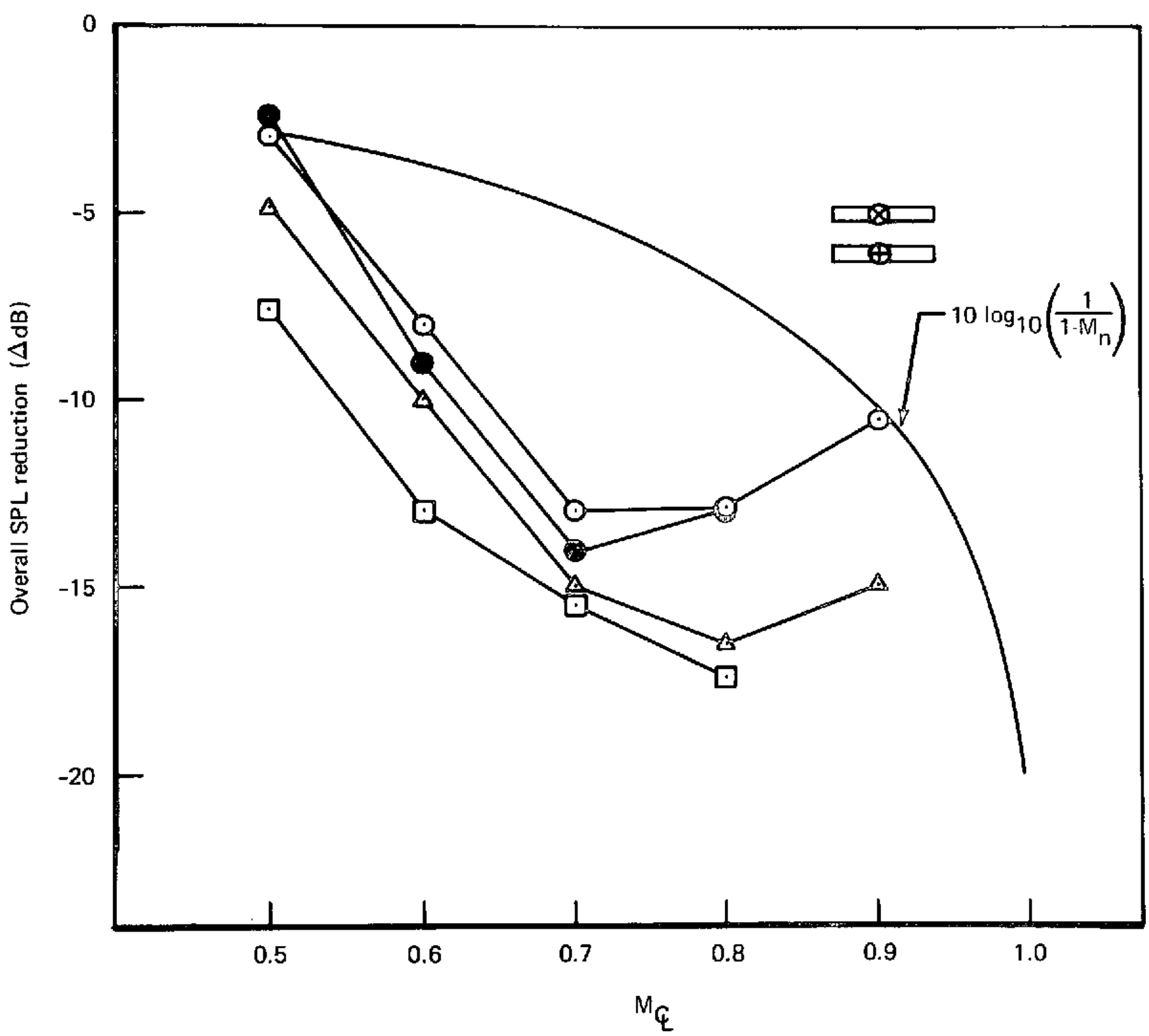

FIGURE E-2.—OVERALL SPL REDUCTION VS FLOW MACH NUMBER

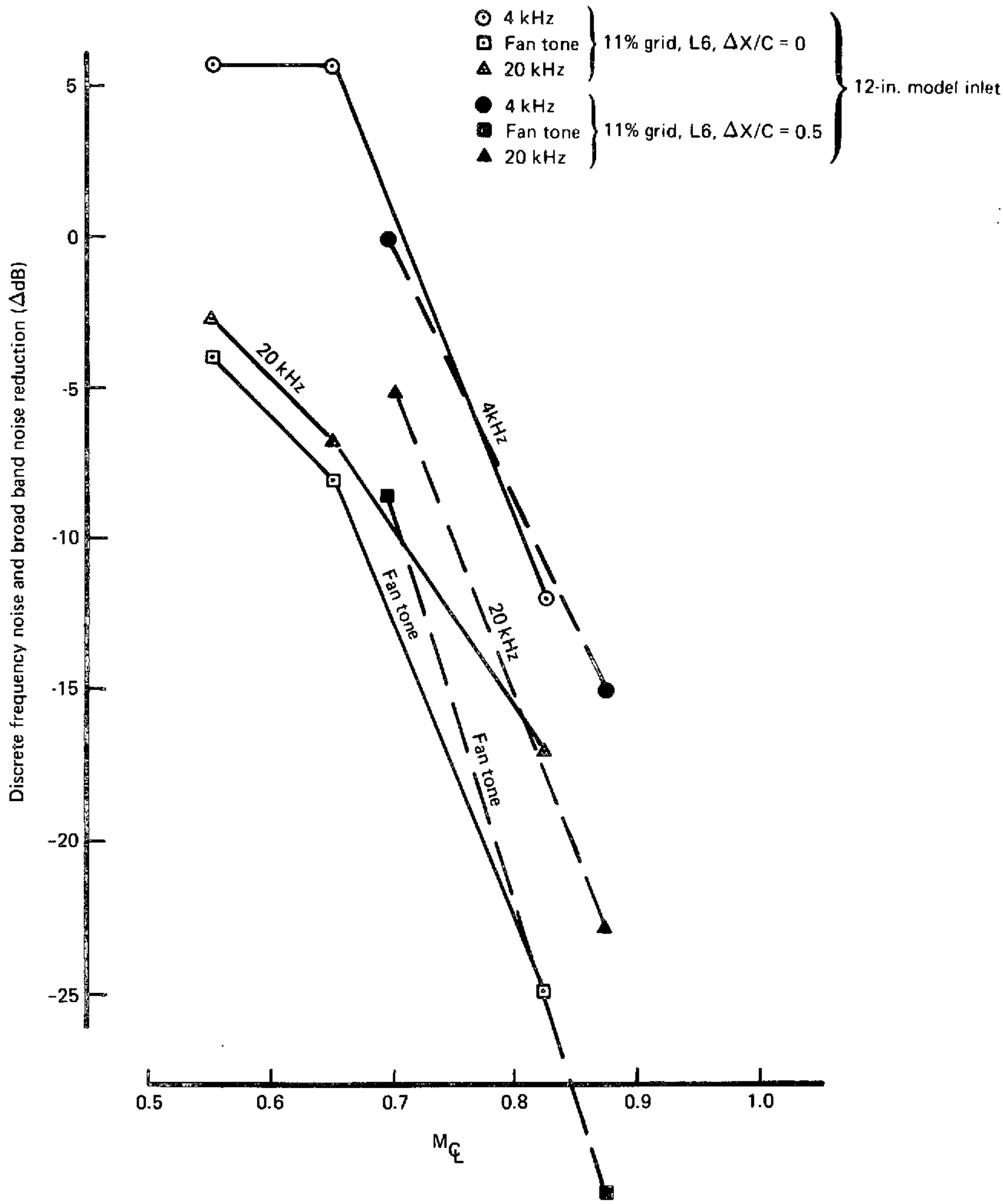

FIGURE E-3.—DISCRETE FREQUENCY NOISE AND BROAD BAND NOISE REDUCTION OF A GRID SONIC INLET

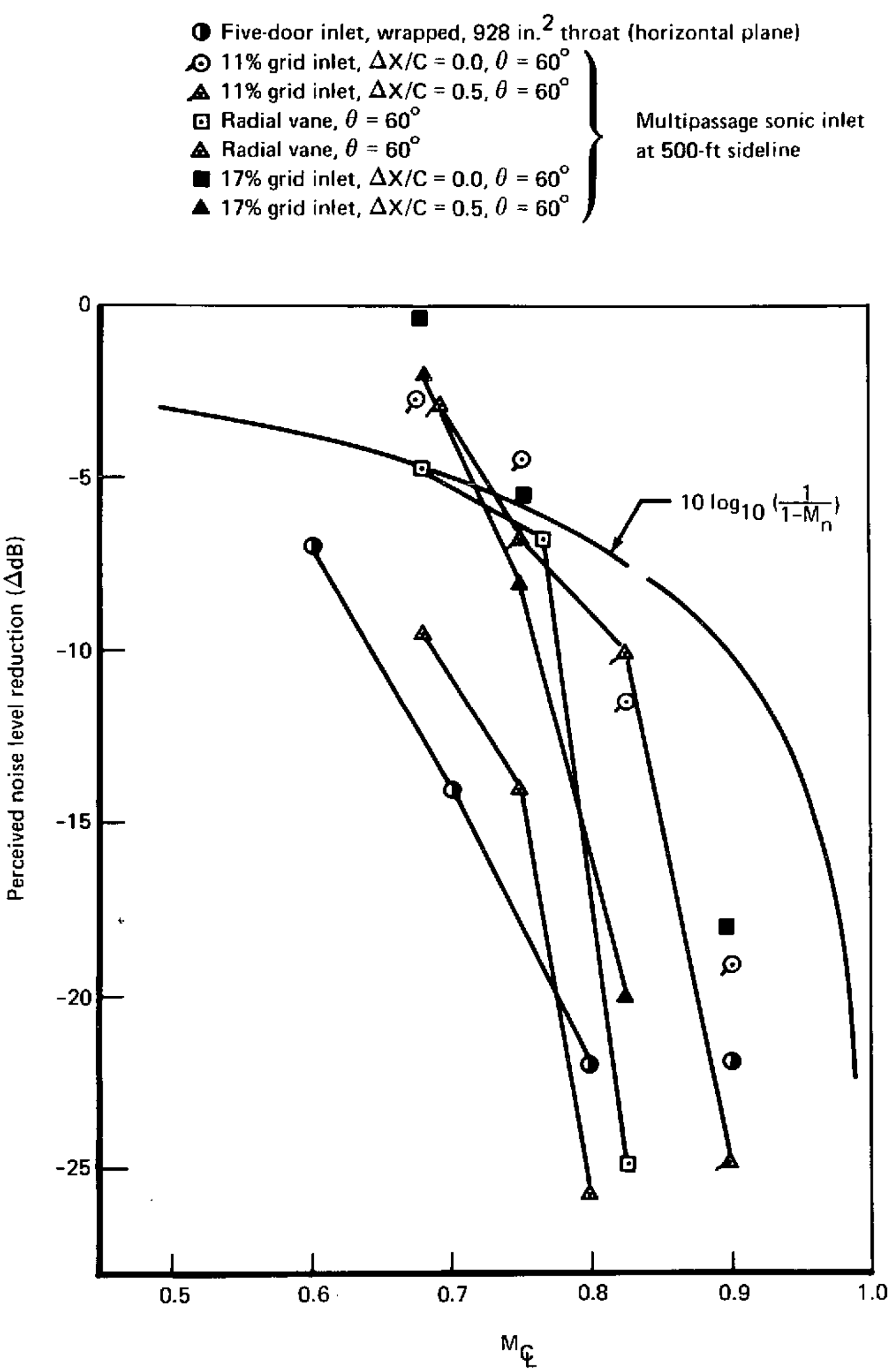

FIGURE E-4.—PERCEIVED NOISE LEVEL REDUCTION VS FLOW MACH NUMBER

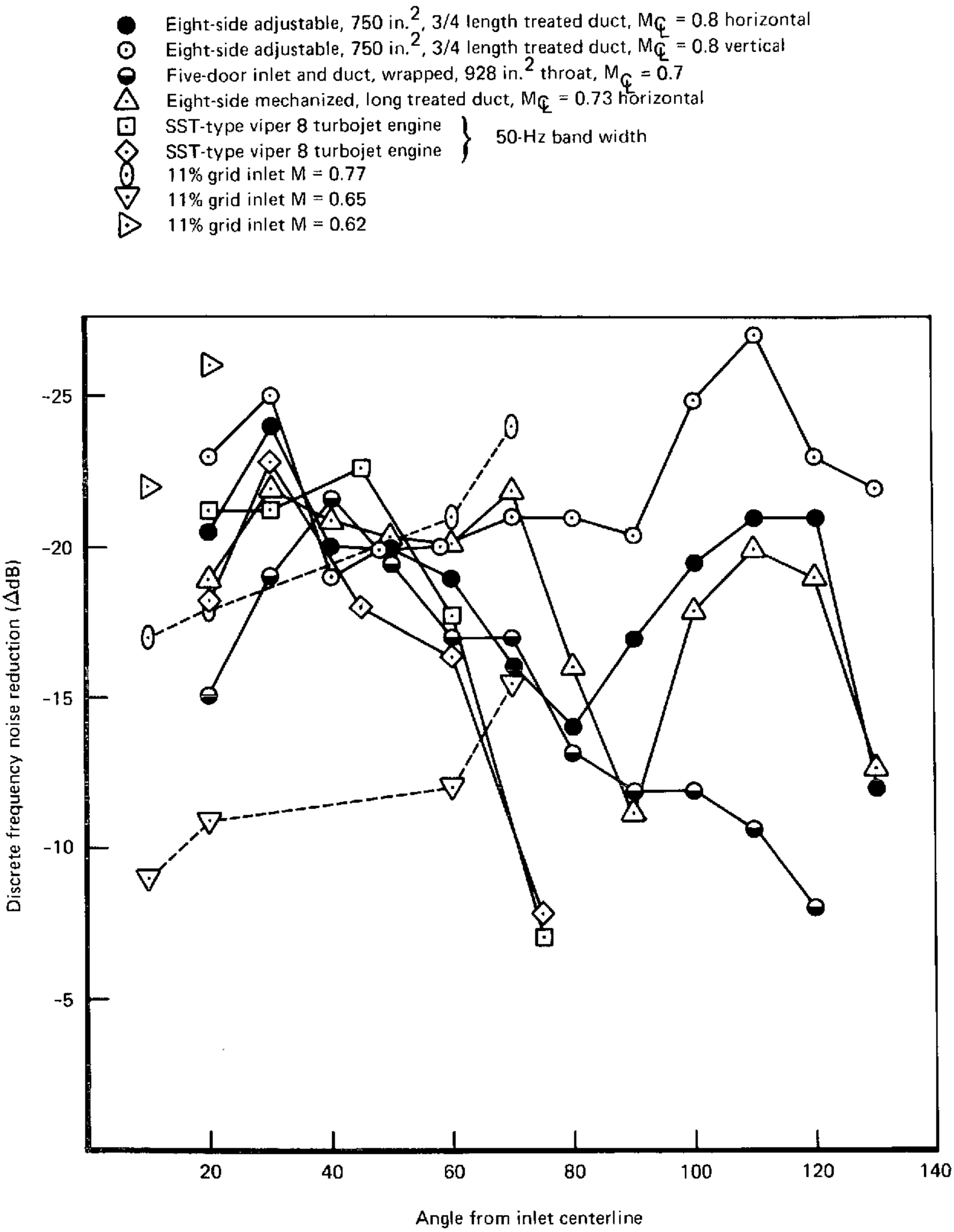

FIGURE E-5.–DIRECTIVITY OF DISCRETE FREQUENCY NOISE REDUCTION

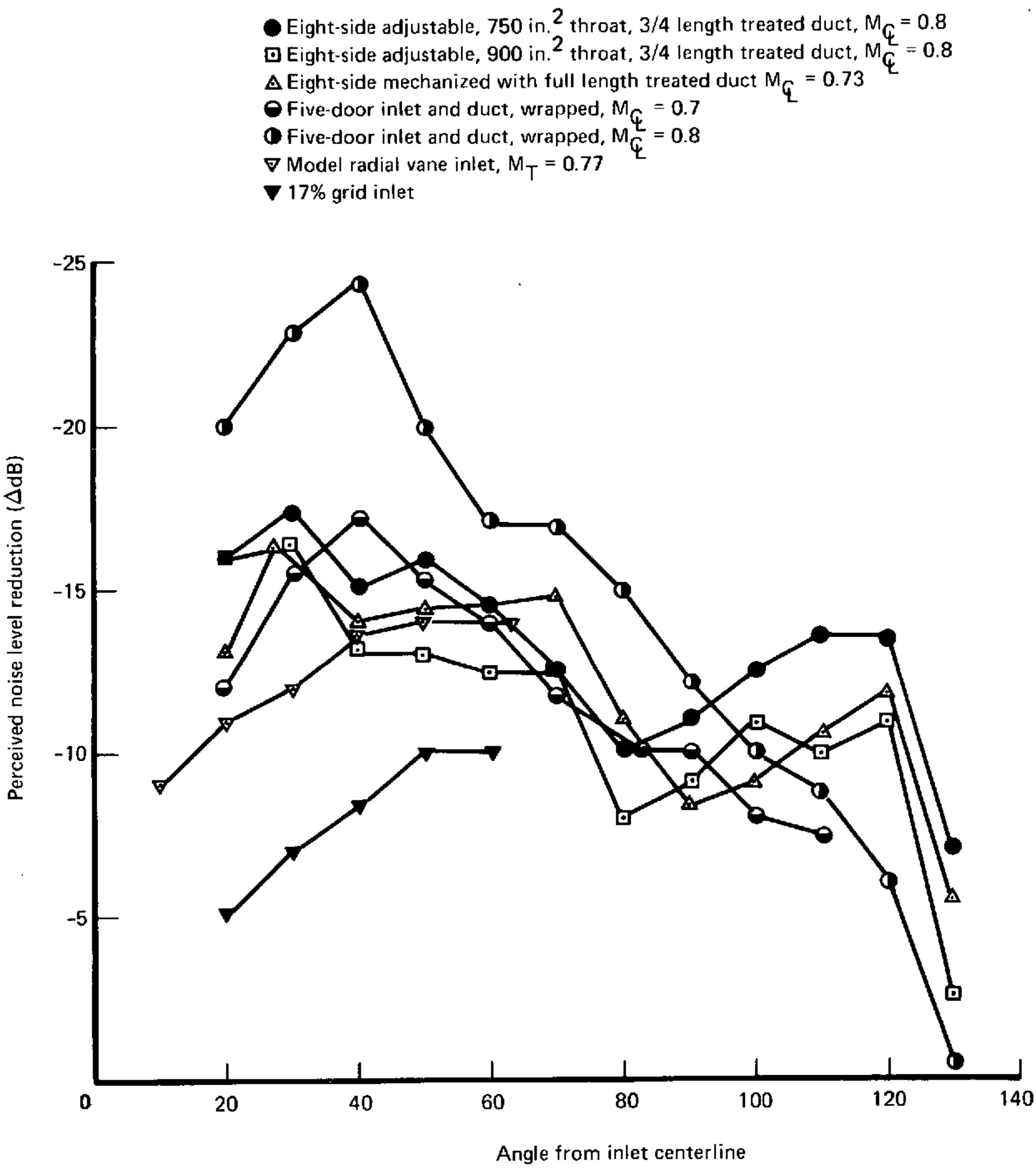

FIGURE E-6.—DIRECTIVITY OF PERCEIVED NOISE LEVEL REDUCTION

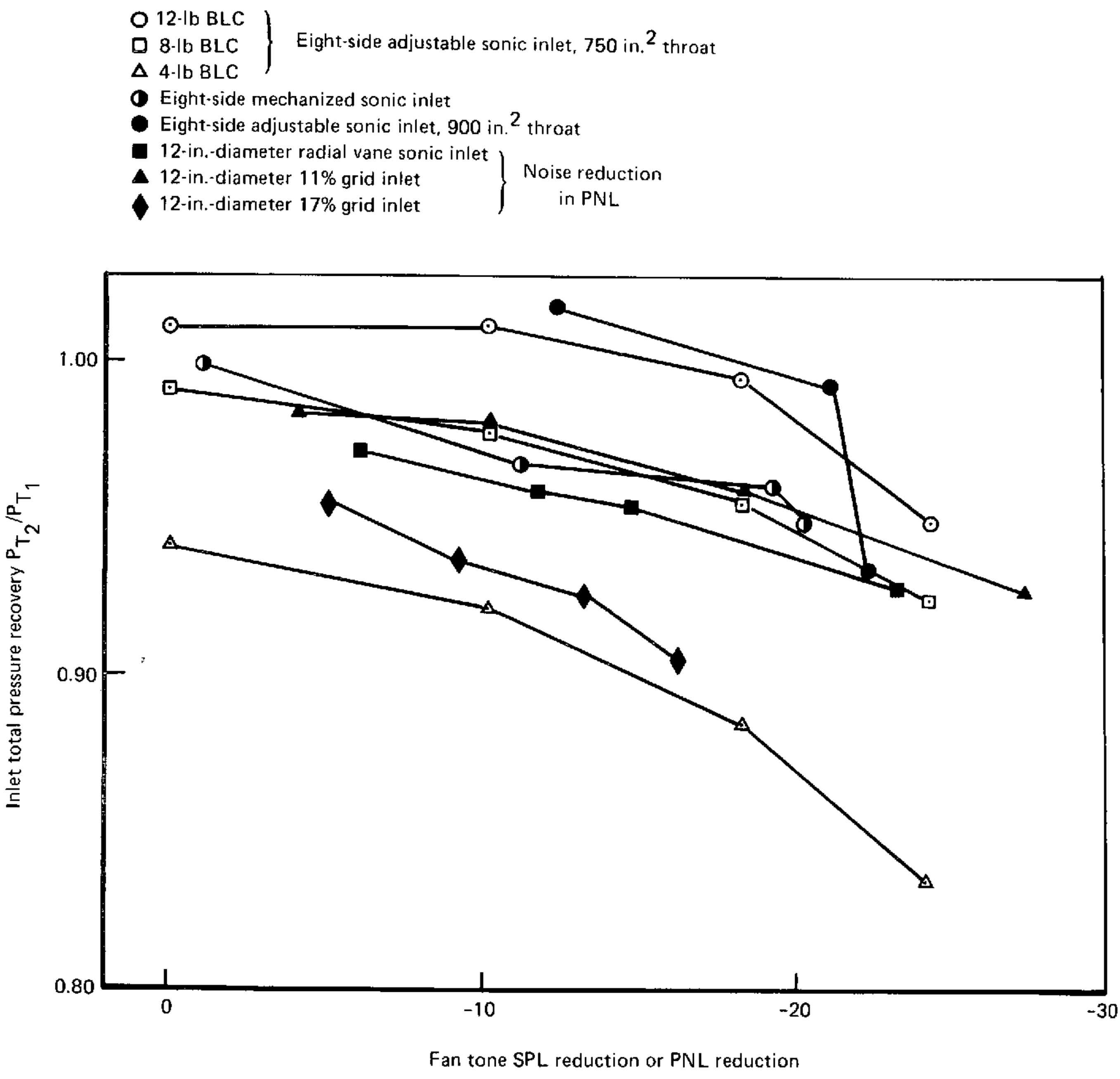

FIGURE E-7.—INLET TOTAL PRESSURE RECOVERY VS NOISE REDUCTION

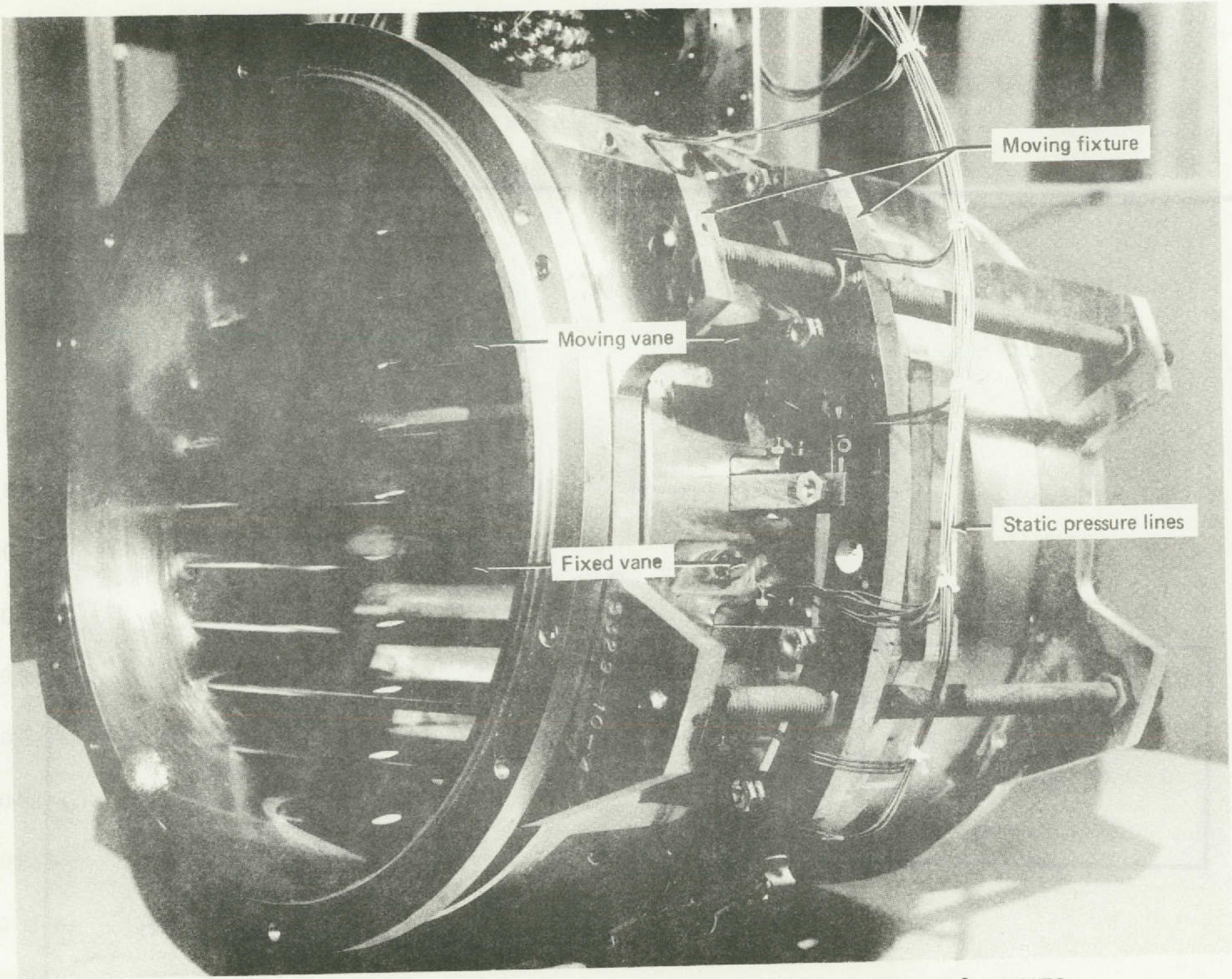

FIGURE E-8.–GRID TEST SECTION, VANE CONFIGURATION, 11° VANES

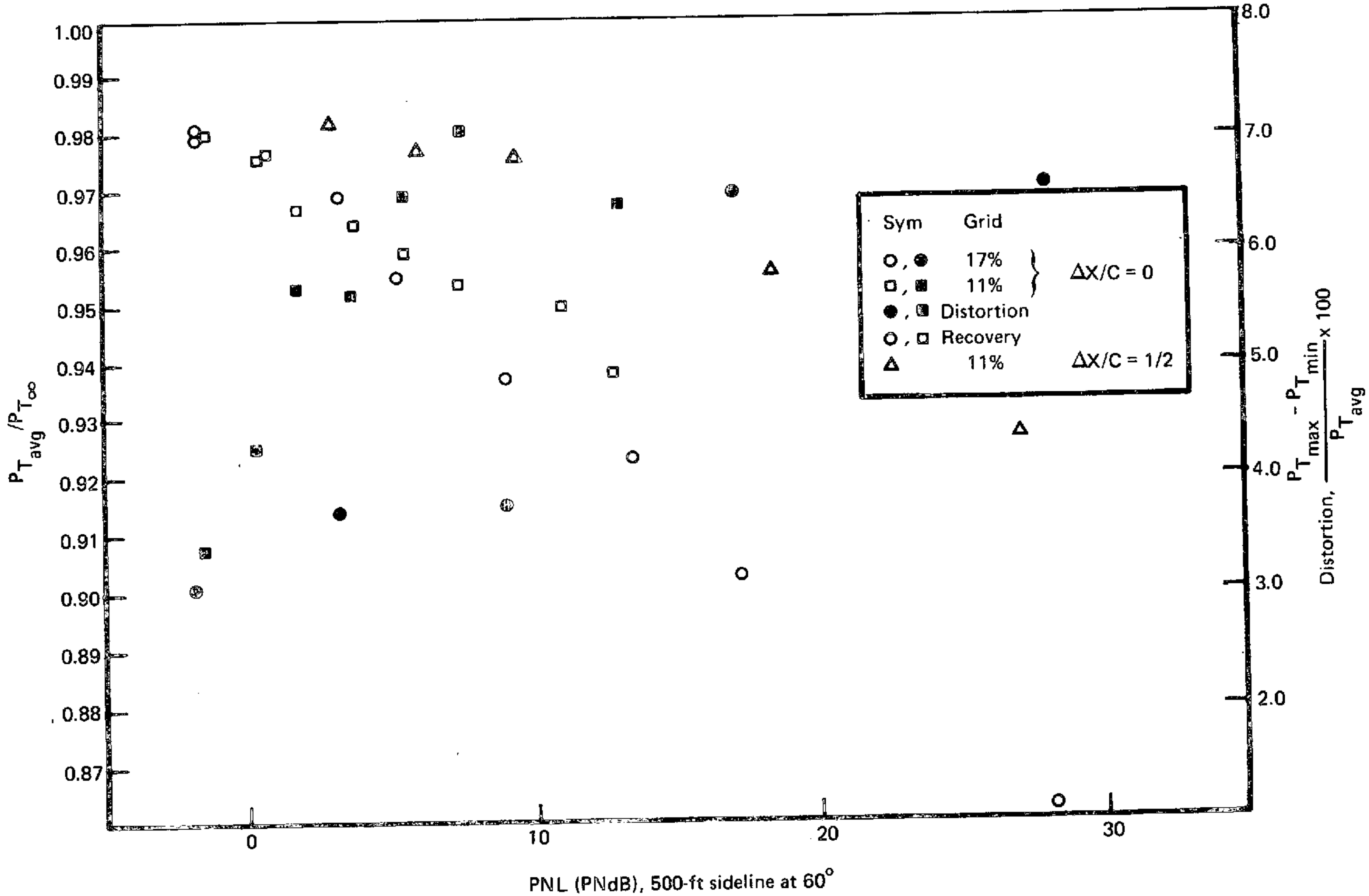

FIGURE E-9.—GRID INLETS, PERCEIVED NOISE LEVEL REDUCTION VS RECOVERY

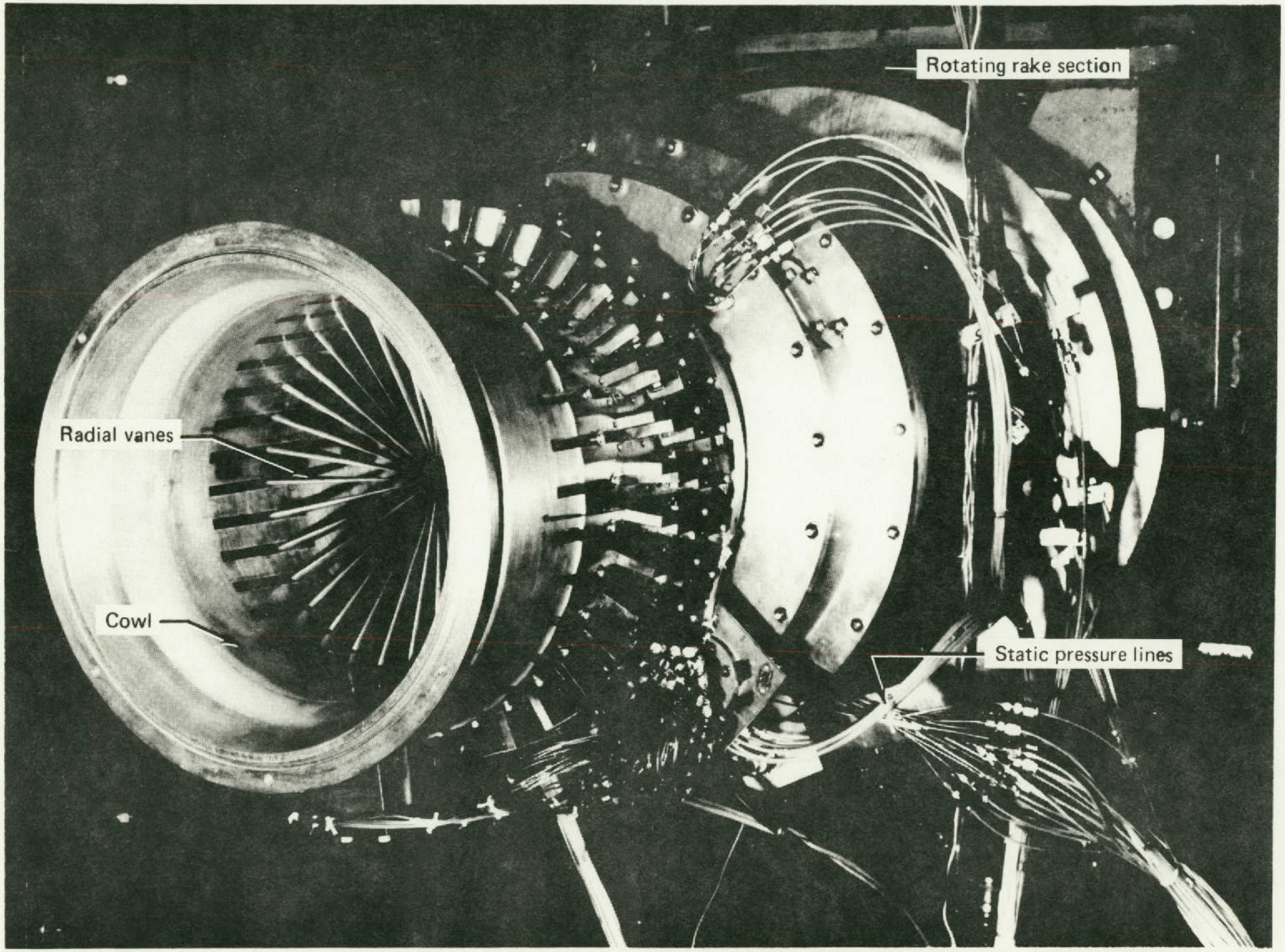

FIGURE E-10.—RADIAL VANE MODEL SONIC INLET

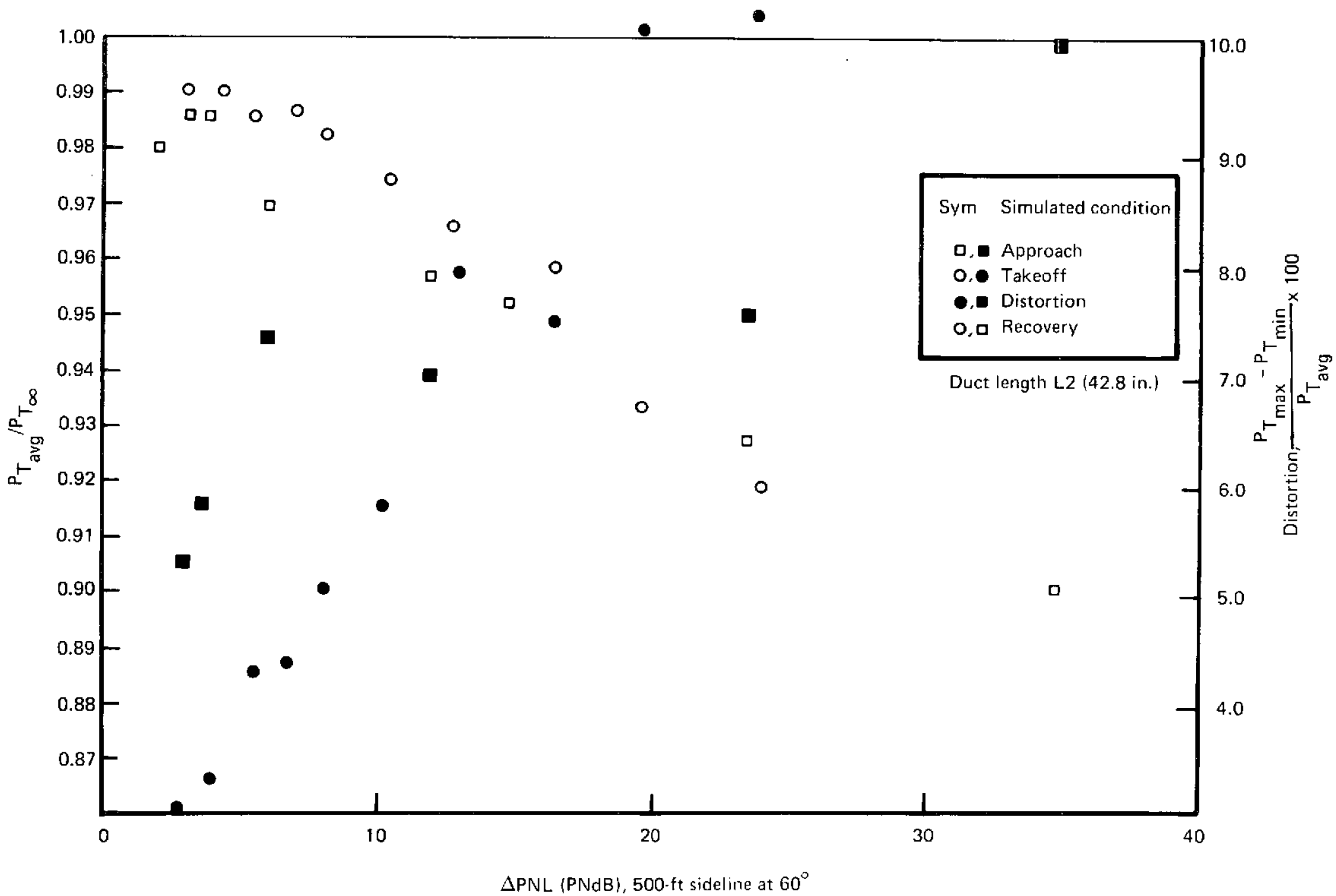

FIGURE E-11.— RADIAL VANE PERCEIVED NOISE LEVEL REDUCTION VS RECOVERY